Planktonic foraminifera as ecological and geochemical palaeoclimate proxies:

Evaluation from Southern Ocean sediment traps

Alexandra Louise King

A thesis submitted in fulfilment of the requirements for the Degree of Doctor of Philosophy at the University of Tasmania.

November, 2003

Institute of Antarctic and Southern Ocean Studies
Hobart

This thesis contains no material which has been accepted for the award of any other degree or diploma in any tertiary institution, and to the best of my knowledge and belief, contains no material previously published or written by another person, except where due reference is made in the text.

PUBLICATIONS ARISING FROM THIS THESIS

King, A.L. and Howard, W.R., Seasonality of foraminiferal flux in sediment traps at Chatham Rise, SW Pacific: Implications for paleotemperature estimates, *Deep-Sea Research I*, 48, 1687-1708, 2001.

King, A.L. and Howard, W.R., Planktonic foraminiferal flux seasonality in Subantarctic sediment traps: A test for paleoclimate reconstructions, *Paleoceanography*, 18(1), 1019, doi:10.1029/2002PA000839, 2003.

King, A.L. and W.R. Howard, Planktonic foraminiferal $\delta^{13}C$ records from Southern Ocean sediment traps: New estimates of the oceanic Suess effect, *Global Biogeochemical Cycles,* 18, doi:10.1029/2003GB002162, in press.

ABSTRACT

The analysis of planktonic foraminifera obtained from Southern Ocean sediment traps allows the calibration of several important paleoclimate proxies in this thesis. Foraminifera are analysed to determine the spatial and temporal changes in faunal and isotopic composition. Annual faunal assemblages collected from each sediment trap are compared to a global core top data base to assess the validity of the Modern Analog Technique in estimating sea-surface temperatures. The oxygen isotopic composition of several foraminiferal species also allows calibration of paleotemperature equations for the first time in Southern Ocean settings. The utility of the foraminiferal carbon isotopic record as a nutrient tracer is also tested.

The sediment traps represent two separate deployments. The first deployment consists of two sediment traps moored north and south of Chatham Rise east of New Zealand at 42° and 44°S respectively. These traps sampled Subtropical and Subantarctic waters over an annual cycle. The second deployment consists of an array of traps moored south of Tasmania at 47°S in the Subantarctic Zone, 51°S at the Subantarctic Front, and 54°S in the Polar Frontal Zone. The timing of this second deployment coincides with the dominant period of biological production between September and March. The trap at 47°S was subsequently redeployed for a following year.

Planktonic foraminifera collected in the traps exhibit distinct seasonal and latitudinal distributions. Diversity of foraminiferal species decreases to the south, with water mass boundaries associated with sharp changes in foraminiferal assemblages. The distinct change in species composition is particularly striking north and south of the Subtropical Front. Subtropical waters are dominated by the species *Globorotalia inflata*, while Subantarctic waters (at the 44°S and 47°S traps) are dominated by *Globigerina bulloides*. *G. bulloides* remained dominant at 51°S, but is replaced by *Neogloboquadrina pachyderma* (sinistral coiling) and *Globigerina quinqueloba* in Polar Frontal waters at 54°S.

Despite the significant differences in species abundances and dominance between the sites, seasonal flux patterns appear constant for each of the major species. *G. bulloides* and *G. inflata* are most productive during spring and early summer at all sites, while *N. pachyderma* (s.) and *N. pachyderma* (dextral coiling) tend to be most abundant during summer to autumn. These seasonal succession patterns are associated with changes in

thermal stratification, which drives the depth of the chlorophyll maximum in these regions.

Analysis of the planktonic foraminifera from these sediment traps provides important insights for the interpretation of past climates in sedimentary records. Comparison between the total assemblages from each trap site and regional core tops confirms the relationship between core top material and modern environments, a relationship which is often extrapolated to the interpretation of down core material. Further comparison to core top assemblages, using the Modern Analog Technique, reveals a good consistency between foraminiferal assemblages and sea-surface temperatures in a global core top data base. These results indicate that the Modern Analog Technique allows the estimation of sea-surface temperatures to within 1.2° to 4.5°C of observations in these Southern Ocean environments.

The isotopic composition of *G. bulloides*, *G. inflata* and *N. pachyderma* (s.) is analysed for each sediment trap. The $\delta^{18}O$ content is compared to predictions from various temperature equations, revealing greatest consistency to the equation of Epstein et al. (1953). The depth range for each species is also determined by analysis of their $\delta^{18}O$ content. *G. bulloides* and *N. pachyderma* (s.) dwell at near-surface depths, while a deeper habitat is inferred for *G. inflata*. Similarity between flux weighted sediment trap values and regional core tops reveals the preservation of seasonal flux patterns in the sedimentary records. Changes in seasonal flux patterns down the core and between water masses may therefore overprint temporal or latitudinal gradients in $\delta^{18}O$.

The $\delta^{13}C$ composition of the three foraminiferal species reveals latitudinal trends in disequilibrium. Foraminiferal $\delta^{13}C$ increases from north to south, while the $\delta^{13}C$ of dissolved inorganic carbon decreases across these latitudes. Disequilibrium in *G. bulloides* can be accounted for by changes in temperature and carbonate ion content ($[CO_3^{2-}]$). The relationship between disequilibrium and $[CO_3^{2-}]$ derived for whole shells of *G. bulloides* is consistent with the slope established from individual chambers in laboratory measurements. Corrected $\delta^{13}C$ for *G. bulloides* is closely correlated to changes in nutrients at each site, indicating the utility of *G. bulloides* as a nutrient tracer in Southern Ocean environments. Comparison between flux weighted sediment trap values and nearby core tops indicates a modern depletion in $\delta^{13}C$, attributable to the oceanic Suess effect. The large magnitude of this effect signifies considerable equilibration between the surface waters and the atmosphere in the Subantarctic Zone.

ACKNOWLEDGEMENTS

The production of this thesis and the maintenance of my sanity have benefited incredibly from the support and assistance provided by many colleagues, friends and family.

My thanks must first of all go to my supervisor Will Howard who has shared his passion for science so enthusiastically and provided me with the inspiration to continue on when my own was lacking. When I first met Will I knew next to nothing about palaeoclimatology and had never even set eyes on a foraminifera. He opened the way for me into an exciting and rewarding field of science which I feel privileged to be a part of. Thank you for your unfailing commitment to this project and to my development as a scientist. Thank you also to Leanne Armand for her sound advice, support and constructive feed back on draft manuscripts. You have been a great inspiration and I really value your sound judgement.

All those within the Paleoenvironment group at the Antarctic CRC have been pivotal to the completion of this project. I could not have completed this project without the assistance of Lisette Robertson who thankfully took control of picking and preparing the last of my samples for isotope analysis after I moved from Hobart to Canberra, has kept a check on the accuracy and integrity of my results, has cheerfully taught me all I know about Adobe Illustrator, and even taught me how to play squash! Thank you for your support and friendship. Thank you also to Suenor Woon, who along with Lisette, provided much laboratory assistance and good cheer. Ana Brandao also stepped in to prepare my samples for the mass spec and Steve Bray and Teresa O'Leary also helped in the early stages of sample collection and preparation.

Many people have provided data and offered their advice and ideas along the way. Thank you particularly to Tom Trull and Scott Nodder for providing me with the sediment trap material to work on and for providing on going discussion about the results and data. Thank you to Keith Harris at CSL who analysed the Chatham Rise sediment trap samples for me, and particular thanks to Howie Spero and David Winter who ran the remainder of my samples on the mass spectrometer at UC Davis. Without this very timely assistance this thesis would still be at a stand still. Howie has also provided very valuable insight and ideas regarding the interpretation of the isotope results. Bronte Tilbrook provided unpublished carbonate ion data and isotope data as

well as useful suggestions, and Pat Quilty is thanked for reviewing earlier versions of some of the manuscripts. Matt Walkington is thanked for providing CTD data for the New Zealand trap sites. Many other people have provided discussion, direction, manuscripts and data along the way. Thanks particularly to Helen Neil, Tim Barrows, Joe Ortiz, Jelle Bijma, Cindy Pilskaln, Patrick DeDeckker, Andrew Moy and Stefan Mulitza.

For administrative and technical support my thanks to Margaret Appleton, Frank Sainsbury and Kelvin Michael.

Many thanks also to Neville Exon, my current supervisor at Geoscience Australia, who has been so supportive during the last few months, allowing me the flexibility to complete this thesis. Thanks to Richard Brown and Tony Watson at GA for allowing me access to laboratory facilities.

My parents and family have inspired me to seek and enjoy challenges, and have supported me throughout the process with home cooked meals whenever possible, proof reading of manuscripts and a faith in my abilities.

My many housemates have been a very important part of my life and thank you to them all for putting up with my stress and tension, particularly my most recent housemates who have had to put up with my antisocial behaviour as I have ferreted myself away in my room during these last few months. Thank you particularly to Alison, Debbie, Caroline, Emma, Prachi and Cath for your patience, for nourishing me with your good cooking, for keeping me sane with your good humour, and for helping me to keep sight of the real world.

My bushwalking and mountain biking buddies have greatly assisted in the rejuvenation of my mind by accompanying me to often wild and beautiful places. I have really valued the good company of Caroline, Dave, Lex, Hil, Claire, Prachi and Steve.

Finally, thank you to Troy for your encouragement, love, understanding and prayers. You have been the light at the end of the tunnel inspiring me to make it to the end.

TABLE OF CONTENTS

CHAPTER 1: INTRODUCTION

CHAPTER 2: FORAMINIFERAL FLUX AT CHATHAM RISE

LIST OF FIGURES

CHAPTER 1:

CHAPTER 2:

CHAPTER 3:

CHAPTER 4:

CHAPTER 5:

CHAPTER 6:

CHAPTER 7:

LIST OF TABLES

LIST OF PLATES

CHAPTER 2:

CHAPTER 6:

CHAPTER 1

INTRODUCTION

"The sediments are a sort of epic poem of the earth. When we are wise enough, perhaps we can read in them all of past history. For all is written here"

Rachel Carson, The Sea Around Us (1951)

1.1 BASIS OF THE STUDY

The fossil record of planktonic foraminiferal assemblages in marine sediments is a key tool used by palaeoceanographers to study past environments. The faunal assemblages preserved in marine sediments have been exploited to determine past changes in sea-surface temperature (Hutson, 1979; Imbrie and Kipp, 1971), while their isotopic and trace metal compositions have been applied to interpretations of ocean chemistry (Boyle, 1992; Boyle and Keigwin, 1985/86; Broecker and Peng, 1982; Charles and Fairbanks, 1992; Shackleton et al., 1992). The different techniques, however, have previously yielded different interpretations of past climates. It is therefore important to validate foraminiferal data sets against environmental parameters observed at the time of production. Sediment trap studies provide the opportunity to establish calibrations between the foraminiferal data and measurements of the thermal and chemical characteristics of the water column.

1.1.1 Significance and aims of the study

This study represents the first analysis of planktonic foraminifera derived from sediment traps in the Subantarctic Zone of the Southern Ocean. The traps were deployed in 4 different environments: viz. Subtropical Zone, Subantarctic Zone, Subantarctic Front and the Polar Frontal Zone (Figure 1). The water masses within these zones have distinct biological characteristics, allowing the interplay between Southern Ocean dynamics and marine organisms to be examined. The calibrations obtained from this study will be important for palaeoclimate reconstructions within the Southern Ocean.

The aims of this study are:

1. To determine the seasonal flux variability of planktonic foraminifera, and the factors which may drive seasonal changes in species composition, such as sea-surface temperature (SST), thermal stratification and biomass production.

2. To validate seasonal SST estimates derived from assemblages of planktonic foraminifera. This analysis will relate specifically to the Modern Analog Technique of Hutson (1979) modified by Prell (1985).
3. To advance our understanding of oxygen and carbon isotopic data derived from shells of planktonic foraminifera.
4. To establish seasonal and depth imprints on the sedimentary isotopic composition for various foraminiferal species in each region.
5. To assess the role of the Southern Ocean in the modern carbon cycle.

1.1.2 Format of the thesis

Chapter 1 provides a discussion of relevant background material. The oceanographic features of the Southern Ocean will be described to provide a context for this study. The importance of the Southern Ocean in the global climate system will then be reviewed. The known ecological preferences of foraminiferal species will be presented followed by a discussion of the environmental information that can be obtained from species fluxes and their chemical signatures. The application of the carbon isotopic record to monitoring change in the modern carbon cycle will then be explained. Sediment trap studies face several potential biases in data collection, as will be discussed.

In Chapter 2, the faunal analyses from the Chatham Rise sediment traps are presented. This chapter includes the methodology used for this study, followed by a presentation of the results and their implications for our understanding of seasonal species fluxes and our estimation of SSTs. Faunal analyses for the Subantarctic Zone sites are presented in Chapter 3. In Chapters 4 and 5 the oxygen and carbon isotope results are discussed for the Chatham Rise and the Subantarctic Zone samples. The isotopic analysis of individual foraminifera are presented in Chapter 6. The implications of all of these results for our interpretation of past climate records is discussed in Chapter 7, with application to a down-core record. This final chapter also includes suggestions for future research.

All data collected from the sediment traps as part of this thesis is recorded in the appendices. Appendix I provides the technical details of each trap deployment, Appendix II contains a record of all the species fluxes at each site, and Appendix III records the isotopic data for each species analysed.

1.2 OCEANOGRAPHIC SETTING

1.2.1 Water masses

The Southern Ocean can be divided into three different oceanographic regions. From north to south these are the Subantarctic Zone (SAZ), the Polar Frontal Zone (PFZ) and the Antarctic Zone (AZ) (Figure 1). The Subtropical Zone (STZ) to the north is also included in this study.

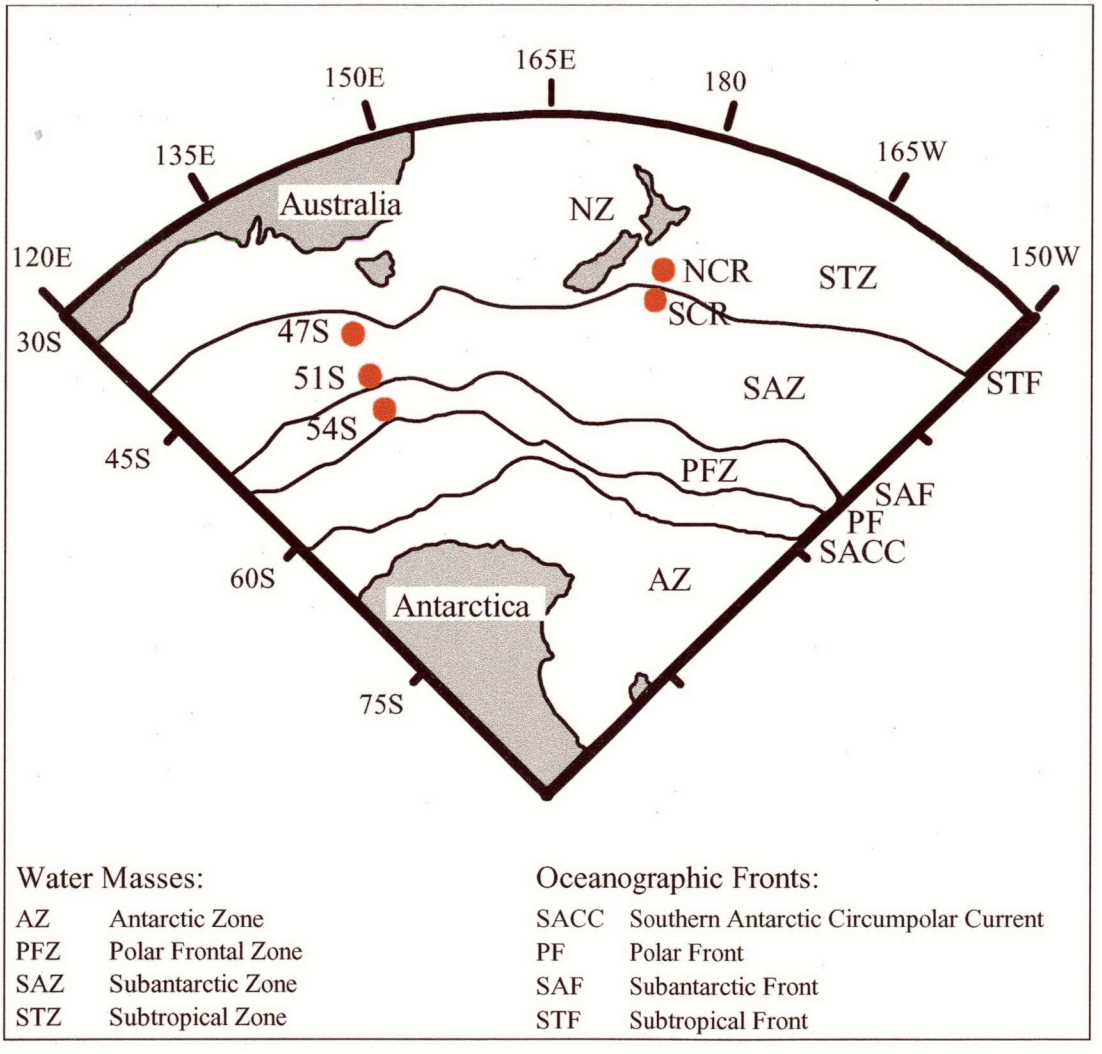

Figure 1: Southern Ocean water mass and frontal locations and their relation to the sediment trap sites (•) included in this study. SCR is the trap moored at South Chatham Rise and NCR the trap at North Chatham Rise. Figure from L. Armand pers. comm., with frontal locations based on Orsi et al. (1995).

The Subtropical water mass originates from the central Pacific Ocean and is warm and saline, with relatively low nutrient concentrations (Heath, 1985). East of New Zealand, summer temperatures and salinity in the STZ are greater than 15°C and 34.7 respectively. The sharp reduction in surface water temperatures across the Subtropical Front means that the STZ marks the southern limit of many warm-water species (Deacon, 1982).

The SAZ extends between ~ 40° and 50°S and is bounded by the Subtropical Front (STF) to the north and the Subantarctic Front (SAF) to the south (Popp et al., 1999). East of New Zealand, Subantarctic Water has surface salinities of <34.4 and temperature <11°C (Burling, 1961). Nutrients in the SAZ region are intermediate between those of the STZ and the PFZ (Rintoul and Trull, 2001). Nutrients are resupplied to the surface SAZ waters via deep winter mixing (> 400 m) and northward spreading of near-surface waters across the SAF (Rintoul and Trull, 2001) (Figure 2). The higher nutrient concentrations in the SAZ region are associated with enhanced biological production compared to subtropical waters (Banse, 1996). The marine biota in this zone is dominated by calcareous organisms including coccolithophorids and planktonic foraminifera. Regional surface sediments are characteristically calcareous oozes, recording a high flux of calcareous organisms from the surface waters (Deacon, 1982; Popp et al., 1999).

Within the Polar Frontal Zone, Antarctic Surface Waters, with temperature <5°C and salinity <34.0 sink beneath the Subantarctic Surface Waters to form Antarctic Intermediate Water (Figure 2) (Tchernia, 1980). Biological productivity in this zone is composed dominantly of siliceous organisms and there is a sharp increase in the concentration of silicate and other nutrients southward across the front.

The Antarctic Zone (AZ) ranges between the Polar Front (PF) and the Antarctic Continental Shelf (Orsi et al., 1995). The properties of Antarctic Surface Water (AASW) are uniform throughout this zone and the water mass is underlain by relatively warm and saline Circumpolar Deep Water (CDW) (Figure 2).

The Southern Ocean is characterised as a high-nutrient, low-chlorophyll (HNLC) oceanic environment with HNLC conditions intensifying to the south (Popp et al., 1999). Ocean colour data suggest that these HNLC conditions persist throughout the year (Comiso et al., 1993), resulting in overall low productivity in the Southern Ocean.

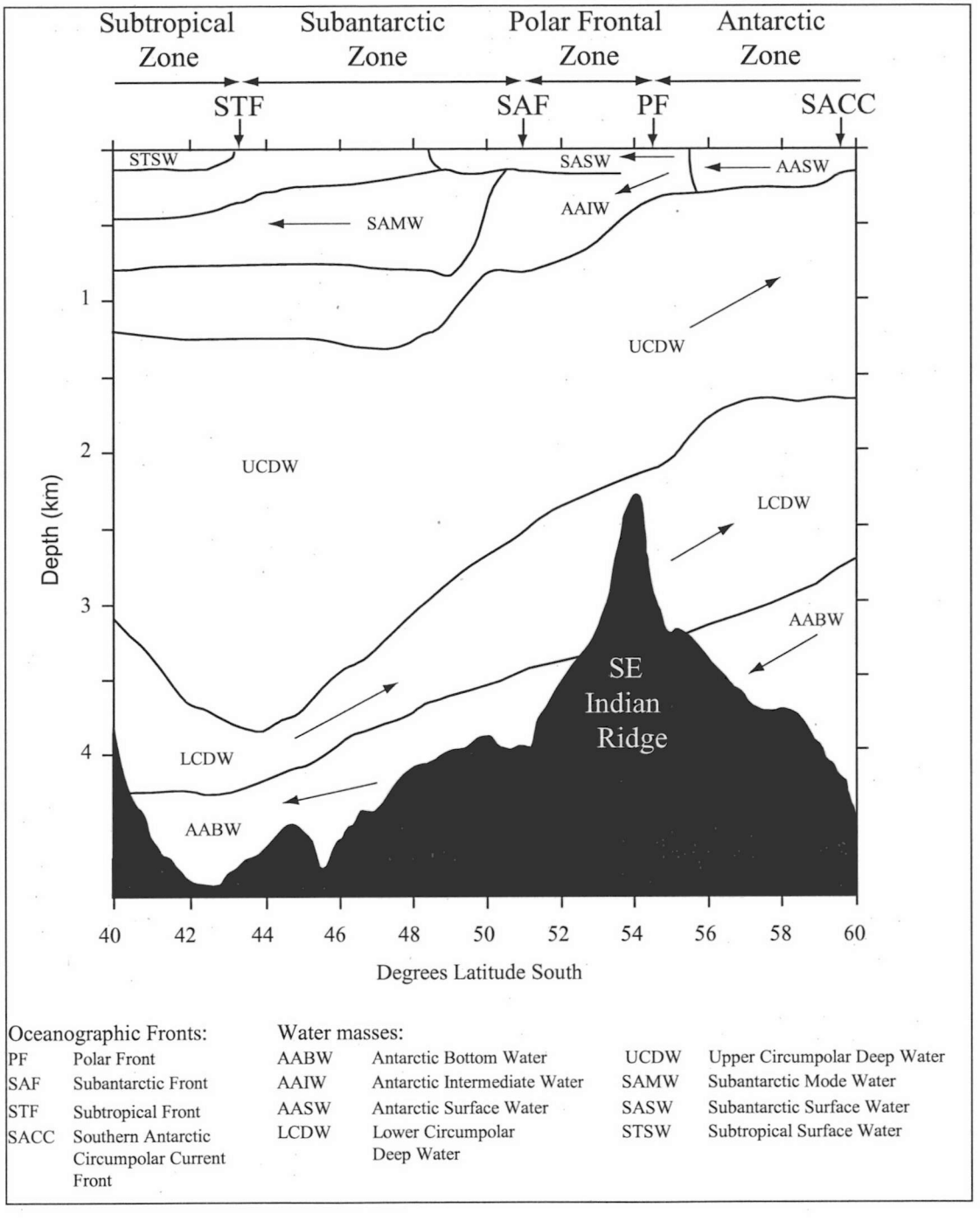

Figure 2: Circulation and deep water masses along ~141°E in the southeast Indian Ocean. Figure adapted from Armand (1997, Figure 1.6) and Trull et al. (2001, Figure 2) with data compiled from Gordon and Molinelli (1986), Braatz and Corliss (1984) and Rintoul and Trull (2001).

1.2.2 Oceanic Fronts

The water masses of the Southern Ocean are bounded on their northern and southern edge by hydrographic fronts which form in response to surface wind fields. From north to south these fronts are: the Subtropical Front, Subantarctic Front and the Polar Front (Figure 1).

The Subtropical Front (STF) is defined by the 11°C isotherm at 150 m (Rintoul et al., 1997). Temperatures across the front at a depth of 100 m range from 10° to 12°C and salinity from 34.6 to 35.0 (Orsi et al., 1995). South of Tasmania the STF is generally located in the trough between the continental shelf and the South Tasman Rise (Rintoul et al., 1997), and east of New Zealand the STF is situated along the crest of Chatham Rise. The STF is bathymetrically trapped along the Chatham Rise (Uddstrom and Oien, 1999), however, in other regions variations in the wind stress fields may cause large shifts in the meridional position of the front (Tomczak and Godfrey, 1994). The frontal band also includes meanders, convolutions and eddies of various sizes which enhance water mass mixing across the front.

The existence of the Subantarctic Front (SAF) south of Australia was first noted by Burling (1961) as a surface-temperature discontinuity at the northern edge of the Polar Frontal Zone. The SAF is marked by the region of largest horizontal temperature gradients at a depth of 300 m (3-8°C) (Rintoul et al., 1997). Additionally, Rintoul et al. (1997) observed a sharp increase in temperature to a depth of 800 m across the front, with steeper gradients on the northern side. The front is maintained by the eastward flow of the Antarctic Circumpolar Current (ACC). The maximum eastward flow marks the core of the SAF, with a mean position south of Tasmania at 51.5°S (Rintoul and Trull, 2001).

The Polar Front (PF) is best defined by the northern-most extent of cold subsurface waters, marked by the 2°C isotherm at ~200 m depth in summer and at the surface in winter (Belkin and Gordon, 1996). The temperature minimum below the surface is maintained by continued sinking of cold Antarctic Surface Water beneath the warmer Subantarctic Surface Water (Deacon, 1982) (Figure 2). The winter position of the PF south of Australia is 54°S (Rintoul and Church, 1993).

The Southern Antarctic Circumpolar Current (SACC) front is situated to the south of the PF in the midst of the AZ. This front was first described as a circumpolar deep-reaching

feature by Orsi et al. (1995). In contrast to the other Southern Ocean fronts, the SACC front does not separate two distinct water masses. The surface water properties of the AZ are generally uniform between the PF and the Antarctic Continental Shelf. The southern ACC front is characterised by steep thermal gradients and a temperature minimum layer at depth caused by a shoaling of Upper Circumpolar Deep Water to near 500 m (Figure 2).

Each of the hydrographic fronts are associated with enhanced biological productivity. SeaWIFS (Sea-viewing Wide Field-of-View Sensor) (Moore et al., 1999) and CZCS (Coastal Zone Color Scanner) (Comiso et al., 1993) data both indicate higher pigment concentrations associated with each of the frontal bands. The topographic highs of the South Tasman Rise and the Chatham Rise are also associated with higher nutrient inputs and therefore higher chlorophyll concentrations (Moore et al., 2000). Surface pigment concentrations obtained from CZCS indicate high concentrations throughout the year at the Chatham Rise while the South Tasman Rise has highest values during spring and summer (Comiso et al., 1993).

1.3 THE ROLE OF THE SOUTHERN OCEAN IN CLIMATE CHANGE

In recent years palaeoceanographers have shown increasing interest in the Southern Ocean as a driver of global climate change. The Southern Ocean forms a link between each of the major ocean basins through the circulation of deep waters. The Southern Ocean is also intricately linked with the atmosphere by exchange during the formation of deep waters and during upwelling along continental margins. Changes in the Southern Ocean should therefore be transmitted rapidly throughout the globe (over time scales of ~2000 years) via deep-water circulation and exchange with the atmosphere. Marine sediments from this region should also record any perturbations of the global climate system.

The Southern Ocean is unique in the global oceans because biological productivity is persistently low, despite high concentrations of the major inorganic nutrients (nitrate and phosphate). The Southern Ocean is therefore a prime candidate for studies proposing the mediation of glacial CO_2 draw down by enhanced biological uptake of carbon, the so-called biological pump (Broecker and Peng, 1982). Production of organic matter involves the incorporation of phosphate, nitrate and carbon in fixed proportions, known as Redfield ratios, where C:N:P $\cong$ 106:16:1 (Redfield et al., 1963). More recent estimates based on analysis along isopycnal surfaces have slightly adjusted these values: 105:15:1

(Broecker and Peng, 1982); 103:16:1 (Takahashi et al., 1985). Full utilisation of nutrients in the Southern Ocean would greatly enhance the uptake of dissolved carbon, and thereby draw atmospheric CO_2 into the oceans. For the last glacial period, calculations of atmospheric CO_2 made on the basis of complete Redfieldian nutrient utilisation in the Southern Ocean, and after allowing for appropriate changes in salinity and temperature, suggest that the partial pressure of carbon dioxide (pCO_2) may have been ~80 ppm lower at this time (Knox and McElroy, 1984). This estimate is in good agreement with polar ice core records which also indicate a reduction in atmospheric CO_2 by ~80 ppm during the last glaciation (Barnola et al., 1987). It is therefore suggested, that enhanced marine productivity may have played a significant role in the glacial draw down of atmospheric CO_2. As a result, research in recent years has focussed on determining changes in Southern Ocean biological production.

The efficiency of the biological pump depends on the balance between upwelling of nutrients and CO_2 and the sinking of particulate biogenic matter into the deep sea. The pump's efficiency will be enhanced in regions with little vertical mixing, since this will minimise the resupply of inorganic nutrients and CO_2 to the surface from intermediate waters (eg. Francois et al., 1997). To determine the efficiency of the biological pump in drawing down CO_2 we need to combine tracers of nutrient utilisation with those which record the rate of biogenic flux from surface waters.

In this study, I will focus on one of these nutrient tracers in particular, the carbon isotopic ratio ($\delta^{13}C$) of planktonic foraminifera. I will attempt to establish the sensitivity of foraminiferal $\delta^{13}C$ records to changes in biological production. Foraminiferal $\delta^{13}C$ records are often compared to other nutrient and biological flux tracers to better constrain interpretations of past biological production. Each of these tracers depend on different assumptions and often lead to different conclusions about past changes in Southern Ocean biological productivity. In the following section, I provide a brief summary of the main nutrient and export production tracers to set the context for the later presentation of the foraminiferal $\delta^{13}C$ records obtained from this study.

1.4 CHEMICAL TRACERS FOR PALAEOCEANOGRAPHIC RECONSTRUCTIONS

1.4.1 Tracers of export production

Foraminifera are just one of the many components of the flux of biogenic material to the sea floor, but they also provide a record of total biological production in their shell

chemistry. In this study I establish the relationships between foraminiferal production and other marine organisms, and test the influence of biological productivity on the foraminiferal $\delta^{13}C$ records. The components and volume of biological production has a significant impact on marine chemistry, as illustrated in the following section.

Export production is defined as the flux of biogenic detritus that escapes remineralisation in the euphotic zone and sinks to the deep sea (Kumar et al., 1995). Various tracers are applied to measure this organic flux, including the accumulation of calcium carbonate ($CaCO_3$), opal, organic carbon and biogenic barite, and radionuclide proxies such as protactinium-231 and thorium-230 ratios ($^{231}Pa/^{230}Th$) and beryllium-10 and thorium-230 ratios ($^{10}Be/^{230}Th$). Authigenic uranium (U_A) also provides a record of sediment accumulation.

Carbonate accumulation rates record the balance between $CaCO_3$ production, non-carbonate flux, and carbonate dissolution (Howard and Prell, 1994). The production of carbonate has a direct effect on the CO_2 content of surface waters. Precipitation of $CaCO_3$ removes carbonate ions (CO_3^{2-}) and thereby increases CO_2, as shown by the following equilibrium relationships:

$$CO_3^{2-} + H^+ \leftrightarrows HCO_3^-$$

$$Ca^{2+} + 2HCO_3 \leftrightarrows CaCO_3 \downarrow + H_2O + CO_2 \uparrow$$

Dissolution of $CaCO_3$, will release CO_3^{2-}, driving the equation towards the production of bicarbonate ions (HCO_3^-), through the uptake of CO_2. It is therefore important to determine relative changes in the production and dissolution of $CaCO_3$ during past climate intervals. Late Quaternary glacial sediments from the south Indian Ocean indicate a reduction in the $CaCO_3$ to organic carbon (C_{org}) ratio driven by a decrease in carbonate preservation and/or production (Howard and Prell, 1994). This effect would drive a decrease in CO_2 concentrations.

The flux of biogenic opal to the sediments represents diatom productivity, which is a major contributor to marine biological production. The effects of diatom production on the carbon cycle are twofold. Firstly, diatoms utilise the inorganic nutrients N, P and C in the production of organic matter, and therefore contribute to the flux of carbon from surface waters. Secondly, in waters where dissolved silicic acid (H_4SiO_4) and iron (Fe) are unlimiting, diatoms may out compete $CaCO_3$ producing organisms for the supply of

N and P, thereby reducing the rate of $CaCO_3$ production (Archer et al., 2000). The reduction in carbonate production will drive alkalinity higher and cause a further decrease in CO_2 concentrations. Diatom production may therefore be a very important constraint on biological CO_2 draw down. Opal burial during the last glacial was highest north of the PF, with a slight increase in the northern SAZ as well (Charles et al., 1991). Regions south of the PF, by contrast, reveal a decrease in opal burial compared to the Holocene. The integration of these patterns suggests that there was little glacial change in overall opal productivity (Charles et al., 1991; François et al., 1997). Recent studies, however, which apply ^{230}Th records to correct the flux for sediment focussing by currents, suggest that the total opal flux was up to twice the magnitude during the last glacial (Kumar et al., 1995). Such a large increase in opal flux would have a major impact on the carbon cycle.

Another recent proxy which was been developed to understand export production is biogenic barite. Measurements from sediment traps indicate a good correlation between the flux of biogenic barite and export production (François et al., 1995). Application to Southern Ocean surface sediments shows a clear relationship between the biogenic Ba rain rate and opal fluxes in the Atlantic and Indian Ocean sectors, once Ba has been corrected for dissolution (François et al., 1997). The greatest uncertainty in the biogenic Ba record is dissolution, which occurs in rapidly accumulating reducing sediments. In the paleo-record, biogenic Ba rain rates in cores north of the Polar Front do not record the increase in export production indicated by other proxies. The one exception is a core where the glacial sedimentation rate was low enough to allow sufficient preservation of Ba. The reliability of the biogenic Ba record therefore needs to be checked against the other proxies.

Measurement of the total organic carbon export can be obtained from radionuclide ratios of $^{231}Pa/^{230}Th$ and $^{10}Be/^{230}Th$. The distribution of ^{231}Pa, ^{230}Th and ^{10}Be is fairly uniform throughout the ocean, and these radionuclides are removed quantitatively from seawater by scavenging to particulate matter (Kumar et al., 1995). ^{231}Pa and ^{10}Be have longer residence times in the ocean than ^{230}Th, and therefore particulate $^{231}Pa/^{230}Th$ and $^{10}Be/^{230}Th$ increase with increasing particle flux. Both of these tracers indicate an increase in export production in the SAZ and a decrease in the AZ during glacial periods. This pattern is particularly notable from the $^{231}Pa/^{230}Th$ record.

Changes in sedimentary uranium also provide a record of particle flux to the sea floor. In the presence of oxygen, uranium remains in a relatively non-reactive hexavalent form (Kumar et al., 1995). When oxygen is limiting, this species enters an amorphous tetravalent phase. Sediments become anoxic when the accumulation of C_{org} exceeds the supply of molecular oxygen by diffusion from bottom waters. Anoxic sediments reveal a positive, though non-linear relationship, between C_{org} flux and the accumulation of authigenic uranium. Increases in authigenic uranium, and therefore of organic carbon flux, are observed in glacial-age sediments in the SAZ region, in agreement with increased production inferred from the radionuclide tracers (Kumar et al., 1995; Rosenthal et al., 1995). South of the Polar Front the glacial accumulation of authigenic U is quite variable, yet tends towards lower accumulation rates overall and therefore lower glacial productivity (Kumar et al., 1995; Rosenthal et al., 1995).

Overall, the export tracers produce a consistent pattern of change within the SAZ (see Table 1) with an increase in biological production inferred from all tracers except $CaCO_3$ burial. These changes imply a consistent decrease in CO_2 concentrations across the region. For the AZ, a more variable pattern emerges (Table 1). The results from the Be/Th ratios and authigenic U are inconclusive for the region as a whole, while reductions in biogenic opal flux, calcite burial and Pa/Th imply decreased productivity and therefore increased CO_2 concentrations. The high production in the SAZ region, however, may have caused an overall uptake of atmospheric CO_2. To help to further determine the total changes in production, tracers of nutrient utilisation need to be employed.

1.4.2 Nutrient tracers

Various tracers have been used to determine changes in surface nutrients. These include the cadmium to calcite ratios (Cd/Ca) in planktonic foraminifera, the carbon isotopic ($\delta^{13}C$) composition of calcite, the $\delta^{13}C$ of organic matter, and the nitrogen isotope ratios ($\delta^{15}N$) in organic matter. These nutrient tracers provide a range of interpretations of last glacial nutrient utilisation, so it is important to establish how these tracers record changes in the marine environment. One of the key motivations for this study is to determine whether the $\delta^{13}C$ record from foraminifera provides an accurate tracer of marine biological production. It is also important to consider how the foraminiferal $\delta^{13}C$ record compares to other nutrient proxies.

The cadmium to calcite ratio from planktonic foraminifera is used to determine changes in the utilisation of P in the ocean. The Cd concentration in seawater is well correlated with nutrient distributions. Cd and P exhibit a consistent linear covariation in the oceans (Boyle et al., 1976). Cd and P are removed from surface waters by incorporation into organic matter, which then sinks and decomposes, releasing nutrients and Cd back into the water. The deep ocean circulation is also superimposed on this biological pattern, creating distinct signatures between water masses. Cd is incorporated into foraminiferal calcite, providing a record of Cd concentration, and therefore of P, through the ratio of Cd to Ca. Interpretation of Cd/Ca ratios in glacial age foraminifera indicates that there is no net change in nutrient utilisation between glacial and interglacial intervals in the SAZ (Elderfield and Rickaby, 2000; Keigwin and Boyle, 1989), while an increase in utilisation is observed in the AZ (Elderfield and Rickaby, 2000). This trend is opposite to that inferred from the radionuclide tracers in the AZ (see summary in Table 1).

$\delta^{13}C_{calcite}$ is also used as a nutrient tracer. The ^{13}C content is expressed in δ(‰), which is defined as follows:

$$\delta = 1000\ (^{13}C/^{12}C \text{ sample}) / (^{13}C/^{12}C \text{ standard}) - 1$$

During biological production, organisms preferentially take up the ^{12}C isotope from the dissolved carbon in surface waters. This leaves the surface water dissolved organic carbon relatively enriched in the ^{13}C isotope (ie. with a higher $\delta^{13}C$). Foraminifera produce their calcite shell from the dissolved organic carbon in the water, so the $\delta^{13}C$ of their shell should reflect changes in biological production. Increased glacial biological production should be recorded as an increase in $\delta^{13}C_{calcite}$. However, glacial aged planktonic foraminifera in Southern Ocean sediments north and south of the Polar Front indicate a $\delta^{13}C$ depletion of between 0.6 and 0.9‰ compared to the Holocene (Charles and Fairbanks, 1990). This implies that there was a decrease in biological production, and therefore of CO_2 uptake during the glacial period. This is contrary to the biological pump model. Charles and Fairbanks (1990) suggest two alternative explanations. The first is that the $\delta^{13}C$ depletion is caused by an increased rate of upwelling, which would resupply nutrients and ^{12}C to the surface waters, and the second is that the upwelled source waters (namely Circumpolar Deep Water) had higher nutrient concentrations during the glacial period. Before these hypotheses can be considered with any certainty it is important through this study to determine how well modern Southern Ocean foraminiferal $\delta^{13}C$ records reflect changes in the $\delta^{13}C$ of seawater.

Another mechanism for determining changes in CO_2 is from the $\delta^{13}C$ of organic matter ($\delta^{13}C_{org}$). Phytoplankton incorporate $\delta^{13}C$ in their organic matter during photosynthesis. The $\delta^{13}C_{org}$ values are offset from that of the dissolved inorganic carbon (DIC), with the offset determined by the concentration of dissolved CO_2 (referred to as $[CO_2]$) in surface waters. High CO_2 levels in surface water are associated with a larger fractionation (Rau et al., 1989). Modern calibrations of the photosynthetic fractionation versus $[CO_2]$ in Southern Ocean surface waters indicate a significant correlation between these two variables, with changes in $[CO_2]$ accounting for ~56% of variations in the $\delta^{13}C$ fractionation (Rosenthal et al., 2000). Measurement of the $\delta^{13}C_{org}$ fractionation from the sediments provides the possibility for reconstructing changes in $[CO_2]$ and therefore pCO_2. However, $\delta^{13}C$ fractionations are also driven by the species composition, diagenesis, cellular growth rate and the cell geometry, complicating $[CO_2]$ reconstructions using this proxy (Bidigare et al., 1999; François et al., 1993; Popp et al., 1998). Estimates of carbon isotopic fractionation from sediments in the SAZ suggest a glacial decrease in this fractionation of ~1.9‰, while AZ sediments indicate an increase of 0.6-1.3‰ (Rosenthal et al., 2000). These trends suggest a decrease in $[CO_2]$ in SAZ surface waters, while in the AZ $[CO_2]$ may have been higher, causing this region to be a source of CO_2 to the atmosphere (Rosenthal et al., 2000).

Analysis of compound-specific $\delta^{13}C$ reduces some of the uncertainties associated with the isotopic analysis of bulk organic samples. By targeting particular compounds for analysis, the source (eg. marine vs terrestrial) and composition (eg. phytoplankton vs zooplankton) of the material can be known. Using molecules or biomarkers which are unique to a particular class of organisms, such as C_{37} alkenones (Volkman et al., 1980), reduces the range of metabolic pathways and cell geometries affecting the carbon isotopic composition. Analysis of the $\delta^{13}C$ composition of sterols is also useful as this eliminates changes in $\delta^{13}C$ caused by remineralisation and diagenesis, and the influence of heterotrophic inputs can be removed by analysis of phytoplankton-derived sterols (O'Leary et al., 2001). Comparative analysis of $\delta^{13}C_{org}$ and $\delta^{13}C_{sterol}$ within the euphotic zone of the Southern Ocean allowed the factors influencing their relationship to $[CO_2]$ to be assessed. The similarity in trend between $\delta^{13}C_{org}$ and $\delta^{13}C_{sterol}$ indicated that factors such as remineralisation, heterotrophic input and biodegradation do not significantly affect changes in $\delta^{13}C_{org}$ with depth. The isotopic composition of organic matter was most strongly associated with changes in growth rate, which in turn was related to water column structure. Sterol isotopes therefore have potential to be used as a proxy for mixed layer depth.

The $\delta^{15}N$ of organic matter provides a record of the utilisation of N by phytoplankton since phytoplankton discriminate against ^{15}N during nitrate uptake (François et al., 1997). SAZ records of $\delta^{15}N$ in diatoms record a slight decrease in isotopic composition during the last glaciation, implying lower biological productivity, whereas regions south of the PF indicate an increase in $\delta^{15}N$ in glacial periods and therefore greater nitrate utilisation (François et al., 1997; Sigman et al., 1999). The increase in nitrate utilisation south of the PF is attributed to increased surface water stratification which would prevent the resupply of nutrients to surface waters. This interpretation is favoured by the tracers of export flux which suggest that glacial export production decreased in this region.

A complex picture of glacial-interglacial change in biological production emerges from these proxies (Table 1). The foraminiferal $\delta^{13}C$ record is the only tracer which records a reduction in biological productivity in the SAZ (and hence an increase in pCO_2), while the Cd/Ca record indicates no change in this region. The Cd/Ca record in the AZ suggests an increase in biological production (and decreased pCO_2) which is in agreement with reduced $CaCO_3$ burial, but contrary to the other tracers in this region. Contradictions between these different proxies may reflect influences from factors such as changes in deep-water circulation and depth of mixing, or the differences may arise due to failure in the assumptions associated with each proxy. To address some of the discrepancies between the different data sources, this study aims to establish the reliability of the foraminiferal tracers. Sediment trap records from the Southern Ocean will be applied to test the utility of deriving nutrient records from the carbon isotopic composition of planktonic foraminifera.

	Subantarctic Zone		Antarctic Zone	
Proxies	Change to proxy	Implied ΔpCO_2	Change to proxy	Implied ΔpCO_2
Tracers of export production				
$CaCO_3$ burial (Howard and Prell, 1994)	Decreased	**Decreased**	Decreased	**Decreased**
Biogenic opal flux (Charles et al., 1991; Kumar et al., 1995)	Increased	**Decreased**	Decreased	Increased
Pa/Th (particle flux) (Kumar et al., 1995)	Increased	**Decreased**	Decreased	Increased
Be/Th (particle flux) (Kumar et al., 1995)	Increased	**Decreased**	Variable	**?**
Burial of authigenic uranium (particle flux) (Kumar et al., 1995; Rosenthal et al., 1995)	Increased	**Decreased**	Variable	Slightly increased?
Nutrient tracers				
Cd/Ca (nutrient utilisation) (Elderfield and Rickaby, 2000)	No change	**No change**	Increased	**Decreased**
$\delta^{13}C$ foraminifera (nutrient tracer) (Charles and Fairbanks, 1990)	Depletion	Increased	Depletion	Increased
$\delta^{13}C$ organic matter (concentration of $[CO_2]$) (Rosenthal et al., 2000)	Decreased	**Decreased**	Increased	Increased

Table 1: Tracers of nutrient utilisation and export production in Southern Ocean sediments during the last glaciation, and the implied change in the concentration of atmospheric CO_2 (ΔpCO_2). These proxies indicate a complex picture of changes in Southern Ocean nutrients and export, particularly south of the Polar Front, highlighting the need for further research to eliminate sources of uncertainty in these proxies. Note that the implied ΔpCO_2 is based only on the perceived forcing by the biological pump. Apparent contradictions between these proxies may reflect the influences of other factors such as changes in deep-water circulation and depth of mixing.

1.5 USE OF FORAMINIFERAL PROXIES TO RECONSTRUCT PAST CLIMATE CHANGE

Planktonic foraminifera provide information on past chemical and physical properties of surface waters. The abundances of different species of foraminifera can be related to sea-surface temperatures and the thermal stratification of surface waters. Past ocean chemistry can be reconstructed from isotopic and trace metal signatures contained within the calcium carbonate shells of planktonic foraminifera. The aim of this thesis is to test calibrations of these various faunal and chemical indices obtained from planktonic foraminifera against observed conditions at the time of production in several Southern Ocean environments. The primary chemical proxies used in this study are the oxygen ($\delta^{18}O$) and carbon ($\delta^{13}C$) isotopic composition. Each of these chemical tracers, as well as the faunal indices, are described in the following sections. I also include a brief discussion of temperature estimates obtained from foraminiferal magnesium/calcium ratios and alkenones since these proxies are often compared to foraminiferal $\delta^{18}O$ SST estimates. I will also discuss cadmium/calcite ratios obtained from planktonic foraminifera as this ratio is another important nutrient tracer from foraminifera.

1.5.1 Environmental controls on foraminiferal populations

A key outcome of this sediment trap study is a record of seasonal production patterns for different species of planktonic foraminifera. The study marks the first results of this kind from Subtropical to Subantarctic environments. Analysis of seasonality in foraminiferal fluxes provides the opportunity to explore the environmental preferences of different species.

Previous studies suggest that species abundances may vary according to food availability, light intensity, temperature and thermal stratification of the water column (Bé and Hutson, 1977; Fairbanks and Wiebe, 1980; Ortiz et al., 1995; Thunell and Reynolds, 1984). Ortiz et al. (1995) suggest that in the north Pacific (42°N) fluxes of non-symbiont bearing species such as *Globigerina bulloides*, *Neogloboquadrina pachyderma* (d.) and *Globigerina quinqueloba* are related to food availability. A similar relationship for *G. bulloides* is found in the subpolar North Pacific (Station PAPA, 50°N) (Reynolds and Thunell, 1985). Abundances of *N. pachyderma* (s.) (eg. Fairbanks and Wiebe, 1980; Fairbanks et al., 1982; Kohfeld et al., 1996) and several tropical species (Ravelo and Fairbanks, 1992) have been associated with the depth of the chlorophyll maximum zone in plankton tow studies, suggesting that the habitat preferences for these species is also influenced by food availability. Species which

harbour photosynthetic symbionts, such as *Neogloboquadrina dutertrei* and *Orbulina universa* are more strongly influenced by light intensity (Hemleben et al., 1989; Ortiz et al., 1995). These species are therefore restricted to the upper water column and may be more susceptible to changes in SST.

Species fluxes may also be associated with thermal stratification of the water column. Fluxes of *N. pachyderma* (d.) (Thunell and Reynolds, 1984) and *N. dutertrei* (Kincaid et al., 2000) have been observed to increase during periods of intense thermal stratification, while fluxes of *G. quinqueloba* and *N. pachyderma* (s.) have been associated with intervals of weak thermal stratification (Reynolds and Thunell, 1985; Sautter and Thunell, 1989; Thunell and Reynolds, 1984). The wide geographic distribution of *G. bulloides* from subpolar to tropical regions suggests that the distribution and abundance of this species is not strongly controlled by SST, however, high fluxes of this species at Station PAPA are coincident with increasing thermal stratification (Sautter and Thunell, 1989).

Understanding the ecological preferences of different species is of key importance to our interpretation of species abundances in sedimentary records. There is little documentation of the ecology of foraminifera in the Southern Ocean, so this study will be significant for determining ecological associations for species in the study region.

1.5.2 Sea-surface temperature estimates from foraminiferal assemblages

Estimates of past sea-surface temperature (SST) are useful in the reconstruction of past ocean circulation since different water masses are commonly delineated by temperature. Strong associations have been observed between foraminiferal species and specific temperature regimes (eg. Bé and Hutson, 1977; Reynolds and Thunell, 1985; Bijma et al., 1990; Ortiz and Mix, 1992; Pflaumann et al., 1996; King and Howard, 2001). Other environmental factors may also influence species distributions, however, temperature may be the strongest control on species distributions at the limit of their thermal tolerance (Ortiz et al., 1995). The relationship between species distributions and SST makes planktonic foraminifera an important tool for establishing past SST change. In this study, fluxes of planktonic foraminifera collected in sediment traps provide a test of faunal SST calibrations which are commonly applied to down-core studies.

The Modern Analog Technique is one of the most successful techniques for estimating SSTs from foraminiferal assemblages (Ortiz and Mix, 1997; Barrows et al., 2000) and is

applied to the sediment trap samples in this study. Calibrations between foraminiferal assemblages from 13 Pacific and Atlantic sediment traps and seasonal SSTs indicate that the Modern Analog Technique (MAT) accurately estimates mean annual SSTs to within a few degrees (Ortiz and Mix, 1997). Summer and winter SSTs are commonly estimated from foraminiferal assemblages, yet sediment trap studies have shown that the flux of species to the sea floor is highly seasonal (Thunell and Honjo, 1987; Deuser and Ross, 1989; Sautter and Thunell, 1989; Ortiz and Mix, 1992; Guptha et al., 1997). The sedimentary record therefore represents an integration of fluxes occurring during different seasons. It is important to test the reliability of MAT estimates in a range of environments with different seasonality in foraminiferal fluxes to determine the effect of seasonal fluxes on the estimation of the annual SST range. The present study encompasses a range of locations, from subtropical to polar frontal environments, providing the opportunity to test the MAT in several settings which are characterised by different seasonal flux patterns (King and Howard, 2001; King and Howard, 2003).

1.5.3 Chemical tracers for palaeo-reconstructions

Foraminiferal $\delta^{18}O$

The $\delta^{18}O$ of foraminiferal calcite is a key tool for determining past changes in temperature and salinity in down core sedimentary records. However, discrepancies between isotopic records and other temperature and salinity proxies, and the large variations in isotopic composition between species, highlights the need for studies such as this one which test calibrations of the foraminiferal records against observations. In this section I provide an overview of the oxygen isotope record and sources of uncertainty in the foraminiferal record.

The $\delta^{18}O$ of surface waters can generally be linearly related to surface salinity (Craig and Gordon, 1965; Charles and Fairbanks, 1990). Higher salinity water has higher $\delta^{18}O$ content due to isotopic fractionation during condensation, while precipitation causes salinity and $\delta^{18}O$ to decrease. There are discernible horizontal gradients in the oxygen isotopic content of surface waters in the modern ocean, reflecting changes in salinity, although it should be acknowledged that this fit is not perfect. The standard error in salinity for known $\delta^{18}O$ of water is 0.4 (Schmidt, 1999). At a regional scale there are large variations in the $\delta^{18}O$ – salinity relationship, and the slope of the relationship also varies over seasonal scales (eg. due to changes in freshwater input) and most likely over glacial-interglacial cycles. These are important constraints on the $\delta^{18}O$ – salinity relationship.

Foraminifera incorporate the oxygen isotopic composition of the seawater in a relationship determined by temperature (Epstein et al., 1953). The $\delta^{18}O$ of calcite therefore provides a record of changes in whole ocean chemistry as well as variations in ocean temperature (Charles and Fairbanks, 1990). Since different water masses are characterised by different isotopic signatures, the isotopic composition of foraminiferal calcite also provides the possibility to trace past variations in ocean circulation and frontal movement (eg. Charles and Fairbanks, 1990; Johannessen et al, 1994). However, the interpretation of past salinity and temperature variations from foraminiferal records is complicated by several factors.

The calibration between $\delta^{18}O$ and temperature varies for different species (Bemis et al., 1998) and in different environments (Bemis et al., 2002). Several biological factors influence the equilibration between the isotopic composition of foraminiferal calcite and seawater. These factors include the carbonate ion concentration of seawater (Russel and Spero, 2000; Spero et al., 1997); photosynthetic activity of algal symbionts (Spero, 1992; Spero and Lea, 1993); genetic variation (Huber et al., 1997; Darling et al., 2000; Stewart et al., 2001; Kucera and Darling, 2002; Bauch et al., 2003); and the foraminiferal shell size (Curry and Matthews, 1981; Donner and Wefer, 1994; Oppo and Fairbanks, 1989; Spero and Lea, 1996). Laboratory experiments indicate that increases in the carbonate ion concentration of seawater ($[CO_3^{2-}]$) cause a decrease in the $\delta^{18}O$ values recorded by each species (Spero et al., 1997). Changes in $[CO_3^{2-}]$ occur latitudinally, and were significantly different during past glacial periods so may have a significant effect on isotopic variability. Size variations are also an important consideration since the isotopic composition of individual species can increase by up to 1‰ as a function of increasing size (Curry and Matthews, 1981). Consistent and narrow size ranges should therefore be used for isotopic studies.

Laboratory experiments suggest that foraminiferal species which possess photosynthetic algae record disequilibrium $\delta^{18}O$ values (Spero, 1992; Spero and Lea, 1993). High light and low light experiments with *Orbulina universa* revealed greater disequilibrium under high light, a trend attributed to enhanced calcification rates due to photosynthesis of algal symbionts (Spero, 1992). Disequilibrium is also observed for the symbiont-bearing species *Globigerinoides sacculifer* (Spero and Lea, 1993). The species analysed in this study are not known to contain algal symbionts.

Another source of uncertainty is genetic variation within a morphospecies. Molecular analysis of *N. pachyderma* in the North Atlantic has revealed that the genetic distinction between the left and right coiling varieties varies with latitude, and the distribution of these different genotypes is associated with changes in $\delta^{18}O$ composition (Bauch et al., 2003). Geotypic variation within Arctic and Antarctic populations is also observed for *G. quinqueloba* and *G. bulloides* (Darling et al., 2000). The genetic variation can not be determined from the samples in this study, so this effect is unknown.

Differences in isotopic composition between species may also reflect the thermal tolerance of each species as reflected in their seasonal production patterns and habitat depth preferences (Curry et al., 1983; Deuser and Ross, 1989; Fairbanks et al., 1982; Kohfeld et al., 1996; Sautter and Thunell, 1991; Williams et al., 1981). Since the isotopic composition of the water column varies seasonally and with depth (Figure 3), species will imprint a unique isotopic signature on the sediments depending on their seasonal and depth preferences. For example, *N. pachyderma* (s.) collected at various depths in Southern Ocean plankton tows exhibits an increase in $\delta^{18}O$ of ~1.5‰ between depths of 50 and 200 m, with calcification concentrated towards the depth of the thermocline (Kohfeld et al., 1996). The habitat depth for *N. pachyderma* (s.) varies in different settings. Studies in the Arctic ocean indicate that the highest concentrations of this species occurs within the upper 50 m, whereas more southerly sites record highest concentrations at depths of between 100 and 200 m. (Bauch et al., 1997).

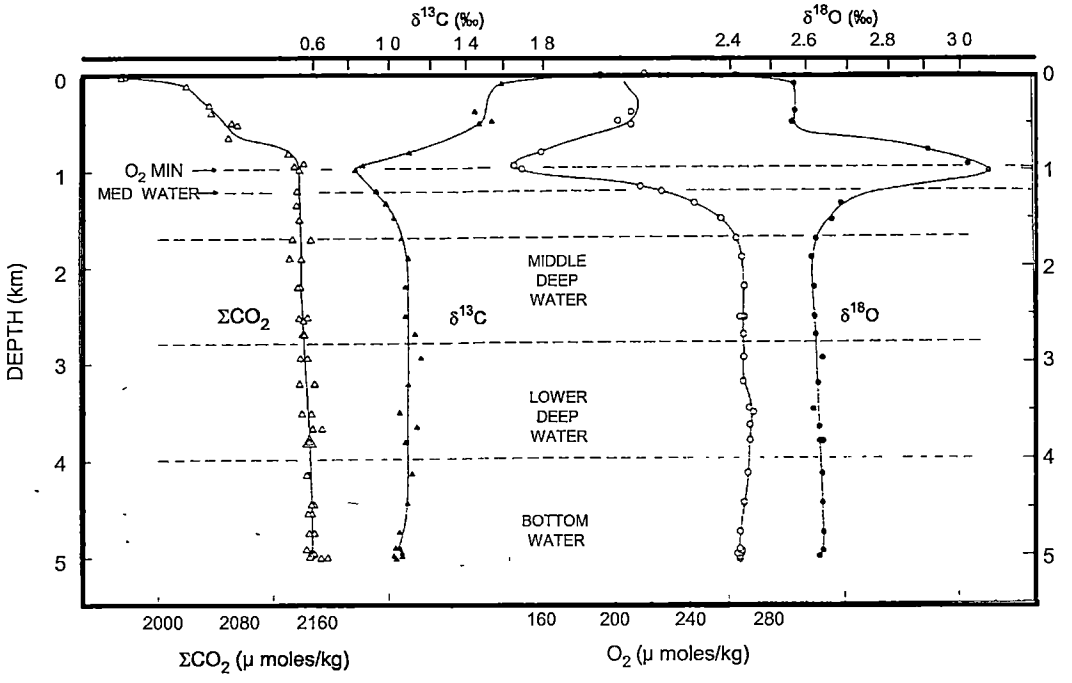

Figure 3: North Atlantic station (35°45'N, 68°00'W), Geosecs II vertical profile of ΣCO_2, $\delta^{13}C$, dissolved O_2 and $\delta^{18}O$ of sea water (Kroopnick et al., 1972). Strong vertical gradients are observed within the upper 2000 m for each of these parameters. The carbon and oxygen isotopic composition recorded in foraminiferal calcite will therefore vary according to their habitat depth.

Temperature estimates derived from a species chemical composition are based around a very different set of criteria to temperature estimates obtained from faunal assemblages. Faunal SST estimates are based on the assumption that the fauna can be closely tied to specific temperatures. Temperature estimates derived from chemical tracers, however, will be most reliable when obtained from species with a broad thermal tolerance. According to the model of Mix (1987) (Figure 4a), the isotopic temperature recorded by a species depends on the overlap between its temperature preference and the temperature range at the site. For a species with a narrow temperature tolerance, the recorded temperature will vary widely from the mean surface temperature above or below the species optimal temperature (Figure 4b). The species will adjust its season or depth of production to match their optimal temperature range. A species with a broad thermal tolerance, by contrast, will record temperatures across a wide range of temperatures.

Adjustments in the habitat depth or season of production for a species through time will mask changes in $\delta^{18}O$ in climate records. Discrepancies between faunal and isotopic sea-surface temperature constructions from Southern Ocean sediments during the last

glaciation, for instance, may reflect an adjustment in the species seasonal or depth preferences. In the Southern Indian Ocean, faunal SST estimates indicate a glacial-interglacial difference of 4 - 6°C, while oxygen isotopic measurements from *Globigerina bulloides* record a shift in oxygen isotopic composition of ~1.6 to 1.8 per mil, representing a maximum SST change of 2°C (Howard and Prell, 1992). The small glacial-interglacial contrast recorded isotopically by *G. bulloides* may reflect a shift in the primary production season or habitat depth of this species to remain within a narrow temperature range.

To successfully apply chemical proxies from individual species to interpretations of past temperature, it is vital to first determine the thermal tolerance ranges of different species and their consistency in chemically recording temperature throughout a whole annual cycle. This sediment trap study provides a record of fluxes of different species of planktonic foraminifera on a continuous basis throughout the year, revealing their seasonal production patterns. Their depth habitats are determined based on their isotopic composition. These records therefore provide detailed information about the ecological preferences of species in each of the study regions, which can then be applied to interpretations of $\delta^{18}O$ in down core sediments.

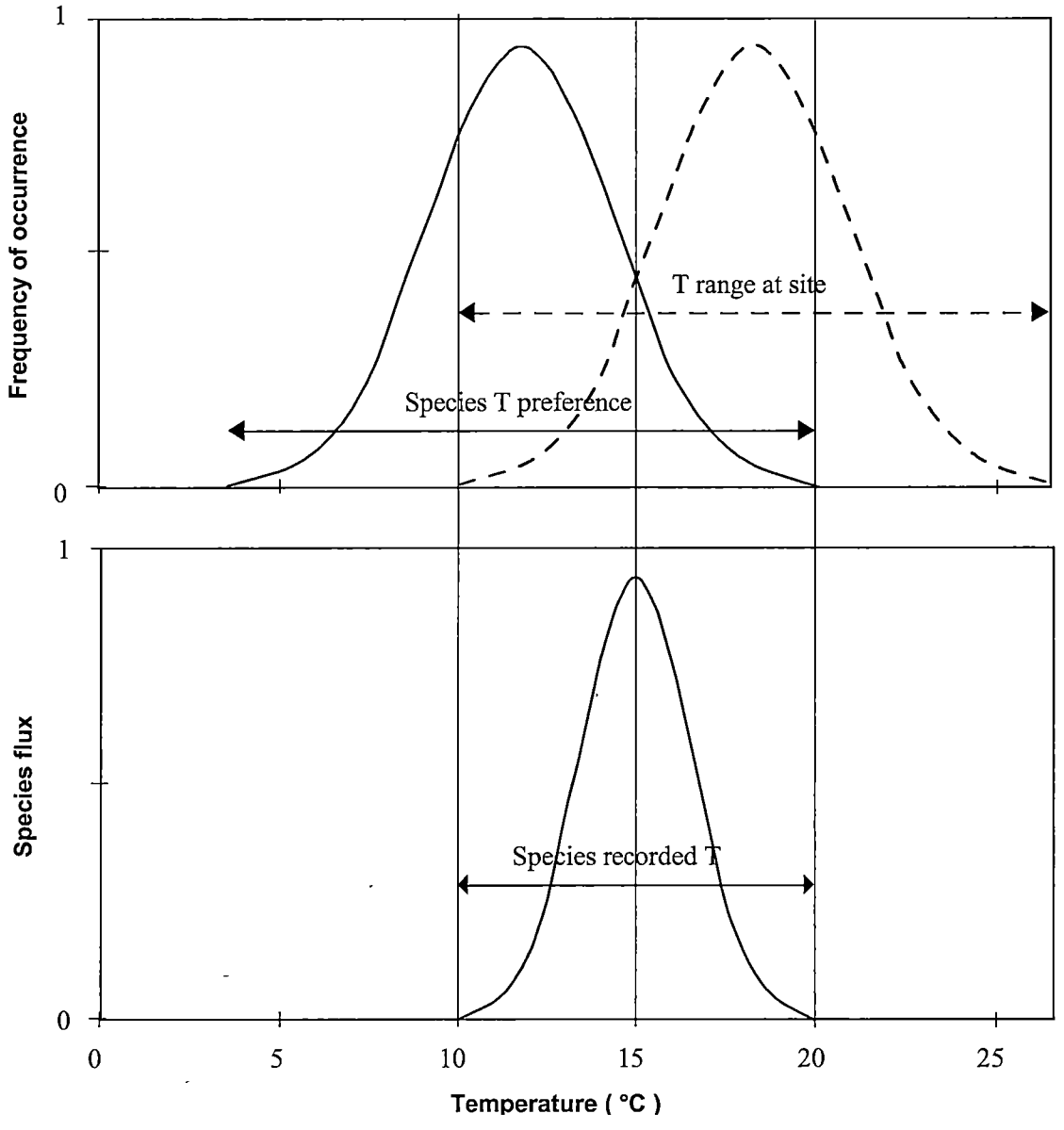

Figure 4a: According to the model of Mix (1987), the overlap between a species temperature preference and the temperature range observed at a site determines the isotopic temperature range which will be recorded by that species.

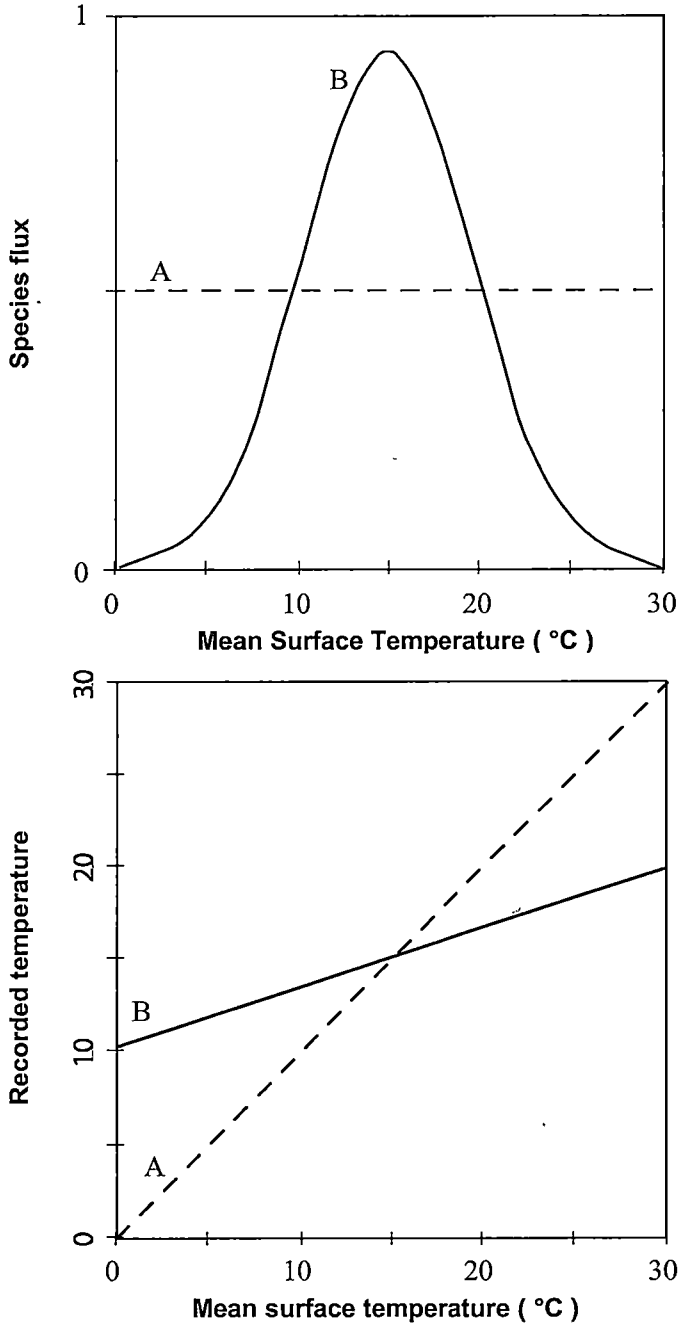

Figure 4b: If a species flux is not restricted by temperature (A), then it should record temperatures throughout the whole range. For species which have a flux that is determined by temperature (B), the recorded temperature will lose accuracy away from the optimal temperature range (From Mix, 1987).

Mg/Ca ratios in foraminifera

The magnesium/calcium ratios in foraminifera form a relatively new method for determining calcification temperature. The results of Mg/Ca analysis from the sediment traps were unfortunately not available in time for this thesis, but it is useful to consider the application of this technique given its increasing use in palaeoclimate studies.

Magnesium and calcium are both conservative tracers, so the Mg/Ca ratio in sea water is constant throughout the water column (Broecker and Peng, 1982). The incorporation of Mg into foraminiferal calcite, however, indicates a temperature dependency. This temperature dependency of Mg uptake offers the possibility to derive past temperatures from foraminiferal Mg/Ca.

Culture experiments with various species of planktonic foraminifera have shown that the ratio of Mg to Ca in their shell calcite co-varies with temperature (Lea et al., 1999; Mashiotta et al., 1999; Nürnberg et al., 1996). The relationship for *Globigerina bulloides* is particularly strong ($r^2 = 0.93$) and an increase in the Mg/Ca ratio of 10.2 per cent with each 1°C increase in temperature is observed (Figure 5) (Lea et al., 1999; Mashiotta et al., 1999). Application of this calibration with *G. bulloides* collected in plankton tow and core top sediments indicates a good consistency between estimated and observed SST. Estimates from plankton tow specimens in the Santa Barbara Channel USA range between 15.1°C and 18.6°C at an observed temperature of 17.5°C (Lea et al., 1999), and temperatures estimated from sub-Antarctic Indian Ocean core tops are within 1-3°C of mean annual SST (Lea et al., 1999; Mashiotta et al., 1999; Rickaby and Elderfield, 1999).

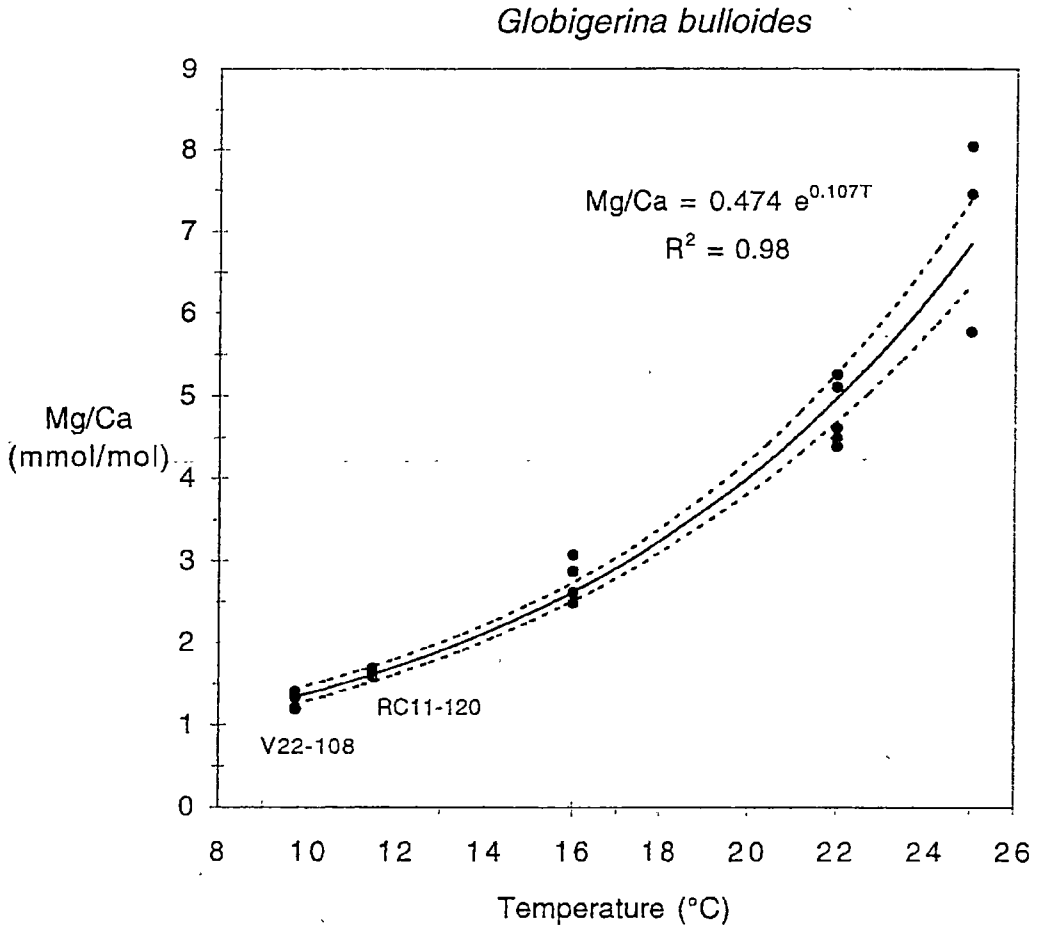

Figure 5: Mg-temperature calibration results from culturing experiments with live *Globigerina bulloides* and core top samples (indicated by the core name) (Mashiotta et al., 1999). Mg/Ca = 0.474exp(0.107 Temp).

There are other parameters apart from temperature, however, which also show a weak correlation to changes in Mg/Ca. At constant temperature in culture experiments, Mg/Ca decreases as pH or salinity increase (Lea et al., 1999). Genetic variation may also prove to cause differences in Mg/Ca incorporation, as for $\delta^{18}O$ (Bauch et al., 2003). In addition, the record of temperature derived from foraminiferal Mg/Ca ratios will reflect the temperature at the depth and during the season of production for a particular species. Core top analyses in the North Atlantic indicate that temperature estimates vary between species (Elderfield and Ganssen, 2000). *Neogloboquadrina pachyderma*, for instance, reflects temperatures at the surface, whereas *Globorotalia inflata* and *Globorotalia truncatulinoides* record temperatures equivalent to that at depths of 300-400 m. Seasonal effects on foraminiferal Mg/Ca are also observed between different latitudes. Analysis of

Mg/Ca from *G. bulloides* in mid-latitude core tops suggests that the SST recorded by this species is weighted towards early spring values, whereas at higher latitudes, the Mg/Ca records suggest that this species records late spring to early summer temperatures. Seasonal variations in production between different environments is a key focus of this study, and future Mg/Ca analyses from these samples have the potential to provide a calibration of this technique in settings with varying seasonal production patterns.

Alkenones as SST proxies

Temperature estimates derived from long chained unsaturated ketones, otherwise known as alkenones, provide a good comparison to foraminiferal temperature estimates. It is therefore important to consider their application, even though no alkenone results are currently available for the sediment trap material in this study.

Alkenones are biosynthesised by haptophyte algae, including coccolithophores (Volkman et al., 1980), and the proportions of various chains are adjusted by the organism depending on its growth temperature (Prahl et al., 1988; Prahl and Wakeham, 1987). Two unsaturation indexes, U^K_{37} and U^K_{37}', are used to track changes in the proportion of the C_{37} ketones. The U^K_{37}' index is defined as the ratio of the di- to tri-unsaturated long chain C_{37} methyl alkenones in a sample (Sikes et al., 1997):

$$U^K_{37}' = [C_{37:2}]/([C_{37.2}] + [C_{37.3}])$$

The unsaturation function U^K_{37} includes the $C_{37:4}$ alkenone:

$$U^K_{37} = [C_{37:2}] - [C_{37\,4}]/([C_{37\cdot2}] + [C_{37.3}] + [C_{37\,4}])$$

The U^K_{37}' index is more commonly used for temperature estimates since the $C_{37\,4}$ alkenone is often not detectable in sediments, and its exclusion improves the SST calibration at lower temperatures (Prahl et al., 1988).

SST calibrations have been derived from the U^K_{37}' values of coccolithophorids in culture experiments (Prahl et al., 1988) and applied in several studies in the Southern Ocean (Ikehara et al., 1997; Müller et al., 1998; Sikes et al., 1997). In general SST estimates from U^K_{37}' values exhibit a close correlation to observed SST. In Southern Ocean core tops, the correlation (r^2) between U^K_{37}' values and observed SST is 0.921 in summer and 0.913 in winter (Sikes et al., 1997). Southeast Atlantic sites exhibited an even closer correlation ($r^2 = 0.981$), with the best relationship for temperatures at 0 to 10 m depth

(Müller et al., 1998). Down-core analyses of U^{K}_{37}' suggest a glacial-interglacial temperature range of 4.4°C (Ikehara et al., 1997). This range is consistent with estimates based on foraminiferal faunas (4-6°C) in Southern Indian Ocean sediments (Howard and Prell, 1992).

There are still some uncertainties associated with the estimation of SSTs from alkenones. Culture studies indicate that the relationship between U^{K}_{37} and SST is variable for different species and strains of haptophyte algae (Conte et al., 1998; Volkman et al., 1995). This may cause inconsistent results if the species composition changes. The correlation between temperature and U^{K}_{37}' is also weakened at higher temperatures (17-26°C) (Goñi et al., 2001) and below ~6°C (Sikes et al., 1997). The limit at higher temperatures may reflect a physiological response of the haptophyte algae to higher temperatures (Conte et al., 1998), a change in species composition, changes in the habitat depth (within the euphotic zone) or a switch in the season of production (Goñi et al., 2001). Southern Ocean calibrations suggest that the lower temperature limit reflects the extent of variations in the unsaturation ratio of U^{K}_{37}'.

Foraminiferal $\delta^{13}C$

The $\delta^{13}C$ composition of foraminiferal calcite provides an important marine nutrient tracer. Foraminifera incorporate $\delta^{13}C$ into their shell calcite from the surrounding sea water, and the sea water composition generally reflects changes in biological productivity and therefore nutrient concentration. However, the factors which influence variations in the $\delta^{13}C$ of sea water are complex and need to be understood before we can establish the efficacy of $\delta^{13}C$ as a nutrient tracer. The foraminiferal $\delta^{13}C$ composition also varies apart from variations in the sea water $\delta^{13}C$ composition. Understanding the $\delta^{13}C$ record produced by planktonic foraminifera therefore forms an important part of this thesis.

The $\delta^{13}C$ of the total dissolved CO_2 ($\sum CO_2$) in surface waters varies as a function of photosynthesis, respiration, remineralisation of organic matter, and air-sea exchange (Gruber et al., 1999). During photosynthesis plants take up carbon from surface waters, preferentially removing ^{12}C relative to ^{13}C. This leaves dissolved inorganic carbon (DIC) in surface waters with relatively enriched $\delta^{13}C$, while marine organic matter has relatively depleted $\delta^{13}C$. The isotopic composition of marine organic matter in the Southern Ocean typically ranges between –20 and –30‰ (Popp et al., 1999). In areas of upwelling, the $\delta^{13}C$ of surface waters decreases due to the input of remineralised organic

matter. Biological productivity and upwelling should cause a consistently negative relationship between nutrient concentrations and $\delta^{13}C$ of seawater (Broecker and Maier-Reimer, 1992). The negative relationship between nutrients (PO_4) and $\delta^{13}C$ along several latitudinal transects is illustrated in Figure 6 (Lynch-Steiglitz et al., 1995).

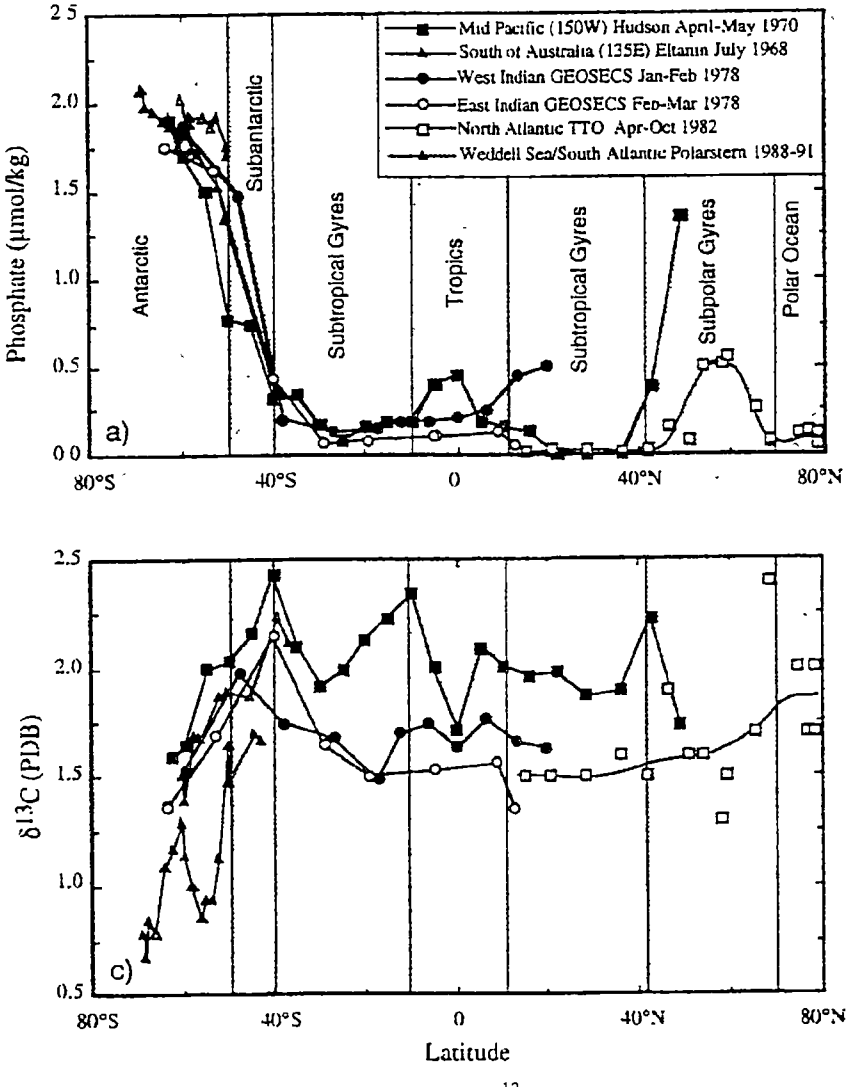

Figure 6: Latitudinal variations in phosphate and $\delta^{13}C$ measured in sea water (Lynch-Steiglitz et al., 1995). As phosphate concentrations decrease the $\delta^{13}C$ concentration increases, and vice versa.

The relationship between $\delta^{13}C$ and biologically mediated uptake of nutrients is as follows:

$$\delta^{13}C - \delta^{13}C_{MO} = (\Delta photo/\Delta CO_{2\,MO})(C/P_{org})(PO_4 - PO_{4\,MO})$$

where MO stands for mean ocean, Δphoto is the carbon isotope separation during marine photosynthesis (~-20 to -30‰ in the Southern Ocean) and C/P_{org} is the carbon to phosphorus ratio in marine organic matter (~ 106); ΣCO_{2MO} ~ 2200 µm; $\delta^{13}C_{MO}$ ~ 0.5; and $PO_{4\,MO}$ ~ 2.2 µmol/kg. The mean ocean values are those which would be present if there were no biological activity. By substituting these values, and inserting the measured phosphate concentration at a particular site, we can calculate the change in $\delta^{13}C$ of sea water since the difference to the mean ocean value should represent the amount of biological uptake. This equation is used in the present study to estimate the $\delta^{13}C$ of sea water where no direct measurements are available.

The relationship between $\delta^{13}C$ and biological production, however, can be complicated by the influence of gas exchange between the ocean surface and the atmosphere. Equilibration with the atmosphere increases the $\delta^{13}C$ of surface waters, although equilibrium is never reached (Mook et al., 1974). Gas exchange is most intense at lower temperatures and fractionation of $\delta^{13}C$ during oceanic uptake causes an enrichment in $\delta^{13}C$ of DIC relative to the atmosphere of ~0.1‰ for every 1 degree of cooling (Broecker and Maier-Reimer, 1992). Equilibration at high Southern latitudes is limited by the short residence time of surface waters and the seasonal sea ice cover (Charles and Fairbanks, 1990), with gas exchange most effective in frontal environments. Highest $\delta^{13}C$ values in the Southern Ocean are recorded at the Polar Front (PF) (Charles and Fairbanks, 1990; McNeil et al., 2001) and the Subantarctic Front due to the increased air-sea exchange and relatively high biological production at these frontal locations (Gruber et al., 1999).

Throughout the year, the influence of air-sea exchange, biological productivity and vertical mixing on the $\delta^{13}C$ of surface waters varies. During spring and summer, biological production in the Southern Ocean is high, causing enhanced uptake of ^{12}C relative to ^{13}C, and therefore higher $\delta^{13}C$ values. Vertical mixing during summer is limited due to intense stratification, maintaining the nutrient depleted and high $\delta^{13}C$ values of the surface waters. During winter, biological production is low and vertical mixing is stronger. As a result, $\delta^{13}C$ values are low. Air-sea gas exchange is also strongest during winter due to the increased CO_2 solubility at lower temperatures. This exchange will tend to further reduced $\delta^{13}C$ values. These seasonal changes in $\delta^{13}C$ should also be imprinted on the foraminiferal $\delta^{13}C$ record.

In this study I attempt to establish the relationship between the $\delta^{13}C$ record of foraminifera and that of surface waters. However, laboratory and plankton tow studies

have revealed several disequilibrium effects in the uptake of $\delta^{13}C$ by planktonic foraminifera. Disequilibrium effects may be driven by 1) temperature (Bemis et al., 2000; Ortiz et al., 1996); 2) the activity of algal symbionts (Bemis et al., 2000); 3) the carbonate ion concentration of seawater (Bemis et al., 2000; Russel and Spero, 2000; Spero et al., 1997); 4) foraminiferal shell size (Curry and Matthews, 1981; Donner and Wefer, 1994; Oppo and Fairbanks, 1989; Ravelo and Fairbanks, 1995; Spero and Lea, 1996; Williams et al., 1981); 5) genetic variation (Huber et al., 1997; Darling et al., 2000; Stewart et al., 2001; Kucera and Darling, 2002; Bauch et al., 2003); and 6) the isotopic composition of the foraminiferal diet (Spero and Lea, 1996). The effect of diet is thought to be small (a 0 - 0.08‰ shift in foraminiferal $\delta^{13}C$ for each 1‰ change in dietary $\delta^{13}C$) and is also difficult to determine. It is also not possible to determine genotypic variation from the samples in this study. The other four factors may have a more predictable effect on $\delta^{13}C$, allowing disequilibrium offsets to be accounted for in foraminiferal $\delta^{13}C$ records. The results from this study will help to determine how well different species capture the overall trends in $\delta^{13}C$ variability, despite disequilibrium effects, and will highlight variability in disequilibrium between species. The following provides a summary of the disequilibrium effects relevant to the interpretation of the $\delta^{13}C$ record in this study.

Temperature changes the metabolic rate of organic compounds, which influences the uptake of $\delta^{13}C$ (Bemis et al., 2000). Metabolic rates increase at higher temperatures causing the shell calcite to incorporate greater proportions of ^{12}C-enriched carbon which is respired during metabolism of organic compounds. Shell $\delta^{13}C$ therefore tends to decrease with increasing temperature. For *G. bulloides* grown in laboratory cultures there is an ~1‰ decrease in $\delta^{13}C$ between 15° and 24°C. The effect of temperature varies between different species, indicating that calculations of the relationship between temperature and $\delta^{13}C$ need to be species specific. *Orbulina universa*, for instance, shows no correlation with increasing temperature under low light conditions and a slight positive correlation under high light levels (Bemis et al., 2000). The effect of temperature at high light levels on this species appears to be due enhanced photosynthetic rates of the algal symbionts at higher temperatures. The photosynthetic activity of algal symbionts will preferentially remove ^{12}C from the foraminiferal microenvironment, leaving the shell enriched in ^{13}C (Spero, 1992; Spero and Lea, 1993). This effect is enhanced at maximum irradiances as well as at higher temperatures (Bemis et al., 2000).

The concentration of carbonate in seawater affects both the carbon and oxygen isotopic composition of planktonic foraminifera (Spero et al., 1997). Laboratory experiments with *O. universa* and *G. bulloides* indicate that as $[CO_3^{2-}]$ increases the $\delta^{13}C$ and $\delta^{18}O$ in calcite decreases. The slope of the carbonate ion effect varies between species, with *G. bulloides* exhibiting a slope twice as steep as that of *O. universa*. The isotopic offset due to $[CO_3^{2-}]$ occurs independently of photosynthesis, as indicated by similar trends for specimens grown under high light and no light. Changes in the $[CO_3^{2-}]$ between glacial and interglacial intervals may have caused significant disequilibrium effects in the $\delta^{13}C$ of foraminiferal calcite and these should be accounted for.

The effect of shell size on $\delta^{13}C$ is more pronounced than for $\delta^{18}O$, with increasing shell size causing increases in the carbon isotopic composition (Curry and Matthews, 1981). For the tropical species *Globgerinoides sacculifer*, the $\delta^{13}C$ range obtained for all size fractions within the one core depth is greater than the glacial-interglacial amplitude recorded by this species in down-core records (Oppo and Fairbanks, 1989). Each species has its own size dependent relationship, generally associated with increasing $\delta^{13}C$, which are consistent between locations (Ravelo and Fairbanks, 1995).

Despite the numerous disequilibrium effects which may alter the carbon isotopic record of planktonic foraminifera, offsets from equilibrium may be constant and therefore predictable for certain water masses and conditions. Comparison between $\delta^{13}C$ measurements of *Neogloboquadrina pachyderma* (s.) in surface sediments and seawater values in the South Atlantic (41° to 60°S) indicate that the foraminiferal $\delta^{13}C$ largely parallels that of equilibrium values with an offset of 1‰ (Charles and Fairbanks, 1990). Ortiz et al. (1996) found that $\delta^{13}C$ values of *N. pachyderma* (s.) in northeast Pacific waters were ~2.4‰ lower than equilibrium $\delta^{13}C$. Laboratory experiments with *Globigerina bulloides* indicate an offset from equilibrium calcite of ~1.75‰ at a temperature of 16°C for shells in the 300 µm size range, although this value varies with both temperature and size (Spero and Lea, 1996). The sediment trap results from this study will help to determine variations in equilibrium fractionation in several different species on a seasonal and regional basis in the Southern Ocean and their relationship to observed parameters.

Cd/Ca in foraminifera

Cadmium is incorporated into the shells of foraminifera, and the ratio of Cd:Ca in foraminiferal calcite has been used to determine past changes in phosphate utilisation

(Boyle, 1988; Boyle, 1992). The incorporation of Cd into foraminiferal shells does not influence the oceanic cadmium distribution since foraminifera and other calcareous organisms are responsible for less than 2 per cent of the vertical Cd transport (Boyle, 1988). Core top studies have indicated a consistent relationship between Cd/Ca of planktonic foraminifera and surface nutrients, although with some offset (McIntyre et al., 1997). Culture experiments with *G. bulloides* indicate that this species faithfully records changes in Cd concentration ($r^2 = 0.96$) with an offset of 1.9± 0.2 when temperature is kept constant (Mashiotta et al., 1997).

Differences in the Cd concentration of seawater and that recorded by planktonic foraminifera may arise due to differences in species vertical distributions (Mashiotta et al., 1997), and temperature (Rickaby and Elderfield, 1999). The Cd/Ca concentration in seawater varies with depth (Mashiotta et al., 1997). Since Cd is a bioactive metal it is characterised by very low surface water concentrations, with a rapid increase through the thermocline. Cd/Ca in planktonic foraminifera may therefore vary widely according to their habitat depth.

An examination of *Globigerina bulloides* in a suite of box cores collected between 35° and 62°N in the northeast Atlantic suggests that temperature may affect Cd/Ca values (Rickaby and Elderfield, 1999). Samples exhibit a latitudinal trend which is opposite to that of phosphate, but consistent with changes in temperature. This suggests that Cd incorporation by *G. bulloides* is temperature dependant. Future analysis of Cd/Ca from the sediment trap data will allow the relationship between variations in Cd and P to be better determined on a seasonal basis, therefore providing a better calibration to down core records.

1.6 MONITORING THE MODERN CARBON CYCLE

The natural carbon cycle has been perturbed since the industrial revolution by human induced changes. The burning of fossil fuels and changes in land use have caused the atmosphere to become relatively enriched in the carbon isotope ^{12}C, therefore lowering the $\delta^{13}C$ (Keeling, 1979). Terrestrial biomass and fossil fuel carbon has a $\delta^{13}C$ of ~-25‰ whereas atmospheric carbon is ~-7‰ and dissolved inorganic carbon in oceanic surface waters is ~+0.5‰. Perturbations to carbon held in any of these three reservoirs will be reflected in the isotopic composition of the carbon held within them. The $\delta^{13}C$ of atmospheric CO_2 has decreased from approximately -6.3‰ in preindustrial times (Friedli

et al., 1986) to approximately -7.8‰ by 1994 (Keeling et al., 1995) due to the addition of relatively light $\delta^{13}C$ since the release of fossil fuel carbon.

The change in the $\delta^{13}C$ of atmospheric CO_2 is reflected in the oceanic carbon reservoir due to air-sea exchange. The size and relative importance of the oceans as a sink for anthropogenic CO_2, however, remains largely unknown. Of the 7 billion tons of CO_2 which have been emitted due to the burning of fossil fuels and tropical forests, about 3.4 billion tons are known to stay in the atmosphere (Kerr, 1992). The fate of the remaining 3 to 4 billion tons is uncertain. Changes in the $\delta^{13}C$ of surface waters can help to determine which regions may act as a sink for atmospheric CO_2. Ortiz et al. (2000) calculate a change in $\delta^{13}C$ of dissolved inorganic carbon in NE Pacific surface waters of -0.62‰ over the span of the industrial revolution. Repeated measurements of $\delta^{13}C$ of dissolved inorganic carbon in Pacific Ocean surface waters has revealed a decrease in $\delta^{13}C$ by about 0.4 between 1970 and 1990 (Quay et al., 1992). This value has been extrapolated globally to indicate a net oceanic CO_2 uptake of 2.1 gigatons of carbon per year. This reduction in the $\delta^{13}C$ of seawater is referred to as the oceanic Suess effect (Broecker and Peng, 1982).

The calcium carbonate tests of planktonic foraminifera also provide a record of the $\delta^{13}C$ of surface waters through time. Beveridge and Shackleton (1994) compared the isotopic composition of planktonic foraminifera collected in sediment trap and plankton tow samples with those from core tops. The core top samples represent the late Holocene period, prior to the industrial revolution, while the sediment trap and tow samples represent the present. This comparison allows an estimate of the oceanic uptake of anthropogenic CO_2 in that region. They noted a drop in $\delta^{13}C$ values in the Eastern Atlantic of between 0.52 and 0.62‰. A similar study in the Arctic Ocean indicated a reduction in $\delta^{13}C$ of ~0.9‰ (Bauch et al., 2000). Such results indicate that some oceanic regions act as a sink for atmospheric CO_2.

Comparison between core top and sediment trap data, however, also needs to take into account the change in carbonate chemistry since the industrial revolution. The addition of anthropogenic CO_2 to the ocean surface has substantially lowered the surface ocean pH, thus affecting the $[CO_3^{2-}]$. *Kohfeld et al.* [2000] estimate a $[CO_3^{2-}]$ decrease since the pre-industrial era in the subantarctic South Atlantic of ~30μmol/kg. If we apply the carbonate ion relationship of *Spero et al.* [1997] then the decrease in $[CO_3^{2-}]$ during pre-industrial times implies a relative enrichment in modern *G. bulloides* of up to 0.40‰

compared to pre-industrial aged core tops. This carbonate ion effect will therefore partly mask the anthropogenic depletion in $\delta^{13}C$ calculated from modern sediment trap samples.

1.7 SEDIMENT TRAP STUDIES

The analysis of planktonic foraminifera collected in sediment traps in this study will help to address many of the issues raised in the forgoing discussion. Foraminifera play a central role in many palaeoclimate studies, so it is important to test and calibrate many of the techniques commonly employed in the interpretation of past climates. Sediment traps provide a unique opportunity to measure the seasonal and regional changes in foraminiferal flux, species composition and shell chemistry. Faunal information can be directly compared to observed climatic variables at the time of their production, enhancing our understanding of the environmental information which can be obtained from foraminiferal records. To further enhance our interpretations of down core records, the sediment trap data are compared to foraminifera deposited in nearby core top sediments. This allows better understanding of the preservation of environmental information in the fossil record.

However, there are a few issues surrounding sediment trap collections which should be considered before interpreting the data, and this particularly applies to the comparison between the foraminiferal data and other observed parameters. The foraminiferal material in this study, and the fluxes of other organic and inorganic particulate matter, is compared to hydrographic data such as dissolved nutrient concentrations, temperature and salinity. When comparing the sediment trap data with other observations, however, it is important to consider sources of bias in the sediment trap collections. For instance, material may be sourced from a large catchment area due to advection by currents, sinking speeds of particles vary and may cause offsets between biological production at the surface and their collection in the traps, and trap collection may be hampered by clogging of particles within the trap cone. These effects can bias the observed timing and magnitude of the fluxes, and will be discussed here in relation to the effects on the foraminiferal record.

Surface and sub-surface currents may transport biogenic material over large distances before deposition in the sediment traps. Traps may therefore have large catchment areas which vary between depths. A model by Siegel and Deuser (1997) indicates that material settles through the water column in a funnel pattern, spreading outwards with depth, and

as a result deeper traps will receive particles from a much wider area than shallower traps. This can result in a larger flux to the deeper trap. Blooms may originally occur outside the smaller catchment area of the shallow trap, but inside that of the deep trap. As the bloom moves laterally it may be recorded in the deep trap prior to the shallower trap.

Fortunately, fluxes of planktonic foraminifera are not easily influenced by the action of currents. Foraminifera are relatively large and have high settling velocities which makes them less susceptible to lateral transport (Gardner et al., 1997; Guptha et al., 1997). Most specimens of planktonic foraminifera >150µm reach a depth of 3800 m within 3 to 12 days (Takahashi and Bé, 1984), and at mean current speeds of up to 22 cm/s Gardner et al. (1997) observed no statistical relationship between currents and vertical flux patterns. The fast sinking speeds of foraminifera and low susceptibility to horizontal advection means that foraminifera collected in sediment traps can be directly related to conditions observed at the sea-surface at the time of collection.

Another complication, however, is that particles deposited in the trap funnel may adhere to the interior wall of the cone, and then slide down the slope and into the collection cup in a series of micro-avalanches (Honjo, 1996). For traps with an aperture of 0.5 m^2, this process may cause a delay of several days between the arrival and collection of material in the trap. In areas of high flux, the material collecting in the cone may cause the trap funnel to become clogged. In PARFLUX Mk7G-21 traps, as employed in this study, Honjo et al. (2000) observed that when mass fluxes reached 400 – 500 $mgm^{-2}d^{-1}$ the sample cups tended to overflow, causing settling particles to clog the bottom of the receiving funnel of the sediment trap. Blockage of the trap cone has also been observed in other studies using 0.5 m^2 diameter traps (Pilskaln et al., 1996). This process may prematurely terminate the sample collection or cause under-collection for the remainder of the record.

Delays caused by sinking speeds and the efficiency of trap collection need to be considered in this study when comparing foraminiferal flux to observed environmental parameters.

1.8 REFERENCES

Archer, D., Winguth, A., Lea, D. and Mahowald, N., 2000. What caused the glacial-interglacial atmospheric pCO_2 cycles. Reviews of Geophysics, 38(2): 159-189.

Armand, L. K., 1997. The use of diatom transfer functions in estimating sea-surface temperature and sea-ice in cores from the southeast Indian Ocean. PhD thesis, Australian National University.

Banse, K., 1996. Low seasonality of low concentrations of surface chlorophyll in the Subantarctic water ring: underwater irradiance, iron, or grazing? Progress in Oceanography, 37: 241-291.

Barnola, J.M., Raynaud, D., Korotkevich, Y.S. and Lorius, C., 1987. Vostok ice core provides 160,000-year record of atmospheric CO_2. Nature, 329: 408-414.

Barrows, T.T., Juggins, S., De Dekker, P., Thiede, J. and Martinez, J.I., 2000. Sea-surface temperatures of the southwest Pacific Ocean during the Last Glacial Maximum. Paleoceanography, 15(1): 95-109.

Bauch, D., Carstens, J. and Wefer, G., 1997. Oxygen isotope composition of living *Neogloboquadrina pachyderma* (sin.) in the Arctic Ocean. Earth and Planetary Science Letters, 146: 47-58.

Bauch, D., Carstens, J., Wefer, G. and Thiede, J., 2000. The imprint of anthropogenic CO_2 in the Arctic Ocean: evidence from planktic $\delta^{13}C$ data from water column and sediment surfaces. Deep-Sea Research II, 47: 1791-1808.

Bauch, D., Darling, K., Simstich, J., Bauch, H.A., Erlenkeuser, H. and Kroon, D., 2003. Palaeoceanographic implications of genetic variation in living North Atlantic *Neogloboquadrina pachyderma*. Nature, 424: 299-302.

Bé, A.W.H. and Hutson, W.H., 1977. Ecology of planktonic foraminifera and biogeographic patterns of life and fossil assemblages in the Indian Ocean. Micropaleontology, 23: 369-414.

Belkin, I.M. and Gordon, A.L., 1996. Southern Ocean fronts from the Greenwich meridian to Tasmania. Journal of Geophysical Research, 101: 3675-3696.

Bemis, B. E. and Spero, H. J., 1998. Reevaluation of the oxygen isotope composition of planktonic foraminifera: Experimental results and revised paleotemperature equations. Paleoceanography, 13(2): 150-160.

Bemis, B.E., Spero, H.J., Lea, D.W. and Bijma, J., 2000. Temperature influence on the carbon isotopic composition of *Globigerina bulloides* and *Orbulina Universa* (planktonic foraminifera). Marine Micropaleontology, 38: 213-228.

Bemis, B. E.; Spero, H. J., and Thunell, R. C., 2002. Using species-specific paleotemperature equations with foraminifera: A case study in the Southern California Bight. Marine Micropaleontology, 46: 405-430.

Beveridge, N.A.S. and Shackleton, N.J., 1994. Carbon isotopes in recent planktonic foraminifera: A record of anthropogenic CO_2 invasion of the surface ocean. Earth and Planetary Science Letters, 126: 259-273.

Bidigare, R.R. et al., 1999. Iron-stimulated changes in ^{13}C fractionation and export by equatorial Pacific phytoplankton: Toward a paleogrowth rate proxy. Paleoceanography, 14(5): 589-595.

Bijma, J., Faber, W.W. and Hemleben, C., 1990. Temperature and salinity limits for growth and survival of some planktonic foraminifers in laboratory cultures. Journal of Foraminiferal Research, 20: 95-116.

Boyle, E.A., 1988. Cadmium: Chemical tracer of deepwater paleoceanography. Paleoceanography, 3: 471-489.

Boyle, E.A., 1992. Cadmium and $\delta^{13}C$ paleochemical ocean distributions during the Stage 2 glacial maximum. Annual Reviews of Earth and Planetary Science, 20: 245-287.

Boyle, E.A. and Keigwin, L.D., 1985/86. Comparison of Atlantic and Pacific paleochemical records for the last 250,000 years: Changes in deep ocean circulation and chemical inventories. Earth and Planetary Science Letters, 76: 135-150.

Boyle, E.A., Sclater, F. and Edmond, J.M., 1976. On the marine geochemistry of cadmium. Nature, 263: 42-44.

Braatz, B.V. and Corliss, B.H., 1984. Bottom water circulation in the South Australian Basin during the last 3.2 million years. Antarctic Journal of the United States, 20: 84-88.

Broecker, W.S. and Maier-Reimer, E., 1992. The influence of air-sea exchange on the carbon isotope distribution in the sea. Global Biogeochemical Cycles, 6: 315-320.

Broecker, W.S. and Peng, T.-H., 1982. Tracers in the Sea. Eldigio, Palisades, N. Y., 690 pp.

Burling, R.W., 1961. Hydrology of circumpolar waters south of New Zealand. New Zealand Department of Science and Industrial Research Bulletin, 143: 66 pp.

Charles, C.D. and Fairbanks, R.G., 1990. Glacial to interglacial changes in the isotopic gradients of Southern Ocean surface water. In: U. Bleil and J. Thiede (Editors), Geological History of the Polar Oceans: Arctic Versus Antarctic. Kluwer, Boston, Mass., pp. 519-538.

Charles, C.D. and Fairbanks, R.G., 1992. Evidence from Southern Ocean sediments for the effect of North Atlantic deep-water flux on climate. Nature, 355: 416-419.

Charles, C.D., Froelich, P.N., Zibello, M.A., Mortlock, R.A. and Morley, J.J., 1991. Biogenic opal in Southern Ocean sediments over the last 450,000 years: Implications for surface water chemistry and circulation. Paleoceanography, 6: 697-728.

Comiso, J.C., McClain, C.R., Sullivan, C.W., Ryan, J.P. and Leonard, C.L., 1993. Coastal Zone Color Scanner pigment concentrations in the Southern Ocean and relationships to geophysical surface features. Journal of Geophysical Research, 98(C2): 2419-2451.

Conte, M.H., Thompson, A., Lesley, D. and Harris, R.P., 1998. Genetic and physiological influences on the alkenone-alkenate versus growth temperature relationship in *Emilinia huxleyi and Gephyrocapsa oceanica.* Geochimica et Cosmochimica Acta, 62(1): 51-68.

Craig, H. and Gordon, L.I., 1965. Deuterium and oxygen 18 variations in the ocean and the marine atmosphere. In: E. Tongiorgi (Editor), Stable Isotopes in Oceanographic Studies and Paleotemperatures. Cons. Naz. di Rech., Spoleto, Italy, pp. 9-130.

Curry, W.B. and Matthews, R.K., 1981. Equilibrium ^{18}O fractionation in small size fraction planktic foraminifera: evidence from Recent Indian Ocean sediments. Marine Micropaleontology, 6: 327-337.

Curry, W.B., Thunell, R.C. and Honjo, S., 1983. Seasonal changes in the isotopic composition of planktonic foraminifera collected in Panama Basin sediment traps. Earth Planet. Sci. Lett., 64: 33-43.

Darling, K. F., Wade, C. M., Stewart, I. A., Kroon, D., Dingle, R., and Brown, A. J. L., 2000. Molecular evidence for genetic mixing of Arctic and Antarctic subpolar populations of planktonic foraminifers. Nature, 405: 43-47.

Deacon, G.E.R., 1982. Physical and biological zonation in the Southern Ocean. Deep-Sea Research, 29(1A): 1-15.

Deuser, W.G. and Ross, E.H., 1989. Seasonally abundant planktonic foraminifera of the Sargasso Sea: succession, deep-water fluxes, isotopic compositions, and paleoceanographic implications. Journal of Foraminiferal Research, 19(4): 268-293.

Donner, B. and Wefer, G., 1994. Flux and stable isotope composition of *Neogloboquadrina pachyderma* and other planktonic foraminifers in the Southern Ocean (Atlantic sector). Deep-Sea Research I, 41: 1733-1743.

Elderfield, H. and Ganssen, G., 2000. Past temperature and $\delta^{18}O$ of surface ocean waters inferred from foraminiferal Mg/Ca ratios. Nature, 405: 442-445.

Elderfield, H. and Rickaby, R.E.M., 2000. Oceanic Cd/P ratio and nutrient utilization in the glacial Southern Ocean. Nature, 405: 305-310.

Epstein, S., Buchsbaum, R., Lowenstam, H.A. and Urey, H.C., 1953. Revised carbonate-water isotopic temperature scale. Geological Society of America Bulletin, 64: 1315-1326.

Fairbanks, R.G., Sverdlove, M., Free, R., Wiebe, P.H. and Bé, A.W.H., 1982. Vertical distribution and isotopic fractionation of living planktonic foraminifera from the Panama Basin. Nature, 298: 841-844.

Fairbanks, R.G. and Wiebe, P.H., 1980. Foraminifera and chlorophyll maxima: Vertical distribution, seasonal succession, and paleoceanographic significance. Science, 209: 1524-1526.

François, R., Altabet,M. A., Goericke,R., McCorkle,D. C., Brunet,C., Poisson,A., 1993. Changes in the $\delta^{13}C$ of surface water particulate organic matter across the Subtropical Convergence in the SW Indian Ocean. Global Biogeochemical Cycles, 7: 627-644.

François, R., Honjo, S., Manganini, S. J., Ravizza, G. E. 1995. Biogenic barium fluxes to the deep sea: Implications for paleoproductivity reconstruction. Global Biogeochemical Cycles, 9: 289-304.

François, R., Altabet,M. A., Yu,E.-F., Sigman,D. M., Bacon,M. P., Frank,M., Bohrmann,G., Bareille,G., Labeyrie,L. D., 1997. Contribution of Southern Ocean surface-water stratification to low atmospheric CO_2 concentrations during the last glacial period. Nature, 389: 929-935.

Friedli, H., Lötscher, H., Oeschger, H., Siegenthaler, U. and Stauffer, B., 1986. Ice core record of the $^{13}C/^{12}C$ ratio of atmospheric CO_2 in the past two centuries. Nature, 324: 237-238.

Gardner, W.D., Biscaye, P.E. and Richardson, M.J., 1997. A sediment trap experiment in the Vema Channel to evaluate the effect of horizontal particle fluxes on measured vertical fluxes. Journal of Marine Research, 55: 995-1028.

Goñi, M.A., Hartz, D.M., Thunell, R.C. and Tappa, E., 2001. Oceanographic considerations for the application of the alkenone-based paleotemperature $U^{K'}_{37}$ index in the Gulf of California. Geochimica et Cosmochimica Acta, 65(4): 545-557.

Gordon, A.L. and Molinelli, E.J., 1986. Thermohaline and chemical distributions and the atlas data set. In: A.L.e.a. Gordon (Editor), Southern Ocean Atlas. A.A. Balkema, Rotterdam, pp. 34 pp.

Gruber, N. et al., 1999. Spatiotemporal patterns of carbon-13 in the global surface oceans and the oceanic Suess effect. Global Biogeochemical Cycles, 13(2): 307-335.

Guptha, M.V.S., Curry, W.B., Ittekkot, V. and Muralinath, A.S., 1997. Seasonal variation in the flux of planktic foraminifera: sediment trap results from the Bay of Bengal, Northern Indian Ocean. Journal of Foraminiferal Research, 27(1): 5-19.

Heath, R.A., 1985. A review of the physical oceanography of the seas around New Zealand - 1982. New Zealand Journal of Marine and Freshwater Research, 19: 79-124.

Hemleben, C., Spindler, M. and Anderson, O.R., 1989. Modern planktonic foraminifera. Springer-Verlag, New York, 363 pp.

Honjo, S., 1996. Fluxes of particles to the interior of the open oceans. In: V. Ittekot, P. Schäfer, S. Honjo and P.J. Depetris (Editors), Particle Flux in the Ocean. Wiley, New York, pp. 92-154.

Honjo, S., Francois, R., Manganini, S., Dymond, J. and Collier, R., 2000. Particle fluxes to the interior of the Southern Ocean in the Western Pacific sector along 170°W. Deep-Sea Research II, 47: 3521-3548.

Howard, W.R. and Prell, W.L., 1992. Late Quaternary surface circulation of the Southern Indian Ocean and its relationship to orbital variations. Paleoceanography, 7: 79-118.

Howard, W.R. and Prell, W.L., 1994. Late Quaternary carbonate production and preservation in the Southern Ocean: Implications for oceanic and atmospheric carbon cycling. Paleoceanography, 9: 453-482.

Huber, B.T., Bijma J. and Darling, K., 1997. Cryptic speciation in the living planktonic foraminifer *Globigerinella siphonifera* (d'Orbigny), Paleobiology, 23: 33-62.

Hutson, W.H., 1979. The Agulhas Current during the Late Pleistocene: Analysis of Modern Faunal Analogs. Science, 207: 64-66.

Ikehara, M. et al., 1997. Alkenone sea surface temperature in the Southern Ocean for the last two deglaciations. Geophysical Research Letters, 24: 679-682.

Imbrie, J. and Kipp, N.G., 1971. A new micropaleontological method for paleoclimatology: Application to a late Pleistocene Caribbean core. In: K.K. Turekian (Editor), The Late Cenozoic Glacial Ages. Yale University Press, New Haven, Conn., pp. 71-181.

Johannessen, T., Jansen, E., Flatøy, A. and Ravelo, A.C., 1994. The relationship between surface water masses, oceanographic fronts and paleoclimatic proxies in surface sediments of the Greenland, Iceland and Norwegian Seas. In: R. Zahn, T.F. Pedersen, M.A. Kaminski and L. Labeyrie (Editors), Carbon Cycling in the Glacial Ocean: Constraints on the Ocean's Role in Global Change. NATO ASI Series. Springer-Verlag, Berlin, pp. 61-85.

Keeling, C.D., 1979. The Suess Effect: ^{13}Carbon-^{14}Carbon interactions, Envioronment International. Pergamon, Tarrytown, New York, pp. 229-300.

Keeling, C.D., Whorf, T.P., Wahlen, M. and van der Plicht, J., 1995. Interannual extremes in the rate of rise of atmospheric carbon dioxide since 1980. Nature, 375: 666-670.

Keigwin, L.D. and Boyle, E.A., 1989. Late Quaternary paleochemistry of high-latitude surface waters. Palaeogeography, Palaeoclimatology, Palaeoecology, 73: 85-106.

Kerr, R.A., 1992. Fugitive carbon dioxide: It's not hiding in the ocean. Science, 256: 35.

Kincaid, E. et al., 2000. Planktonic foraminiferal fluxes in the Santa Barbara Basin: response to seasonal and interannual hydrographic changes. Deep-Sea Research II, 47: 1157-1176.

King, A.L. and Howard, W.R., 2001. Seasonality of foraminiferal flux in sediment traps at Chatham Rise, SW Pacific: Implications for paleotemperature estimates. Deep-Sea Research I, 48: 1687-1708.

Knox; F. and McElroy, M.B., 1984. Changes in atmospheric CO_2: Influence of the marine biota at high latitude. Journal of Geophysical Research, 89(D3): 4629-4637.

Kohfeld, K.E., Fairbanks, R.G., Smith, S.L. and Walsh, I.D., 1996. *Neogloboquadrina pachyderma* (sinistral coiling) as paleoceanographic tracers in polar oceans: Evidence from Northeast Water Polynya plankton tows, sediment traps, and surface sediments. Paleoceanography, 11: 679-699.

Kohfeld, K.E., Anderson, R.F. and Lynch-Stieglitz, J., 2000. Carbon isotopic disequilibrium in polar planktonic foraminifera and its impact on modern and Last Glacial Maximum reconstructions, Paleoceanography, 15: 53-64.

Kucera, M. and Darling, K.F., 2002. Cryptic species of planktonic foraminifera: their effect on palaeoceanographic reconstructions, Philosophical Transactions of the Royal Society of London Series a-Mathematical Physical and Engineering Sciences, 360(1793): 695-718.

Kumar, N. et al., 1995. Increased biological productivity and export production in the glacial Southern Ocean. Nature, 378: 675-680.

Lea, D.W., Mashiotta, T.A. and Spero, H.J., 1999. Controls on magnesium and strontium uptake in planktonic foraminifera determined by live culturing. Geochimica et Cosmochimica Acta, 63(16): 2369-2379.

Lynch-Steiglitz, J.; Stocker, T. F.; Broecker, W. S., and Fairbanks, R. G., 1995. The influence of air-sea exchange on the isotopic composition of oceanic carbon: Observations and modeling. Global Biogeochemical Cycles, 9:653-665.

Mashiotta, T.A., Lea, D.W. and Spero, H.J., 1997. Experimental determination of cadmium uptake in shells of the planktonic foraminifera *Orbulina universa* and *Globigerina bulloides:* Implications for surface water paleoreconstructions. Geochimica et Cosmochimica Acta, 61(9): 4053-4065.

Mashiotta, T.A., Lea, D.W. and Spero, H.J., 1999. Glacial-interglacial changes in Subantarctic sea surface temperature and $\delta^{18}O$-water using foraminiferal Mg. Earth and Planetary Science Letters, 170: 417-432.

McIntyre, K., Ravelo, A.C., Delaney, M.L., Anderson, L.D. and Johannessen, T., 1997. Ground truthing the Cd/Ca-carbon isotope relationship in foraminifera of the Greenland-Iceland-Norwegian Seas. Marine Geology, 140: 61-73.

McNeil, B.I., Tilbrook, B. and Matear, R.J., 2001. Carbon export in the sub-Antarctic zone, South of Australia based on seasonal changes in DIC and $\delta^{13}C_{DIC}$. Deep-Sea Research.

Mix, A.C., 1987. The oxygen-isotope record of glaciation. In: W.F. Ruddiman and H. Wright (Editors), North America and Adjacent Oceans During the Last Deglaciation. The Geology of North America. Geological Society of America, Boulder, Colo., pp. 111-135.

Mook, W.G., Bommerson, J.C. and Staverman, W.H., 1974. Carbon isotope fractionation between dissolved bicarbonate and gaseous carbon dioxide. Earth and Planetary Science Letters, 22: 169-176.

Moore, J.K., Abbott, M.R., Richman, J.G. and Nelson, D.M., 2000. The Southern Ocean at the last glacial maximum: A strong sink for atmospheric carbon dioxide. Global Biogeochemical Cycles, 14(1): 455-475.

Moore, J.K. et al., 1999. SeaWIFS satellite ocean color data from the Southern Ocean. Geophysical Research Letters, 26(10): 1465-1468.

Müller, P.J., Kirst, G., Ruhland, G., von Storch, I. and Rosell-Melé, A., 1998. Calibration of the alkenone paleotemperature index $U^{K'}_{37}$ based on core-tops form the eastern South Atlantic and the global ocean (60°N-60°S). Geochimica et Cosmochimica Acta, 62: 1757-1772.

Nürnberg, D., Bijma, H. and Hemleben, C., 1996. Assessing the reliability of magnesium in foraminiferal calcite as a proxy for water mass temperatures. Geochimica et Cosmochimica Acta, 60(5): 803-814.

O'Leary, T., Trull, T., Griffiths, B., Tilbrook, B., and Revill, A.T., 2001. Euphotic zone variations in bulk and compound specific $\delta^{13}C$ of suspended organic matter in the subantarctic Ocean, south of Australia. Journal of Geophysical Research, 106(C12): 31,669-31,684.

Oppo, D.W. and Fairbanks, R.G., 1989. Carbon isotope composition of tropical surface water during the past 22,000 years. Paleoceanography, 4: 333-351.

Orsi, A., Whitworth, T. and Nowlin, W.D., 1995. On the meridional extent and fronts of the Antarctic Circumpolar Current. Deep-Sea Research, 42: 641-673.

Ortiz, J.D. and Mix, A.C., 1992. The spatial distribution and seasonal succession of planktonic foraminifera in the California Current off Oregon, September 1987 - September 1988. In: C.P. Summerhayes, W.L. Prell and K.C. Emeis (Editors), Upwelling Systems: Evolution Since the Early Miocene. Geological Society Special Publication. Geological Society, London, pp. 197-213.

Ortiz, J.D. and Mix, A.C., 1997. Comparison of Imbrie-Kipp transfer function and modern analog temperature estimates using sediment trap and core top foraminiferal faunas. Paleoceanography, 12: 175-190.

Ortiz, J.D., Mix, A.C. and Collier, R.W., 1995. Environmental control of living symbiotic and asymbiotic foraminifera of the California Current. Paleoceanography, 10(6): 987-1009.

Ortiz, J.D., Mix, A.C., Rugh, J.M., Watkins, J.M. and Collier, R.W., 1996. Deep-dwelling planktonic foraminifera of the northeastern Pacific Ocean reveal environmental control of oxygen and carbon isotopic disequilibria. Geochimica et Cosmochimica Acta, 60: 4509-4523.

Pflaumann, U., Duprat, J., Pujol, C. and Labeyrie, L.D., 1996. SIMMAX: A modern analog technique to deduce Atlantic sea surface temperatures from planktonic foraminifera in deep-sea sediments. Paleoceanography, 11(1): 15-36.

Popp, B.N. et al., 1998. Effect of phytoplankton cell geometry on carbon isotopic fractionation. Geochimica et Cosmochimica Acta, 62(1): 69-77.

Popp, B.N. et al., 1999. Controls on the carbon isotopic composition of Southern Ocean phytoplankton. Global Biogeochemical Cycles, 13(4): 827-843.

Prahl, F.G., Muehlhausen, L.A. and Zahnle, D.L., 1988. Further evaluation of long-chain alkenones as indicators of paleoceanographic conditions. Geochimica et Cosmochimica Acta, 52: 2303-2310.

Prahl, F.G. and Wakeham, S.G., 1987. Calibration of unsaturation patterns in long-chain ketone compositions for palaeotemperature assessment. Nature, 330: 367-369.

Prell, W.L., 1985. The stability of low-latitude sea-surface temperatures: An evaluation of the CLIMAP reconstruction with emphasis on the positive SST anomalies. 025, U.S. Department of Energy, Washington, D. C.

Quay, P.D., Tilbrook, B. and Wong, C.S., 1992. Oceanic uptake of fossil fuel CO_2: Carbon-13 evidence. Science, 256: 74-79.

Rau, G.H., Takahashi, T. and Des Marais, D.J., 1989. Latitudinal variations in plankton $\delta^{13}C$: Implications for CO_2 and productivity in past oceans. Nature, 341: 516-518.

Ravelo, A.C. and Fairbanks, R.G., 1992. Oxygen isotopic composition of multiple species of planktonic foraminifera: Recorders of the modern photic zone temperature gradient. Paleoceanography, 7: 815-831.

Ravelo, A.C. and Fairbanks, R.G., 1995. Carbon isotopic fractionation in multiple species of planktonic foraminifera from core-tops in the tropical Atlantic. Journal of Foraminiferal Research, 25(1): 53-74.

Redfield, A.C., Ketchum, B.H. and Richards, F.A., 1963. The influence of organisms on the composition of seawater. In: M.N. Hill (Editor), The Sea. Wiley Interscience, New York, pp. 26-79.

Reynolds, L. and Thunell, R.C., 1985. Seasonal succession of planktonic foraminifera in the subpolar North Pacific. Journal of Foraminiferal Research, 15: 282-301.

Rickaby, R.E.M. and Elderfield, H., 1999. Planktonic foraminiferal Cd/Ca: Paleonutrients or Paleotemperature? Paleoceanography, 14(3): 293-303.

Rintoul, S.R. and Church, J.A., 1993. A late winter section between Tasmania and Antarctica: circulation, transport and water mass formation, Fourth International Conference on Southern Hemisphere Meterology and Oceanography. Australia Preprint Volume. American Meterological Society, Hobart, pp. 21-22.

Rintoul, S.R., Donguy, J.R. and Roemmich, D.H., 1997. Seasonal evolution of upper ocean thermal structure between Tasmania and Antarctica. Deep-Sea Research Part I, 44(7): 1185-1202.

Rintoul, S.R. and Trull, T.W., 2001. Seasonal evolution of the mixed layer in the Subantarctic Zone south of Australia. Journal of Geophysical Research.

Rosenthal, Y., Boyle, E.A., Labeyrie, L.D. and Oppo, D., 1995. Glacial enrichments of authigenic Cd and U in Subantarctic sediments: A climatic control on the elements' oceanic budget? Paleoceanography, 10: 395-414.

Rosenthal, Y., Dahan, M. and Shemesh, A., 2000. Southern Ocean contributions to glacial-interglacial changes of atmospheric pCO_2: An assessment of carbon isotope records in diatoms. Paleoceanography, 15(1): 65-75.

Russel, A.D. and Spero, H.J., 2000. Field examination of the oceanic carbonate ion effect on stable isotopes in planktonic foraminifera. Paleoceanography, 15(1): 43-52.

Sautter, L.R. and Thunell, R.C., 1989. Seasonal succession of planktonic foraminifera: Results from a four-year time-series sediment trap experiment in the Northeast Pacific. Journal of Foraminiferal Research, 19: 253-267.

Sautter, L.R. and Thunell, R.C., 1991. Seasonal variability in the $\delta^{18}O$ and $\delta^{13}C$ of planktonic foraminifera from an upwelling environment: Sediment trap results from the San Pedro Basin, Southern California Bight. Paleoceanography, 6(3): 307-334.

Schmidt, G.A., 1999. Error analysis of paleosalinity calculations. Paleoceanography, 14(3): 422-429.

Shackleton, N.J., Le, J., Mix, A.C. and Hall, M.A., 1992. Carbon isotope records from Pacific surface waters and atmospheric carbon dioxide. Quaternary Science Reviews, 11: 387-400.

Siegel, D.A. and Deuser, W.G., 1997. Trajectories of sinking particles in the Sargasso Sea: modeling of statistical funnels above deep-ocean sediment traps. Deep-Sea Research I, 44(9-10): 1519-1541.

Sigman, D.M., Altabet, M.A., Francois, R., McCorkle, D.C. and Gaillard, J.-F., 1999. The isotopic composition of diatom-bound nitrogen in Southern Ocean sediments. Paleoceanography, 14(2): 118-134.

Sikes, E.L., Volkman, J.K., Robertson, L.G. and Pichon, J.-J., 1997. Akenones and alkenes in surface waters and sediments of the Southern Ocean: Implications for paleotemperature estimation in polar regions. Geochimica et Cosmochimica Acta, 61: 1495-1505.

Spero, H.J., 1992. Do planktic foraminifera accurately record shifts in the carbon isotopic composition of seawater ΣCO_2? Marine Micropaleontology, 19: 275-285.

Spero, H.J., Bijma, J., Lea, D.W. and Bemis, B.E., 1997. Effect of seawater carbonate concentration on foraminiferal carbon and oxygen isotopes. Nature, 390: 497-500.

Spero, H.J. and Lea, D.W., 1993. Intraspecific stable isotope variability in the planktic foraminifera *Globigerinoides sacculifer*: Results from laboratory experiments. Marine Micropaleontology, 22: 221-234.

Spero, H.J. and Lea, D.W., 1996. Experimental determination of stable isotope variability in *Globigerina bulloides*: implications for paleoceanographic reconstructions. Marine Micropaleontology, 28: 231-246.

Stewart, I.A., Darling, K.F., Kroon, D., Wade, C.M., Troelstra, S.R., 2001. Genotypic variability in subarctic Atlantic planktic foraminifera, Marine Micropaleontology, 43(1-2): 143-153.

Takahashi, K. and Bé, A.W.H., 1984. Planktonic foraminifera: factors controlling sinking speeds. Deep-Sea Research A, 31(12): 1477-1500.

Takahashi, T., Broecker, W.S. and Langer, S., 1985. Redfield ratio based on chemical data from isopycnal surfaces. Journal of Geophysical Research, 90(C4): 6907-6924.

Tchernia, P., 1980. Descriptive Regional Oceanography. Pergamon Marine Series, 13. Pergamon Press, Oxford.

Thunell, R.C. and Honjo, S., 1987. Seasonal and interannual changes in planktonic foraminiferal production in the North Pacific. Nature, 328: 335-337.

Thunell, R.C. and Reynolds, L.A., 1984. Sedimentation of planktonic foraminifera: Seasonal changes in species flux in the Panama Basin. Micropaleontology, 30: 241-260.

Tomczak, M. and Godfrey, J.S., 1994. Regional Oceanography: An introduction. Pergamon Press, UK.

Uddstrom, M.J. and Oien, N.A., 1999. On the use of high-resolution satellite data to describe the spatial and temporal variability of sea surface temperatures in the New Zealand region. Journal of Geophysical Research, 104(C9): 20,749-20,751.

Volkman, J.K., Barrett, S.M., Blackburn, S.I. and Sikes, E.L., 1995. Alkenones in *Geophyrocapsa oceanica:* Implications for studies of paleoclimate. Geochimica et Cosmochimica Acta, 59(3): 513-520.

Volkman, J.K., Eglinton, G., Corner, E.D.S. and Forsberg, T.E.V., 1980. Long-chain alkenes and alkenones in the marine coccolithophorid *Emiliania huxleyi*. Phytochemistry, 19: 2619-2622.

Williams, D.F., Bé, A.W.H. and Fairbanks, R.G., 1981. Seasonal stable isotopic variations in living planktonic foraminifera from Bermuda plankton tows. Palaeogoegraphy, Palaeoclimatology, Palaeoecology, 33: 71-102.

Williams, D.F. and Healy-Williams, N., 1980. Oxygen isotopic-hydrographic relationships among Recent planktonic foraminifera from the Indian Ocean. Nature, 283: 848-852.

CHAPTER 2

CHATHAM RISE FORAMINIFERAL FLUX

"None of the world's oceans cast such a glamour of adventure over us as the Pacific, none has stirred man's imagination, and none affords more enticing problems to the student"
G. L Wood and P. McBride, The Pacific Basin (1930)

Published as: King, A.L. and Howard, W.R., 2001. Seasonality of foraminiferal flux in sediment traps at Chatham Rise, SW Pacific: Implications for paleotemperature estimates. Deep-Sea Research I 48, 1687-1708

Abstract

Analysis of sediment traps located either side of the Subtropical Front (STF) east of New Zealand, reveals a strong association between water masses and foraminiferal assemblages. The composition and timing of foraminiferal productivity is distinct between waters north and south of the front, and these differences are also reflected in the assemblages of nearby core-tops. The sediment trap data indicate highly seasonal flux patterns in this region, so sedimentary records may represent flux during a particular season, rather than throughout the annual cycle. This pronounced seasonality has implications for our estimates of the annual temperature range based on faunal assemblages. This study shows that despite strong flux seasonality the annual sea-surface temperature (SST) range is reliably estimated from the sediment trap foraminiferal assemblages by the Modern Analog Technique. The successful estimation of the annual SST range also indicates that the annual flux obtained from these sediment traps is representative of the longer term flux preserved in surface sediments. Core-top assemblages from this region can therefore be directly related to modern sea-surface conditions, providing an analogue for interpreting past environmental change from fossil assemblages.

2.1 Introduction

The fossil record of planktonic foraminiferal assemblages in marine sediments is a key tool used by paleoceanographers to study past environments. Sediment trap studies allow critical review of some of the potential sources of variability in our interpretation of fossil assemblages. Fossil assemblages may be altered after deposition by processes

including dissolution, bioturbation and resuspension. These may substantially change the faunal composition of an assemblage. In addition, the calibrations between sedimentary assemblages and seasonal sea-surface temperatures (SSTs) may miss the season of maximum production. Sediment trap and core-top assemblages are compared to determine whether post-depositional changes and flux seasonality significantly affect our interpretation of sedimentary assemblages. The basic structure of sediment trap and core-top faunal assemblages from studies at Atlantic and Pacific sites are mostly similar, though the largest discrepancies occurred at mid-latitude sites (Ortiz and Mix, 1997). In this study, foraminiferal assemblages derived from two sediment trap sites moored north and south of the Chatham Rise (NCR and SCR respectively), east of New Zealand, are compared to several nearby core-tops (Figure 1 and Table 1).

The Subtropical Front (STF) is situated along the crest of Chatham Rise. The frontal zone is characterised by steep temperature and salinity gradients which separate cold, low salinity, nutrient-rich subantarctic waters from warm, saline, nutrient-depleted subtropical waters (Deacon, 1982; Heath, 1985; Belkin and Gordon, 1996). The front is typically defined by the 10-14°C winter and 14-18°C summer isotherms (Heath, 1985). The temperature contrast between water masses north and south of the front is illustrated by the surface temperature cycles and vertical profiles at the two sediment trap sites (Figure 2). The STF is associated with high biological productivity (Bradford-Grieve et al., 1997; Bradford-Grieve et al., 1999). Coastal Zone Color Scanner data indicate that surface pigment concentrations in the region remain high throughout the year (Comiso et al., 1993). The global importance of this region is highlighted by studies inferring that the uptake of carbon dioxide is enhanced in the area (Murphy et al., 1991), a pattern partly attributed to the high biological productivity (Currie and Hunter, 1998).

The high biological productivity of this region makes it an ideal location in which to undertake particle flux studies with sediment trap deployments. Two sediment traps were deployed for almost a full annual cycle at sites just to the north and south of the STF (Figure 1). Comparison of these two sites permits an understanding of the dynamics of the subtropical and subantarctic environments, and of the extent and variability of the STF during an annual productivity season. Gaining an understanding of the interactions between particulate flux and environmental variables in the modern ocean is a key to understanding past environmental change recorded in deep-sea sediments.

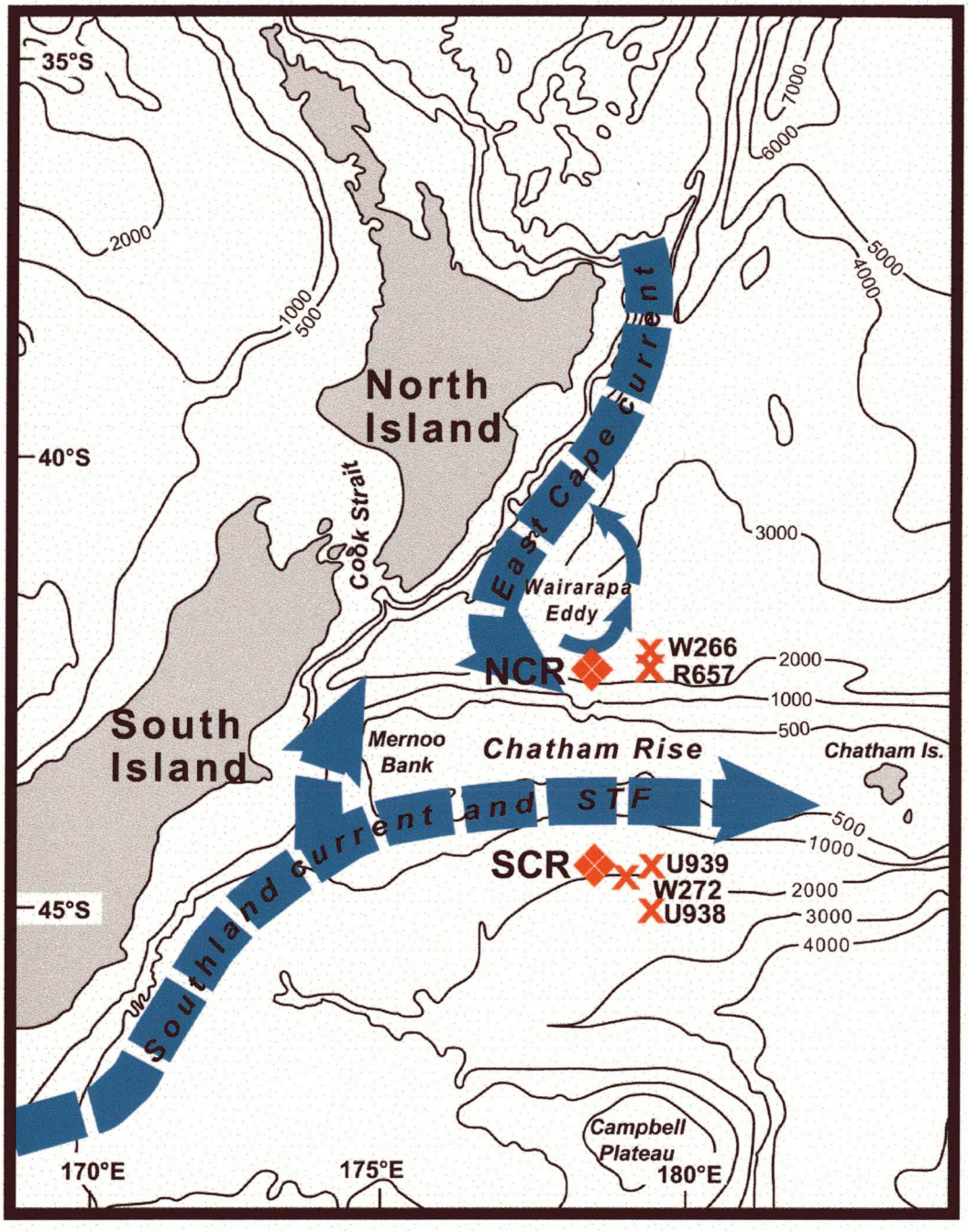

Figure 1: Locations of the sediment trap sites, NCR and SCR, and the core-tops used in this study (viz. W266, R657, U939, W272 and U938). The Subtropical Front (STF) is located along the crest of Chatham Rise, separating subantarctic from subtropical water masses. Current and frontal locations based on Heath (1985) and Roemmich and Sutton (1998).

Location and core	Latitude/longitude	Water depth (m)	MAT SST estimates (°C)		Average dissimilarity
			Summer	Winter	
NCR 300 m/1000 m	42°42'S; 178°38'E	1500	20.3 ± 4.3 20.1 ± 4.3	14.6 ± 3.5 14.4 ± 3.4	0.17 0.17
AVHRR(N)	42°30'S; 178°30'E	-	18.0	11.7	-
GOSTA(N)	42°30'S; 178°30'E	-	17.5	11.8	-
W266(N)	42°13'44"S; 179°21'54"E	2540	18.9 ± 3.7	13.7 ± 3.1	0.12
R657(N)	42°32'00"S; 179°29'55"E	1408	19.3 ± 1.8	14.6 ± 1.9	0.12
SCR 300 m/1000 m	44°37'S; 178°37'E	1500	11.6 ± 2.6 13.8 ± 2.0	8.0 ± 2.1 9.1 ± 1.5	0.19 0.14
AVHRR(S)	44°30'S; 178°30'E	-	15.1	8.9	-
GOSTA(S)	44°30'S; 178°30'E	-	15.5	9.7	-
U939 (S)	44° 29.7'S; 179°30.1'E	1300	10.8 ± 2.2	7.1 ± 2.0	0.16
W272(S)	44°41'21"S; 179°04'33"E	1841	11.7 ± 2.1	7.9 ± 1.9	0.09
U938(S)	45° 04.5'S; 179°29.9'E	2700	12.9 ± 1.5	8.9 ± 1.0	0.20

Table 1: Chatham Rise core-top and sediment trap locations and SST estimates. GOSTA SSTs derived from long-term observations at the sediment trap sites are shown for comparison (Bottomley et al., 1990) as are the AVHRR SSTs observed during the trap deployment period (Advanced Very High Resolution Radiometer, 1999). N denotes cores located north of the Subtropical Front and S, south of the front.

Several sediment trap studies have shown that the species composition and abundance of planktonic foraminifera deposited on the sea floor varies seasonally (Thunell and Honjo, 1987; Deuser and Ross, 1989; Sautter and Thunell, 1989; Ortiz and Mix, 1992; Guptha et al., 1997). The dominance of seasonal flux patterns on the sedimentary record has implications for how we interpret the fossil record, since fluxes may represent a particular season, rather than the entire annual cycle. Methods such as the Modern Analog Technique (MAT), which derives summer and winter temperature estimates

from the fossil assemblages, may need to be recalibrated to account for the seasonal structure embedded within the preserved assemblages.

Estimates of past sea-surface temperature (SST) change are useful in the reconstruction of past oceanic circulation, since different water masses are commonly delineated by temperature. In theory, it should be possible to determine the past position of ocean fronts based on SST variability, however, other factors also need to be considered. Some researchers contend that the STF east of New Zealand remains bathymetrically trapped over the Chatham Rise today (Uddstrom and Oien, 1999) and in the past (Fenner et al., 1992; Weaver et al., 1998; Nelson et al., 2000), but others suggest that it migrates on a seasonal basis today (Chiswell, 1994) and during interglacial intervals of the late Quaternary (Wells and Okada, 1997). Further understanding of the modern dynamics of this frontal system and variations in planktonic foraminiferal assemblages north and south of the front will aid our interpretation of paleoceanographic conditions in this region.

2.2 Methods

2.2.1 Sediment trap moorings

The two sediment trap moorings were deployed for approximately one year during 1996 and 1997. The south Chatham Rise (SCR) record was deployed from R.V. *Tangaroa* and spans the interval 9 June 1996 to 15 May 1997. The deployment of the northern trap (NCR) by the R.V. *Kaharoa* was delayed until 14 September 1996 due to logistical difficulties, and this record also concludes on the 15 May 1997.

Each mooring consists of two McLane PARFLUX Mk 7G-21 time-incremental sediment traps at depths of 300 and 1000 m. Traps at SCR were pre-programmed to collect particles sinking through the water column over approximately 16-day intervals. The traps at NCR collected samples over 7-8 day intervals during the predicted spring bloom period, changing to a 16-day sampling period which coincided with that of the SCR traps in late December 1996. No data were obtained from the 300m trap at NCR between the 18th November and the 5th January because of cup damage.

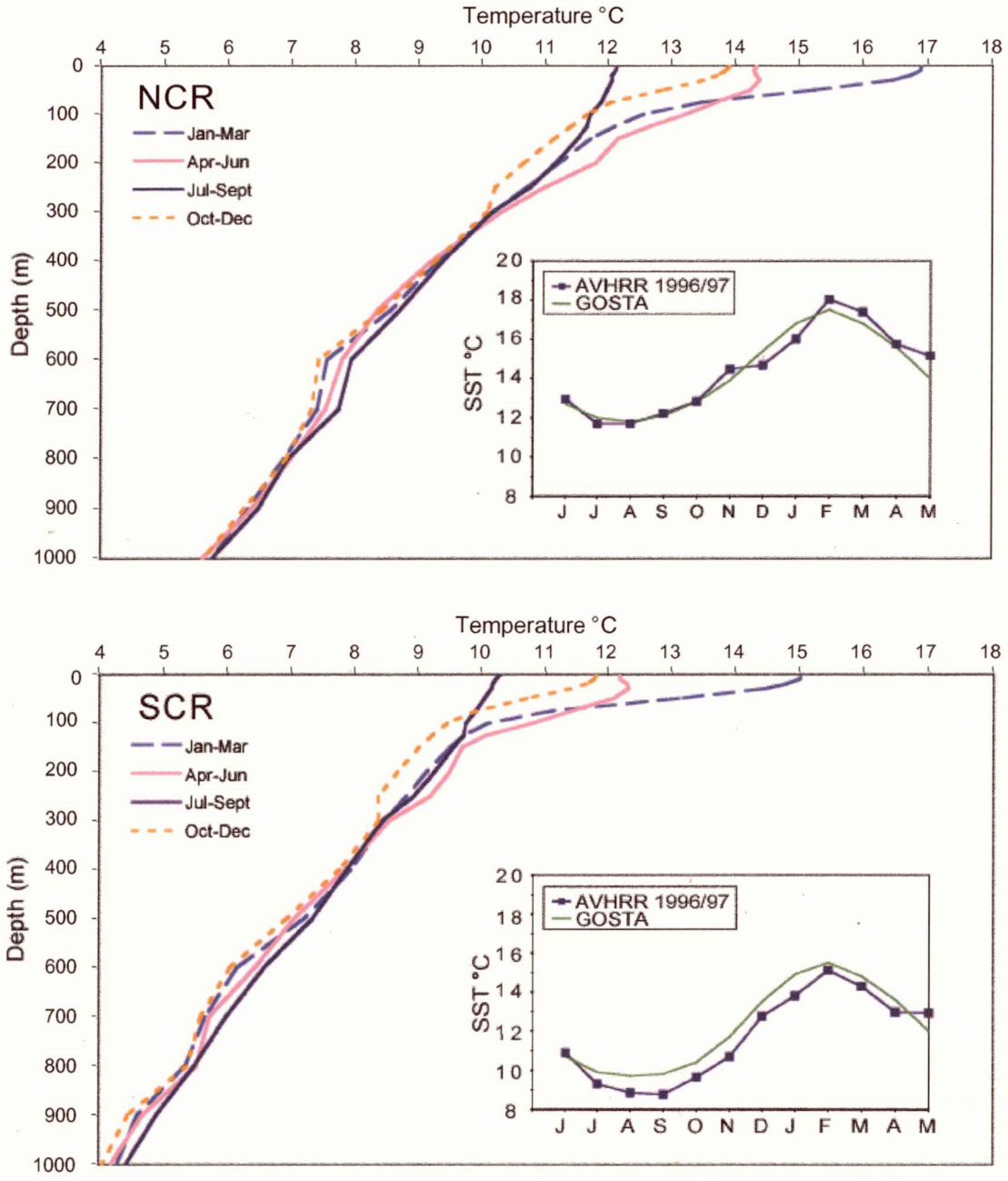

Figure 2: The temperature profile between 0 and 1000 m at NCR and SCR (Levitus, 1994). The thermal stratification of surface waters is least during July-September, and gradually strengthens throughout October-December and January-March. Monthly SST variability from the AVHRR (1996-1997) and GOSTA (since 1851) (Bottomley et al., 1990) data sets are shown in the insets. The GOSTA climatology compares well with the AVHRR data, indicating that SSTs during the trap deployment period were representative of long-term SST variability at the two sites.

Trap solutions at each mooring site were prepared from filtered seawater collected at the nominal depth of the traps. The samples at the southern site were poisoned with formaldehyde to make up a 6% solution; a 0.3% solution of mercuric chloride ($HgCl_2$) was used at the northern sites. Trap solutions at both sites were borax-buffered and were made up to a high-density brine by adding excess NaCl (5-6% excess).

2.2.2 Sample analysis

Samples were initially washed through a 1 mm sieve and then split for analyses. A quarter split was originally taken for faunal analyses, but high flux samples were further split. Results from the particulate analyses have been presented elsewhere (Nodder and Northcote, 2001). Each sample from the faunal split was soaked in a buffered 3% peroxide solution for 5 to 6 hours to dissolve the organic matter. The samples were then washed through a 150μm stainless steel sieve using pH 7–8 deionised water buffered with sodium borate, and then filtered onto 0.8μm filters.

The planktonic foraminifera in the 150μm to 1mm size fraction were identified according to the taxonomy of Parker (1962) and Kipp (1976), although the "*pachyderma-dutertrei* intergrade" was not recognised. This taxonomy is consistent with the core-top data set employed in this study, which was derived from the global data base of Brown University (Prell et al., 1999). Examples of five species that tend to intergrade morphologically with other taxa and may cause taxonomic differences between studies are shown in Plate 1. The faunal assemblages were used to estimate the summer and winter SSTs using the MAT (which incorporates the GOSTA SST dataset of Bottomley, 1990) to assess the relationship between preserved assemblages and observed AVHRR SSTs (Advanced Very High Resolution Radiometer, 1999). The AVHRR data provides satellite derived sea-surface temperatures obtained during the trap deployment period with a spatial resolution of 9 km. Foraminiferal assemblages were then compared to those of nearby core-tops. Foraminiferal flux estimates were made in terms of number of specimens/m^2/day, taking into account the duration of each collection period and the cross-sectional area of the trap (0.5 m^2).

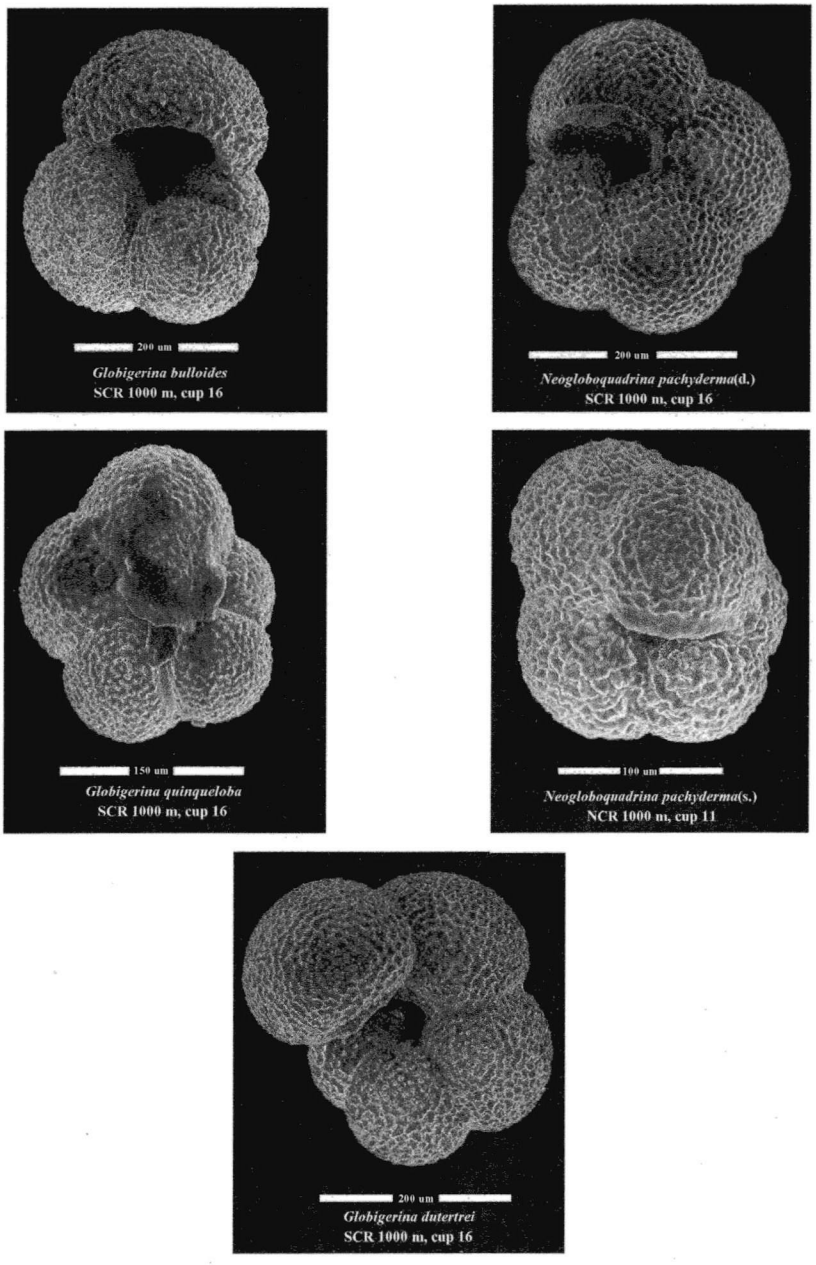

Plate 1: Foraminiferal species from sediment traps at SCR and NCR. These are examples of species whose morphology tends to intergrade with other taxa. Images were obtained with an electroscan environmental scanning electron microscope at the Central Sciences Laboratory, University of Tasmania.

2.3 Results

2.3.1 Mass flux and foraminiferal flux

North Chatham Rise. The total mass flux of the Chatham Rise sediment traps is presented and discussed in Nodder and Northcote (2001) and is here compared to the total foraminiferal flux (Figure 3). The mass flux at NCR (Figures 3A and 3B) exhibits distinct peaks during October, with moderate fluxes at the deeper trap recorded throughout the December to May sampling interval. The timing of peak mass flux events is similar to peaks in foraminiferal flux. The major peaks in foraminiferal and mass flux in the shallower trap are recorded as single peaks during October (the foraminiferal flux is ~6000 shells/m^2/day). This Spring production peak is also recorded in the deep trap. There are two peaks in foraminiferal flux at 1000 m (~6000 shells/m^2/day each), with the initial peak occurring one sample period prior to the 300 m peak. The mass flux at 1000 m lags behind both the peaks in foraminiferal production at both depths and the mass flux in the 300 m trap by one sample interval. The highest foraminiferal flux peak in the deeper trap (~9000 shells/m^2/day) occurs during December at a time of only moderate mass flux. There is another minor flux peak in foraminifera during early April. Unfortunately, no data could be obtained from the 300 m trap during either period due to cup damage (cups were found to be broken upon recovery).

There are consistently higher mass and foraminiferal fluxes in the 1000 m trap than in the 300 m trap. These higher deep fluxes are most pronounced during the latter half of October and November when no flux is recorded in the 300 m trap despite moderate fluxes to the deeper trap. Particulate flux to moored sediment traps may be affected by advection of material into or away from the traps by sub-surface currents, and failure during collection. Current speed data at NCR shows no consistent correlation to foraminiferal flux patterns and remain relatively low throughout the collection period with averages of 12.3±4.3 cm/sec and 8.3±2.5 cm/sec for the 300 m and 1000 m traps respectively (Nodder and Northcote, 2001). Gardner et al. (1997) observed that at mean current speeds of up to 22 cm/sec there is no statistical relationship to vertical flux patterns. The high settling velocities of foraminiferal shells makes these particles less susceptible to advection by sub-surface currents, so significant differential advection between traps is not likely (Guptha et al., 1997). The low fluxes observed in the shallow trap most likely reflects blockage of the trap cone as observed in other studies using 0.5 m^2 diameter traps (Pilskaln et al., 1996). Clogging probably occurred following the high spring flux, resulting in under-collection by the trap for the remainder of the record.

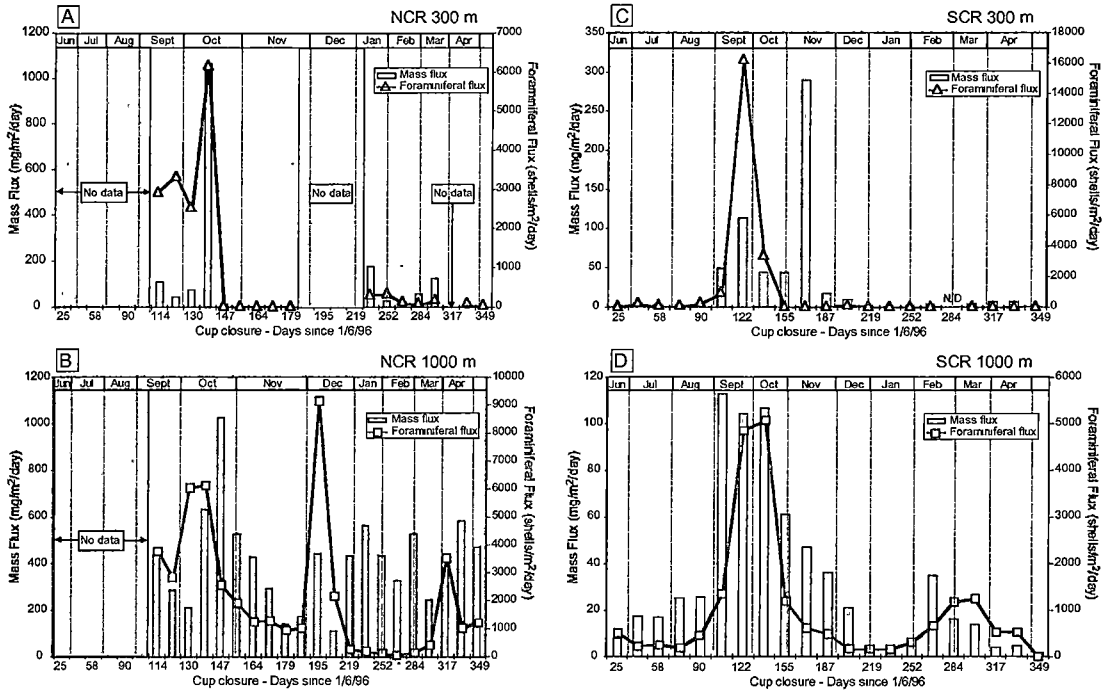

Figure 3: Mass and foraminiferal flux at NCR 300 m (A) and 1000 m (B), and SCR 300 m (C) and 1000 m (D). The timing of peaks in mass and foraminiferal flux are mostly consistent, however, at SCR 300 m the major peak in mass flux occurs during November, while the major foramininiferal peak is in September. At NCR distinct peaks in mass and foraminiferal flux occur during the same intervals, but the relative amplitude is not necessarily the same. At NCR 1000 m the maximum mass flux occurs during October, whereas the maximum foraminiferal flux is during December. Note that scales differ between graphs. Mass flux from Nodder and Northcote (2001).

South Chatham Rise. The foraminiferal and mass flux at SCR is episodic (Figures 3C and 3D). The major peak in mass flux recorded by the shallow trap occurs during November, with a minor peak during September. Throughout the remainder of the record the mass flux remains below 50 mg/m^2/day. The foraminiferal flux exhibits one production peak in September of ~16,000 shells/m^2/day, coinciding with the minor peak in mass flux. The 1000 m data set is also clearly dominated by the September event in both the mass (>100 mg/m^2/day) and foraminiferal fluxes (~5000 shells/m^2/day). Otherwise, fluxes remain low but detectable throughout the sampling period with another minor peak during February and March. The September peak in the 300 m record reaches a much higher amplitude than in the 1000 m record. The high amplitude of this peak in the shallow trap may, however, be overestimated due to difficulties splitting the foraminifera in this sample. Current speeds at SCR average 15.9±3.2 cm/sec and 10.5±1.3 cm/sec at 300 m and 1000 m depths (Nodder and Northcote, 2001).

Intervals during which currents were stronger show no consistent relationship to changes in foraminiferal flux. The very low mass and foraminiferal fluxes at 300 m during the latter half of this record are probably due to blockage of the cone after the high mass flux event in November.

Site comparisons. The flux of foraminifera, as well as the total mass flux, is greater at the northern than the southern trap (Nodder and Northcote, 2001). The average foraminiferal flux to the northern 1000 m trap (the more complete data set of the two depths) is twice that of the flux at the southern trap (1841 shells/m^2/day compared to 970 shells/m^2/day), while mass flux at NCR is greater than at SCR by a factor of 13. Both sites, however, record similar fluxes to those observed at other subpolar sites. Fluxes at Station P in the Northeast Pacific, for instance, recorded an average annual foraminiferal flux ranging between 1471 and 4918 shells/m^2/day between October 1982 and August 1986 (Sautter and Thunell, 1989), and the average foraminiferal flux recorded at the most productive site in the California current off Oregon was 780 shells/m^2/day (Ortiz and Mix, 1992).

2.3.2 Foraminiferal composition

North Chatham Rise. The foraminifera trapped at NCR are composed predominantly of *Globorotalia inflata*, which constitutes 68% of the total shell flux at 300 m and 59% at 1000 m (Table 2). The remaining flux is composed of *Neogloboquadrina pachyderma* (d.) (10% at 300 m, 14% at 1000 m), *Globigerina bulloides* (9% and 14% respectively) and several other species present with abundances of less than 5%. These percentage abundances are consistent throughout the year, with no apparent seasonal succession among minor species (not shown here). The species fluxes for the six key species at 300 and 1000 m are shown in Figure 4. The timing of species fluxes are very similar between the two trap depths, excluding the data gaps in the 300 m record and the absence of any foraminiferal flux at this trap during late October and November. The lead by the deep trap observed from the total flux estimates for the October peak is also exhibited by the most dominant species at this trap (listed above).

South Chatham Rise. The dominant species at SCR is *G. bulloides*, however, its relative abundance differs between the two trap depths (Table 2, Figure 4D). In the 300 m trap this species comprises 78% of the fauna, while at 1000 m it accounts for only 45% of the total flux (Table 2). Absolute foraminiferal fluxes are considerably different between the two traps. The abundances of *N. pachyderma* (d.) (Figure 4F) at 1000 m are up to three

times that recorded by the 300 m trap, peaks in *G. inflata, G. bulloides* and *N. pachyderma* (s.) (Figure 4B, 4D, 4J respectively) are close to double that of the 300 m trap, and *G. quinqueloba* (Figure 4L) peaks at six times that of the shallower trap. Peak fluxes of *G. glutinata* (Figure 4H) are, however, higher in the 300 m trap. Despite these differences in amplitude the flux seasonality is consistent between the two traps, although there is a slight lag in the flux to the 1000 m trap. Inconsistencies in flux amplitudes between the traps during the latter half of the record is most likely due to blockage of the cone at 300 m. Based on fluxes to the 1000 m trap, however, the 300 m trap appears to have captured the main flux event so should still be representative of the annual flux over this site.

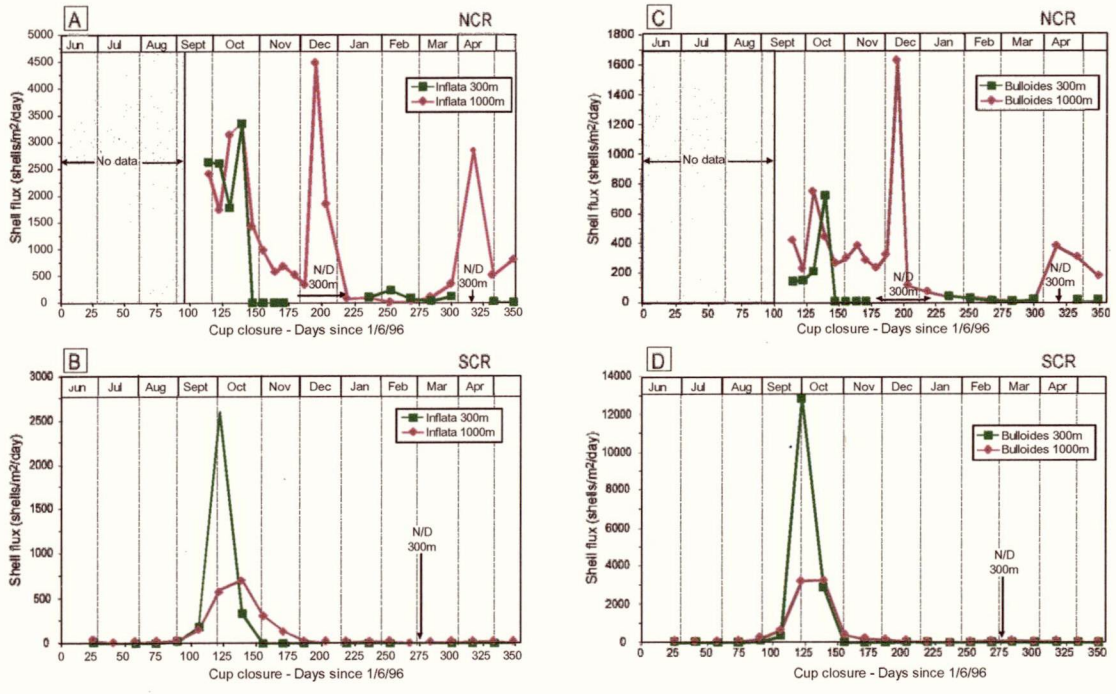

Figure 4: Species fluxes for the six main species of planktonic foraminifera at NCR and SCR. At NCR peaks at 300 m and 1000 m are generally of similar magnitude and timing, although there is a slight lead by the 1000 m trap by *G. inflata, G. bulloides* and *N. pachyderma* (d.). At SCR peaks in the 1000 m trap generally occur one sample period after the peak at 300 m. Note that scales differ between graphs. N/D 300 m = no data at 300 m trap. Pachy R = *N. pachyderma* (d.) and Pachy L = *N. pachyderma* (s.).

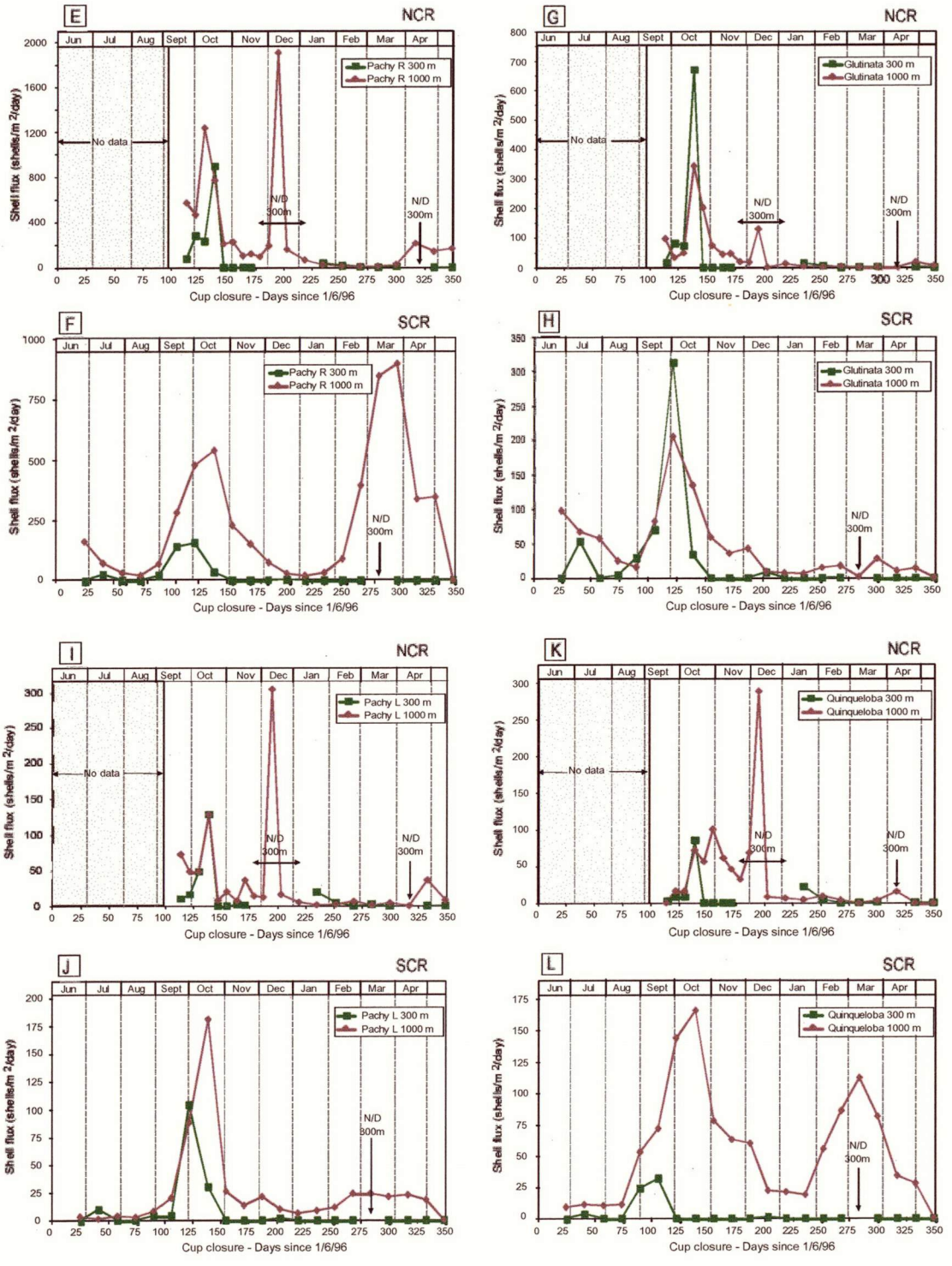

Figure 4 (continued)

Species	NCR		SCR	
	NCR 300	1000	SCR 300	1000
Globigerina bulloides	8.62	13.84	77.59	44.74
Globigerina falconensis	0.00	0.26	0.31	0.01
Globigerina calida	0.18	0.31	0.00	0.00
Globigerina quinqueloba	1.00	1.58	0.29	5.58
Globigerinita glutinata	5.48	2.14	2.41	4.57
Globigerinella aequilateralis	0.20	0.24	0.00	0.00
Globigerinoides ruber	0.00	0.06	0.00	0.00
Orbulina universa	1.27	2.17	0.13	1.22
Neogloboquadrina pachyderma (s.)	1.56	1.58	0.73	2.55
Neogloboquadrina pachyderma (d.)	10.03	13.82	1.80	24.90
Neogloboquadrina dutertrei	1.43	1.08	0.00	1.11
Globorotalia truncatulinoides (s.)	0.80	0.30	1.68	3.00
Globorotalia truncatulinoides (d.)	0.05	0.00	0.00	0.04
Globorotalia crassaformis	0.29	0.01	0.00	0.00
Globorotalia scitula	0.97	3.43	0.05	1.64
Globorotalia inflata	68.13	56.04	14.95	10.62

Table 2: Species percent of total shell flux at the northern and southern trap sites.

2.3.3 Faunal sea-surface temperature estimates from the sediment trap assemblages

SST estimates were obtained from the sediment trap assemblages by the MAT (Prell, 1985). These temperatures are compared to mean monthly AVHRR data (Advanced Very High Resolution Radiometer, 1999) in Figure 5.

The SST estimates obtained from the MAT at NCR exhibit a similar seasonal range to AVHRR SSTs over the site (Figure 5 and Table 1). The MAT and AVHRR SST values agree within the error of the MAT estimates, although the AVHRR temperatures are consistently lower. The relatively warm temperature estimates obtained from the traps may be caused by the missing winter data between June and August at this site. There is also a fairly good correspondence between the observed SSTs and the trap estimates at SCR during August and February at both trap depths, with differences ranging from 0.2°C to 3.5°C (Figure 5 and Table 1). The winter temperatures are particularly well estimated; the summer temperatures are slightly cooler at the trap sites. This close similarity suggests that the annual flux of foraminifera received over this site is representative of the climatological flux recorded by the core-top sediments. SSTs

recorded by AVHRR data during the deployment period are also representative of the long-term SST variability since 1851, contained within the GOSTA dataset (Figure 2). The MAT SST estimates were derived using this GOSTA climatology, so faunal estimates calibrated using the GOSTA data can be directly compared to AVHRR observations at the trap sites.

The 10 closest analogue sites from the global data base of Brown University (Prell et al., 1999) were used to obtain SST estimates from the trap assemblages. A dissimilarity index obtained for each site defines how close the core-top assemblages are to the trap assemblage. A squared chord distance dissimilarity of <0.2 is considered to indicate a close analogue (Ortiz and Mix, 1997). At NCR the 10 closest analogues provide dissimilarities that are consistently below 0.20 at both trap depths (see Table 1 for average dissimilarities). At SCR the dissimilarities range up to 0.27 at the 300m trap and 0.16 at the 1000m trap. Including only those analogues with dissimilarities of <0.2 at the 300m trap causes SSTs to be slightly less accurate (by up to 0.2°C) than if all 10 analogue samples are included. However, the SST estimates would be slightly improved (to within 2.9°C of the observations) if the 10th analogue site was excluded. Ortiz and Mix (1997) note that stretching the dissimilarity limits well beyond 0.2 does not significantly reduce the quality of the SST values obtained for most of their sediment trap sites. The higher dissimilarities observed in the sediment trap assemblages are most likely the result of interannual variability in the foraminiferal flux not captured by the shorter-term trap deployments.

The location of the 10 core-top analogue sites matched to the trap assemblage provides additional information about the types of environments in which similar assemblages are deposited. Each of the 10 closest analogue sites at SCR 300 and eight of the analogues for the other three traps were located in the Southern Hemisphere, and most of those for SCR were located within the Subantarctic. Very few of the analogue sites were derived from the Southwest Pacific sector, but this mainly reflects the deficiency of Southwest Pacific sites in the global data base.

The MAT was re-run incorporating an additional 33 core-top assemblages located in the Chatham Rise region to determine how well the sediment trap assemblages represent regional core-tops. These additional core-top samples were derived from the data set of Weaver et al. (1997) excluding the Eltanin cores (for which data was not available), and additional sites from data at the University of Tasmania (viz. W266 and W272) and three

from Neil (1997) (Q213, U939 and W268). Duplicate counts of sites U938 and R657, which are already included in the Weaver et al. (1997) data base, were also incorporated. The Weaver et al. (1997) foraminiferal counts include the "*pachyderma-dutertrei* intergrade" category not recognised by this study or the global data base of Brown University (Prell et al., 1999). The Weaver et al. (1997) data base was therefore adjusted by assigning intergrade samples to *Neogloboquadrina pachyderma* (d.).

The Chatham Rise core-top data set provides several close analogues for the trap assemblages. At NCR 300, two of the 10 closest analogue samples obtained were located in the Chatham Rise region, and for the 1000 m trap five regional analogue sites were obtained. Of these sites, all but one was located north of the Subtropical Front (STF). At SCR an even stronger preference for regional core-tops was observed. For the 300 m trap five of the 10 closest analogues were located in the Chatham Rise region, and all 10 sites at the 1000 m trap were from the Chatham Rise data set. All but one of these regional analogue sites were located south of the STF. These results indicate that the faunal assemblages collected by the sediment traps during this one year deployment are distinctive of Southwest Pacific waters north and south of the STF respectively for the NCR and SCR traps.

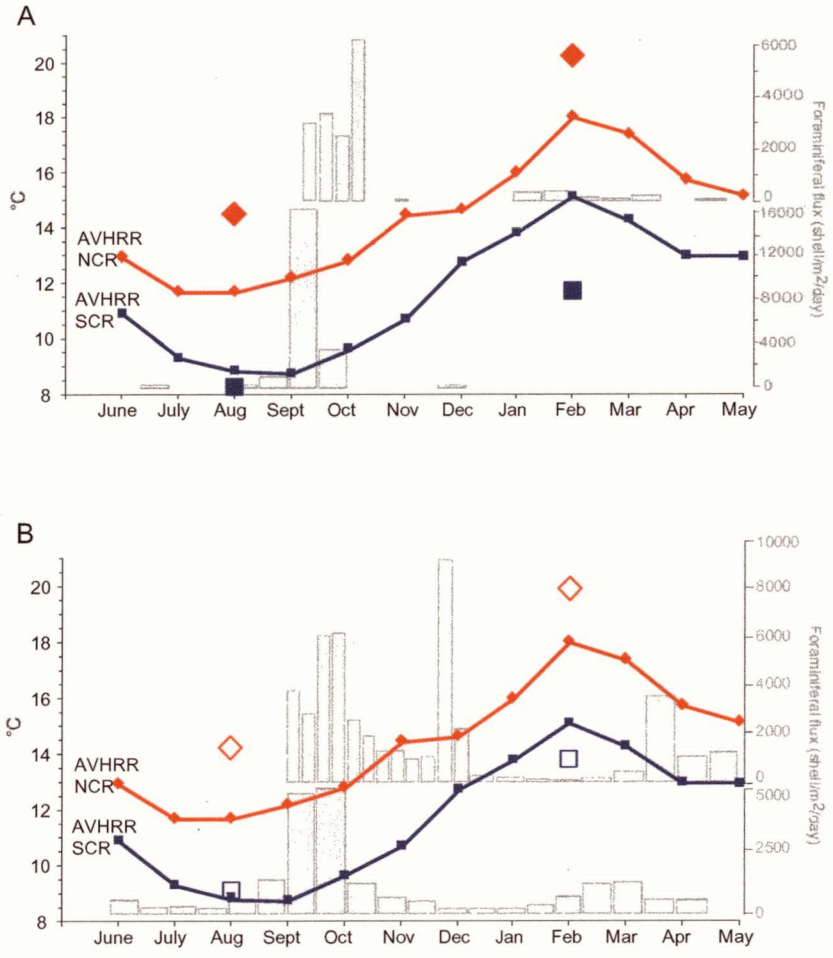

Figure 5: Observed AVHRR SST data from June 1996 to May 1997 at NCR and SCR are compared to the MAT estimates derived from the annual faunal composition collected from each trap site. These data overlie the foraminiferal flux at the 300 m (A) and 1000 m (B) traps. In both (A) and (B) the top flux graph relates to NCR and the lower graph to SCR. The SSTs estimated by the MAT are represented by diamonds at NCR (◆ 300 m and ◇ 1000 m traps); the squares represent the estimated SST at SCR (■ 300 m and □ 1000 m traps). The August and February SST estimates do not correspond to periods of peak foraminiferal flux.

2.3.4 Sediment trap to core-top comparison

A more detailed comparison between the sediment trap assemblages and those at five core-tops located close to each mooring was conducted to assess the relationship between preserved faunal assemblages and the modern fluxes. This comparison is vital since preserved core-top assemblages are related to currently observed sea-surface conditions, forming the framework within which down-core records are investigated. The location and core-top SST estimates for these five sites are listed in Table 1 (see

also locations on Figure 1). There are slight differences between the MAT estimated and observed GOSTA SSTs at these sites. These differences probably reflect the stability of SST gradients in the Chatham Rise region, compared to the analogue sites derived from the Prell et al. (1999) global data base at which similar assemblages are deposited in environments which may be more variable due to seasonal frontal migration. Table 3 provides a summary of the dissimilarities between each of the core-top and sediment trap sites. The dissimilarity values are clearly delineated by the STF, with the lowest dissimilarities calculated for assemblages derived from within each water mass.

The core-top records at W266 and R657 are compared to the assemblages collected from the NCR sediment trap (Figure 6). The core-top and trap assemblages are all dominated by *G. inflata*. The sediment trap assemblages are most similar to the species abundances at W266 with dissimilarities of 0.09 and 0.07 for the 300 m and 1000 m traps respectively (Table 3). These low dissimilarities suggest that flux to both the 300 m and 1000 m traps are representative of the long term faunal variability experienced at site W266. Site R657 records slightly different faunal abundances from the trap data, particularly for *G. inflata* and *N. pachyderma* (d.), and dissimilarities are higher (0.23 for the 300 m trap and 0.17 for the 1000 m trap). Differences between these two core-top assemblages reflect the spatial variability in the region, typical of frontal zones.

	N300	**N1000**	**W266**	**R657**	**S300**	**S1000**	**U939**	**W272**	**U938**
N300	0	*North of STF*							
N1000	0.036	0							
W266	0.088	0.068	0						
R657	0.226	0.168	0.105	0					
S300	0.645	0.560	0.537	0.569	0	*South of STF*			
S1000	0.457	0.350	0.336	0.289	0.297	0			
U939	0.764	0.658	0.655	0.619	0.179	0.162	0		
W272	0.490	0.419	0.350	0.297	0.393	0.063	0.176	0	
U938	0.510	0.457	0.400	0.264	0.578	0.138	0.323	0.090	0

Table 3: Matrix of dissimilarity (squared chord distance) between each of the regional core-tops and sediment trap sites. Dissimilarities among core-tops and sediment traps are highest between sites north and south of the STF (upper left and lower right quadrants respectively).

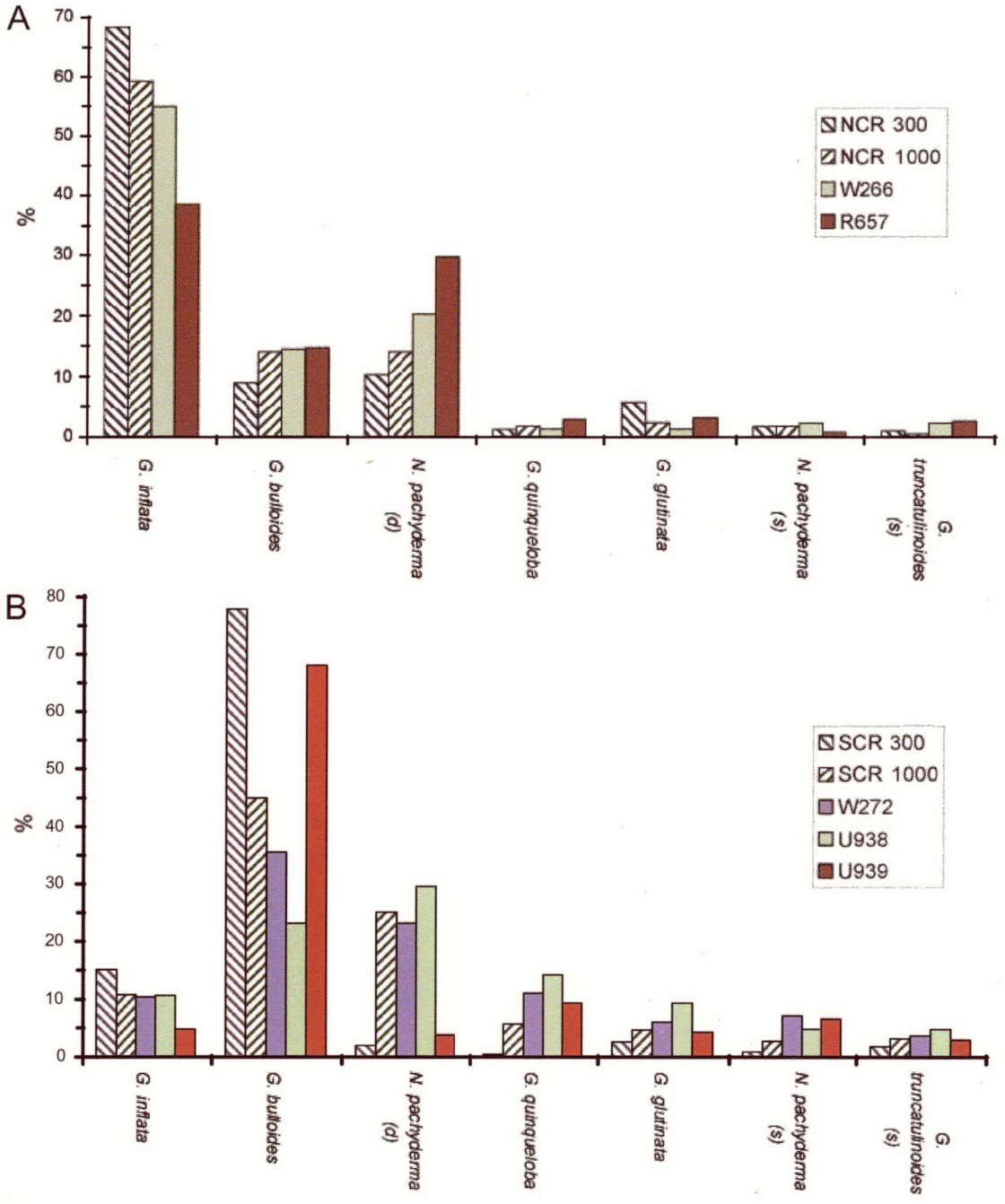

Figure 6: Comparison between core-top and sediment trap assemblages at NCR and SCR.

Three core-top sites are compared to the sediment trap assemblages at the southern site, viz. W272, U938 and U939 (Figure 6). The faunal assemblages collected from the 300 and 1000 m traps are quite different, and are consistent with differences between some of the core-top assemblages. The assemblage at 300 m is most similar to that at sites U939 and W272 with dissimilarities of 0.18 and 0.39 respectively (Table 3). Site U939 and the 300 m trap both exhibit very high abundances of *G. bulloides* (65-80%) and low abundances of *N. pachyderma* (d.) (<5%), in contrast to the other core-top sites and the 1000 m trap which have moderately high abundances of *G. bulloides* (25-45%) and *N. pachyderma* (d.) (25-30%). The 1000 m trap has a dissimilarity index of 0.06 and 0.14 respectively for cores W272 and U938. Differences in the species abundances, particularly the relative abundances of *G. bulloides* and *N. pachyderma* (d.) between the core-top sites, suggests that there may be significant local-scale variability in this region. These regional variations in species abundances are also reflected by the two traps, suggesting that the differences between the two trap depths may be influenced by the same factors driving spatial variability in this region. Such factors may involve the horizontal advection of material by sub-surface currents and meso-scale eddies, although the current speed data suggests that foraminiferal advection, at least at the trap depths, was minimal.

2.4 Discussion

2.4.1 Foraminiferal production and its relation to environmental variables

Peaks in foraminiferal production do not always coincide with those of mass flux (Figure 3), or other particulate fluxes, including particulate phosphorus, nitrogen and biogenic silica (Nodder and Northcote, 2001). These differences suggest that foraminiferal production does not always respond to the environment in the same way as other zooplankton and phytoplankton. Studies at Station P (North Pacific) also exhibit differences in the timing of foraminiferal production compared to peaks in primary productivity and zooplankton biomass (Thunell and Honjo, 1987).

Foraminiferal production is closely associated with the temperature characteristics of the surface mixed layer (Bé and Hutson, 1977). The temperature profiles at NCR and SCR both indicate an increase in surface layer stratification during early spring, intensifying throughout the summer and decreasing again during autumn (Figure 2). Spring peaks in foraminiferal flux at both SCR and NCR coincide with the evolution of the surface mixed layer, and other major peaks at NCR also occur during intervals of moderate thermal stratification. Mass flux also tends to peak during these intervals. Throughout

the summer, however, mass flux at NCR remains relatively high, whereas foraminiferal fluxes are very low during this interval. These low fluxes may be caused by the high thermal stratification during this period, as this would provide only a narrow depth range for species thermal tolerances (Thunell and Honjo, 1987). The relationship among foraminiferal flux, mass flux and thermal stratification suggests that foraminiferal production is primarily affected by the thermal structure of the water column, with food availability (as measured by mass flux) probably of secondary importance in explaining foraminiferal flux variability.

Some differences in the timing of peak foraminiferal fluxes between NCR and SCR occur despite similarities in the seasonal surface layer stratification at the two sites. Both sites record a major spring peak in foraminiferal flux, but peaks during December and March are observed only at NCR. These differences reflect the influence of different water masses on foraminiferal production. However, substantial variability also occurs within the Subantarctic region. A study of sediment traps deployed between May 1997 and June 1998 on the Campbell Plateau, south of New Zealand, record quite different seasonality from that at SCR. A major bloom is recorded during May 1997 (H. Neil, pers. comm.), in contrast to the September peak observed at SCR during the previous year. This difference may reflect spatial heterogeneity within the Subantarctic zone, or interannual variability in foraminiferal production in the region.

2.4.2 Comparison between foraminiferal assemblages at NCR and SCR

The species composition at NCR and SCR reflects the influence of distinctly different water masses over the two sites. The foraminifera at the northern site are dominated by *G. inflata,* which is usually found within a temperature range of ~17 ± 4°C (Bé and Hutson, 1977). The southern assemblage is dominated by *G. bulloides* which has an optimal temperature range of ~13 ± 8°C. Subtropical species such as *Globigerina calida, Globigerinella aequilateralis, Globorotalia crassaformis* and *Globorotalia scitula* are more abundant at the NCR site than in the SCR traps, while subpolar species, including *Globigerina quinqueloba*, reach much higher abundances at the southern site.

Previous research has shown that *G. crassaformis* became extinct south of the Subtropical Front (STF) during Marine Isotope Stage 9 (~300 ka) (Williams, 1976; Howard and Prell, 1992), so its absence in the SCR traps and presence at NCR, provides further confirmation that the STF acts as a barrier between the subtropical and subantarctic water masses in this region. The subtropical faunas present at the northern

trap are influenced by subtropical gyres such as the Wairarapa Eddy which is a permanent warm core eddy with an anticyclonic circulation over the site (Figure 1). The cooler water species present at the southern site reflect the influence of subantarctic waters advected over the site by the West Wind Drift.

The separation of water masses and faunal assemblages across the front suggests that any seasonal migration of the STF in this region is, if it occurs at all, minimal. This is in agreement with the satellite SST analyses of Uddstrom and Oien (1999). The distinction in faunal assemblages north and south of the front also imply that it should be possible to determine the paleo-position of the front from assemblages in down-core records in this region, if frontal migration has occurred over these longer time scales.

2.4.3 Implications for interpreting the down-core record

Sediment trap studies offer the means to validate our approach to paleoclimate research. We can obtain a better environmental interpretation from sedimentary records after comparing modern fluxes, occurring under observed oceanic conditions, with preserved sedimentary records. The results from the present study provide insights into water mass mixing and frontal dynamics in the region of the STF and these results can be applied to down-core studies of sediments.

Foraminiferal assemblages as water mass tracers. Separation of the NCR and SCR sediment traps by the STF creates distinctly different foraminiferal compositions between the two sites, despite a separation of <200 km between them. The faunal differences between subtropical and subantarctic water masses provides a basis for detecting changes in the circulation and characteristics of these water masses in down-core records. The dominance of *G. inflata* over *G. bulloides* seems to be a clear indication of subtropical waters, while the reverse pattern reflects the influence of subantarctic water masses (Prell et al., 1979). The relative abundances of several more minor subtropical species such as *G. crassaformis, G. scitula, G. aequilateralis* and *G. calida* can also be used to detect the influence of subtropical waters. Conclusions based on species abundances should, however, proceed with care since not all variability in faunal composition reflects large-scale oceanic gradients. There is considerable small-scale faunal variability in this region, as seen from the core-top assemblages, and these occur despite little variation in environmental parameters such as SST.

The relationship between foraminiferal faunas and SST needs to be considered in the light of seasonal flux variations. The sediment trap data, at least from this annual record, indicate a seasonal dependency in the flux of foraminifera through the water column. This seasonal cycle, however, differs between the subtropical and subantarctic waters. South of the Chatham Rise the major foraminiferal flux occurs during September, whereas to the north the flux occurs throughout spring, summer and autumn. These northern sediments may therefore capture much more of the intra-annual variability, although no seasonal variability in species composition is observed. The consistency of species composition throughout the year contrasts to other regions, such as the North Pacific (Sautter and Thunell, 1989) and the San Pedro Basin (Sautter and Thunell, 1991) where there is distinct seasonal succession of foraminiferal species related to changes in surface hydrography.

SST estimates. Planktonic foraminifera are a widely used paleoceanographic tool for obtaining estimates of past SST. One technique commonly used for obtaining these SST estimates is the MAT of Hutson (1979), modified by Prell (1985). The MAT has been tested against core-top assemblages and shown to successfully estimate SSTs at core-top and sediment trap sites (Ortiz and Mix, 1997). The MAT relies on the assumption that faunal assemblages are representative of the overlying environment as expressed by SST. This assumption may fail if there has been substantial post-depositional alteration of the assemblage, or greater environmental variability during the time interval represented by the core-top assemblage than is captured by modern SST observations at the site. Sediment trap assemblages allow further validation of the MAT since the SSTs observed at the time of production can be directly compared to the assemblages living within the water column at that time. The study by Ortiz and Mix (1997) found that the MAT provided relatively accurate SST estimates for most of the sediment trap faunas they analysed, with SST estimates ranging within 0.1 and 4.2°C of the observed temperatures at the sites.

The estimation of summer and winter temperatures using the MAT does not account for differences in the seasonal flux of foraminifera to the sea floor. Faunal SST estimates are typically obtained for February and August since these months generally capture the annual temperature range; however, foraminiferal fluxes during these months are relatively low at both SCR and NCR (Figure 5). The two sediment traps used in this study, therefore provide the opportunity to assess how reliably the annual temperature range can be estimated from sites with strong seasonal flux variability.

Comparison between observed and estimated SSTs at NCR and SCR indicate that the MAT estimates summer and winter SSTs ranging between 0.2°C and 3.5°C of the observed values and generally agree within the MAT error. The most consistent match between the observed and estimated SSTs was obtained from SCR 1000 (within 1.3°C), despite the dominant September flux in this record. The SST estimates at SCR 300 are within 3.5°C of the observations even though 80% of the foraminiferal flux is recorded during September at this trap. These results suggests a stable seasonal cycle at the analogue core-top sites. Since the seasonal structure at these sites is consistent with that at the sediment trap site, the spring time foraminiferal flux is sufficient to accurately estimate the annual temperature range. However, for reliable SST estimates to be obtained from down-core samples, the core-top analogues must be located in regions with a similar seasonal structure to that which operated at the time of deposition.

Assemblages at nearby core-top sites were compared to those at the sediment traps to determine the correspondence between the sediments preserved at the surface and conditions in the overlying environment. There are several factors which may create differences between the foraminiferal assemblages preserved in core-tops and the modern assemblages inhabiting the water column. Firstly, the core-top samples represent the average conditions over hundreds and sometimes thousands of years. These mean conditions may deviate from the modern conditions at the same sites. In addition, this study represents collection over one annual cycle, so we cannot evaluate interannual variability and its effect on foraminiferal fluxes. Secondly, the assemblages may have been altered since deposition. Processes which may alter the core-top assemblages include: 1) dissolution within the water column 2) corrosion of calcium carbonate by CO_2 produced by degradation of organic matter within the sediments (Sautter and Sancetta, 1992), 3) bioturbation of the sediments by living benthic organisms, and 4) winnowing of fine-grained material (Wu and Berger, 1991). The effects of these processes can be assessed by comparing the annual assemblages collected from sediment trap samples with those of nearby core-tops.

The sediment traps and nearby core-top assemblages compared in this study are very similar as expressed by the low square chord distances. The close match between the trap and core-top assemblages indicates that the sediments have not been significantly altered since deposition. Preservation of the environmental signature in these core-top assemblages has not been lost since deposition, indicating that they can be interpreted in

terms of the observed modern annual cycle in the near-surface ocean. Since the sediment trap faunas also represent the longer term variability in this region, they provide a good analogue for environmental interpretation of similar faunas deposited in the past.

2.5 References

Advanced Very High Resolution Radiometer (AVHRR), 1999. AVHRR sea surface temperature data. (NOAA/NASA), 20th October 1999, WWW page, http://podaac.jpl.nasa.gov/sst/.

Bé, A.W.H., Hutson, W.H., 1977. Ecology of planktonic foraminifera and biogeographic patterns of life and fossil assemblages in the Indian Ocean. Micropaleontology 23, 369-414.

Belkin, I.M., Gordon, A.L., 1996. Southern Ocean fronts from the Greenwich meridian to Tasmania. Journal of Geophysical Research 101, 3675-3696.

Bottomley, M., Folland, C.K., Hsiung, J., Newell, R.E., Parker, D.E., 1990. Global ocean surface temperature atlas "GOSTA". Meteorological Office Department of Earth, Atmospheric and Planetary Sciences, Massachusetts Institute of Technology, Bracknell, UK, Cambridge, MA, USA, 20 pp.

Bradford-Grieve, J.M., Boyd,P.W., Chang,F.H., Chiswell,S., Hadfield,M., Hall,J.A., James,M.R., Nodder,S.D., Shushkina,E.A., 1999. Pelagic ecosystem functioning in the Subtropical Front region east of New Zealand in austral winter and spring 1993. Journal of Plankton Research 21(3), 405-428.

Bradford-Grieve, J.M., Chang, F.H., Gall, M., Pickmere, S., Richards, F., 1997. Size-fractionated phytoplankton standing stocks and primary production during austral winter and spring 1993 in the Subtropical Convergence region near New Zealand. New Zealand Journal of Marine and Freshwater Research 31, 201-224.

Chiswell, S.M., 1994. Variability in sea surface temperature around New Zealand from AVHRR images. New Zealand Journal of Marine and Freshwater Research 28, 179-192.

Comiso, J.C., McClain, C.R., Sullivan, C.W., Ryan, J.P., Leonard, C.L., 1993. Coastal Zone Color Scanner pigment concentrations in the Southern Ocean and relationships to geophysical surface features. Journal of Geophysical Research 98(C2), 2419-2451.

Currie, K.I., Hunter, K.A., 1998. Surface water carbon dioxide in the waters associated with the subtropical convergence, east of New Zealand. Deep-Sea Research I 45, 1765-1777.

Deacon, G.E.R., 1982. Physical and biological zonation in the Southern Ocean. Deep-Sea Research 29(1A), 1-15.

Deuser, W.G., Ross, E.H., 1989. Seasonally abundant planktonic foraminifera of the Sargasso Sea: succession, deep-water fluxes, isotopic compositions, and paleoceanographic implications. Journal of Foraminiferal Research 19(4), 268-293.

Fenner, J., Carter, L., Stewart, R., 1992. Late Quaternary paleoclimatic and paleoceanographic change over Chatham Rise, New Zealand. Marine Geology 108, 383-404.

Gardner, W.D., Biscaye,P.E., Richardon,M.J., 1997. A sediment trap experiment in the Vema Channel to evaluate the effect of horizontal particle fluxes on measured vertical fluxes. Journal of Marine Research 55, 995-1028.

Guptha, M.V.S., Curry, W.B., Ittekkot, V., Muralinath, A.S., 1997. Seasonal variation in the flux of planktic foraminifera: sediment trap results from the Bay of Bengal, Northern Indian Ocean. Journal of Foraminiferal Research 27(1), 5-19.

Heath, R.A., 1985. A review of the physical oceanography of the seas around New Zealand - 1982. New Zealand Journal of Marine and Freshwater Research 19, 79-124.

Howard, W.R., Prell, W.L., 1992. Late Quaternary surface circulation of the Southern Indian Ocean and its relationship to orbital variations. Paleoceanography 7, 79-118.

Hutson, W.H., 1979. The Agulhas Current during the Late Pleistocene: Analysis of Modern Faunal Analogs. Science 207, 64-66.

Kipp, N.G., 1976. New transfer function for estimating past sea-surface conditions from sea-bed distribution of planktonic foraminiferal assemblages in the North Atlantic. In: R.M. Cline and J.D. Hays (Eds), Investigation of Late Quaternary Paleoceanography and Paleoclimatology. Geological Society of America Memoirs. Geological Society of America, Boulder, Colorado, pp. 3-42.

Levitus, S., 1994. Levitus94: World Ocean Atlas 1994. (NOAA Office of Global Programs and Lamont-Doherty Earth Observatory of Columbia University), 23rd May 2000, WWW Page, http://ingrid.ldgo.columbia.edu/SOURCES/.LEVITUS94/

Murphy, P.P., Feely,R.A., Gammon,R.H., Harrison,D.E., Kelly,K.C., Waterman,L.S., 1991. Assessment of the air-sea exchange of CO_2 in the South Pacific during austral autumn. Journal of Geophysical Research 96(C11), 20,455-20,465.

Neil, H.L., 1997. Late Quaternary variability of surface and deep water masses - Chatham Rise, SW Pacific. Ph.D. Thesis, University of Waikato, Hamilton, New Zealand, unpublished.

Nelson, C.S., Hendy, I.L., Neil, H.L., Hendy, C.H., Weaver, P.P.E., 2000. Last glacial jetting of cold waters through the Subtropical Convergence zone in the Southwest Pacific off eastern New Zealand, and some geological implications. Palaeogeography, Palaeoclimatology, Palaeoecology 156, 103-121.

Nodder, S.D., Northcote, L.C., 2001, Episodic particulate fluxes at southern temperate mid-latitudes (42-45°S) in the Subtropical Front region, east of New Zealand. Deep-Sea Research 48(3), 833-864.

Ortiz, J.D., Mix, A.C., 1992. The spatial distribution and seasonal succession of planktonic foraminifera in the California Current off Oregon, September 1987 - September 1988. In: C.P. Summerhayes, W.L. Prell and K.C. Emeis (Editors), Upwelling Systems: Evolution Since the Early Miocene. Geological Society Special Publication. Geological Society, London, pp. 197-213.

Ortiz, J.D., Mix, A.C., 1997. Comparison of Imbrie-Kipp transfer function and modern analog temperature estimates using sediment trap and core top foraminiferal faunas. Paleoceanography 12, 175-190.

Parker, F.L., 1962. Planktonic foraminiferal species in Pacific sediments. Micropaleontology 8, 219-254.

Pilskaln,C.H., Paduan,J.B., Chavez,F.P., Anderson,R.Y., Berelson,W.M., 1996. Carbon export and regeneration in the coastal upwelling system of Monterey Bay, central California. Journal of Marine Research 54, 1149-1178.

Prell, W.L., 1985. The stability of low-latitude sea-surface temperatures: An evaluation of the CLIMAP reconstruction with emphasis on the positive SST anomalies. Rep. TR 025, U.S. Department of Energy, Washington, D. C.

Prell, W.L., Hutson, W.H., Williams, D.F., 1979. The subtropical convergence and late Quaternary circulation in the southern Indian Ocean. Marine Micropaleontology 4, 225-234.

Prell, W., Martin, A., Cullen, J., Trend, M., 1999. The Brown University Foraminiferal Data Base. (IGBP PAGES/World Data Center-A for Paleoclimatology, Boulder CO, NOAA/NGDC Paleoclimatology Program), 3 April 2000, WWW Page, ftp://ftp.ngdc.noaa.gov/paleo/paleocean/brown_foram.

Roemmich,D., Sutton,P., 1998. The mean and variability of ocean circulation past northern New Zealand: Determining the representativeness of hydrographic climatologies. Journal of Geophysical Research 103(C6), 13,041-13,054.

Sautter, L.R., Sancetta, C., 1992. Seasonal associations of phytoplankton and planktic foraminifera in an upwelling region and their contribution to the seafloor. Marine Micropaleontology 18, 263-278.

Sautter, L.R., Thunell, R.C., 1989. Seasonal succession of planktonic foraminifera: Results from a four-year time-series sediment trap experiment in the Northeast Pacific. Journal of Foraminiferal Research 19, 253-267.

Sautter, L.R., Thunell, R.C., 1991. Planktonic foraminiferal response to upwelling and seasonal hydrograpic conditions: sediment trap results from San Pedro Basin, Southern California Bight. Journal of Foraminiferal Research 21(4), 347-363.

Thunell, R.C., Honjo, S., 1987. Seasonal and interannual changes in planktonic foraminiferal production in the North Pacific. Nature 328, 335-337.

Uddstrom, M.J., Oien, N.A., 1999. On the use of high-resolution satellite data to describe the spatial and temporal variability of sea surface temperatures in the New Zealand region. Journal of Geophysical Research 104(C9), 20,749-20,751.

Weaver, P.P.E., Carter, L., Neil, H.L., 1998. Response of surface water masses and circulation to late Quaternary climate change east of New Zealand. Paleoceaongraphy 13, 70-83.

Weaver, P.P.E., Neil, H., Carter, L., 1997. Sea surface temperature estimates from the Southwest Pacific based on planktonic foraminifera and oxygen isotopes. Palaeogeography, Palaeoclimatology, Palaeoecology 131, 241-256.

Wells, P., Okada, H., 1997. Response of nannoplankton to major changes in sea-surface temperature and movements of hydrological fronts over Site DSDP 594 (south Chatham Rise, southeastern New Zealand), during the last 130kyr. Marine Micropaleontology 3, 341-363.

Williams, D.F., 1976. Late Quaternary fluctuations of the Polar Front and Subtropical Convergence in the Southeast Indian Ocean. Marine Micropaleontology 1, 363-375.

Wu, G., Berger, W.H., 1991. Pleistocene $\delta^{18}O$ records from Ontong-Java Plateau: Effects of winnowing and dissolution: Marine Geology 96, 193-209.

CHAPTER 3

FORAMINIFERAL FLUX FROM SUBANTARCTIC SEDIMENT TRAPS

"Preserve the old but know the new"
Chinese Proverb

Published as: King, A.L. and W.R. Howard, Planktonic foraminiferal flux seasonality in Subantarctic sediment traps: A test for paleoclimate reconstructions, *Paleoceanography, 18*(1), 1019, doi:10.1029/2002PA000839, 2003

Abstract

Sediment trap moorings deployed during 1997 and 1998 in the Subantarctic to Polar Frontal regions of the Southern Ocean reveal distinct seasonality in foraminiferal flux. Foraminiferal assemblages vary between each site, yet major species exhibit very similar patterns of seasonal succession which can be associated with changes in mixed layer depth. Enhanced foraminiferal productivity is also associated with periods of high biogenic silica and particulate organic carbon flux. On a broader scale, foraminiferal assemblages are strongly delineated by temperature. Temperature estimates derived from the assemblages using the Modern Analog Technique (MAT) are mostly within 2.5°C of the satellite AVHRR temperatures observed during the deployment period. This indicates that core top sediments included in the MAT data base do reflect modern observed conditions at the sea-surface, providing a robust technique for estimating past temperature change from foraminiferal assemblages in Southern Ocean environments.

3.1 Introduction

Analyses of planktonic foraminiferal assemblages form a key component of paleoceanographic reconstructions. The utility of foraminifera as tracers of sea-surface temperature (SST) change has been exploited widely in the reconstruction of past climate change in down-core sediments. Sediment trap studies have shown that species fluxes vary seasonally, and that sedimentary records retain an integration of the seasonal flux patterns (Thunell and Honjo, 1987; Deuser and Ross, 1989; King and Howard, 2001). Flux seasonality may be driven by factors other than changes in temperature. It is

therefore important to validate estimates of SST from foraminiferal fluxes in a range of settings with different seasonal flux patterns.

In this study, we analyse planktonic foraminifera derived from sediment traps in three distinct Southern Ocean environments south of Tasmania (the Subantarctic Zone, the Subantarctic Front and within the Polar Frontal Zone). Total fluxes of foraminifera collected by the traps are compared to core top sediments to determine how seasonal fluxes over the collection period are reflected in the sedimentary record. The total fluxes are also used to estimate the annual SST range using the Modern Analog Technique (MAT). Comparison between observed SST and estimates from the trap assemblages allows validation of this technique in Southern Ocean settings.

3.2 Oceanographic Setting

The northernmost sediment trap mooring is located within the Subantarctic Zone (SAZ) (Figure 1). The SAZ extends between ~ 40° and 50°S and is bounded by the Subtropical Front (STF) to the north and the Subantarctic Front (SAF) to the south (Popp et al., 1999; Rintoul and Trull, 2001). In the region south of Tasmania, the STF is generally located near 43°S (Rintoul and Trull, 2001), and is defined by the 11°C isotherm at 150 m (Rintoul et al., 1997). The SAZ marks the transition between subtropical nutrient-depleted waters and nutrient-rich waters of the southern Polar Frontal zone (PFZ) (Rintoul and Trull, 2001). The SAF is marked by the region of largest horizontal temperature gradients at a depth of 300 m (3-8°C), and is associated with the eastward flow of the Antarctic Circumpolar Current (ACC) (Rintoul et al., 1997). The SAF represents the boundary between SAZ and PFZ water masses, and south of Tasmania, the core of the SAF is located at 51.5°S (Rintoul and Trull, 2001). The second mooring is located within the SAF zone at 51°S. The most southerly mooring is located at 54°S, near the mean position of the Polar Front (PF) (Popp et al., 1999). The PF is best defined by the northern-most extent of cold subsurface waters, marked by the 2°C isotherm at ~200 m depth in summer and at the surface in winter (Belkin and Gordon, 1996). The PFZ is located between the southern ACC and the SAF to the north (Figure 1).

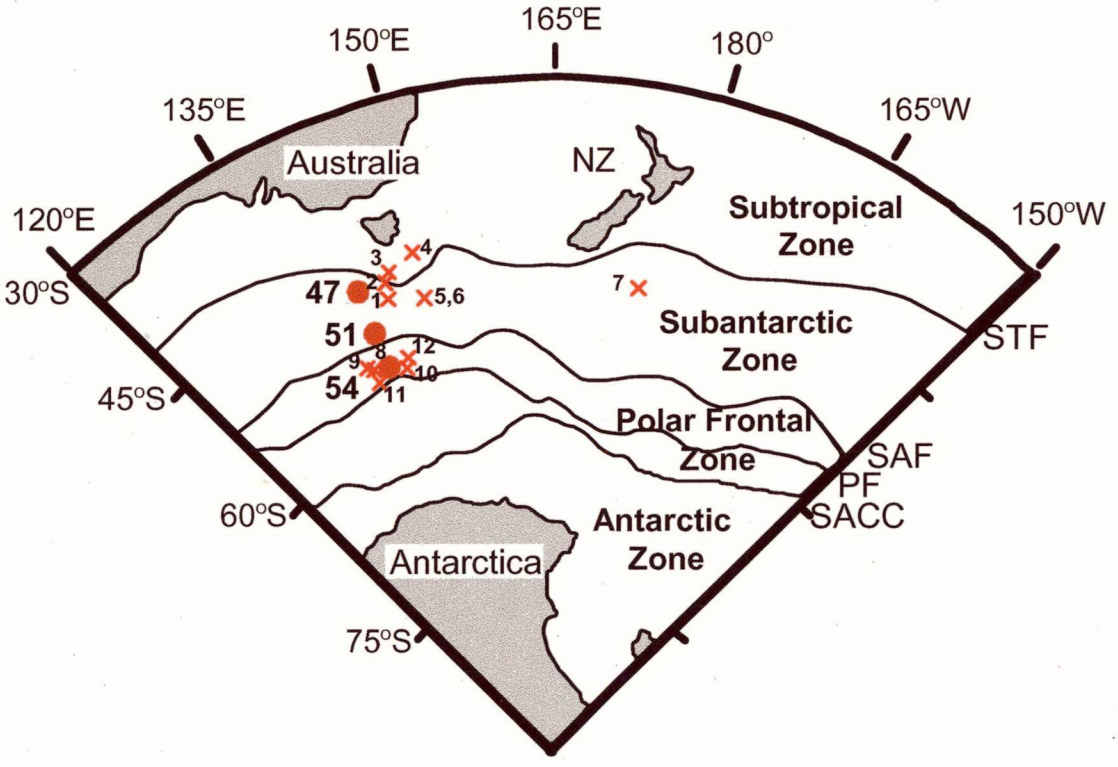

Figure 1: Trap (•) and core top (x) locations in relation to water masses and fronts. Core tops are as follows: 1: RS147-17G; 2: RS147-14G; 3: MD972-106G; 4: RS147-31G; 5: SO136-147B; 6: MD972-108B; 7: MD972-110G; 8: ELT36-1PH; 9: ELT36-5PC; 10: ELT53-14PC; 11: ELT36-6PC; 12: ELT53-13PC. (G refers to gravity core, B to box core, PH to phleger core and PC to piston core). Figure adapted from L. Armand pers. comm., with frontal locations based on Orsi et al. (1995).

The Southern Ocean fronts create biological as well as thermal boundaries. The SAZ region is marked by enhanced biological production compared to waters north of the STF (Banse, 1996), and is dominated by calcareous organisms, including high coccolithophorid abundances (Deacon, 1982; Popp et al., 1999), and other prymnesiophytes, cyanobacteria and autotrophic flagellates (Kopczynska et al., 2001). South of the PF biological production is dominated by siliceous organisms, with flagellates and coccolithophores exhibiting much lower abundances. Surface sediments throughout the Southern Ocean similarly reflect this biological zonation (eg. Deacon, 1982). The fronts themselves are associated with enhanced biological productivity. SeaWiFS (Sea-viewing Wide Field-of-view Sensor) (Moore et al., 1999) and CZCS (Coastal Zone Color Scanner) (Comiso et al., 1993) data both indicate higher pigment concentrations associated with each of the frontal bands. During the sediment trap

deployment, SeaWiFS data indicate a December peak in chlorophyll-a concentrations in the southern SAZ, at the SAF and in the PFZ (Trull et al., 2001).

Biological production in the SAZ and PFZ is highly seasonal, with most production occurring during the austral spring and summer. The consistency of the spring and summer blooms within the Subantarctic and Polar Frontal regions south of Tasmania is revealed by 8 years of ocean color data (Comiso et al., 1993). Annual sediment trap moorings deployed as part of the AESOPS program between 53° and 66° south along 170°W, also clearly reveal the dominance of biological production between September and March, with very little production throughout the remainder of the year (see Honjo et al., 2000). Foraminiferal records obtained from a year long trap deployment south of Chatham Rise east of New Zealand, indicate that 85% of the foraminiferal production at this Subantarctic site occurs between September and March (King and Howard, 2001). The sediment trap deployments in the present study were therefore planned to sample the peak biological productivity throughout the austral spring and summer.

3.3 Methods

3.3.1 Sediment trap moorings

Sediment trap moorings were deployed between September 1997 and February 1998 along 142°E longitude in the central SAZ (47°S, traps at 1060, 2050 and 3850 m – hereafter referred to as 47-1000, 47-2000 and 47-3800), at the SAF (51°S, one trap a 3080 m – referred to as 51-3100) and within the PFZ (54°S, two traps at 830 and 1580 m – referred to as 54-800 and 54-1500) (Figure 1) (see Bray et al., 2000, Trull et al., 2001). Each mooring was recovered successfully and here we present data for the deeper traps from each site. Data for the shallower traps are archived at the World Data Center A for Paleoclimatology[1]. Moorings at 47°S were redeployed during the following year between 15th March 1998 and 5th February 1999, while traps at 54°S were deployed between 24th March 1998 and 5th February 1999. During the 1998/99 deployment, a complete record was obtained for the 47-3800 mooring only. The 1000 m trap at 47°S failed to collect material after the fourth sampling interval, and a technical failure prevented collection by the 2000 m trap. At 54°S, material was deposited only in the first sample cup at both depths, presumably due to clogging of the trap funnel. The 47-3800 record and the first cup at 54°S are presented here in conjunction with the 1997 results. For mooring locations refer to Table 1.

[1] All data is available electronically via the World Data Center A for Paleoclimatology, NOAA/NGDC, 325 Broadway, Boulder, Colorado (URL: http://www.ngdc.noaa.gov/paleo)

Each mooring consisted of a McLane 21-cup trap with a current meter deployed 20 m below each trap (see Bray et al., 2000). The current meters measured speed, direction, pressure and temperature. Temperature was measured each time a cup was changed. For the 1997 deployment the cups were open for 8.5 days for the majority of the time, changing to 4.25 days throughout January. During the 1998 deployment, cups were open for 15.5 days, except for the first cup at 47°S which was open for 24.5 days to coincide with the remainder of the collection times at 54°S. Traps were placed at least 700 m above the bottom to avoid collection of resuspended material.

Each cup was prepared with a solution of unfiltered seawater buffered with borate and made up to a high-density brine with sodium chloride. Mercuric chloride was used as a preservative (see Bray et al., 2000 for details). Upon recovery samples were repoisoned with 100 µl of saturated mercuric chloride and stored at 4°C in the dark.

Foraminiferal assemblages from nearby core top sites are compared to each trap assemblage. Core tops were derived from Rig Seismic cruise 147 (RS147), Marion Dufresne cruise 972 (MD972), Sonne cruise 136 (SO136) and Eltanin cruises 36 and 53 (ELT36 and ELT53). Locations are shown in Figure 1.

Table 1: Sediment trap deployments

Location and core	Latitude/longitude	Trap depth (m)	Water depth (m)	Deployment period
47-1000	46°45.6'S; 142°4.2'E	1060	4540	21/09/97 to 21/02/98
47-3800 1997	46°45.6'S; 142°4.2'E	3850	4540	21/09/97 to 21/02/98
47-3800 1998	46°45.6'S; 142°4.2'E	3850	4540	15/03/98 to 05/02/99
51-3100	51°0.01'S; 141°44.3'E	3080	3780	21/09/97 to 21/02/98
54-800	53°44.8'S; 141°45.5'E	830	2280	21/09/97 to 21/02/98
54-1500 1997	53°44.8'S; 141°45.5'E	1580	2280	21/09/97 to 21/02/98
54-1500 1998	53°44.8'S; 141°45.5'E	1580	2280	24/03/98 to 05/02/99

3.3.2 Sample analysis

Samples were washed through a 1 mm sieve and the <1 mm fraction split into ten aliquots with a McLane rotary splitter. One aliquot was used for foraminiferal analyses for the 1997 season, and two or three aliquots were analysed for the 1998 season. Foraminifera were extracted by washing each sample through a series of stainless steel sieves (500µm, 425µm, 355µm, 250µm and 150µm) using pH 7–8 deionised water buffered with sodium borate. Samples containing large amounts of organic matter were

soaked in a buffered 3% peroxide solution for up to 1 hour to dissolve the organic matter prior to sieving. Samples were then filtered onto 0.45 or 0.8 μm filters, with filters retained for future analysis.

The planktonic foraminifera (>150μm) were identified according to the taxonomy of Parker (1962)and Kipp (1976), although the "*pachyderma-dutertrei* intergrade" category was not recognized. This taxonomy is consistent with the global core top data set employed in this study which was derived from the global data base of Brown University (Prell et al., 1999). At least 300 individuals were counted where available in each sample. Foraminiferal flux estimates were made in terms of number of specimens $m^{-2}d^{-1}$, taking into account the duration of each collection period and the cross-sectional area of the trap (0.5 m^2). Further work is currently underway to derive the isotopic and trace metal composition for various species of planktonic foraminifera from the traps. This work will be published shortly, together with results from Chatham Rise, east of New Zealand (see for example King and Howard, 2001).

Sea-surface temperatures (SSTs) were estimated from the total assemblage collected from each trap using the Modern Analog Technique (MAT) of Hutson (1979), modified by Prell (1985). The MAT is a commonly used technique in paleoclimate studies to estimate SSTs from foraminiferal assemblages. SSTs are obtained by comparing the sample assemblage to assemblages in the Brown University global core top data base (Prell et al., 1999), incorporating the Global Ocean Surface Temperature Atlas (GOSTA) climatological SST data set (Bottomley et al., 1990). Similarity between the trap and core top foraminiferal assemblages is determined by the squared chord distance dissimilarity, where a dissimilarity of <0.2 is considered to indicate a close analog (Ortiz and Mix, 1997). The summer and winter SSTs at sites exhibiting the closest similarity in foraminiferal assemblages (with a dissimilarity cut off of 0.2) are assigned to the sample. By estimating SSTs from the trap samples, at which the SSTs at the time of deposition are known, we can test the accuracy of the MAT estimates.

Monthly sea-surface temperatures (SST) during the deployment period were determined from the average observed satellite AVHRR data at each site (Advanced Very High Resolution Radiometer (AVHRR), 1999). Climatological SSTs (compiled from data between 1961-1990) were derived from the GOSTA data set (Bottomley et al., 1990), and provide the basis for estimating SSTs from core top foraminiferal assemblages. The AVHRR sea-surface temperatures measured during the deployment

period are generally close to the long term mean SSTs recorded in the GOSTA data set (Global Ocean Surface Temperature Atlas) (Bottomley et al., 1990) (Table 2). The similarity between the satellite and climatological SST observations indicate that conditions during the deployment period were representative of the long term climatic conditions in the region, although AVHRR temperatures at 47°S during the summer of 1998 are warmer than average observations in the GOSTA data set. There are larger differences between the AVHRR and GOSTA temperatures at 51°S and 54°S, however data points in the GOSTA data set at these southerly sites are sparse.

The World Ocean Atlas 1994 (Levitus, 1994) is also employed in this study since this data set provides a monthly climatological temperature record with depth. Mixed layer depth at each site is derived from this atlas, with the climatological depths consistent with observed mixed layer depths during September and March cruises during the deployment period.

3.4 Results

3.4.1 Foraminiferal flux to traps

47°S mooring. In this section we present results from the 3800 m trap only, although there is very good consistency in fluxes between the 3800 m and 1000 m traps. The complete data set for the 3800 m and 1000 m traps is available from the World Data Center A for Paleoclimatology[1]. Foraminiferal flux at 47°S exhibited two peaks in production during the 1997 deployment (Figure 2a). These occurred during October and mid-January with fluxes of 950 shells $m^{-2}d^{-1}$ and 3250 shells $m^{-2}d^{-1}$ respectively. The 1998 record at 3800 m commenced 3 weeks after the conclusion of the 1997 deployment. High summer foraminiferal fluxes continued at the start of the 1998 deployment (Figure 2a). The highest foraminiferal flux occurred during late March (1660 shells $m^{-2}d^{-1}$) with peaks of ~1350 shells $m^{-2}d^{-1}$ during May (Figure 2a). Fluxes decreased between July and September (<200 shells $m^{-2}d^{-1}$), and increased in October to 970 shells $m^{-2}d^{-1}$, similar to the magnitude of flux during October 1997. A slight increase in foraminiferal flux was observed at the end of January 1999.

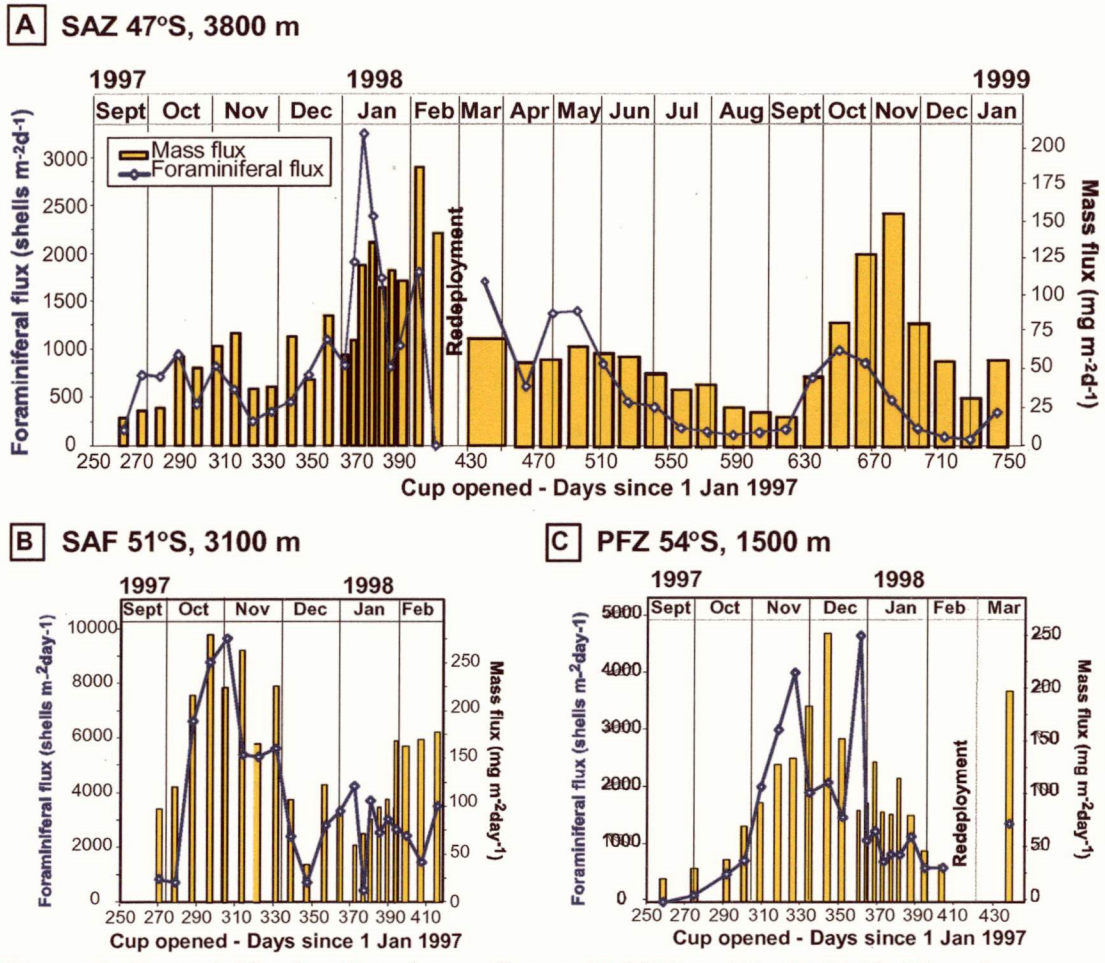

Figure 2: Foraminiferal and total mass flux at 47-3800 m (**A**), 51-3100 (**B**) and 54-1500 (**C**). Seasonal fluxes vary between each site. At 47°S, summer fluxes dominate, while spring fluxes are highest at 51°S, and high fluxes occur during late spring and summer at 54°S. Total mass flux data from Trull et al. (2001).

51°S mooring. The foraminiferal flux at 51-3100 (1997 deployment) displays quite a different seasonal pattern to that at the 47°S mooring (Figure 2b). At this trap there was a broad peak in foraminiferal flux throughout October and November, with relatively lower values during the austral summer. The foraminiferal flux was also much higher at 51°S than at the 47°S mooring. The major October foraminiferal flux was >9500 shells $m^{-2}d^{-1}$ while the relatively low summer fluxes exhibited peaks of up to 4270 shells $m^{-2}d^{-1}$, higher than peak fluxes recorded at the 47°S site.

54°S mooring. Foraminiferal fluxes are presented here for the 1500 m trap, with results from the trap at 800 m available electronically from the World Data Center for Paleoclimatology[1]. Maximum foraminiferal fluxes at 54-1500 were recorded during

November (4000 shells $m^{-2}d^{-1}$) and early January (4800 shells $m^{-2}d^{-1}$) (Figure 2c). The overall foraminiferal flux at the 54°S site during the 1997 deployment was lower than at the 51°S site, but much higher than in the 47°S trap.

During the 1998 deployment, material was only collected in the first cup at both trap depths. The absence of material throughout the remainder of the deployment period was probably due to clogging of the trap cone as observed in other studies using 0.5 m^2 diameter traps (Pilskaln et al., 1996; Honjo et al., 2000).

3.4.2 Foraminiferal composition

47°S mooring. The species composition at 47-3800 exhibited considerable seasonal variability (Figure 3a). The most abundant species overall was *Neogloboquadrina pachyderma* (d.), accounting for 25% of the total flux during the 1997 deployment and 35% in the 1998 deployment. This species was dominant from January to June 1998. During September and the early part of October in both the 1997 and 1998 records, *Globigerina bulloides* dominated the assemblage (up to 70%), with increased abundances of *Globorotalia inflata* (30%) during the latter part of October and early November in the 1997 record.

The species abundances and total flux between December and February differed between the 1997 and 1998 deployments. During December 1997 the assemblage was dominated by *Globigerina quinqueloba* (40%), and there were peaks in *N. pachyderma* (d.) (up to 45%) and *N. pachyderma* (s.) (~15%) during January and February. In the 1998 deployment fluxes during December and January dropped to very low values, with a slight increase in mid-January by *G. bulloides*, *G. quinqueloba* and *N. pachyderma* (d.), each making up 25 to 30% of the flux at this time.

Minor species, with abundances of less than 20%, showed a seasonal succession which was generally consistent between the 1997 and 1998 records. During September of 1997 and 1998 *Globigerina falconensis* was present with abundances of up to 4%. *Globorotalia scitula* peaked during November and December (with a maximum of 12% in 1997 and 20% in 1998). *Orbulina universa* had a distinct peak of 10% towards the end of December 1997 and of 2% in 1998. This species was also abundant during July to September 1998 with peaks up to 7%. *Neogloboquadrina dutertrei* was present during January 1997 and April and May 1998 with abundances of a few percent. These minor species predominantly occupy subtropical waters (Bé and Hutson, 1977). We speculate

that they may indicate brief intervals during which warmer waters were advected over the site, possibly at depth since warm water incursions were not apparent in the satellite SST data. Warmer waters may be mixed southwards by eddies associated with the East Australia Current which 'leak' beneath Tasmania and enter the SAZ during the summer months (Cresswell, 2000). High abundances of *O. universa* between July and September suggest that warmer waters may also have been advected into the SAZ during winter and early spring.

51°S mooring. The dominant species at 51°S was *G. bulloides* (Figure 3b). This species accounted for over 50% of the total foraminiferal flux received at the site, but was most abundant during October and November when there were also relatively high abundances of *G. inflata*. Fluxes of *N. pachyderma* (s.) and *N. pachyderma* (d.) increased throughout December, dominating the assemblage during January and February. *N. pachyderma* (s.) accounted for up to 40% of the assemblage during this summer period. The seasonal succession patterns at 51°S were consistent with those observed at 47°S for the major species, despite differences in the season of peak production. Minor species were very rare at the 51°S site indicating a much lower species diversity than at the 47°S mooring.

54°S mooring. The foraminiferal assemblage at 54°S was composed primarily of five species (viz. *N. pachyderma* (s.), *G. quinqueloba, G. bulloides*, *G. glutinata* and *N. pachyderma* (d.) listed in order of abundance) (Figure 3c). The dominance by *N. pachyderma* and *G. quinqueloba* at this site is similar to the pattern of foraminiferal flux at the station PAPA sediment trap mooring in the northeast Pacific (Sautter and Thunell, 1989). *N. pachyderma* (s.) was present throughout the deployment period at the 54°S site, reaching peaks of over 85% during late January to early February and 80% during late October. Overall, this species accounted for 45% of the flux at 1500 m (Appendix I). Fluxes of *G. quinqueloba* were highest during November and December with peaks of up to 70%. *G. bulloides* reached maximum abundances during December and January (up to 15% of the assemblage at this time). *G. inflata* was also present during this interval reaching abundances of up to 9% during September at 1500 m.

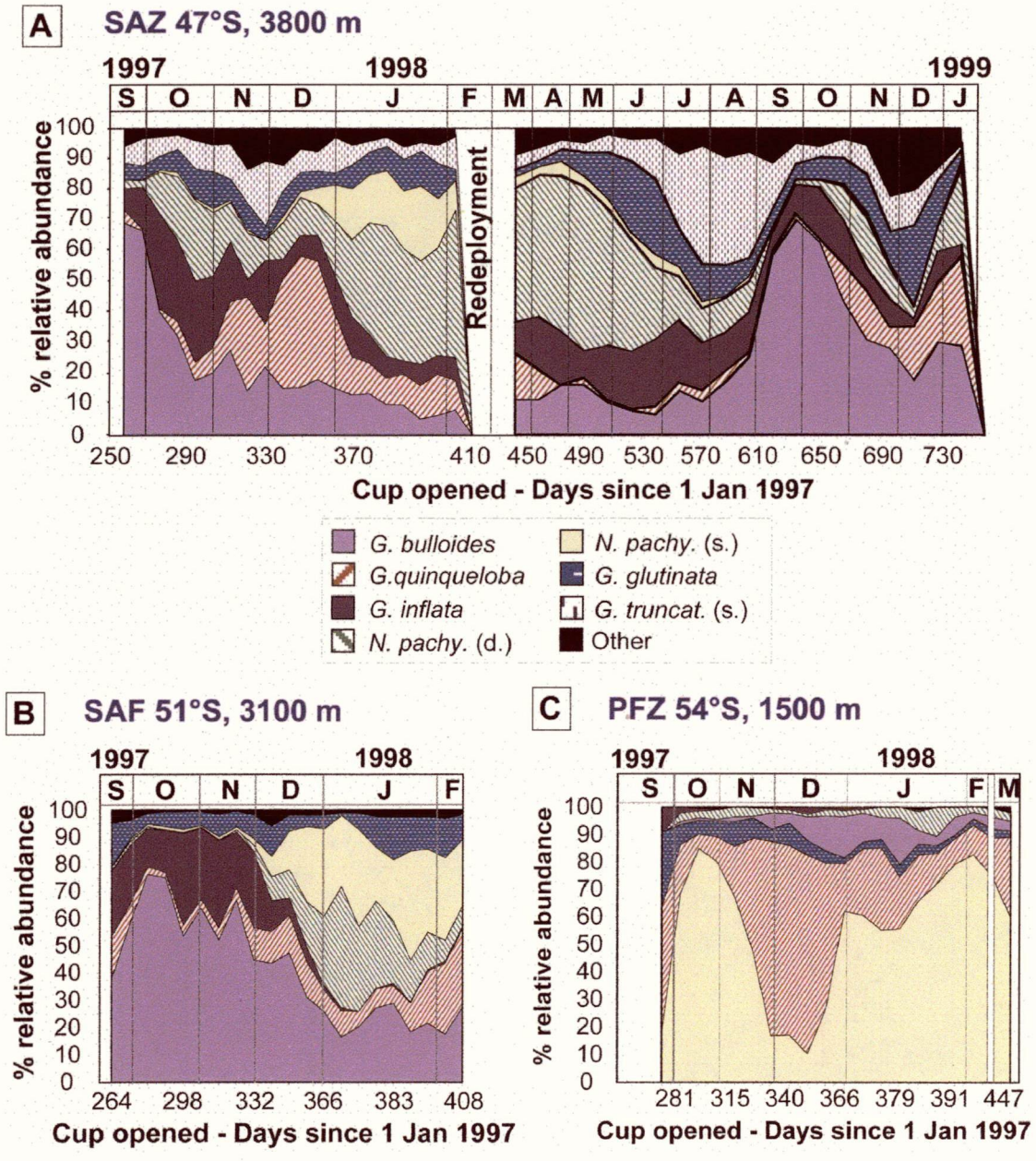

Figure 3: Species relative abundances at 47-3800 (**A**), 51-3100m (**B**) and 54-1500 m (**C**). Species seasonal succession patterns are consistent between each region. *G. bulloides* dominates the spring fluxes at 47°S and 51°S, while *N. pachyderma* (s. and d.) is the most abundant species during the summer months at all sites.

3.4.3 Core tops and interannual variability

We compared several core tops collected from the South Tasman Rise to the integrated sediment trap assemblages (see Figure 1 for locations). The core tops were distributed between 44° and 48°S, and near 54°S and represent accumulation integrated

over centuries to millennia. Comparison between the surface sediments and the trap assemblages allowed us to determine how well the 6 month sediment trap deployments represent the long term mean fluxes in this region. Comparison between the 1997 and 1998 deployments at the SAZ site also provided insight into the interannual variability in foraminiferal fluxes at this site.

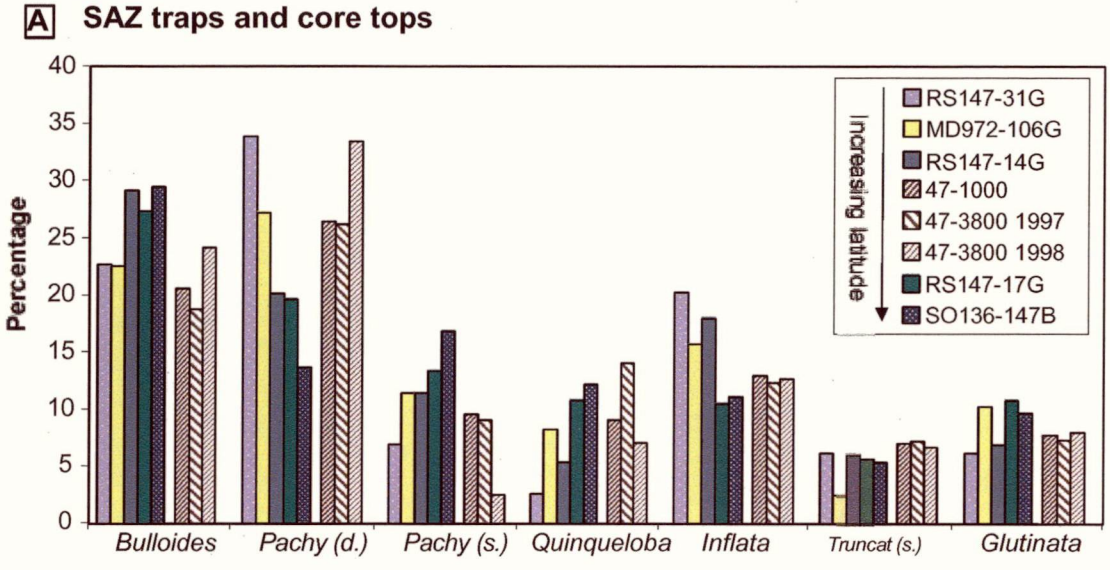

Dissimilarity to core tops

	47-1000	47-3800 1997	47-3800 1998
RS147-31G	0.070	0.092	0.064
MD972-106G	0.052	0.050	0.084
RS147-14G	0.050	0.056	0.078
RS147-17G	0.050	0.047	0.099
SO136-147B	0.070	0.070	0.146

Figure 4: Core top and sediment trap assemblages in the region of 47°S (**A**), 51°S (**B**) and 54°S (**C**) sites. Assemblages from both the 1000 m and 3800 m traps are shown for the 47°S site, and from the 800 m and 1500 m trap at 54°S. Also shown (in inset table) are the dissimilarities between the assemblages at each site. At the 47°S site dissimilarities are generally lower for the 1997 than the 1998 deployment. Higher dissimilarities during 1998 reflect the lower abundance of *N. pachyderma* (s.), and relatively high abundances of *N. pachyderma* (d.). At the 51°S sediment trap, abundances of *G. bulloides* and *G. inflata* are generally higher than in the core tops, while other species have lower abundances. In the PFZ, abundances of *G. quinqueloba* are much higher than in the core tops, while *N. pachyderma* (s.) is generally less abundant. This results in relatively high dissimilarities with PFZ core tops.

B **SAF traps and core tops**

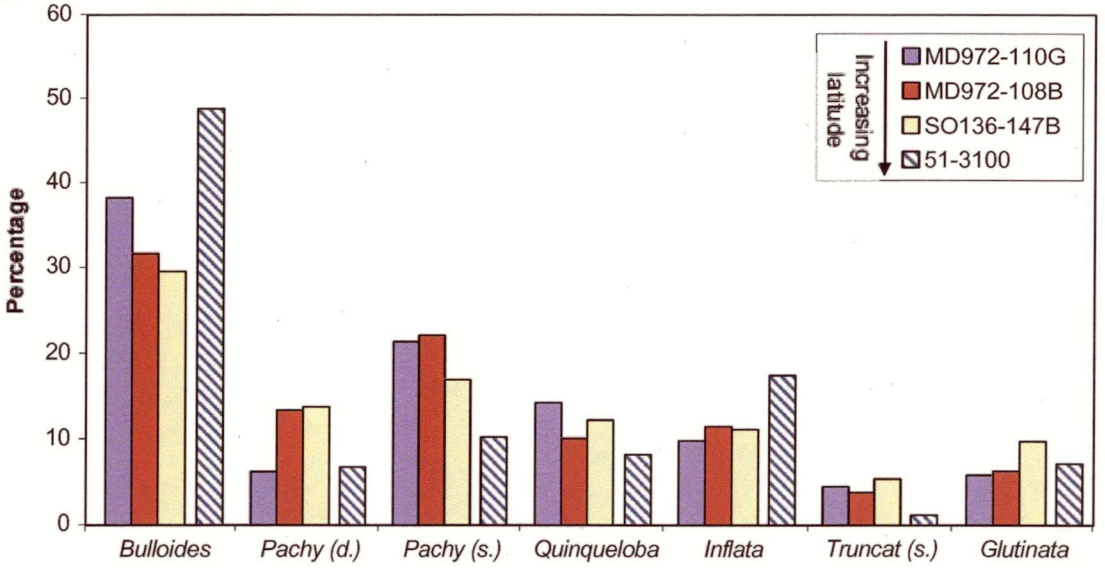

Dissimilarity to core tops

	51-3100
MD972-110G	0.066
MD972-108B	0.094
SO136-147B	0.099

C **PFZ traps and core tops**

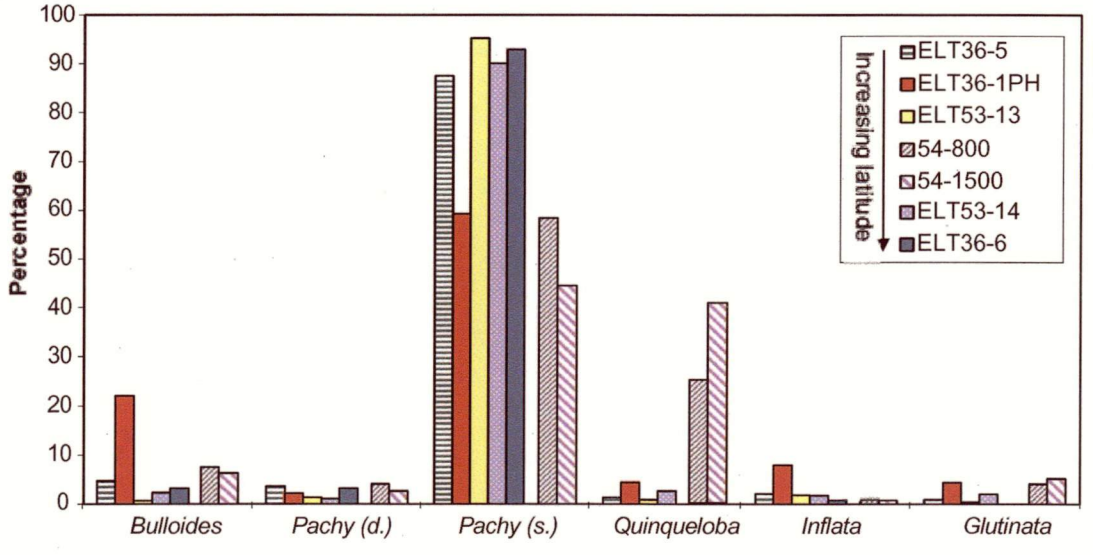

Dissimilarity to core tops

	54-800	54-1500
ELT36-5G	0.188	0.383
ELT36-1PH	0.166	0.288
ELT53-13G	0.270	0.472
ELT53-14	0.166	0.339
ELT36-6	0.324	0.559

Figure 4 (continued)

SAZ core tops. The core tops from the SAZ region exhibited close similarity with the sediment trap assemblages at 1000 m and 3800 m at the 47°S mooring. Five core tops within close proximity of the 47°S trap (numbers 1 to 5 on Figure 1) each had dissimilarities of between 0.05 and 0.1 (Figure 4a) indicating a close correspondence between the assemblages. The 1997 data set had lower dissimilarities to the core tops than the 1998 data, despite the shorter collection period for the 1997 traps. This suggests that the September to February interval captured most of the annual variability recorded by the sediments. The higher dissimilarities for the 1998 traps implies that the species fluxes during this year were not typical of the longer term flux patterns in this region. It is likely that there was some interannual variability in the foraminiferal fluxes to this region.

The 1998 trap contained relatively low proportions of the sub-polar species *N. pachyderma* (s.), and higher abundances of the temperate dextral form of *N. pachyderma* compared to the core tops (Figure 4a). Subtropical species (including *N. dutertrei, O. universa, G. calida* and *G. falconensis*) were also found in higher abundances in the 1998 traps than in the core tops. This change in flux patterns implies that warmer water masses drifted over the site during 1998, consistent with higher-than-average AVHRR summer SSTs at 47°S in 1998/1999 (Table 2).

SAF core tops. Several core tops from 48°S compared well with the assemblage from the 51°S sediment trap. The core tops MD972-110, MD972-108 and SO136-147 each had dissimilarities of < 0.1 with the 51-3100 assemblage (Figure 4b). The greatest difference between the trap and core top assemblages were higher abundances of *G. bulloides* and lower abundances of *N. pachyderma* at the 51-3100 trap.

PFZ core tops. Several Eltanin cores are located close to the 54°S trap mooring. The sites ELT36-1PH, ELT53-14 and ELT36-5 yielded dissimilarities of <0.2 against the 800 m sediment trap mooring and <0.4 against the 1500 m assemblage (Figure 4c). Abundances of *G. quinqueloba* at each of these sites were much lower than at the sediment trap site, suggesting that the flux of this species was anomalously high during the deployment interval. The relatively lower abundances of *G. quinqueloba* in the core tops may also reflect alteration of the surface sediments since deposition by dissolution or other processes. The core top sediments contained little fragmentation of shells which

suggests that foraminifera were well preserved, but core top material may have been lost through the piston coring process.

3.4.4 Sea-surface temperature estimates

SST estimates were derived from the total foraminiferal assemblage at each trap site to test results from the Modern Analog Technique (MAT) against observed satellite AVHRR (AVHRR, 1999) data.

47°S mooring. SST estimates from 47-1000 and 47-3800 were very similar to each other for the 1997 deployment, and were consistent with observed AVHRR data (AVHRR, 1999) and the longer term GOSTA climatology (Bottomley et al., 1990) (Table 2, Figure 5a). The SST estimates from the 1998 data set were a few degrees warmer than those for the 1997 traps, consistent with warmer observed AVHRR temperatures. Winter SSTs estimated from the 1997 trap samples were within 0.2°C of the AVHRR temperatures and 0.5°C of the GOSTA data, while summer temperatures were up to 1.2°C warmer than the observations. The 1998 estimates had a greater deviation from the observed data. Winter temperatures were 2.3°C warmer than AVHRR and 1.3°C warmer than the GOSTA data, while summer temperatures were up to 1.8°C warmer than the AVHRR data and 2.6°C warmer than GOSTA. The AVHRR temperatures, however, were close to within 1 standard deviation of the MAT estimates (Table 2). Dissimilarities for the ten closest analogs at 47-3800 range between 0.09 and 0.17.

51°S mooring. Winter SST estimates at 51-3100 were within 2.8°C and 1.2°C of the AVHRR and GOSTA data, and summer estimates were within 1.8° to 1.5°C (Table 2, Figure 5b). Differences between the estimated and observed temperatures were generally within one standard deviation of the analog values. The 10 analog sites had a maximum dissimilarity of 0.1 and were located between 41° and 54°S.

54°S mooring. The MAT temperatures derived from the 54°S site were consistently overestimated compared to the AVHRR and GOSTA values at both the 800 m and 1500 m trap (Table 2, Figure 5c). Winter values were 2.5°C higher than AVHRR and 1°C higher than GOSTA. Summer temperatures were up to 4.6°C too high compared to AVHRR and 3°C higher than GOSTA. These offsets from observed temperatures mainly reflect the relatively warm SSTs at coretop analog sites identified by the MAT. The warm estimates are due, in part, to a greater proportion of *G. quinqueloba* in the

traps than is normally found in Southern Ocean cores (Figure 4c). The foraminiferal assemblages at the 800 m and 1500 m traps consisted of 24 and 41% *G. quinqueloba* respectively, while the highest abundance of *G. quinqueloba* in nearby core tops was 4% (Figure 4c). North Atlantic sites tend to have relatively high abundances of *G. quinqueloba*, so all analogs at this site were derived from North Atlantic core tops. The warmer temperatures of the North Atlantic in similar subpolar environments resulted in the overestimation of SSTs from the foraminifera at 54°S. An advantage of using the Modern Analog Technique is that a dissimilarity index is generated with the estimates, providing one indication of the reliability of the temperature estimates. At 54-1500, the dissimilarities for the ten closest analogs range between 0.12 and 0.18.

Table 2: Observed and estimated SST from the sediment trap sites. GOSTA SSTs (Bottomley et al., 1990) derived from long-term observations at the trap sites are compared to the AVHRR SSTs observed during the trap deployment period (AVHRR, 1999).

Location and core	MAT SST estimates (°C)		Average dissimilarity
	Summer	Winter	
47-1000	12.9±1.73	8.89±1.37	0.14
47-3800 1997	13.03±1.69	8.55±1.25	0.14
47-3800 1998	14.85±1.79	10.37±1.63	0.12
AVHRR 1997	11.85	8.7	_
AVHRR 1998	13.05	8.1	
GOSTA	12.2	9.1	_
51-3100	9.71±2.22	6.33±2.29	0.09
AVHRR	7.95	3.45	_
GOSTA	8.2	5.1	_
54-800	9.49±1.07	4.01±1.29	0.09
54-1500	9.34±1.03	3.96±1.23	0.14
AVHRR	4.95	1.5	_
GOSTA	6.7	3.0	_

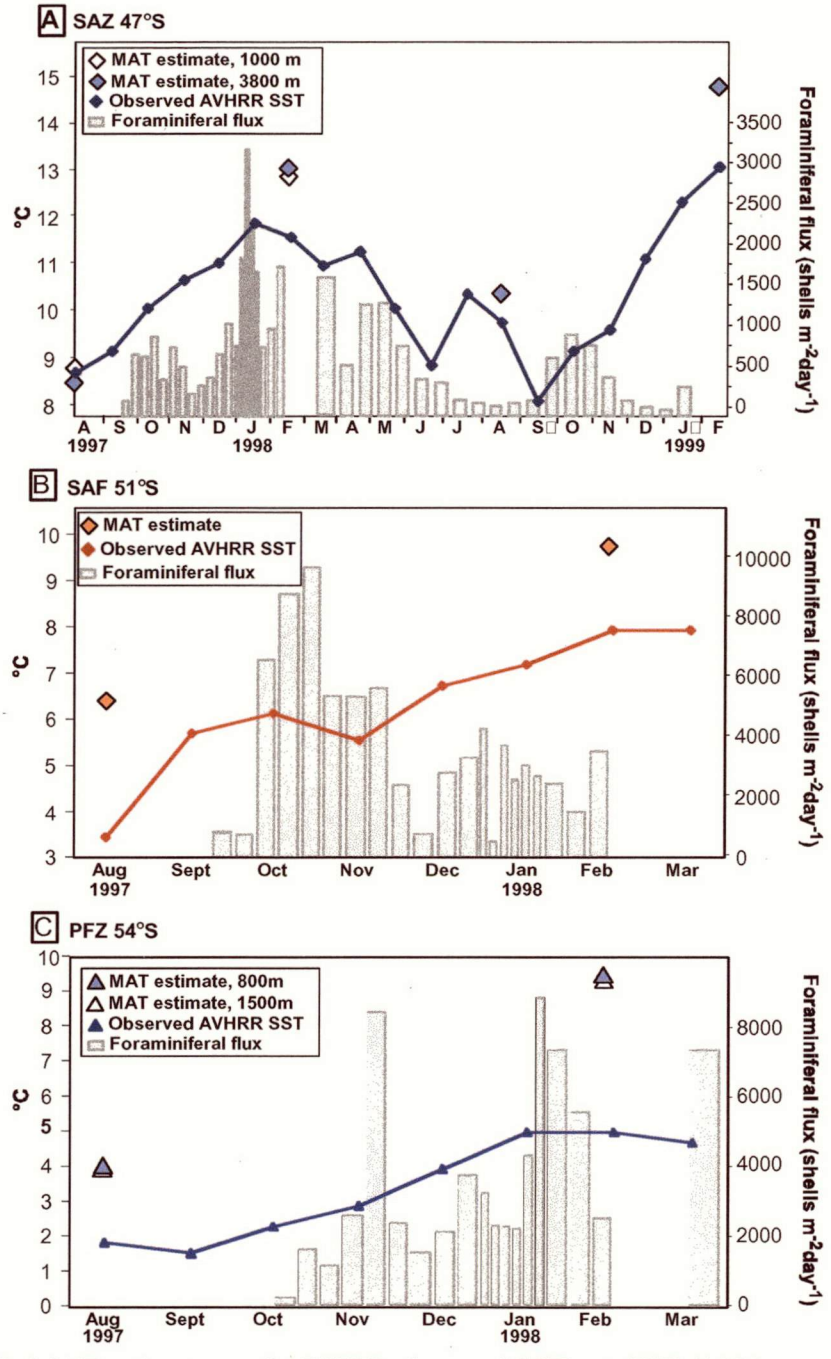

Figure 5: MAT estimates and AVHRR observed SSTs at 47°S (1000 m and 3800 m trap) (**A**), 51°S (3100 m trap) (**B**) and 54°S (800 m and 1500 m traps) (**C**). Also shown are the foraminiferal fluxes at each site. Foraminiferal fluxes are highly seasonal at each site, yet the annual SST range is well estimated by the MAT. Larger offsets between observed and estimated SST at 54°S are due to the higher proportion of *G. quinqueloba* in these sediment traps than is normally found in Southern Ocean core tops.

3.5 Discussion

3.5.1 Control of seasonal patterns of foraminiferal flux.

Species distributions and abundances on a global scale have been strongly associated with specific thermal regimes (eg. Bé and Hutson, 1977). Within these optimal thermal limits, however, there are other factors which may provide more significant constraints on seasonal productivity. These factors include food availability, light intensity, and mixed layer depth (Fairbanks and Wiebe, 1980; Thunell and Reynolds, 1984; Ortiz et al., 1995). This sediment trap study allows the opportunity to explore relationships between species fluxes and environmental parameters on a seasonal and regional basis.

In this section, we compare foraminiferal fluxes from this study to those from a subantarctic sediment trap located south of Chatham Rise (44°S), east of New Zealand (King and Howard, 2001). This comparison allows the assessment of species seasonal fluxes at nominally subantarctic sites in different sectors. Total foraminiferal fluxes at both the 47°S and South Chatham Rise (SCR) sites show distinct seasonality from each other. At SCR, highest total fluxes occur during October with low fluxes throughout the summer (Figure 6a), while at 47°S, summer fluxes dominate between January and May with only moderate fluxes during October (Figure 6b). The 51°S site shows similar flux patterns to those at SCR, even though these sites are in very different oceanographic settings (Figure 6c), and the 54°S trap exhibits maximum fluxes during late November / early December and January (Figure 6d and e).

Despite these differences in total foraminiferal fluxes, the seasonal succession of foraminiferal species exhibits a consistent pattern at all four sites (Figure 7). The spring flux in each region is dominated by *G. bulloides* (excluding 54°S) and the summer flux is dominated by *N. pachyderma*. The transition between *G. bulloides* and *N. pachyderma* dominated assemblages is consistent with the distinct seasonal cycles observed for these two species at trap sites in the Santa Barbara Basin (Kincaid et al., 2000). The similarity in seasonal flux patterns in each of the Southern Ocean trap sites suggests that the environmental variables important for species production vary with a consistent seasonal pattern at all of these sites. This indicates that surface temperature in itself is not a key control on species fluxes on a seasonal scale, so variables such as mixed layer depth and food availability may be more important.

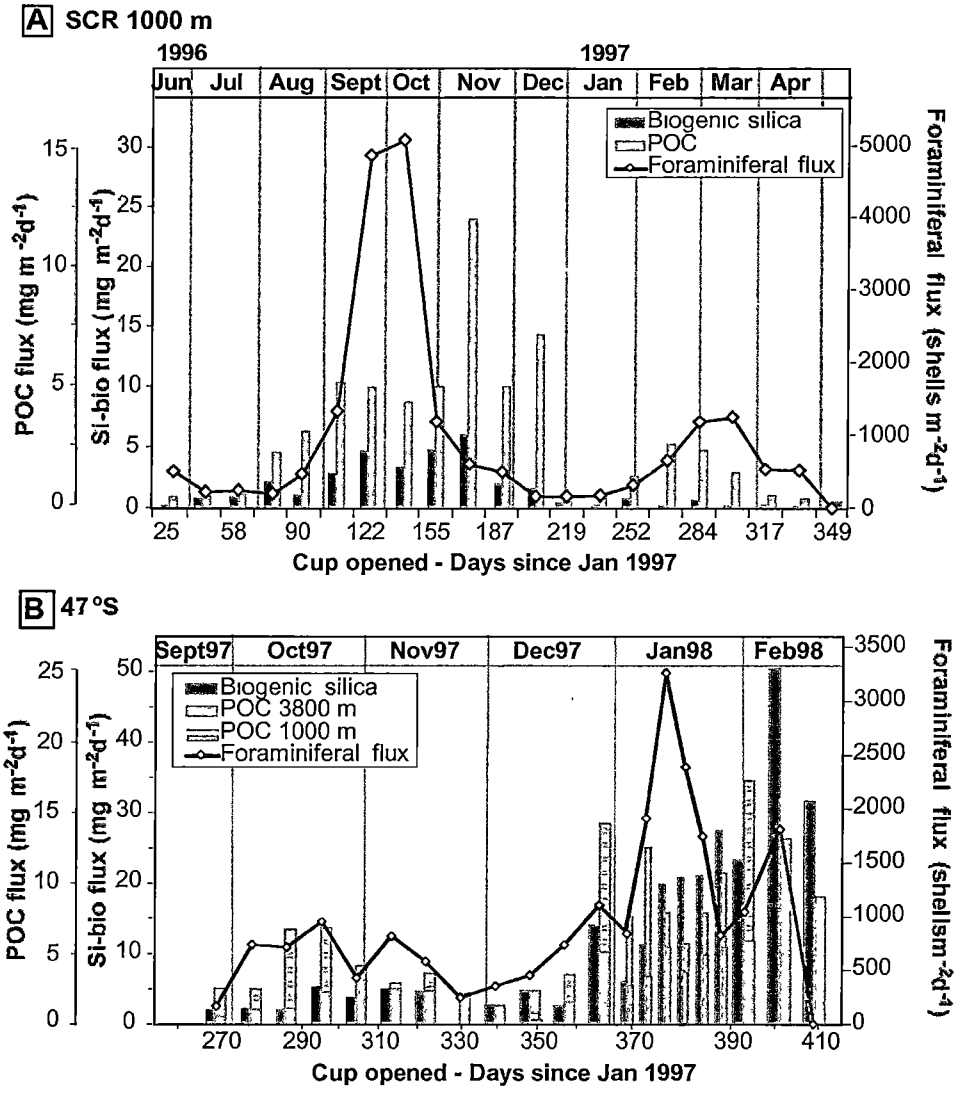

Figure 6: Total foraminiferal, biogenic silica and particulate organic carbon (POC) flux at SCR **(A),** 47-3800 m **(B)**, 51-3100 m **(C)**, 54-800 m **(D)** and 54-1500 m **(E)**. POC at 47-1000 is also plotted. POC flux is generally higher at 1000 m compared to the 3800 m, indicating some remineralisation between these depths, but this does not affect the seasonal pattern of POC flux recorded by the deeper trap. Within the resolution of their relative sinking speeds, high POC and biogenic silica flux is associated with high foraminiferal production at the SCR, 47°S and 54°S sites, but not at 51°S. The relatively low summer foraminiferal flux at 51°S, despite high food availability, implies that other factors important for the production of the summer species are limiting at this site. At 54°S we have plotted data for the 800 and 1500 m traps, revealing the differences in the timing of foraminiferal flux peaks recorded between these depths. Despite these differences, there is still a general correlation between foraminiferal production and biogenic silica and POC. Biogenic silica and POC data for SCR from Nodder and Northcote (2001), for other sites from Trull et al. (2001). Note that the data from SCR commences during June while the other sites are plotted from September.

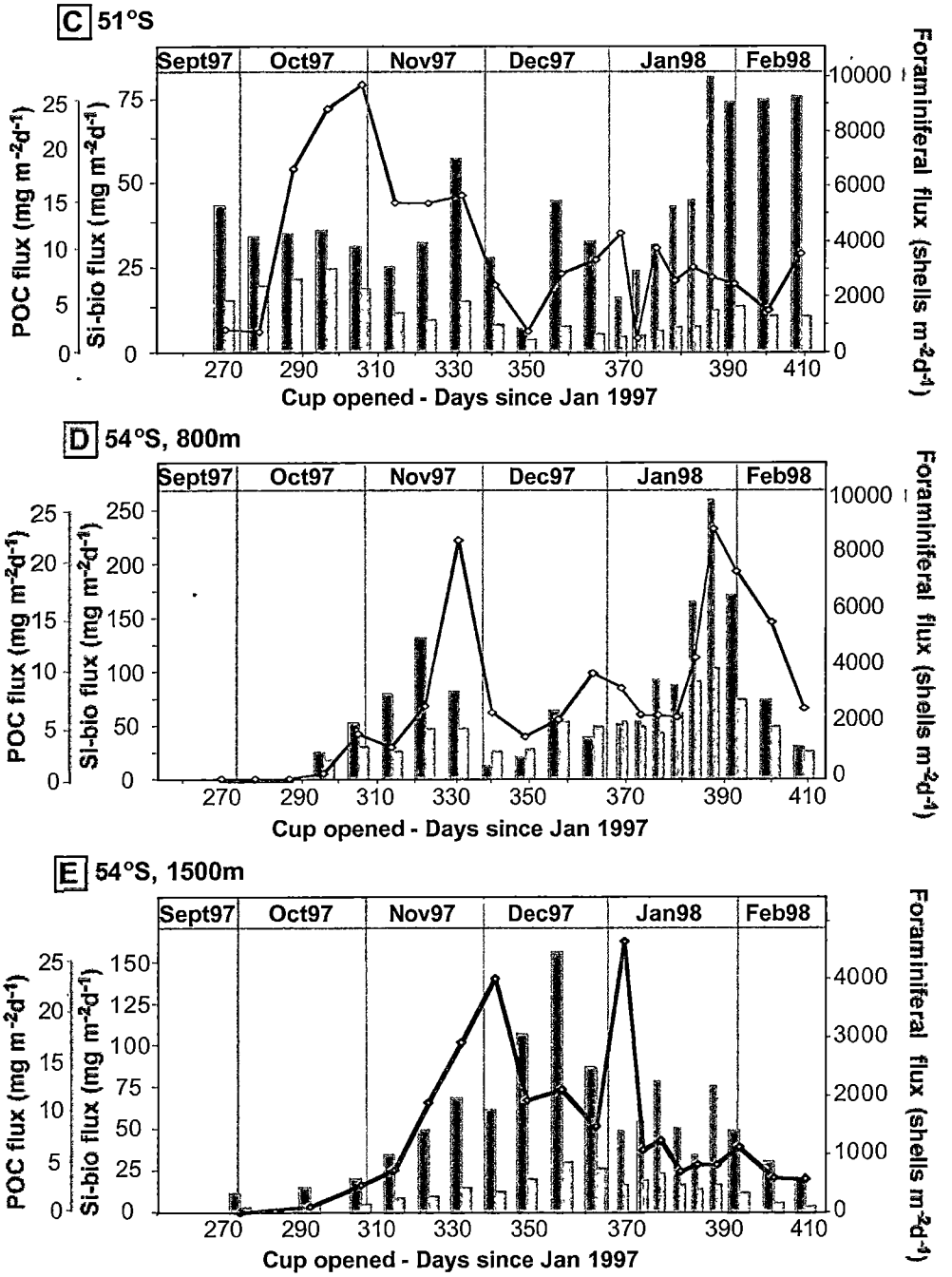

Figure 6 (continued)

Mixed layer depth varies consistently at all of the sites in this study (Figure 7) and may therefore provide a mechanism for similar patterns of species production between different regions. The depth of the mixed layer is often associated with the chlorophyll maximum zone. At each of the sediment trap sites the mixed layer first shallows during spring, reaching shallowest depths during summer. Unfortunately there was only one

measurement of the chlorophyll maximum during the deployment, taken during March 1998, however, several transects have been conducted during other years and seasons between 48° and 62°S south of Tasmania. These measurements indicate a close association between the chlorophyll maximum and the mixed layer depth in the PFZ, and in the SAZ the chlorophyll maximum extended between the surface and the depth of the mixed layer (Parslow et al., 2001). Shallowing of the mixed layer during late spring and summer may therefore reduce the depth of the chlorophyll maximum, enhancing food supply at the surface.

At each of the sediment trap sites, the September/October shallowing of the mixed layer depth and the concurrent increase in chlorophyll-a concentrations (also observed by SeaWiFS, see Trull et al., 2001) is associated with maximum fluxes of *G. bulloides*. Maximum fluxes of *N. pachyderma* (s. and d.), by contrast, are consistently related to intervals when the mixed layer is near the surface, chlorophyll-a concentrations are high, and the water column is strongly stratified. High abundances of *N. pachyderma* have also been linked to intervals of intense summer stratification in the Panama Basin (Thunell and Reynolds, 1984). Subpolar North Pacific sediment trap studies, however, indicate a reverse association between stratification and maximum fluxes of these two species. At Station PAPA, *N. pachyderma* is most abundant during spring while *G. bulloides* is most productive during summer (Sautter and Thunell, 1989). The comparison between these studies highlights the importance of applying seasonal flux patterns on a regional scale only.

The influence of food availability on overall foraminiferal production can be assessed from these trap sites using mass flux as a proxy for overall biogenic production, and measurements of biogenic silica and particulate organic carbon (POC) flux to further characterise biological production and therefore food availability. The fluxes of these components to the traps may only represent a small fraction of the surface production, yet the timing of surface production established from these records are broadly consistent with maximum concentrations of chlorophyll-a in surface waters as observed by SeaWiFS (Trull et al., 2001) and measurements taken with depth (Parslow et al., 2001). Fluxes of total mass, POC, silica and chlorophyll-a concentrations are generally highest during summer at each of the 47°S, 51°S and 54°S sites (Figures 2 and 6), and during spring at SCR (Figure 6a) (Nodder and Northcote, 2001). These production patterns are also well correlated with peaks in total foraminiferal production (within the resolution of the relatively slower sinking speeds for silica and POC) at all sites apart

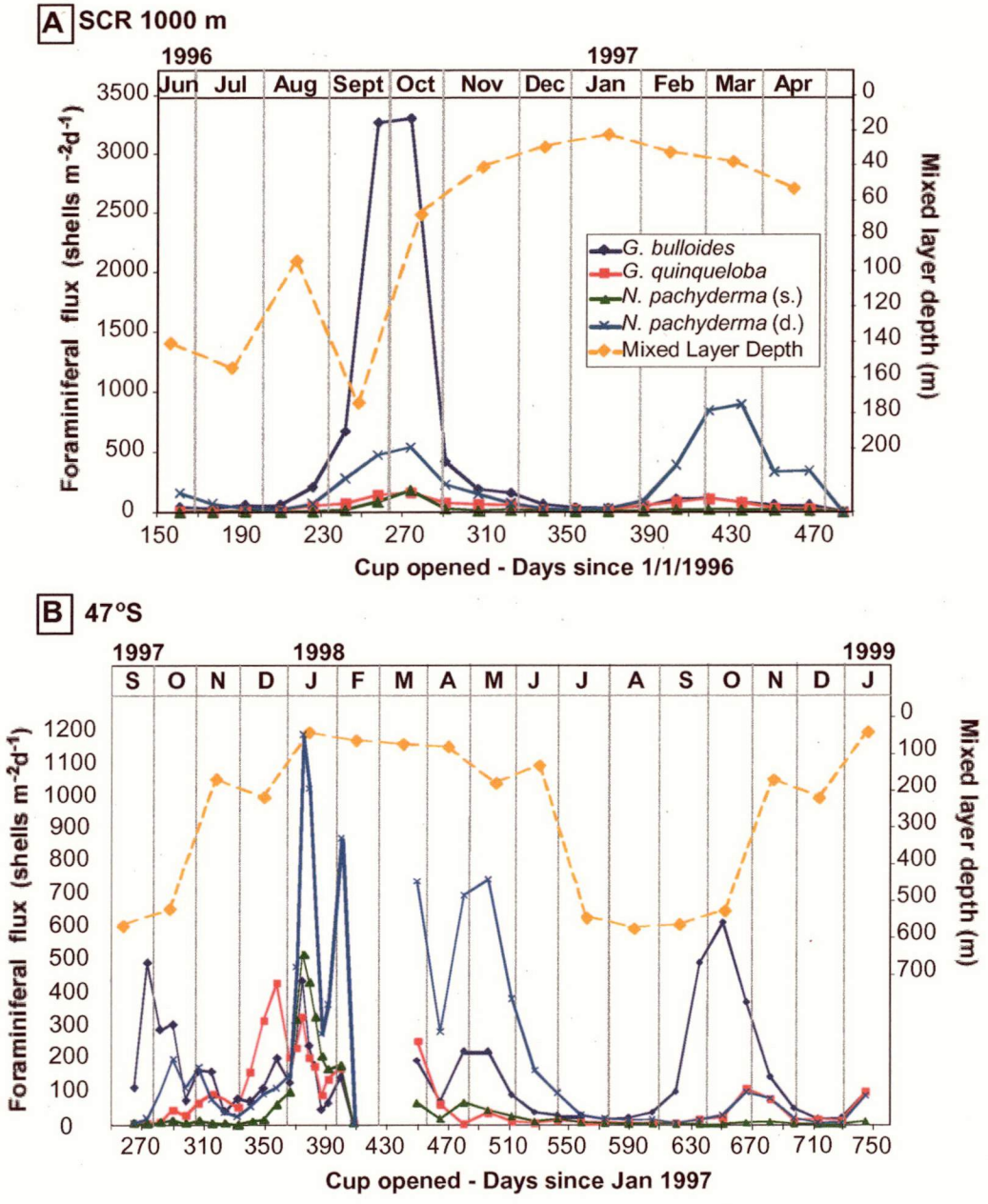

Figure 7: Species fluxes and mixed layer depth at South Chatham Rise (SCR) **(A)**, 47-3800 m **(B)**, 51-3100 m **(C)**, and 54-1500 m **(D)**. At SCR, 47°S and 51°S, highest fluxes of *G. bulloides* occur during September and October when the mixed layer is deep, while fluxes of *N. pachyderma* (d. and s.) are highest during January when the mixed layer is closest to the surface. Mixed layer depth was obtained from the Levitus climatology (Levitus, 1994) since there are no continuous seasonal measurements from the trap sites, and measurements were made only at the very beginning and end of the deployment period. Foraminiferal data at SCR is from King and Howard (2001). This dataset is plotted from June rather than September to show the earlier onset of the spring flux at this site compared to the sites south of Tasmania.

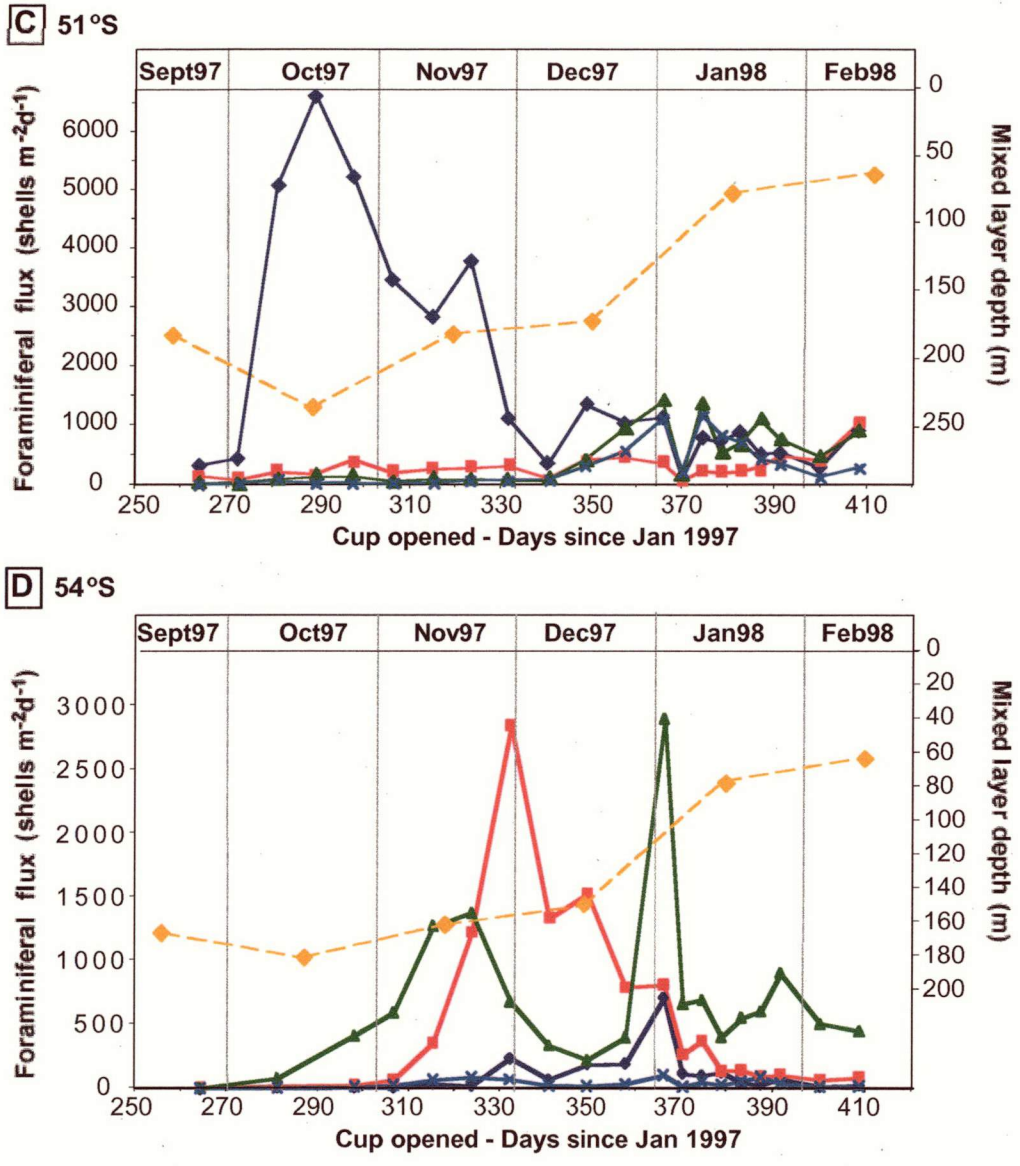

Figure 7 continued

from 51°S. At 51°S foraminiferal production is highest during spring, despite maximum fluxes of POC, silica and chlorophyll-a concentrations during summer. The consistency of peaks in total mass and foraminiferal fluxes at 51-3100 indicates that the foraminiferal flux accounts for a large proportion of the total mass flux at this site.

Closer examination of the record from the 51°S site reveals some consistency between the foraminiferal fluxes and food availability (POC and silica). The spring flux

at the 51°S trap is dominated by *G. bulloides*, with a flux up to 8 times greater than at the 47°S site. The spring fluxes of POC and silica at 51°S are also approximately 7 times higher than maximum fluxes at 47°S (Trull et al., 2001). These patterns suggest that the relationship between food availability and *G. bulloides* flux is consistent between these sites. The influence of food availability on *G. bulloides* abundance is supported by plankton tow data indicating highest abundances of this species at the depth of the chlorophyll maximum zone (Ortiz et al., 1995).

Total foraminiferal, POC and biogenic flux is shown for both trap depths at 54°S (Figure 6d and e). Although foraminiferal flux patterns are broadly similar between both trap depths, we do see a depth dependent difference in the timing and amplitude of foraminiferal flux at 54°S. Fluxes to the deeper trap at this site are generally recorded one sample period after peaks in the shallower trap, and are lower overall. The major late January peak at 800 m is particularly small at 1500 m (4800 shells $m^{-2}d^{-1}$ at 800 m compared to 1130 shells $m^{-2}d^{-1}$ at 1500 m). Despite these differences, there is an overall consistency between the timing of foraminiferal fluxes and POC and biogenic silica at 54°S. This trend is particularly clear from the 54-800 record.

Measurements of POC and silica are only crude estimates of the amount of food available for foraminiferal consumption. Analysis of foraminiferal and phytoplankton fluxes in San Pedro Basin sediment traps indicate that fluxes of *N. pachyderma* and *G. quinqueloba* are associated with certain species of diatoms, suggesting that these foraminiferal species may have specific dietary preferences for certain species of phytoplankton (Sautter and Sancetta, 1992). *G. bulloides*, by contrast, exhibits no clear associations to particular species (Sautter and Sancetta, 1992). The low summer foraminiferal fluxes at 51°S, despite high POC and silica, may reflect the dietary preferences of *N. pachyderma* and *G. quinqueloba* for phytoplankton species which are not abundant during this interval.

The relatively low summer flux at the 51°S site may also reflect the temperature limits of the summer species. *N. pachyderma* (d.), for instance, tends to be most abundant in warmer temperate regions, while the sinistral form of this species is more abundant in cooler sub-polar to polar environments (Bé and Hutson, 1977). Temperatures at 51°S may be outside the optimal temperatures for both of these species, resulting in their relatively low abundance at the 51°S site.

In summary, observations from each of these sites constrains the relative importance of three environmental parameters affecting species seasonal fluxes and productivity. Seasonal changes in mixed layer depth, and the associated changes in chlorophyll-a concentrations, show a strong association to seasonal changes in species fluxes, consistent with the findings of Thunell and Reynolds (1984) and Sautter and Thunell (1989). Within this context, high food availability may enhance production of the species present (see also Ortiz et al., 1995) if dietary preferences (Sautter and Sancetta, 1992) and/or thermal conditions are optimal for production of that species (eg. Bé and Hutson, 1977).

3.5.2 Implications of seasonal fluxes for paleoclimate reconstructions

The stability of seasonal flux patterns between the traps located within the SAZ and SAF provides the potential for tracking changes in spring conditions, through analysis of *G. bulloides*, and summer conditions, with analysis of *N. pachyderma*, in down-core sediments from these regions. These findings are particularly relevant for interpretation of isotopic records from sediments which will be weighted towards the season of maximum production for each species (Curry et al., 1983).

The stability of seasonal succession patterns across regions indicates that species fluxes are not determined solely by temperature. It is therefore particularly relevant to test estimates of SSTs from assemblages at these sites. SST estimates derived with the MAT indicate a very good consistency to observed SSTs, particularly at 47°S and 51°S. The success of the MAT reinforces the validity of the assumption that the factors which influence foraminiferal production are closely associated with regional-scale climatological temperature patterns. Comparison of the trap assemblages to core top sediments near the 47°S and 51°S trap sites indicates that flux patterns have remained consistent over the span of centuries to millennia, implying that seasonally varying parameters such as mixed layer depth and biomass production have remained similar enough to modern patterns to produce similar assemblages.

The success of the MAT also lies in the distributions of relatively minor species. Diversity clearly decreases poleward among the trap sites, creating distinct foraminiferal assemblages within each water mass. Minor occurrences of *Globorotalia scitula, Neogloboquadrina dutertrei, Globigerina falconensis* and *Orbulina universa* at 47°S distinguish the foraminiferal assemblage at this site from the 51°S assemblage, while relatively high abundances of *N. pachyderma* (d.), *G. inflata* and *Globorotalia*

truncatulinoides (s.) at 51°S distinguishes this assemblage from the 54°S site which is dominated by *N. pachyderma* (s.) and *G. quinqueloba*. Changes in the abundances of minor species constrain variations in water mass boundaries, and associated temperatures. The low species diversity at high latitudes, however, also creates higher uncertainties in the temperature estimates. The results from 54°S therefore provide important constraints on SST estimates from high latitude environments.

SST estimates obtained using the MAT in this study may also be affected by interannual anomalies and/or calcium carbonate dissolution of the core top sediments. At 54°S, for example, the overestimation of SSTs is partly a reflection of the relatively high abundances of *G. quinqueloba*. The MAT indicates the occurrence of this "no-analog" situation with high dissimilarities to Southern Ocean core tops.

Differences between the assemblages in the traps and the regional core top sediments near 54°S suggests that there is either 1) significant interannual variability over this site with the 97/98 season atypical of the longer term mean, 2) there is substantial foraminiferal flux between March and August (the interval not sampled) with relatively low abundances of *G. quinqueloba* during this period, or 3) *G. quinqueloba*, which is a solution susceptible species, has been selectively dissolved from core top sediments (Parker and Berger, 1971). Further studies during different years and seasons, and addition of core tops spanning a wider range of preservation states are required to distinguish among these hypotheses.

A key outcome of this study is that we are now able to determine the likely error range for SST estimates derived from Southern Ocean foraminiferal records. The results from this study indicate that SST estimates to within 2°C of the observations can be obtained from the sediment trap records at 47° and 51°S, which is a good result considering that we are comparing a single record to the long-term averaged core top sediments. The estimates derived from 54°S have a slightly greater offset from the observations, but considering that this site lies towards the edge of the range for the technique, with low species diversity, it is reassuring that the temperature estimate are within 2.5-4.6°C of the observations. Calibrations of other faunal SST indices, such as factor based transfer functions, show that these techniques are much less accurate in comparison to the MAT, and they exhibit much higher offsets than we observe in this study (eg. Ortiz and Miz, 1997; Barrows et al, 2000). The main weakness of the MAT highlighted by this study is its dependence on a large core top data base. The larger

offset between estimated and observed temperatures at the 54°S site emphasises the need for additional sub-polar to polar Southern Ocean core tops in the MAT database to capture more of the regional variations.

3.6 Conclusions

This analysis of Subantarctic sediment traps reveals some important features of foraminiferal fluxes. At each of the sites we observe a clear seasonal succession of species which can be related most directly to variations in mixed layer depth. Close similarity between the sediment trap assemblages and those of nearby core tops indicates that the sedimentary record retains an integration of these seasonal flux patterns, implying that seasonal changes in mixed layer depth and food availability have remained stable during recent centuries to millennia. The long term consistency of the foraminiferal flux patterns and their strong association with environmental variables is also revealed by the reliability of the MAT SST estimates from the sediment trap assemblages. The MAT successfully estimates SSTs to within 2.5°C of the observed temperatures for the 47°S and 51°S trap sites. The sensitivity of the MAT is further highlighted by the estimation of warmer SSTs from the 1998 compared to 1997 assemblage at 47°S, coherent with the warmer observed temperatures during 1998. These results signify that the MAT provides a reliable means of obtaining SST estimates from foraminiferal assemblages, despite high flux seasonality driven by factors other than temperature.

3.7 REFERENCES

Advanced Very High Resolution Radiometer (AVHRR), 1999. AVHRR sea surface temperature data. (NOAA/NASA), 20th October 1999, WWW page, http://podaac.jpl.nasa.gov/sst/.

Banse, K., 1996. Low seasonality of low concentrations of surface chlorophyll in the Subantarctic water ring: underwater irradiance, iron, or grazing? Progress in Oceanography, 37: 241-291.

Barrows, T. T.; Juggins, S.; De Dekker, P.; Thiede, J., and Martinez, J. I., 2000. Sea-surface temperatures of the southwest Pacific Ocean during the Last Glacial Maximum. Paleoceanography, 15(1):95-109.

Bé, A.W.H. and Hutson, W.H., 1977. Ecology of planktonic foraminifera and biogeographic patterns of life and fossil assemblages in the Indian Ocean. Micropaleontology, 23: 369-414.

Belkin, I.M. and Gordon, A.L., 1996. Southern Ocean fronts from the Greenwich meridian to Tasmania. Journal of Geophysical Research, 101: 3675-3696.

Berger, W.H. and Piper, J.W., 1972. Planktonic foraminifera: Differential settling, dissolution, and redeposition. Limnology and Oceanography, 17(2): 275-287.

Bottomley, M., Folland, C.K., Hsiung, J., Newell, R.E. and Parker, D.E., 1990. Global ocean surface temperature atlas "GOSTA". Meteorological Office Department of Earth, Atmospheric and Planetary Sciences, Massachusetts Institute of Technology, Bracknell, UK, Cambridge, MA, USA, 20 pp.

Bray, S., Trull, T. and Manganini, S., 2000. SAZ project moored sediment traps: Results of the 1997-1998 deployments. Report no. 15, Antarctic CRC, Hobart.

Broecker, W.S. and Takahashi, T., 1978. The relationship between lysocline depth and *in situ* carbonate ion concentration. Deep-Sea Research, 25: 65-95.

Comiso, J.C., McClain, C.R., Sullivan, C.W., Ryan, J.P. and Leonard, C.L., 1993. Coastal Zone Color Scanner pigment concentrations in the Southern Ocean and relationships to geophysical surface features. Journal of Geophysical Research, 98(C2): 2419-2451.

Cresswell, G., 2000. Currents of the continental shelf and upper slope of Tasmania. In: M.R. Banks and M.J. Brown (Editors), Tasmania and the Southern Ocean. Papers and Proceedings of the Royal Society of Tasmania, Hobart, pp. 21-30.

Curry, W.B., Thunell, R.C. and Honjo, S., 1983. Seasonal changes in the isotopic composition of planktonic foraminifera collected in Panama Basin sediment traps. Earth and Planetary Science Letters, 64: 33-43.

Deacon, G.E.R., 1982. Physical and biological zonation in the Southern Ocean. Deep-Sea Research, 29(1A): 1-15.

Deuser, W.G. and Ross, E.H., 1989. Seasonally abundant planktonic foraminifera of the Sargasso Sea: succession, deep-water fluxes, isotopic compositions, and paleoceanographic implications. Journal of Foraminiferal Research, 19(4): 268-293.

Fairbanks, R.G. and Wiebe, P.H., 1980. Foraminifera and chlorophyll maxima: Vertical distribution, seasonal succession, and paleoceanographic significance. Science, 209: 1524-1526.

Gardner, W.D., Biscaye, P.E. and Richardson, M.J., 1997. A sediment trap experiment in the Vema Channel to evaluate the effect of horizontal particle fluxes on measured vertical fluxes. Journal of Marine Research, 55: 995-1028.

Guptha, M.V.S., Curry, W.B., Ittekkot, V. and Muralinath, A.S., 1997. Seasonal variation in the flux of planktic foraminifera: sediment trap results from the Bay of Bengal, Northern Indian Ocean. Journal of Foraminiferal Research, 27(1): 5-19.

Honjo, S., Francois, R., Manganini, S., Dymond, J. and Collier, R., 2000. Particle fluxes to the interior of the Southern Ocean in the Western Pacific sector along 170°W. Deep-Sea Research II, 47: 3521-3548.

Hutson, W.H., 1979. The Agulhas Current during the Late Pleistocene: Analysis of Modern Faunal Analogs. Science, 207: 64-66.

Kincaid, E. et al., 2000. Planktonic foraminiferal fluxes in the Santa Barbara Basin: response to seasonal and interannual hydrographic changes. Deep-Sea Research II, 47: 1157-1176.

King, A.L. and Howard, W.R., 2001. Seasonality of foraminiferal flux in sediment traps at Chatham Rise, SW Pacific: Implications for paleotemperature estimates. Deep-Sea Research I, 48: 1687-1708.

King, A. L. and Howard, W. R., 2001. Seasonality of foraminiferal flux and isotopic composition in southern Ocean sediment traps: Implications for paleo-reconstructions. 7th International Conference on Paleoceanography; Sapporo, Japan.

Kipp, N.G., 1976. New transfer function for estimating past sea-surface conditions from sea-bed distribution of planktonic foraminiferal assemblages in the North Atlantic. In: R.M. Cline and J.D. Hays (Editors), Investigation of Late Quaternary Paleoceanography and Paleoclimatology. Geological Society of America Memoirs. Geological Society of America, Boulder, Colorado, pp. 3-42.

Kopczynska, E.E., Dehairs, F., Elskens, M. and Wright, S., 2001. Phytoplankton and microzooplankton variability between the Subtropical and Polar Fronts south of

Australia: Thriving under regenerative and new production in late summer. Journal of Geophysical Research, 106(C12): 31,597-31,610.

Levitus, S., 1994. Levitus94: World Ocean Atlas 1994. NOAA Office of Global Programs and Lamont-Doherty Earth Observatory of Columbia University, 23 May 2000, WWW page, http://ingrid.ldgo.columbia.edu/SOURCES/.LEVITUS94/.

Moore, J.K. et al., 1999. SeaWIFS satellite ocean color data from the Southern Ocean. Geophysical Research Letters, 26(10): 1465-1468.

Nodder, S.D. and Northcote, L.C., 2001. Episodic particulate fluxes at southern temperate mid-latitudes (42-45°S) in the Subtropical Front region, east of New Zealand. Deep-Sea Research I, 48(3): 833-864.

Orsi, A., Whitworth, T. and Nowlin, W.D., 1995. On the meridional extent and fronts of the Antarctic Circumpolar Current. Deep-Sea Research I, 42: 641-673.

Ortiz, J.D. and Mix, A.C., 1997. Comparison of Imbrie-Kipp transfer function and modern analog temperature estimates using sediment trap and core top foraminiferal faunas. Paleoceanography, 12: 175-190.

Ortiz, J.D., Mix, A.C. and Collier, R.W., 1995. Environmental control of living symbiotic and asymbiotic foraminifera of the California Current. Paleoceanography, 10(6): 987-1009.

Parker, F.L., 1962. Planktonic foraminiferal species in Pacific sediments. Micropaleontology, 8: 219-254.

Parker, F.L. and Berger, W.H., 1971. Faunal and solution patterns of planktonic foraminifera in surface sediments of the South Pacific. Deep-Sea Research, 18: 73-107.

Parslow, J. S., Boyd, P. W., Rintoul, S. R., and Giffiths, F. B., 2001. A persistent subsurface chlorophyll maximum in the Interpolar Frontal Zone south of Australia: Seasonal progression and implications for phytoplankton-light-nutrient interactions. Journal of Geophysical Research, 106(C12):31,543-31,557.

Pilskaln, C.H., Paduan, J.B., Chavez, F.P., Anderson, R.Y. and Berelson, W.M., 1996. Carbon export and regeneration in the coastal upwelling system of Monterey Bay, central California. Journal of Marine Research, 54: 1149-1178.

Popp, B.N. et al., 1999. Controls on the carbon isotopic composition of Southern Ocean phytoplankton. Global Biogeochemical Cycles, 13(4): 827-843.

Prell, W., Martin, A., Cullen, J. and Trend, M., 1999. The Brown University Foraminiferal Data Base. IGBP PAGES/World Data Center-A for Paleoclimatology, Boulder CO, NOAA/NGDC Paleoclimatology Program.

Prell, W.L., 1985. The stability of low-latitude sea-surface temperatures: An evaluation of the CLIMAP reconstruction with emphasis on the positive SST anomalies. 025, U.S. Department of Energy, Washington, D.C.

Rintoul, S.R., Donguy, J.R. and Roemmich, D.H., 1997. Seasonal evolution of upper ocean thermal structure between Tasmania and Antarctica. Deep-Sea Research I, 44(7): 1185-1202.

Rintoul, S.R. and Trull, T.W., 2001. Seasonal evolution of the mixed layer in the Subantarctic Zone south of Australia. Journal of Geophysical Research, 106(C12): 31,447-31,462.

Sautter, L.R. and Sancetta, C., 1992. Seasonal associations of phytoplankton and planktic foraminifera in an upwelling region and their contribution to the seafloor. Marine Micropaleontology, 18: 263-278.

Sautter, L.R. and Thunell, R.C., 1989. Seasonal succession of planktonic foraminifera: Results from a four-year time-series sediment trap experiment in the Northeast Pacific. Journal of Foraminiferal Research, 19: 253-267.

Takahashi, K. and Bé, A.W.H., 1984. Planktonic foraminifera: factors controlling sinking speeds. Deep-Sea Research A, 31(12): 1477-1500.

Thunell, R.C. and Honjo, S., 1987. Seasonal and interannual changes in planktonic foraminiferal production in the North Pacific. Nature, 328: 335-337.

Thunell, R.C. and Reynolds, L.A., 1984. Sedimentation of planktonic foraminifera: Seasonal changes in species flux in the Panama Basin. Micropaleontology, 30: 241-260.

Trull, T., Bray, S., Manganini, S., Honjo, S. and François, R., 2001. Moored sediment trap measurements of carbon export in the Sub-Antarctic and Polar Frontal zones of the Southern Ocean, south of Australia. Journal of Geophysical Research, 106(C12): 31,489-31,510.

Note added after publication:

A study of planktonic foraminifera collected from sediment traps in the northwestern North Pacific Ocean by Kuroyanagi et al. (2002)[1] found that fluxes of *N. pachyderma* and *G. bulloides* are closely associated with the availability of organic matter, consistent with the relationship determined in this study for *G. bulloides*. A study in the central North Pacific by Eguchi et al. (2003)[2] demonstrates the correspondence between fluxes of *G. bulloides* and *G. inflata*, both of which peak during periods of low stratification. They also find that fluxes of *G. bulloides* and *N. pachyderma* (d.) are out of phase with

each other. These two results from the study of Eguchi et al. are consistent with the results from our Southern Ocean sediment traps.

[1] Kuroyanagi, A.; Kawahata, H. Nishi H., and Honda, M. C., 2002. Seasonal changes in planktonic foraminifera in the northwestern North Pacific Ocean: sediment trap experiments from subarctic and subtropical gyres. Deep-Sea Research II, 49: 5627-5645.
[2] Eguchi, N. O.; Ujiie, H.; Kawahata, H., and Taira, A., 2003. Seasonal variations in planktonic foraminifera at three sediment traps in the Subarctic, Transition and Subtropical zones of the central North Pacific Ocean. Marine Micropaleontology, 48: 149-163.

Appendix I: Species percent of total yearly shell flux at the trap sites.

Species	**47- 1000**	**47- 3800 97**	**47- 3800 98**	**51- 3100**	**54-800**	**54-1500**
Globigerina bulloides	20.62	18.77	24.20	51.50	6.78	6.18
Globigerina falconensis	0.43	0.23	0.60	0.02	0	0
Globigerina calida	0	0.08	0.09	0	0	0
Globigerina quinqueloba	9.13	14.10	7.08	7.75	23.66	40.94
Globigerinita glutinata	7.77	7.36	8.00	7.09	3.83	5.11
Globigerinoides ruber	0	0.02	0	0	0	0
Orbulina universa	1.98	0.80	1.71	0.01	0	0
Neogloboquadrina pachyderma (s.)	9.57	9.12	2.52	9.55	60.91	44.47
Neogloboquadrina pachyderma (d.)	26.47	26.25	33.40	5.94	3.85	2.53
Neogloboquadrina dutertrei	1.09	0.65	1.24	0	0	0
Globorotalia truncatulinoides (s.)	7.05	7.22	6.76	1.12	0.07	0.06
Globorotalia truncatulinoides (d.)	0.19	0.23	0.21	0.07	0	0.02
Globorotalia scitula	2.63	2.53	1.18	0.03	0	0.01
Globorotalia hirsuta	0.07	0	0	0.01	0	0
Globorotalia inflata	12.98	12.39	12.69	16.84	0.77	0.65

CHAPTER 4

PLANKTONIC FORAMINIFERAL $\delta^{18}O$ IN SOUTHERN OCEAN SEDIMENT TRAPS

"Nature goes her own way, and all that seems an exception is really according to order"
Johann Wolfgang von Goethe (1749-1832)

4.1 Abstract

The oxygen isotopic record obtained from *Globigerina bulloides*, *Globorotalia inflata* and *Neogloboquadrina pachyderma* (s.) was analysed for 5 sediment traps moored in the Southern Ocean and Southwest Pacific. The traps extend from Subtropical to the Polar Frontal environments, providing the first analysis of seasonal foraminiferal $\delta^{18}O$ records from these latitudes. Comparison between the foraminiferal records and various equilibrium $\delta^{18}O$ equations reveals that the expected equilibrium is best captured by the equation of Epstein et al. (1953), with constant offsets from this equilibrium $\delta^{18}O$ exhibited by *G. bulloides* and *N. pachyderma* (s.) across the full range of latitudes. The seasonal range in $\delta^{18}O$ values for these two species implies a surface to sub-surface habitat across all sites, while *G. inflata* most likely dwells at ~50m depth. The sediment trap records reveal distinct seasonal flux patterns for each species. Comparison between flux-weighted isotopic values calculated from the sediment traps and the isotopic composition of nearby surface sediments indicates that the sedimentary records retain this seasonal imprint. Differences in seasonal flux patterns between sites has important implications for the reconstruction of temperature and salinity gradients in paleoclimate records from this region.

4.2 Introduction

The oxygen isotopic composition of planktonic foraminifera provides one of the most widely used tools for reconstructing past changes in ocean temperature and salinity. However, there are still large discrepancies between isotopic records and other temperature and salinity proxies, and there are also large variations in isotopic composition between foraminiferal species. Various attempts have been made to better calibrate the foraminiferal isotopic records under modern observed conditions through data obtained from plankton tow and sediment trap studies (Erez and Honjo, 1981; Williams et al., 1981; Fairbanks et al., 1982; Deuser and Ross, 1989; Sautter and

Thunell, 1991). A recent study of South Atlantic plankton tows marks the first such data set from the Southern Ocean (Mortyn and Charles, 2003). Since calibrations to equilibrium calcite vary between species and areas (eg. Bemis et al., 2002), it is important to test equilibrium relationships in a range of environments and across the full range of conditions which may be encountered in paleoclimate records.

There is a confusing choice of temperature equations which can be applied in the interpretation of $\delta^{18}O$ records. Some of these equations have been developed in both field and laboratory relationships for use with specific foraminiferal taxa (eg. Bemis et al., 1998; von Langen et al., 2000; Bemis et al., 2002), others with mollusks (eg. Epstein et al., 1953), while others relate to the inorganic precipitation of calcite (eg. Kim and O'Neil, 1997). The large variability between these equations highlights the importance of testing their relationship to foraminiferal isotopic variability in field settings.

Previous paleoclimate studies from the Southern Ocean have sought to apply isotopic signals to the reconstruction of past oceanographic and climate conditions. The migration of ocean fronts and, in some areas, the intensification of circulation have been inferred on the basis of latitudinal gradients in $\delta^{18}O$ (eg. Charles and Fairbanks, 1990; Nelson et al., 1994; Labeyrie et al., 1996; Matsumoto et al., 2001). However, conflicting results from isotopic and biotic reconstructions for past climate cycles highlight the potential problem for isotopic records to become overprinted by changes in seasonal flux patterns for the species analysed (Howard and Prell, 1992; Brathauer and Abelmann, 1999). More recently, attempts have been made to establish changes in seasonal flux patterns through the analysis of individual foraminifera (Bemis, 2000). Sediment trap studies provide a unique opportunity to determine the impact that seasonal and depth distributions of foraminifera may have on sedimentary interpretations.

In this study, we test the utility of foraminiferal $\delta^{18}O$ records for paleoclimate reconstructions based on results from five sediment traps located in four distinct water masses of the southwestern Pacific and Southern Oceans. Firstly, we test a range of equilibrium equations against measured foraminiferal $\delta^{18}O$, focussing on three species of planktonic foraminifera (viz. *G. bulloides*, *G. inflata* and *N. pachyderma* (s.)) which are commonly used in paleoclimate reconstructions. Secondly, we evaluate the habitat depth for each species based on the seasonal amplitude of their $\delta^{18}O$ values. We also assess how well each species tracks seasonal changes in equilibrium $\delta^{18}O$ at their inferred habitat depth. Finally, we assess the influence of seasonal flux patterns on isotopic

records. Previous studies of faunal seasonality from this region (King and Howard, 2001; King and Howard, 2003) sought to test the implications of foraminiferal flux patterns for biotic reconstructions. In this paper, we examine this impact of foraminiferal flux seasonality on the stable-isotopic record preserved in sediments.

4.3 Oceanographic setting

The five sediment traps were moored in distinct environments of the Pacific/Southern Ocean (Figure 1). These zones are characterised as Subtropical, Subantarctic, Subantarctic Frontal and Polar Frontal. Two traps were moored within the Subantarctic Zone (SAZ). One was located east of New Zealand, and the other south of Tasmania, Australia. Each of the traps are associated with major oceanic fronts which mark the transition between water masses with unique temperature, salinity and nutrient characteristics. Traps moored at 42° and 44°S at North and South Chatham Rise east of New Zealand are separated by the Subtropical Front (STF). This front separates Subantarctic waters which are characteristically cold, low salinity, and nutrient-rich, from warm, saline, nutrient-depleted Subtropical waters (Deacon, 1982; Heath, 1985; Belkin and Gordon, 1996).

The Australian sector traps capture the distinct environments of the SAZ, the Subantarctic Front (STF) and the Polar Frontal Zone (PFZ). The Subantarctic Front forms a transition zone between the warmer, more saline, nutrient-depleted waters of the SAZ and the southern waters of the PFZ (Rintoul and Trull, 2001). The salinity and temperature of the southern SAZ in this sector is controlled by the mixture of warmer, more saline sub-tropical waters advected southwards across the STF, and fresher Antarctic Surface Waters advected northwards across the SAF by strong Ekman transport (Rintoul and Trull, 2001). At present, there is no direct input of meltwater to 54°S, however the influx of Antarctic Surface Waters contributes to the low salinity and temperature at this site. The decrease in salinity to the south from the Subtropical to Polar Frontal water masses causes the $\delta^{18}O$ content of surface waters to decrease by ~0.8‰ between the most northern and southern traps sites (42°S and 54°S respectively). Surface temperature also varies by up to 14°C across these sites. This large contrast in temperature and salinity provides a broad basis for establishing latitudinal variations in $\delta^{18}O$ for planktonic foraminifera.

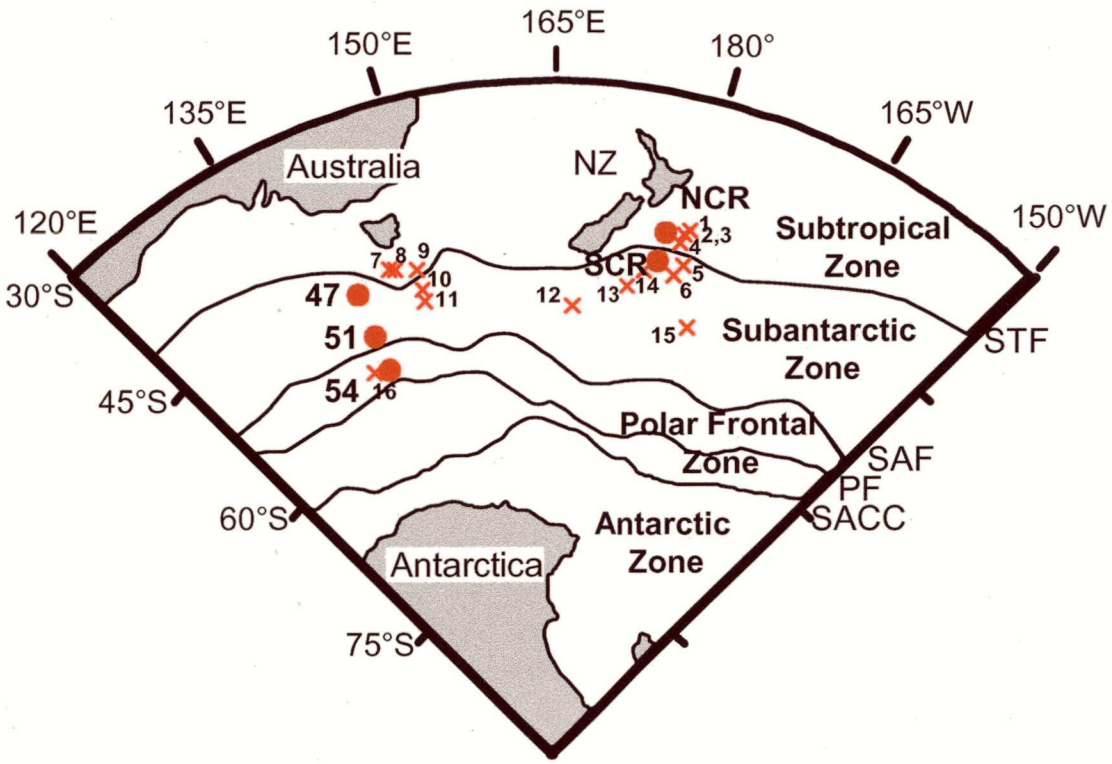

Figure 1: Trap (•) and core top (x) locations in relation to water masses and fronts. Core tops are as follows: 1: W266-K; 2: R657-K; 3: S924-K; 4: W268-P; 5: U939-P; 6: W272-P, 7: MD972-106-G; 8: SO136-165-BX; 9: SO136-161-BX; 10: SO136-153-BX; 11: SO136-147-BX; 12: D84-D 13: H564-G; 14:Q216-G; 15: Q585-G; 16: ELT36-1-PH. (G refers to gravity core, K to Kasten core, BX to box core, D to dredge, PH to phleger core and PC to piston core). Figure adapted from L. Armand pers. comm., with frontal locations based on Orsi et al. (1995)(Orsi et al., 1995). Core 1 from Neil (1997), cores 3, 12, 13, 14 and 15 from Weaver et al. (1997).

4.4 Methods

4.4.1 Sediment trap moorings

Two sediment traps were moored north and south of Chatham Rise for approximately one year during 1996 and 1997. The South Chatham Rise (SCR) record spans the interval 9th June 1996 to 15th May 1997 while the deployment at North Chatham Rise (NCR) covers the interval from 14th September 1996 to 15th May 1997 (see Nodder and Northcote, 2001). Here we present results from the 1000 m traps at both sites.

Moorings from a separate deployment from the Australian sector of the Southern Ocean are also presented here. Sediment trap moorings were deployed between September

1997 and February 1998 along 142°E longitude in the central SAZ (47°S), at the SAF (51°S) and within the PFZ (54°S) (Figure 1) (see Bray et al., 2000; Trull et al., 2001). Moorings at 47°S were redeployed during the following year between 15th March 1998 and 5th February 1999, while traps at 54°S were deployed between 24th March 1998 and 5th February 1999. In this second deployment at 54°S, however, material was only collected in the first sample cup. Here we present results from the 1997 and 1998 deployments for traps at 3850 m at 47°S (47-3800), 3080 m at 51°S (51-3100) and 830 m at 54°S (54-800).

The Australian sector and Chatham Rise deployments both used McLane PARFLUX Mk 7G-21 time-incremental sediment traps. For sampling intervals and other details of the trap deployments at Chatham Rise refer to Nodder and Northcote (2001) and King and Howard (2001) and for the Australian sector deployments to Bray et al. (2000) and King and Howard (2003).

4.4.2 Isotopic analysis

The carbon and oxygen isotopic composition of three species were obtained from the sediment traps (viz. *Globigerina bulloides, Neogloboquadrina pachyderma* (s.) and *Globorotalia inflata*). Ten specimens in the 250-355 µm size fraction were analysed per sample for *G. bulloides* and *G. inflata*, and 15-20 specimens in the 150-250 µm size fraction were analysed for *N. pachyderma* (s.). Prior to analysis, samples were rinsed and sonicated in methanol, and then roasted at 375°C for 60 minutes to eliminate any water and volatile organic compounds.

The carbon and oxygen isotopic ratios were measured on two machines and expressed using standard "δ" notation. The Chatham Rise samples were analysed at the Central Sciences Laboratory, University of Tasmania on an individual reaction-vial automated carbonate line coupled to a Micromass Optima mass spectrometer. Analytical precision was ±0.08 for $\delta^{13}C$ and ±0.09 for $\delta^{18}O$ (N = 51). Most of the Australian sector samples were analysed on a Micromass Optima at UC Davis (see Bemis et al., 2002 for methods). The average analytical precision for these measurements was ±0.05 for $\delta^{13}C$, and ±0.06 for $\delta^{18}O$ (N = 28). The isotopic ratios are reported as per mil (‰) deviations from the Pee Dee belemnite (PDB) standard using Carrara marble as a laboratory standard.

4.4.3 Comparison between trap and core top $\delta^{18}O$ values

We compare trap $\delta^{18}O$ values to published core top values and analyses which we have made on additional core tops. The published core tops all use *G. bulloides*, providing a much larger core top data base for this species than for *G. inflata* or *N. pachyderma* (s.). Sources of the published material are shown on the figures.

To compare the sediment trap values to the core tops we obtained a flux-weighted $\delta^{18}O$ average for the three foraminiferal species. The flux-weighted value ($\hat{I}$) is calculated for each sediment trap by multiplying each isotope value (I) by the percentage abundance (f) of the species (i) in that cup, and then summing all values together to produce a single value for each trap deployment as follows:

$$\hat{I} = \sum_{1}^{n} f_i I_i / \Sigma f$$

These flux-weighted values are an approximation of a 'core top' value, assuming that seasonal flux patterns have remained similar to present over the time span represented by each core top (eg. Mix, 1987). An assumption in determining flux-weighted estimates is that the flux in the size fraction analysed remains proportional to the total flux of that species. To refine this estimate we would need to weight the isotopic value according to the flux in each size fraction, but this would cause statistical problems at low flux intervals.

4.4.4 Equilibrium $\delta^{18}O$ calculations

The $\delta^{18}O$ of seawater was calculated using salinity measured from CTD casts and the Levitus data base (Levitus, 1994) in accordance with the equation of Duplessy (1970):

$$\delta^{18}O_{water} = 0.66*\text{salinity} - 22.6$$

The $\delta^{18}O_{water}$ values are expressed as ‰ SMOW. The equilibrium calcite composition was predicted with depth using observed temperatures obtained from CTD casts and the Levitus data base (Levitus, 1994). Sea-surface temperatures obtained from the AVHRR (Advanced Very High Resolution Radiometer, 1999) satellite during the deployment period were also used to obtain a better estimate of surface water $\delta^{18}O$ at each site. Unfortunately there are few water column measurements of $\delta^{18}O_{water}$ from the trap sites with which to better calibrate the $\delta^{18}O_{water}$/salinity relationship. Measurements of $\delta^{18}O_{water}$ have been obtained from two casts north and south of Chatham Rise, and these correspond well to the relationship of Duplessy (1970). For the Subantarctic region

measured $\delta^{18}O_{water}$ is within 0.1‰ of calculated values, while measurements within the Subtropical Zone are offset from calculations by up to 0.3‰.

The sediment trap data was used to test the calibration of several commonly used equilibrium equations. These equations are as follows:

1. The Epstein et al. (1953) equation, developed from mollusks:

$$T_{water} = 16.5 - 4.3\,(\delta^{18}O_{calcite} - \delta^{18}O_{water}) + 0.14\,(\delta^{18}O_{calcite} - \delta^{18}O_{water})^2$$

2. The inorganic equation of Kim and O'Neil (1997):

$$T_{water} = 16.1 - 4.64\,(\delta^{18}O_{calcite} - \delta^{18}O_{water}) + 0.09\,(\delta^{18}O_{calcite} - \delta^{18}O_{water})^2$$

3. The 12 chambered *G. bulloides* equation of Bemis et al. (1998):

$$T_{water} = 13.2 - 4.89\,(\delta^{18}O_{calcite} - \delta^{18}O_{water})$$

4. The *G. bulloides* (9-24°C) equation of Bemis et al. (2002):

$$T_{water} = 13.4 - 4.48\,(\delta^{18}O_{calcite} - \delta^{18}O_{water})$$

5. The *N. pachyderma* equation of von Langen et al. (2000):

$$T_{water} = 16.4 - 4.57\,(\delta^{18}O_{calcite} - \delta^{18}O_{water}) + 0.349\,(\delta^{18}O_{calcite} - \delta^{18}O_{water})^2$$

The $\delta^{18}O_{water}$ values were corrected to PDB by applying an offset of -0.2‰ when using the $\delta^{18}O$ calcite equation of Epstein (1953), and -0.27‰ when applying the more recent $\delta^{18}O$ calcite equations (see Bemis et al., 1998).

4.5 Results

4.5.1 Paleotemperature equations

Each of the paleotemperature equations predict significant differences in the seasonal amplitude in $\delta^{18}O$ and exhibit substantial offsets from each other. At 44°S, for example, the $\delta^{18}O$ calculated with the Epstein et al. (1953) equation exhibits a large seasonal range compared to the equations of Kim and O'Neil (1997) and von Langen (2000) (Figure 2). The seasonal amplitude recorded by the foraminifera may help to constrain our choice of these equations. The Epstein et al. (1953) equation also shows the most

enriched $\delta^{18}O$ values, with an enrichment of 1‰ compared to the Bemis et al. 1998 and 2002 equations. The offset between the equations increases with latitude. The range between the Bemis et al. (1998) and Epstein et al. (1953) equations increases from ~0.8‰ at NCR to 1.6‰ at 54°S. This large variation between the temperature equations could lead to differences in temperature estimates of as much as 7.2°C at more southerly latitudes. It is therefore critical to determine which of these equations provides the best fit to Southern Ocean foraminiferal $\delta^{18}O$ records.

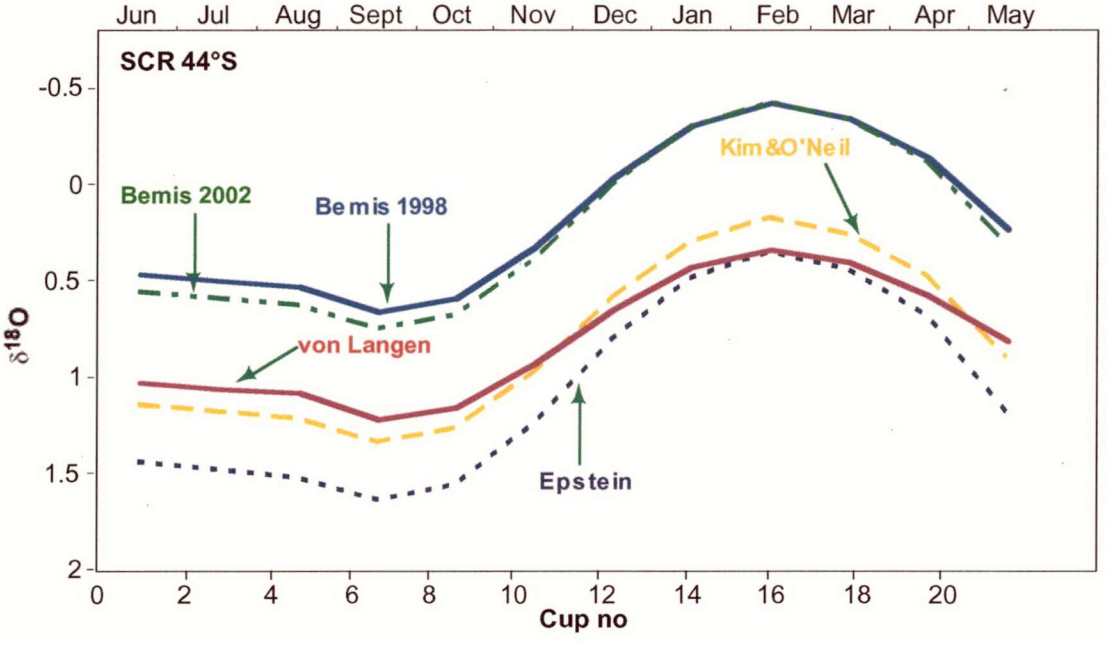

Figure 2: Predicted equilibrium $\delta^{18}O$ at 44°S based on the 12-chambered *G. bulloides* relationship of Bemis et al. (1998), the revised *G. bulloides* relationship of Bemis et al. (2002), the *N. pachyderma* (s.) relationship of von Langen (2000), the inorganic relationship of Kim and O'Neil (1997), and the mollusk relationship of Epstein et al. (1953). These equilibrium calibrations are based on the Levitus surface temperature and salinity and CTD casts during May.

4.5.2 A test of the paleotemperature equations

Linear regression between the predicted equilibrium $\delta^{18}O$ ($\delta^{18}O_{EQ}$) calculations and foraminiferal $\delta^{18}O$ allows us to assess the correlation between predicted and observed $\delta^{18}O$. The $\delta^{18}O_{EQ}$ calculations have been made on the basis of observed AVHRR SSTs during each cup period. The linear regressions illustrate several useful aspects of each equation: 1) the slope of the regression line compared to the 1:1 relationship; 2) the scatter in the data points relative to the linear regression; and 3) the distance of the

regression line from the 1:1 relationship. We use each of these aspects to determine the variations between each of the relationships across the sites for the three species. We combine data from all 5 sites to test these equations across a wide range of environments, spanning 12° of latitude from subtropical to polar frontal environments. A test of this nature is critical since the Polar Front is thought to have shifted northward by at least 5-7° during glacial periods of the Pleistocene (Prell et al., 1979; Morley, 1989; Howard and Prell, 1992) , emphasising the importance of applying temperature equations which are consistent across a wide range of latitudes and environments.

G. bulloides: The regression of shell versus calculated $\delta^{18}O_{EQ}$ for *G. bulloides* across all sites is shown for five different temperature relationships in Figure 3a. The slope of each calibration varies, revealing inconsistencies in some relationships across the full range of values. The calibration of Bemis et al. (1998), for instance, yields a slope against the measured $\delta^{18}O$ of 1.34. The range in $\delta^{18}O_{EQ}$ values predicted from this relationship is therefore much smaller than the range measured from *G. bulloides*, so application of this calibration would underestimate the temperature range at these sites. The relationship of Epstein et al. (1953), by contrast, yields a slope of 0.99 for the measured versus predicted $\delta^{18}O_{EQ}$. Equilibrium values calculated using this equation are depleted by ~0.37±0.28‰ compared to measured $\delta^{18}O$ for *G. bulloides*, but the offset remains almost constant across the full range of values. There is some scatter in values around this relationship, but the R^2 is higher than for the other calibrations with a value of 0.87.

N. pachyderma (s.): Measured $\delta^{18}O$ for *N. pachyderma* (s.) versus predicted $\delta^{18}O_{EQ}$ displays a fairly similar pattern to *G. bulloides* (Figure 3b). The Bemis et al. (1998) relationship has the steepest slope (1.33), while the slope derived from Epstein et al. (1953) relationship (0.96) provides an almost consistent offset from the expected equilibrium throughout the whole record. The Epstein relationship yields a disequilibrium offset for *N. pachyderma* (s.) of ~-0.50±0.37‰. The consistency of this offset through the whole record means that it is possible to correct the $\delta^{18}O$ values for *N. pachyderma* (s.) to expected equilibrium, with an uncertainty of ±0.37‰ if the Epstein calibration is employed. None of the other equations provide such consistency in their relationship to *N. pachyderma* (s.) $\delta^{18}O$. The *N. pachyderma* calibration of von Langen (2000) provides a very poor correlation to this data, with a slope of 1.74 and an R^2 of 0.77.

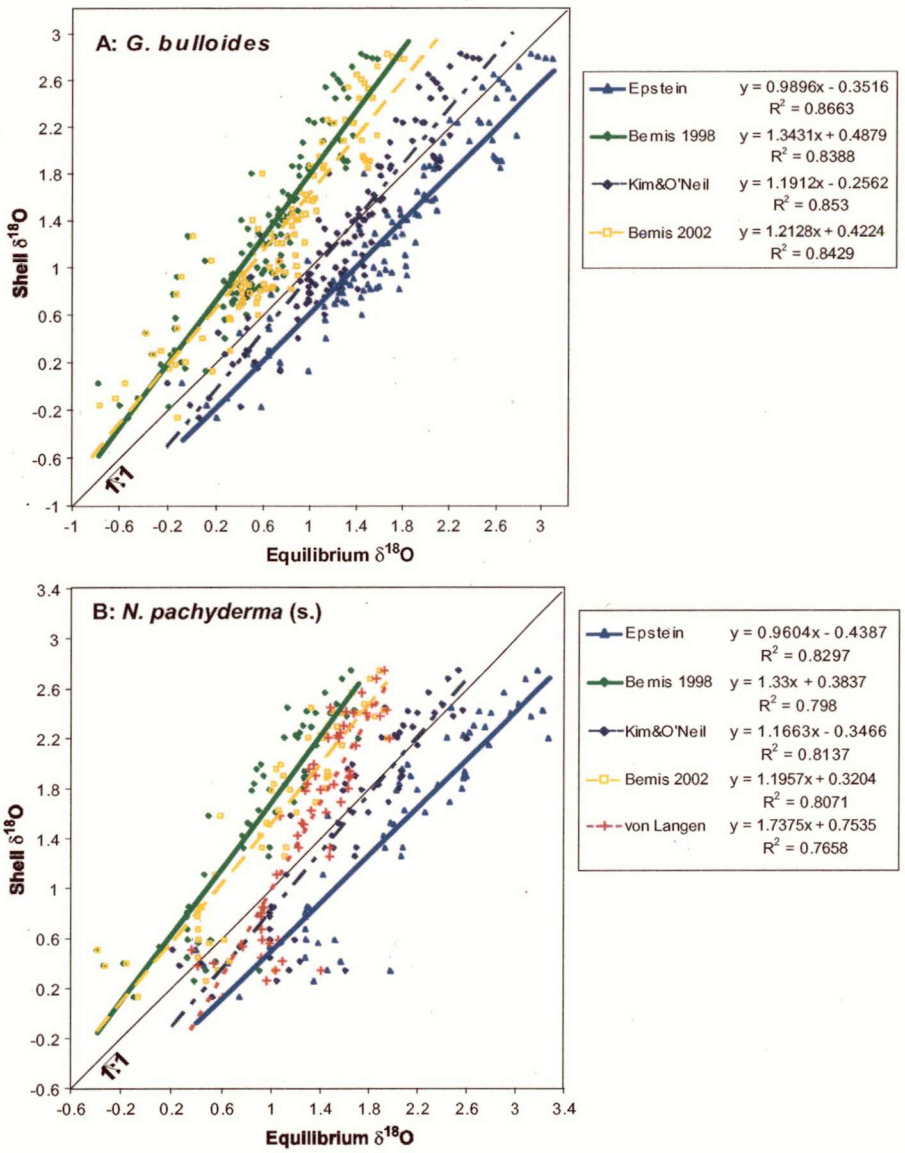

Figure 3: Shell $\delta^{18}O$ versus predicted equilibrium $\delta^{18}O$ across all sites for *G. bulloides* (A), *N. pachyderma* (s.) (B) and *G. inflata* (C). Equilibrium values are calculated using the 12-chambered *G. bulloides* relationship of Bemis et al. (1998), the revised *G. bulloides* relationship of Bemis (2002), the inorganic equation of Kim and O'Neil (1997), and the mollusk relationship of Epstein et al. (1953). The Epstein relationship provides the most consistent offset from predicted equilibrium for both *G. bulloides* and *N. pachyderma* (s.). *G. inflata* displays a lower range in $\delta^{18}O$ than expected equilibrium, suggesting that this species dwells below the surface. Equilibrium values have been calculated based on the observed AVHRR (1999) sea surface temperatures during the deployment, with surface salinity from Levitus (1994).

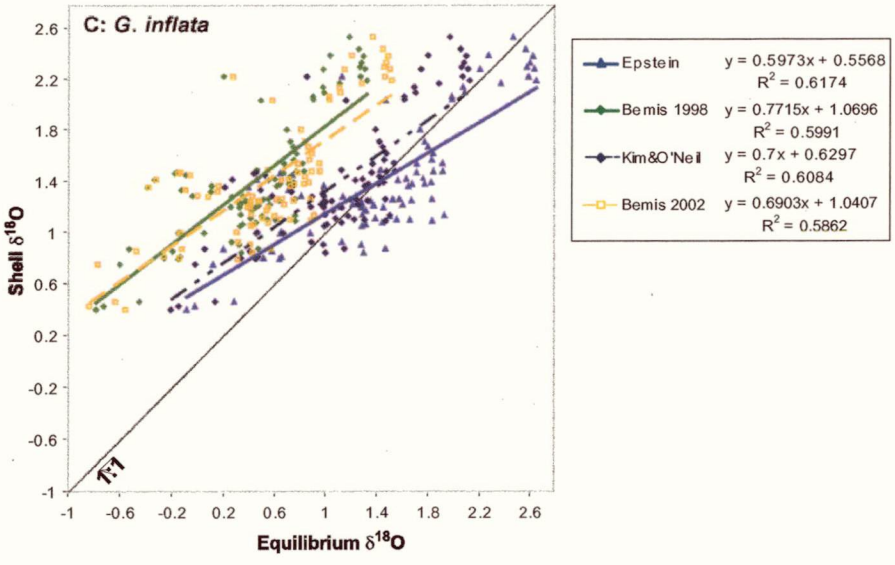

Figure 3 continued

G. inflata: The relationship between shell and $\delta^{18}O_{EQ}$ shows much larger scatter for *G. inflata* than for *G. bulloides* or *N. pachyderma* (s.) (Figure 3c). The R^2 values across all calibrations for *G. inflata* are between 0.59 and 0.62, compared to 0.77 to 0.87 for *N. pachyderma* (s.) and *G. bulloides*. The slope of the relationships for *G. inflata* are also quite shallow for each calibration, indicating that there is a greater range in surface equilibrium than is measured for *G. inflata*, regardless of the relationship used. These patterns suggest that *G. inflata* does not inhabit surface waters at these sites. We assess the habitat depth for each species in the following section.

4.5.3 Habitat depth

Comparison between the seasonal range in the $\delta^{18}O$ values for each species and the seasonal amplitude exhibited in the predicted equilibrium relationships can be used to determine the habitat depths for each species. We calculate the equilibrium range in $\delta^{18}O$ based on the Epstein equation, using the AVHRR surface temperatures and Levitus temperatures at depth.

G. bulloides: The seasonal range observed for each of the species is compared to the predicted equilibrium range in Table 1. For *G. bulloides*, the seasonal range in $\delta^{18}O$ observed across each of the trap deployments compares well with the seasonal amplitude predicted from the Epstein equation using the surface AVHRR temperatures. A surface

to near-surface habitat is inferred across all sites for *G. bulloides*, apart from during the 1998 deployment at 47°S (Table 2) (see later discussion).

	SEASONAL AMPLITUDE IN $\delta^{18}O$			
	$\delta^{18}O_{EQ}$	*G. bulloides*	*N. pachyderma* (s.)	*G. inflata*
NCR	1.4 (AVHRR) 1.2 (Lev. 0m) 0.95 (Lev. 50m)	1.17	NA	0.97
SCR	1.65 (AVHRR) 1.3 (Lev. 0m) 0.95 (Lev. 50m)	1.74	1.45	1.0
47°S	0.71 (AVHRR 1997) 1.1 (AVHRR 1998) 1.1 (Lev. 0m) 0.93 (Lev. 50m)	0.8 (1997) 0.6 (1998)	NA	0.8 (1997) 0.83 (1998)
51°S	0.67 (AVHRR) 1.05 (Lev. 0m) 0.5 (AVHRR, Sept-Dec) 0.51 (L. 0m, Sept-Dec) 0.49 (L. 50m, Sept-Dec)	0.8	0.67	0.36 (Sept-Dec)
54°S	0.8 (AVHRR Nov –Mar) 1.16 (Lev. 0m Nov – Mar)	0.7 (Nov – Mar)	0.6 (Nov – Mar)	NA

Table 1: Seasonal range in $\delta^{18}O$ for the Epstein equilibrium calculations and for *G. bulloides*, *N. pachyderma* (s.) and *G. inflata*. The seasonal range for *G. bulloides* and *N. pachyderma* (s.) generally compares well to the range in surface equilibrium values, while the seasonal range for *G. inflata* is consistent with the range at depths of ~50 m. Equilibrium $\delta^{18}O$ values for 0m and 50m are calculated according to the climatological temperature and salinity (Levitus, 1994).

	INFERRED HABITAT DEPTHS		
	G. bulloides	*N. pachyderma* (s.)	*G. inflata*
NCR	Near-surface	NA	~50 m
SCR	Surface	Near-surface	~50 m
47°S	Near-surface (1997) ? 100 m (1998)	NA	Surface (1997) ~50 m (1998)
51°S	Surface	Surface	0 – 100 m
54°S	Surface	Near-surface	NA

Table 2: Habitat depths inferred from the seasonal amplitude in $\delta^{18}O$ values compared to equilibrium for *G. bulloides*, *N. pachyderma* (s.) and *G. inflata*.

N. pachyderma (s.): This species also tends to dwell in the surface to near-surface environment. At SCR, the seasonal $\delta^{18}O$ range for *N. pachyderma* (s.) is consistent with the predicted equilibrium values from just below the surface (Table 1 and 2). At 47°S it is difficult to discern the seasonal amplitude due to the lack of data points, but at 51°S, *N. pachyderma* (s.) captures the surface range in $\delta^{18}O_{EQ}$. At 54°S, *N. pachyderma* (s.) has a slightly lower range in $\delta^{18}O$ than observed at the surface, suggesting that this species dwells slightly below the surface in the PFZ (Table 1 and 2).

G. inflata: *G. inflata* exhibits a relatively low seasonal amplitude in $\delta^{18}O$, equivalent to predicted equilibrium at ~50 m at both NCR and SCR (Table 1 and 2). At 47°S, *G. inflata* appears to change habitat depth between the 1997 and 1998 deployment. The seasonal amplitude in $\delta^{18}O$ recorded by this species is similar for both years, however, there is a change in $\delta^{18}O_{EQ}$. Comparison to the predicted equilibrium values implies a surface habitat for *G. inflata* during 1997, and of ~50 m during 1998. At 51°S, isotopic analysis of *G. inflata* was restricted to the interval between September and December. Due to the weak stratification of the water column during this interval it is not possible to distinguish between $\delta^{18}O_{EQ}$ values between 0 and 100 m, so we cannot define the habitat depth for *G. inflata* at this site.

We can test the consistency of the deeper habitat for *G. inflata* by plotting predicted equilibrium $\delta^{18}O$ at 50 m against the measured $\delta^{18}O$ for *G. inflata* across all sites (Figure 4). Each of the equilibrium calibrations shown in Figure 4 exhibit a steeper slope against measured $\delta^{18}O$ than for the surface calibrations, however, none achieve a 1:1 fit between the shell and calculated equilibrium values. The inconsistency between the shell and predicted equilibrium $\delta^{18}O$ at 50 m implies that either *G. inflata* does not dwell at 50 m throughout the season at all sites, or that the Levitus salinity and temperature climatology does not adequately capture the conditions during the deployment period. These possibilities are explored in more detail in the following section.

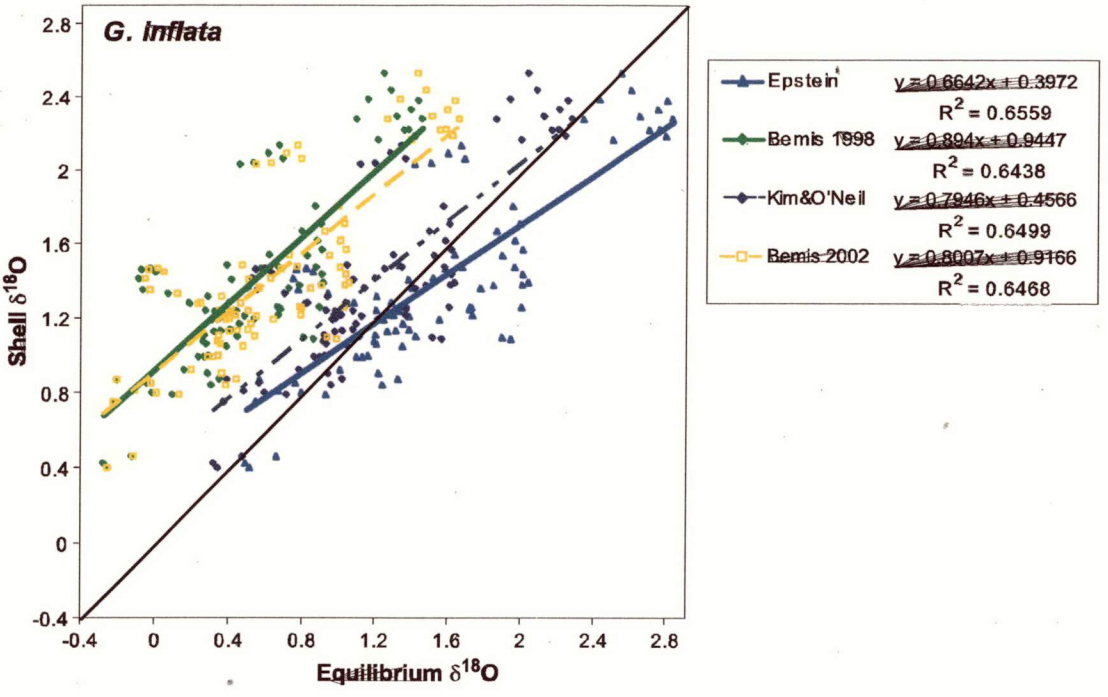

Figure 4: *G. inflata* $\delta^{18}O$ versus predicted equilibrium $\delta^{18}O$ at 50 m across all sites. Equilibrium values are calculated using the equations as stated in Figure 3 and are based on the Levitus (1994) temperature and salinity climatologies at a water depth of 50 m.

4.5.4 Habitat depth variations with season

The broad patterns in habitat depth are consistent across the sites for each species (Tables 1 and 2), but there are some variations in habitat depth throughout the season (Figures 4-6). These seasonal variations may reflect offsets between the collection and precipitation of foraminiferal tests by the traps, small variations in temperature and/or salinity not captured by the monthly AVHRR and Levitus values, or even seasonal changes in the salinity to $\delta^{18}O_{water}$ relationship. Examples of each of these situations are highlighted in the following section. For comparison to the seasonal trend in $\delta^{18}O_{EQ}$, we have corrected the $\delta^{18}O$ values for *G. bulloides* and *N. pachyderma* (s.) according to the offsets from predicted equilibrium determined by the regression analysis (0.37‰ and 0.50‰ respectively).

There is only one site at which we observe a significant lag between the shell and equilibrium $\delta^{18}O$ values. The seasonal trend in $\delta^{18}O$ exhibited by *G. bulloides* at SCR suggests an offset of approximately one month between the precipitation and collection

of the foraminiferal tests by the trap. This pattern is most pronounced between September and February (Figure 5b).

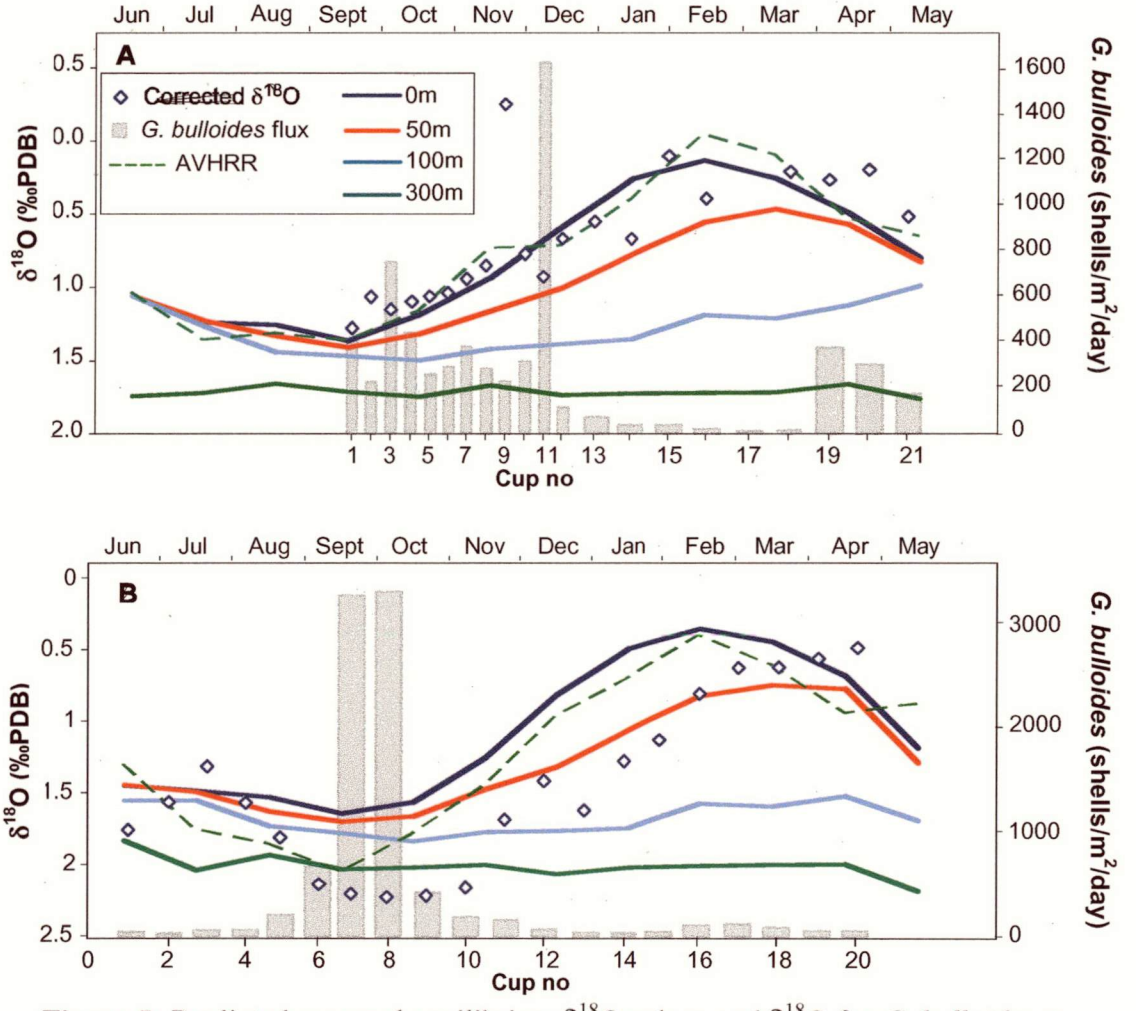

Figure 5: Predicted seasonal equilibrium $\delta^{18}O$ values and $\delta^{18}O$ for *G. bulloides* at NCR (A), SCR (B), 47°S (C), 51°S (D) and 54°S (E). *G. bulloides* $\delta^{18}O$ has been corrected according to the offset of -0.37‰ from the Epstein relationship. The fluxes of *G. bulloides* collected in each cup is also shown to illustrate seasonal flux patterns at each site.

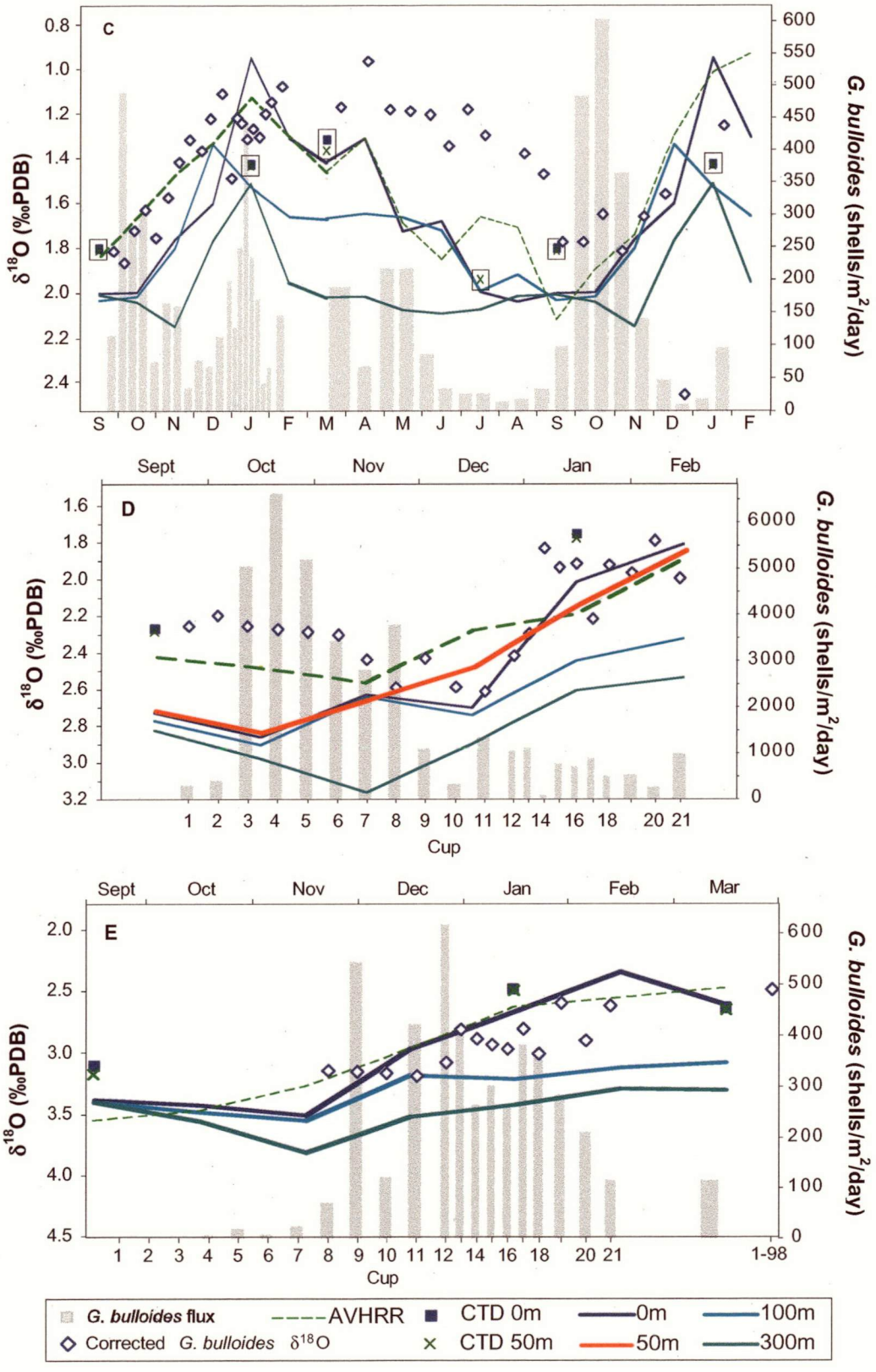

Figure 5 continued

The $\delta^{18}O$ records for both *G. bulloides* and *G. inflata* at 47°S exhibit strong depletions of up to 0.6‰ compared to predicted equilibrium between March and September 1998 (Figures 4c and 6c). The occurrence of this depletion in both species suggests that the calculated equilibrium values do not fully reflect the real equilibrium conditions during this interval, possibly due to unrecorded changes in temperature or salinity. The observed AVHRR surface temperatures at this time are similar to the long term averages recorded in the Levitus dataset, apart from the warmer temperatures during July and August which cause a depletion in $\delta^{18}O_{EQ}$. There is only one water column measurement of temperature and salinity from during the deployment and this is from March 1998. This one measurement is consistent with salinity and temperature obtained from the Levitus climatology, but we have no means of calibrating the remaining observations during this interval. We can therefore only speculate that the depleted $\delta^{18}O$ values throughout this March to September interval represent either a slight reduction in salinity, or a change in the $\delta^{18}O$ sea water relationship to salinity.

At 51°S, the AVHRR temperatures between September and December are between 0.4° and 1.4°C warmer than the Levitus surface values. This offset between the two data sets results in a difference of up to 0.4‰ for equilibrium $\delta^{18}O$ calculated from the AVHRR and the Levitus data. This difference between the AVHRR and surface Levitus values makes it difficult to predict equilibrium $\delta^{18}O$ values at depth for this interval, causing some inconsistency between the *G. inflata* $\delta^{18}O$ and predicted equilibrium $\delta^{18}O$ at 50 m as shown in Figure 4.

At the other sites, the seasonal trends in $\delta^{18}O$ recorded by each of the species remain fairly consistent with predicted equilibrium values at their inferred habitat depths. Slight variations in $\delta^{18}O_{foram}$ compared to equilibrium may reflect small changes in salinity and temperature not captured by our monthly and climatological data.

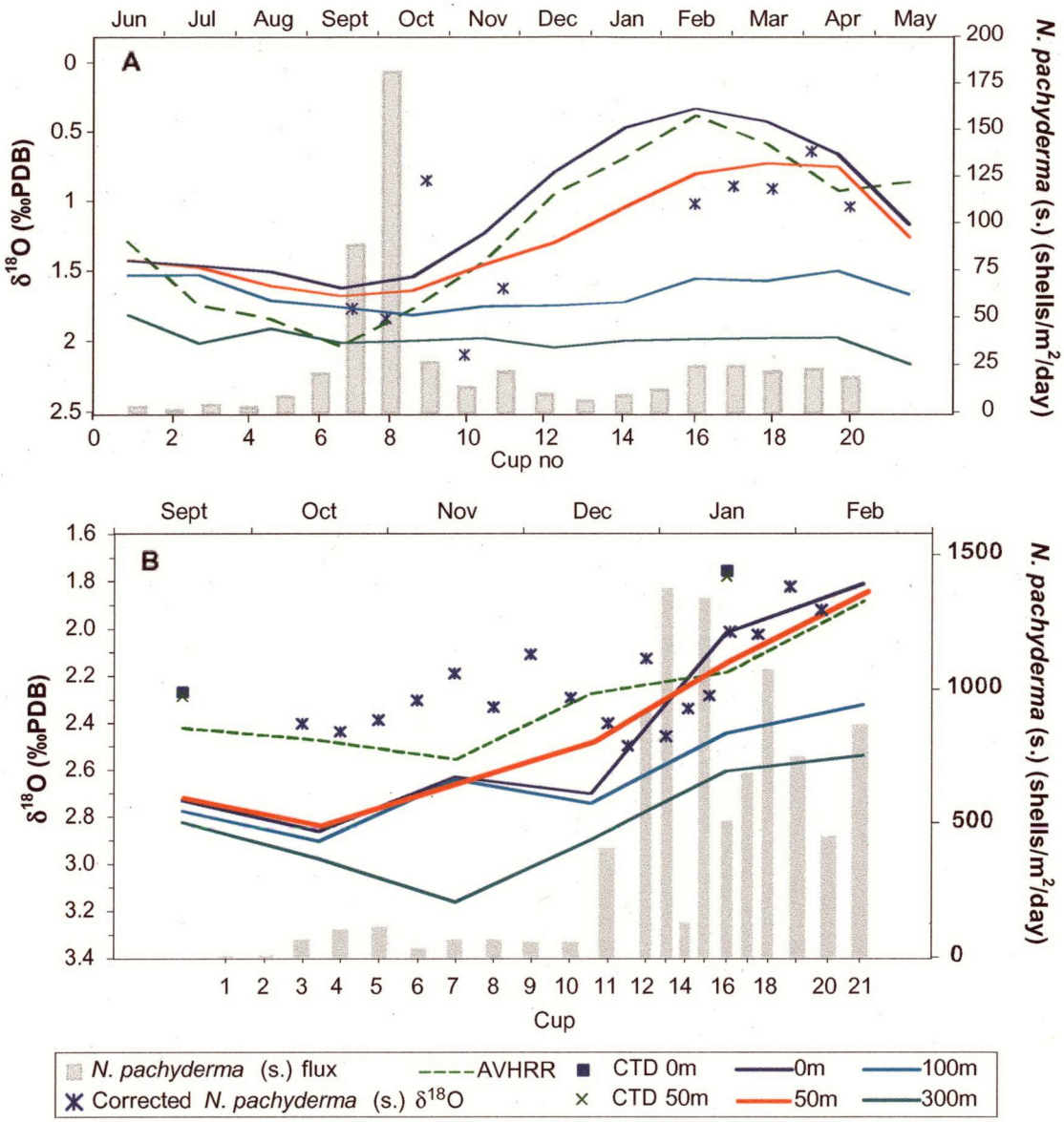

Figure 6: Predicted seasonal equilibrium $\delta^{18}O$ values and $\delta^{18}O$ for *N. pachyderma* (s.) at SCR (A), 51°S (B) and 54°S (C). *N. pachyderma* (s.) $\delta^{18}O$ values have been corrected according to the offset of -0.50‰ from the Epstein equilibrium calibration. Fluxes of *N. pachyderma* (s.) collected in each cup are also shown, indicating a change in seasonal fluxes from spring at SCR to summer at 51°S and 54°S.

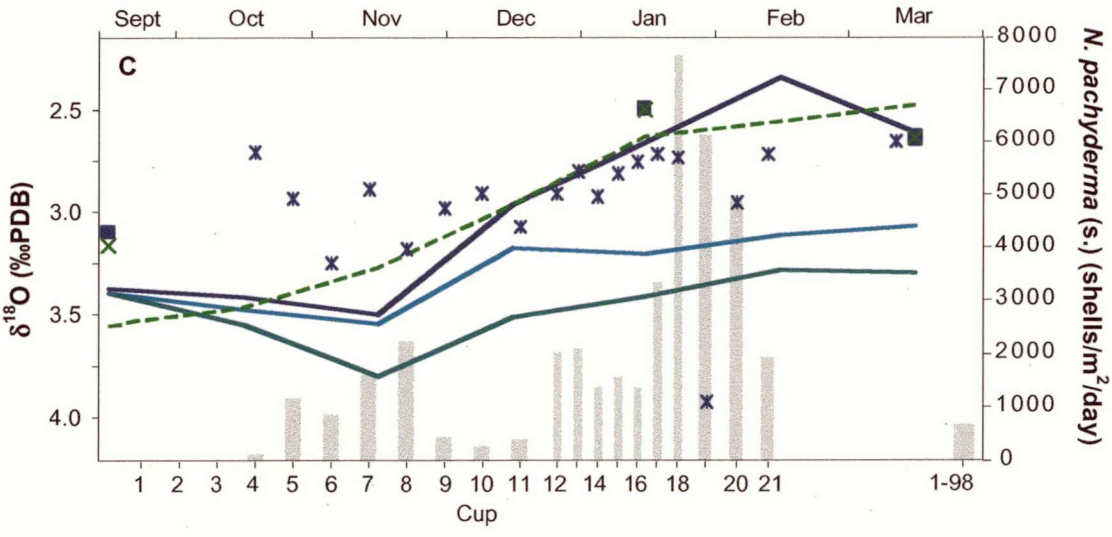

Figure 6 continued

4.5.6 Seasonality in flux and $\delta^{18}O$

Sediment trap deployments provide the opportunity to consider the influence of seasonal flux patterns on $\delta^{18}O$ records. Previous analysis of the foraminiferal assemblages from these sediment trap sites has indicated that foraminiferal production displays distinct seasonality at each site (see King and Howard, 2001; King and Howard, 2003). The timing of the dominant flux intervals are mostly consistent between the sites, but there are differences in the timing of minor fluxes. *G. bulloides*, for instance, has its maximum production during December at NCR, with slightly higher fluxes during October (Figure 5a), while at SCR, *G. bulloides* production occurs almost exclusively between September and October (Figure 5b). At 47°S, production of *G. bulloides* occurs predominantly during October, with higher production also during January (Figure 5c). At 51°S, production occurs during October and November for *G. bulloides* (Figure 5d), while at 54°S greatest flux for this species occurs during November to January, with barely any flux during September and October (Figure 5e). We examine the significance of these latitudinal changes in seasonal flux patterns in the following section by deriving the flux-weighted isotopic composition for each species at each site. We then compare these values to the isotopic composition obtained from nearby core tops to establish the seasonal imprint on the sedimentary isotopic records.

G. bulloides: The flux-weighted foraminiferal $\delta^{18}O$ values are compared to the seasonal maximum and minimum calculated equilibrium $\delta^{18}O$ values across each of the sites in

Figures 7a-c. The flux-weighted values for *G. bulloides* exhibit a much steeper latitudinal gradient between NCR and SCR than observed for the calculated equilibrium values, reflecting the change in production season between these sites (Figure 8a). At NCR, the *G. bulloides* flux is spread across September to December and April to May, when predicted equilibrium $\delta^{18}O$ values are moderate in the seasonal range. The flux-weighted values therefore fall part way between the extremes in the equilibrium values. At SCR, by contrast, 85% of the *G. bulloides* flux occurs during September and October, when calculated equilibrium $\delta^{18}O$ values are most enriched. The flux-weighted trap values are therefore strongly weighted towards the maximum equilibrium $\delta^{18}O$ values at this site. The change in seasonal production for *G. bulloides* between these two sites creates a steeper latitudinal gradient than observed during any one season. At 47°S and 54°S, flux-weighted values tend to be distributed between the maximum and minimum envelope of the predicted equilibrium values. This reflects the spring to summer fluxes of *G. bulloides* at these sites. At 51°S, flux-weighted values reflect the relatively high spring flux at this site, with values weighted more strongly towards the maximum $\delta^{18}O$ values at this site.

N. pachyderma (s.): Flux-weighted values for *N. pachyderma* (s.) largely reflect the seasonal flux patterns for this species. At SCR, flux predominantly occurs during September and October when $\delta^{18}O$ values are most enriched, however, 20% of the total flux for this species also falls during February to April (Figure 6a), causing a slight depletion in the flux-weighted $\delta^{18}O$ values (Figure 8b). At 47°S, production is strongly weighted towards January when predicted equilibrium $\delta^{18}O$ is most depleted. The flux-weighted values are therefore very close to the minimum equilibrium estimates. At 51°S and 54°S the highest flux for *N. pachyderma* (s.) occurs during late spring to summer, resulting in moderate flux-weighted values at these sites. The change in flux seasonality for *N. pachyderma* (s.) has most impact on the gradient in $\delta^{18}O$ values between SCR and 47°S and across the SAF between 47°S and 51°S.

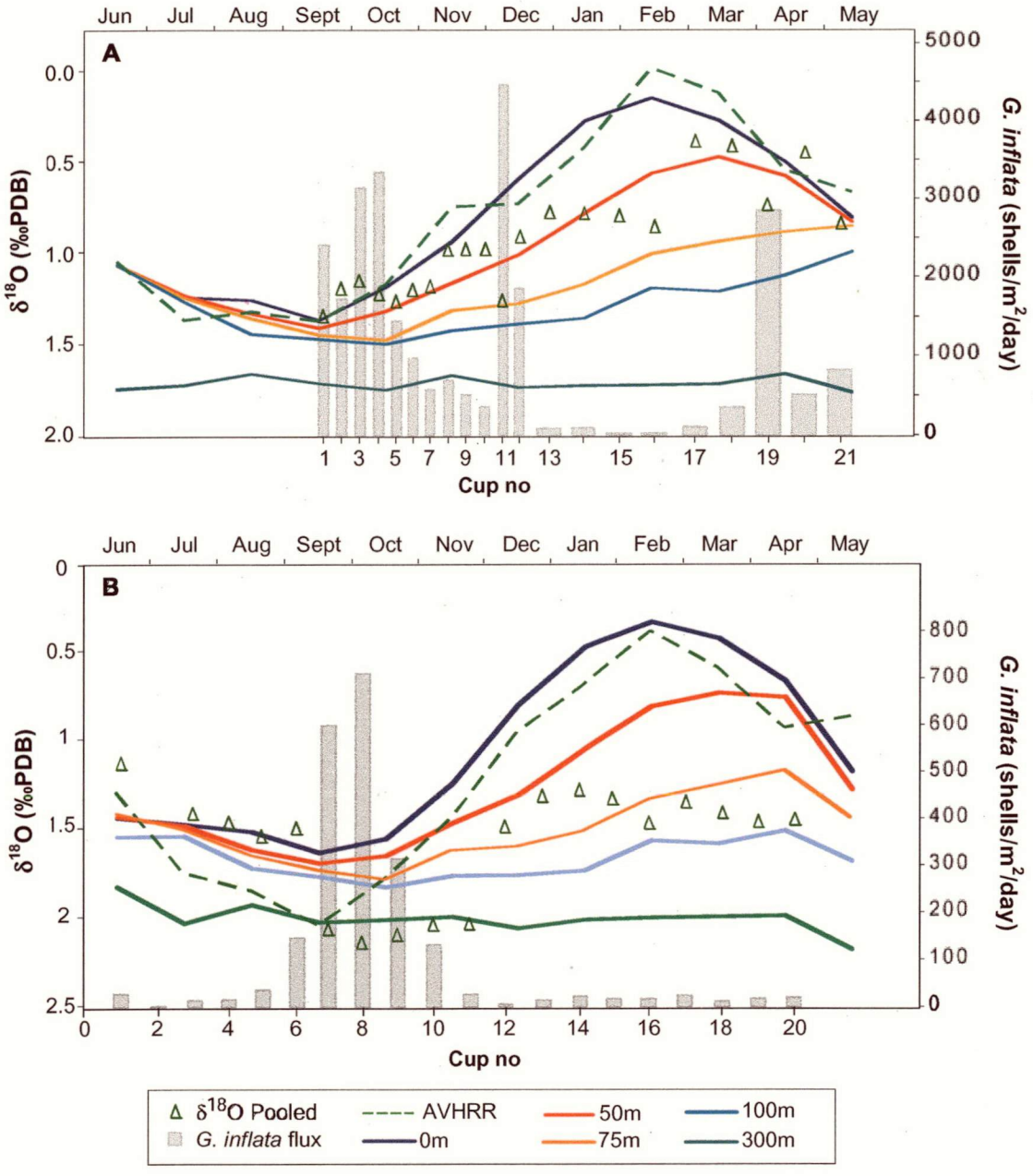

Figure 7: Predicted seasonal equilibrium $\delta^{18}O$ values and $\delta^{18}O$ for *G. inflata* at NCR (A), SCR (B), 47°S (C) and 51°S (D). The enrichment in $\delta^{18}O$ for *G. inflata* and the low seasonal amplitude compared to surface equilibrium values suggest that this species dwells at depths of ~50 m at each site. Fluxes of *G. inflata* collected in each cup display a change in seasonal fluxes across each site.

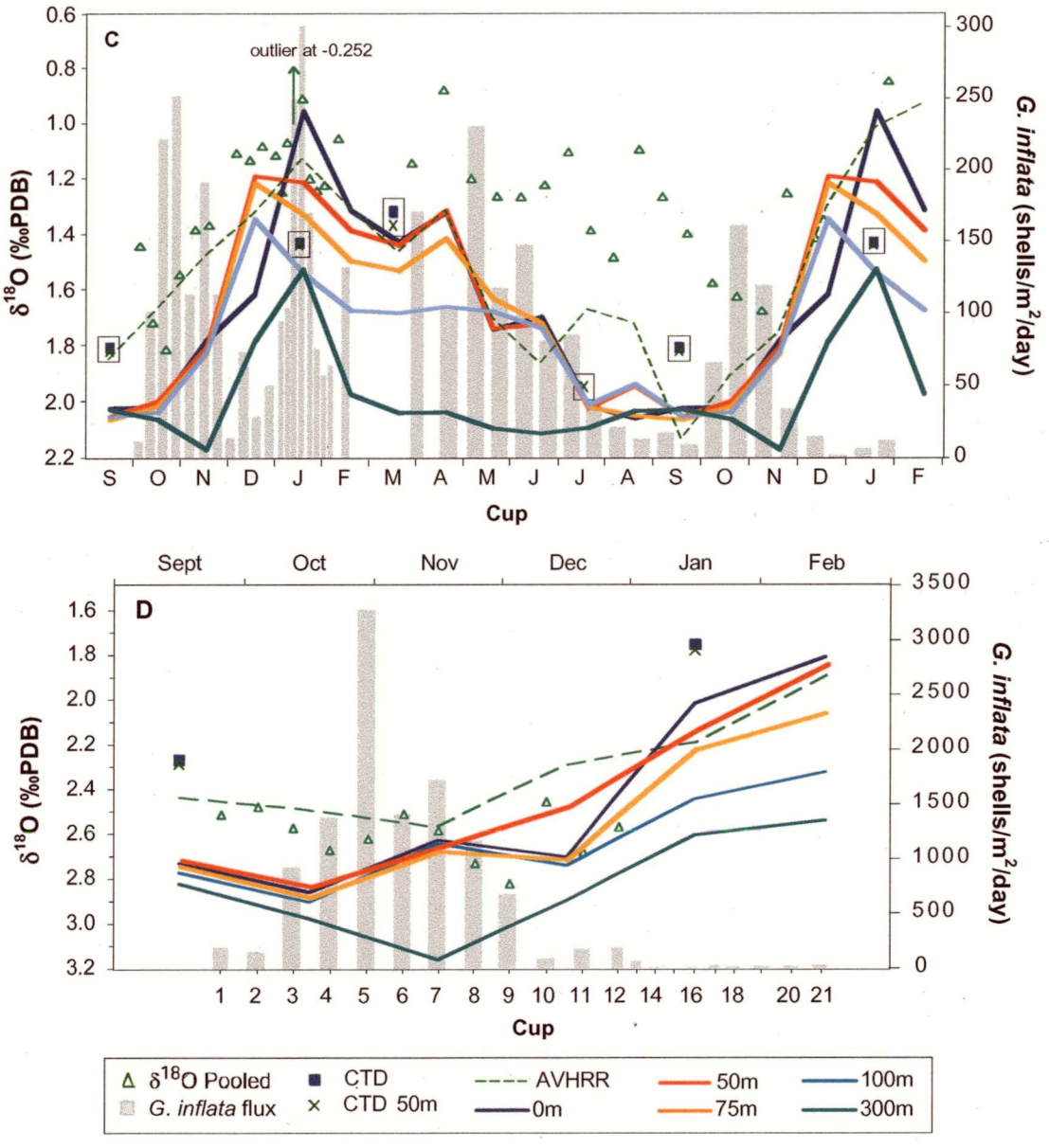

Figure 7 continued

G. inflata: We compare the flux-weighted $\delta^{18}O$ for *G. inflata* against the minimum and maximum predicted equilibrium values at 50 m (Figure 8c). Fluxes of *G. inflata* at NCR are spread across September to December and April to May (Figure 7a). The flux-weighted $\delta^{18}O$ values are therefore intermediate between the minimum and maximum values at NCR. At SCR, 82% of the flux occurs during September and October (Figure 7b), causing flux-weighted values to reflect the minimum equilibrium values at this site, and creating a steeper $\delta^{18}O$ gradient between NCR and SCR than would occur during any one time. There is a large difference in flux-weighted $\delta^{18}O$ values between SCR and 47°S, since high fluxes of *G. inflata* at 47°S are associated with the most depleted $\delta^{18}O$ values during summer and autumn (Figure 7c). At 51°S, flux-weighted $\delta^{18}O$ values lie within the seasonal range of $\delta^{18}O_{EQ}$, reflecting the predominantly late spring fluxes of *G. inflata* at this site (Figure 7d).

4.5.7 Preservation of seasonal fluxes in regional core tops

The flux-weighted isotopic values are compared to regional core top values to determine whether the core top sediments reflect the modern seasonal flux patterns observed from the sediment trap deployments. This comparison provides a means of testing the calibration between the core tops and modern oceanographic conditions, and establishes whether the results from the traps can be applied to other sedimentary records. It is important to consider the impact of seasonal flux patterns on the sedimentary record since differences in seasonal fluxes between sites or down the core may exaggerate or weaken the true isotopic gradients. This is illustrated clearly by the steep gradients in the flux-weighted trap values observed for both *G. bulloides* and *G. inflata* between NCR and SCR, reflecting the change from summer to spring fluxes (Figures 7a and c).

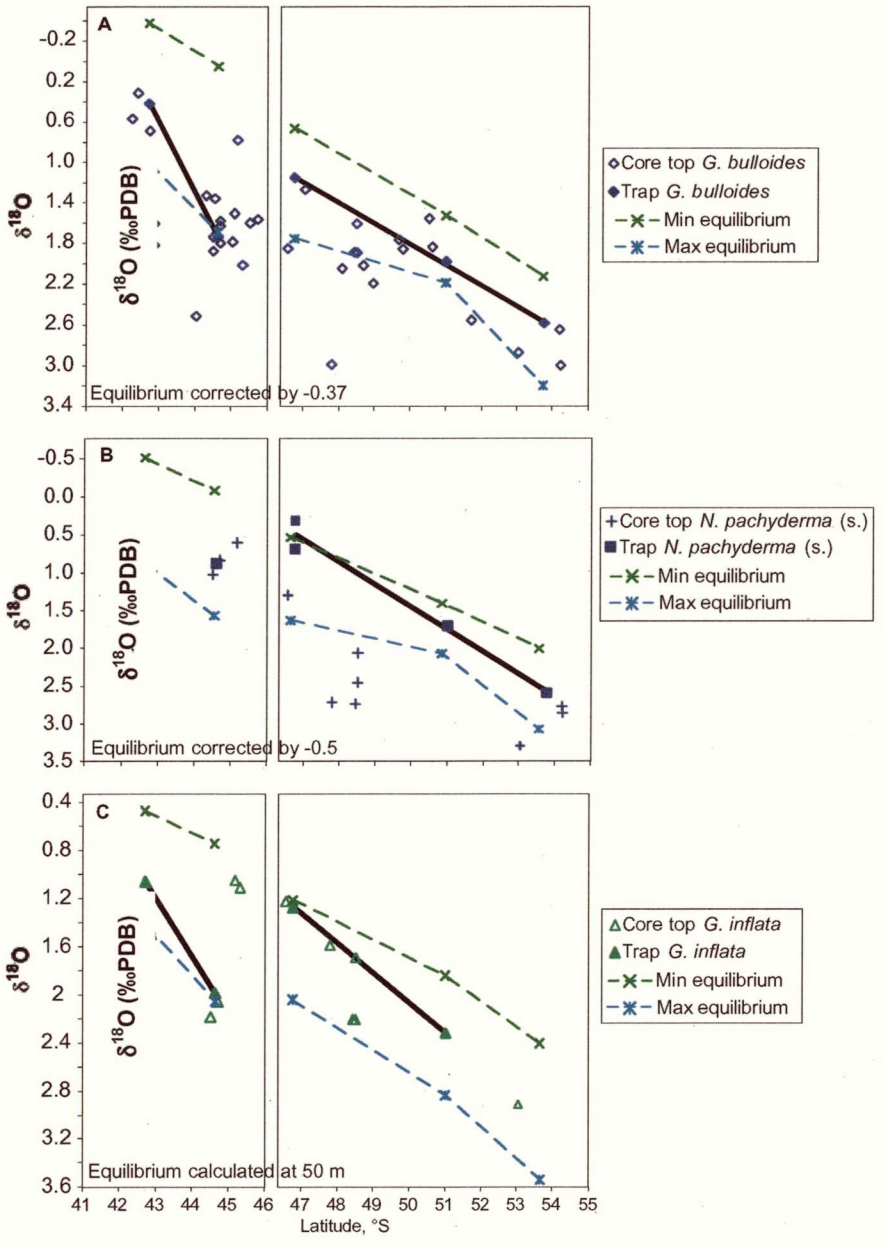

Figure 8: Flux-weighted $\delta^{18}O$ values for each sediment trap are compared to $\delta^{18}O$ values from regional core tops for *G. bulloides* (A), *N. pachyderma* (s.) (B) and *G. inflata* (C). The minimum and maximum equilibrium $\delta^{18}O$ values calculated from the Epstein equation are also displayed. Equilibrium values for *G. bulloides* are offset by -0.37‰ and for *N. pachyderma* (s.) by -0.50‰ to correct for disequilibrium. For *G. inflata* we show equilibrium calculated at 50 m. Flux-weighted values compare well with the core top $\delta^{18}O$ for *G. bulloides* and *G. inflata*, while core tops for *N. pachyderma* (s.) exhibit a large enrichment in $\delta^{18}O$. The core top values for *G. bulloides* and *G. inflata* are mostly well within the interannual range in $\delta^{18}O$ variability, and exhibit similar seasonal weightings as for the sediment trap values.

The core top $\delta^{18}O$ values for *G. bulloides* show some scatter around the sediment trap values, however, many of the core tops are within at least 0.2‰ of the trap values (Figure 8a), less than the interannual variability in sea water $\delta^{18}O$ at these sites. The core tops are also generally weighted towards the most enriched equilibrium $\delta^{18}O$ values, indicating a similar seasonal weighting as the sediment traps. *G. inflata* displays very good coherency between the weighted sediment trap values and the nearby core tops (Figure 8c). The $\delta^{18}O$ values from nearly all of the core top sediments are well within 0.2‰ of the trap values along the latitudinal transects. A larger scatter in core top $\delta^{18}O$ values relative to the sediment traps is observed for *N. pachyderma* (s.) (Figure 8b). For this species, many of the core top $\delta^{18}O$ values are enriched compared to the maximum modern annual $\delta^{18}O$ range, suggesting that the core top values for *N. pachyderma* (s.) do not reflect modern sediments. The low abundance of this species in the Subantarctic core tops, and the large number of specimens required per analysis compared to *G. bulloides* and *G. inflata*, make this species more prone to the incorporation of bioturbated glacial material with an enriched $\delta^{18}O$ signal. The general similarity between the flux-weighted sediment trap values and the core tops for *G. inflata* and *G. bulloides*, by contrast, indicates that seasonal flux patterns in this region have been consistent to those observed during the trap deployment throughout the Holocene.

4.6 Discussion

4.6.1 Disequilibrium in G. bulloides

Given the often large disequilibrium offsets cited for *G. bulloides*, it is important to consider the impact that this may have on our interpretations of $\delta^{18}O$ at these sites. Laboratory studies show that disequilibrium in $\delta^{18}O$ for *G. bulloides* is affected by the carbonate ion concentration of the sea water (Spero et al., 1997; Russell and Spero, 2000). We have estimated $[CO_3^{2-}]$ for the sediment trap sites based on the relationship between $[CO_3^{2-}]$ and temperature derived during transects conducted between 44°S and 65°S during January 1995, March 1998 and September 1996, and from WOCE lines P15S and P14S east and south of New Zealand during February 1996 [Tilbrook pers. comm.]. This data indicates that for the sediment trap sites the average $[CO_3^{2-}]$ is ~65 µmol/kg higher at NCR than 54°S. According to the equation of Spero et al. (1997), this should cause an increase in $\delta^{18}O$ relative to equilibrium of 0.33‰ between the trap sites. The evidence from this study, however, suggests that $[CO_3^{2-}]$ is not the dominant effect driving $\delta^{18}O$ disequilibrium at these sites (Figure 9). The offset from predicted equilibrium $\delta^{18}O$ appears constant (Figure 3a), and although the mechanism for this offset is not clear, its consistency across sites means that it can be applied uniformly to

G. bulloides $\delta^{18}O$ records from this region. For the carbon isotopes, we find a strong correlation between disequilibrium in *G. bulloides* and temperature, following the equation of Bemis et al. (2000) (King and Howard, submitted manuscript). However, there is also no evidence for a relationship between $\delta^{13}C$ disequilibrium and $[CO_3^{2-}]$ once this temperature effect has been taken into account. We therefore conclude that the carbonate ion concentration is not the dominant effect on isotopic disequilibrium in *G. bulloides* at these sites. The results from this study contrast with those from laboratory studies which show a strong isotopic response to $[CO_3^{2-}]$. This difference may reflect genotypic variability between the Southern Ocean fauna and the South California Bight derived laboratory cultures. No genetic analyses have been done on these Southern Ocean samples, however variations in isotopic calibrations have been inferred between genotypes in the North Atlantic (Bauch et al., 2003).

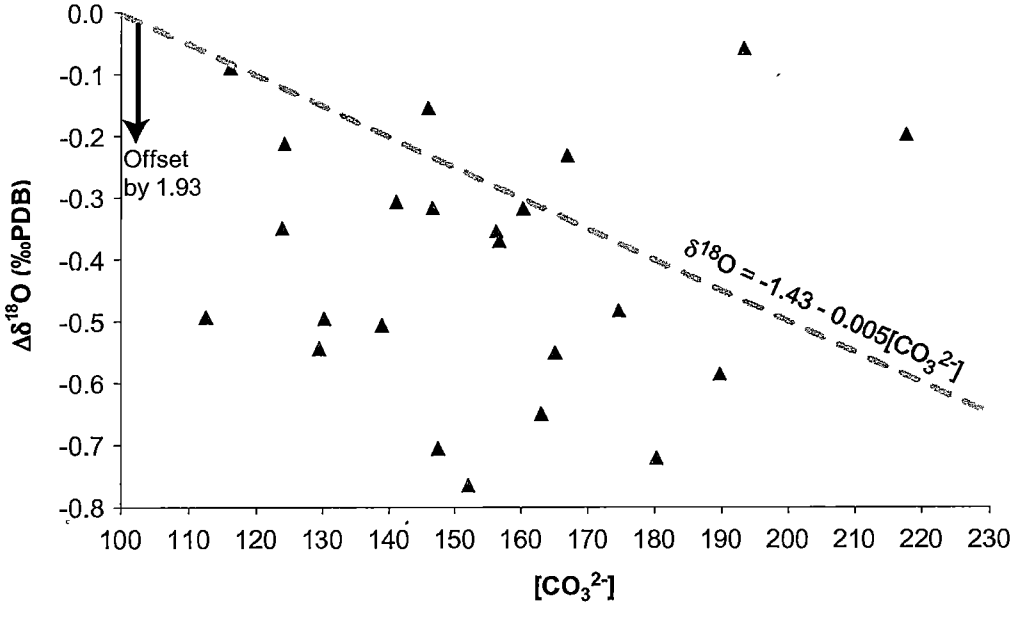

Figure 9: Carbonate ion concentration versus $\delta^{18}O$ disequilibrium in *G. bulloides* across each sediment trap site. $\delta^{18}O$ disequilibrium ($\Delta\delta^{18}O$) is measured as $\delta^{18}O_{G.\ bulloides} - \delta^{18}O_{Epstein}$. There is no trend in disequilibrium and $[CO_3^{2-}]$ at the sediment trap sites and values are much more enriched than would be calculated from the relationship of Spero et al. (1997) (dotted line). This line is plotted with an offset of 1.93‰ to show the trend relative to our values. Carbonate ion concentration is determined based on measurements of Tilbrook (pers. comm.).

4.6.2 Implications for interpreting paleo $\delta^{18}O$ records

The seasonal and depth distributions of each of the three species analysed in this study provide important insights for paleoclimate reconstructions from Southern Ocean environments as outlined in the following sections.

Habitat depth: The habitat depth for *G. bulloides* has been associated with the depth of the chlorophyll maximum in other regions (Fairbanks et al., 1982; Ortiz et al., 1995; Mortyn and Charles, 2003). *N. pachyderma* has also been found at this depth in Subantarctic waters of the South Atlantic (Mortyn and Charles, 2003), while *G. inflata* has highest abundances at depths below the chlorophyll maximum (Fairbanks et al., 1980; Mortyn and Charles, 2003). In the region of the sediment traps at 47°S and 51°S, highest cell densities for phytoplankton measured during late summer occur at ~30 m, while at 54°S this maximum occurs at 50-90 m (Kopczynska et al., 2001). During other seasons, the chlorophyll maximum has been observed to extend from the surface to the depth of the mixed layer within the SAZ, with maximums in the PFZ more closely tied to the depth of the mixed layer (Parslow et al., 2001). It is not possible from our data to determine a definitive relationship between foraminiferal habitat depth and the chlorophyll maximum, however, the near-surface habitat for *G. bulloides* and *N. pachyderma* (s.) at each of the sites is consistent with the relatively shallow chlorophyll maximum in these regions. The $\delta^{18}O$ values for *G. inflata*, by contrast, imply deeper habitat depths than for either *G. bulloides* or *N. pachyderma* (s.), consistent with the observed pattern in other ocean basins.

The difference in $\delta^{18}O$ between shallow and deep dwelling foraminifera has been exploited as a proxy for water mass stratification in the interpretation of sedimentary records (eg. Mulitza et al., 1997; Ganssen and Kroon, 2000). However, the isotopic difference between deep and shallow dwelling foraminifera will also vary depending on their season of maximum production. Stratification tends to be very weak during winter and spring and therefore the contrast in $\delta^{18}O$ with depth is low. During summer, stratification is strong, so there is a stronger contrast in the $\delta^{18}O$ values between species living at different depths.

Our $\delta^{18}O$ data are consistent with a surface habitat for *G. bulloides* during spring and summer, whereas *G. inflata* $\delta^{18}O$ suggests calcification at ~50 m. These two species therefore provide the possibility to trace water mass stratification, as in the NE Atlantic (Ganssen and Kroon, 2000). *G. inflata* could also be compared to *N. pachyderma* (s.),

but the seasonal production patterns are slightly different between these two species so differences in their $\delta^{18}O$ composition will reflect both seasonal and depth contrasts (Figure 10). The contrast between *G. inflata* and *G. bulloides* flux-weighted $\delta^{18}O$ values captures the summer stratification well at 42°S (Figure 10), while 44°S and 47°S show less difference in $\delta^{18}O$. The low contrast at these two sites reflects the dominant September flux at 44°S (when stratification is low) and the similar habitat depths of these two species at 47°S. At 51°S there is a stronger contrast between *G. bulloides* and *G. inflata*, capturing the stratification during early summer.

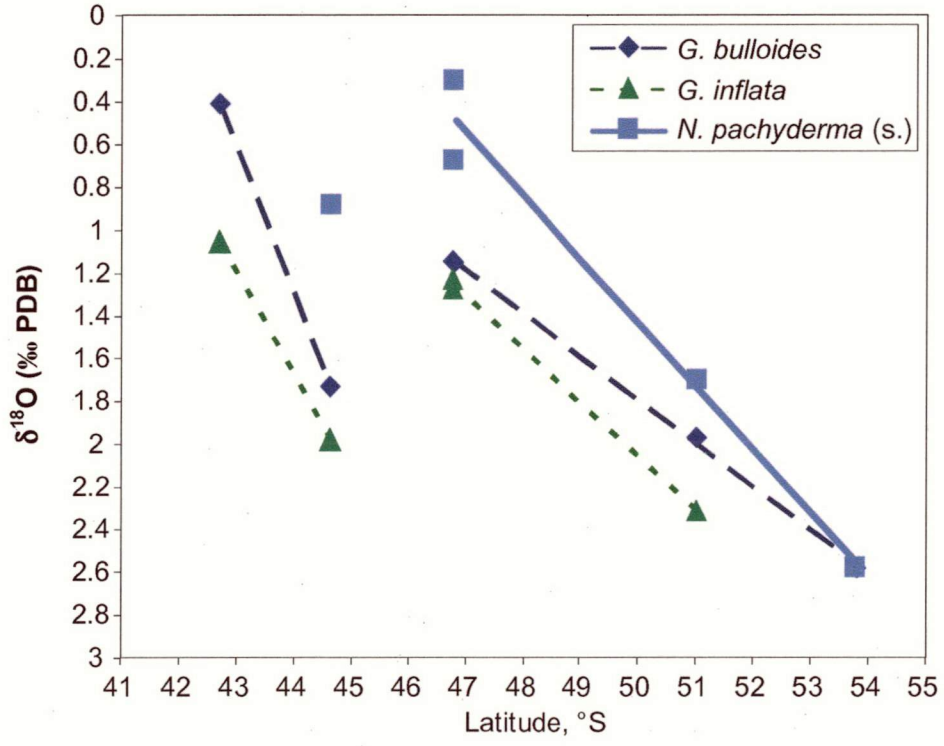

Figure 10: Flux-weighted $\delta^{18}O$ for *G. bulloides*, *N. pachyderma* (s.) and *G. inflata*. *G. bulloides* and *N. pachyderma* (s.) values have been corrected to predicted equilibrium $\delta^{18}O$. The contrast in $\delta^{18}O$ between *G. bulloides* and *G. inflata* reflects stratification during early summer at 42°S and 51°S. At 44°S, there is little difference between these species, reflecting the weak stratification during September and October, while at 47°S these species dwell at similar depths. The relatively depleted values for *N. pachyderma* (s.) at 44°S, 47°S and 51°S reflect the dominant summer flux compared to the spring fluxes of *G. bulloides* and *G. inflata* at these sites. At 54°S, *G. bulloides* has a spring to early summer flux so $\delta^{18}O$ values are similar to *N. pachyderma* (s.).

Implications of seasonal production patterns: Consistency between flux-weighted $\delta^{18}O$ values from the traps and core tops reveals that sedimentary isotopic records are clearly weighted towards the season of maximum production. Seasonal production patterns vary for some species between the trap sites, implying that changes in the environment in down-core records may also cause changes in seasonal production. Such changes in seasonal fluxes down the core will affect the magnitude of isotopic variability in both time and space. The possible effects of such flux changes must be taken into account in interpretations of past climate change.

Differences in seasonal production between regions will affect reconstructions of water mass boundaries. The $\delta^{18}O$ gradient across the STF, for instance, reflects changes in seasonality as well as the foraminiferal isotopic composition. *G. bulloides* has a shift in production from summer to spring across the front, and therefore exhibits a much steeper latitudinal gradient in $\delta^{18}O$ than expected. There is also a change in seasonal production between SCR and 47°S, despite the Subantarctic location of both sites (although at different longitudes). The foraminiferal $\delta^{18}O$ gradient between NCR and 47°S is much more consistent with the observed gradient across the STF, suggesting that the seasonal patterns observed at SCR, with strong weighting towards spring time fluxes, are anomalous. Latitudinal gradients between 47°S and 54°S in the Australian sector are more consistent with the observed $\delta^{18}O$ gradients in these regions.

N. pachyderma (s.) and *G. inflata* also display a $\delta^{18}O$ gradient across the sites which is consistent with the observed $\delta^{18}O$ gradients for all sites (apart from SCR). This consistency results from the similarity in seasonal flux patterns, and these findings confirm the applicability of foraminiferal $\delta^{18}O$ to the reconstruction of gradients across ocean fronts. The results from SCR, however, also reveal the potential danger posed by inconsistencies in seasonal fluxes between sites. To achieve better interpretation of paleoclimate records we require an understanding of past seasonality in foraminiferal fluxes. One way in which this has been attempted is by analysing individual foraminifera, with the range in values interpreted as representing the seasonal range in $\delta^{18}O$ (Billups and Spero, 1995; Bemis, 2000). Individual *G. bulloides* analysed from core tops near Chatham Rise (Bemis, 2000) yield a much smaller range than the seasonal range which we observe from the sediment traps, reflecting the short production season in this region.

4.7 Conclusions

Foraminiferal isotopic records from Southern Ocean sediments record the seasonal and depth information observed in the sediment traps. The preservation of seasonal and depth information in the isotopic records has the potential to form a powerful tool for paleoclimate reconstructions from this region. However, we have also demonstrated the importance of deciphering the seasonal imprint on the sedimentary record. For valid reconstructions of past climatic conditions in these regions it is critical to first establish the seasonal signature in the isotopic record as this may overprint the true climatic signal. This will be particularly important in the reconstruction of latitudinal gradients since we observe significant variations in seasonal flux patterns between the sediment trap sites. The most extreme example of this seasonal weighting in $\delta^{18}O$ occurs at SCR where fluxes occur primarily during the one season, thereby biasing the $\delta^{18}O$ record. The habitat depth may also vary between sites and on an interannual basis, as shown by the deeper habitat for *G. bulloides* at 47°S during 1998 compared to the surface depth implied at each of the other sites and at 47°S during 1997. Given these modern-day examples of differences in habitat depth and seasonal flux patterns between sites, it is likely that down-core records are similarly affected by changes in seasonal and depth distributions, particularly as water masses boundaries migrate. We also propose that the most consistent climate reconstructions from $\delta^{18}O$ records in this region can be obtained using the Epstein (1953) equilibrium relationship. *G. bulloides* exhibits a constant offset from surface equilibrium calculated with this equation of 0.37±0.28‰, while *N. pachyderma* (s.) is offset from surface equilibrium by 0.50±0.37‰. *G. inflata* exhibits $\delta^{18}O$ values which are equivalent to equilibrium values at depths of ~50 m.

4.8 References

AVHRR, Advanced Very High Resolution Radiometer. 1999. AVHRR sea surface temperature data. NOAA/NASA.

Bauch, D., Darling, K., Simstich, J., Bauch, H.A., Eriendeuser H. and Kroon, D., 2003. Palaeoceanographic implications of genetic variation in living North Atlantic *Neogloboquadrina pachyderma*, Nature, 424: 299-302.

Belkin, I.M. and Gordon, A.L., 1996. Southern Ocean fronts from the Greenwich meridian to Tasmania. Journal of Geophysical Research, 101: 3675-3696.

Bemis, B.E., 2000. Controls on the Oxygen and Carbon Isotopic Composition of Planktonic Foraminifera: Implication for Paleoceanographic Reconstructions. Ph.D. Thesis, University of California, Davis.

Bemis, B.E., Spero, H.J., Bijma, J. and Lea, D. W., 1998. Reevaluation of the oxygen isotope composition of planktonic foraminifera: Experimental results and revised paleotemperature equations. Paleoceanography, 13(2): 150-160.

Bemis, B.E., Spero, H.J., Lea, D.W., and Bijma, J., 2000. Temperature influence on the carbon isotopic composition of *Globigerina bulloides* and *Orbulina universa* (planktonic foraminifera). Marine Micropaleontology, 38: 213-228.

Bemis, B.E., Spero, H.J., and Thunell, R.C., 2002. Using species-specific paleotemperature equations with foraminifera: A case study in the Southern California Bight. Marine Micropaleontology., 46: 405-430.

Billups, K. and Spero, H.J., 1995. Relationship between shell size, thickness and stable isotopes in individual planktonic foraminifera from two equatorial Atlantic cores. Journal of Foraminiferal Research, 25(1): 24-37.

Brathauer, U. and Abelmann, A., 1999. Late Quaternary variations in sea surface temperatures and their relationship to orbital forcing recorded in the Southern Ocean (Atlantic sector). Paleoceanography, 14(2): 135-148.

Bray, S., Trull, T., and Manganini, S., 2000. SAZ project moored sediment traps: Results of the 1997-1998 deployments. Antarctic CRC, Hobart.

Charles, C.D. and Fairbanks, R.G., 1990. Glacial to interglacial changes in the isotopic gradients of Southern Ocean surface water. In: U. Bleil and J. Thiede (Editors), Geological History of the Polar Oceans: Arctic Versus Antarctic. Kluwer, Boston, Mass., pp. 519-538.

Deacon, G.E.R., 1982. Physical and biological zonation in the Southern Ocean. Deep-Sea Research, 29(1A): 1-15.

Deuser, W.G. and Ross, E.H., 1989. Seasonally abundant planktonic foraminifera of the Sargasso Sea: succession, deep-water fluxes, isotopic compositions, and paleoceanographic implications. Journal of Foraminiferal Research, 19(4): 268-293.

Duplessy, J.-C., 1970. Note préliminaire sur les variations de la composition isotopique des eaux supericielles de l'Ocean Indien: La relation ^{18}O-salinité. C.R. Acad Sci. Paris, 271: 1075-1078.

Epstein, S., Buchsbaum, R., Lowenstam, H.A., and Urey, H.C., 1953. Revised carbonate-water isotopic temperature scale. Geological Society of America Bulletin, 64: 1315-1326.

Erez, J. and Honjo, S., 1981. Comparison of isotopic composition of planktonic foraminifera in plankton tows, sediment traps and sediments. Palaeogeography, Palaeoclimatology, Palaeoecology, 33: 129-156.

Fairbanks, R.G., Sverdlove, M., Free, R., Wiebe, P.H., and Bé, A.W.H., 1982. Vertical distribution and isotopic fractionation of living planktonic foraminifera from the Panama Basin. Nature, 298: 841-844.

Fairbanks, R.G., Wiebe, P.H., and Bé, A.W.H., 1980. Vertical distribution and isotopic composition of living planktonic foraminifera in the western North Atlantic. Science, 207: 61-63.

Ganssen, G.M. and Kroon, D., 2000. The isotopic signature of planktonic foraminifera from NE Atlantic surface sediments: implications for the reconstruction of past oceanic conditions. Journal of the Geological Society, 157: 693-699.

Heath, R.A., 1985. A review of the physical oceanography of the seas around New Zealand - 1982. N.Z. Journal of Marine and Freshwater Research, 19: 79-124.

Howard, W.R. and Prell, W.L., 1992. Late Quaternary surface circulation of the Southern Indian Ocean and its relationship to orbital variations. Paleoceanography, 7: 79-118.

Kim, S.-T. and O'Neil, J.R., 1997. Equilibrium and non-equilibrium oxygen isotope effects in synthetic carbonates. Geochimica Cosmochimica Acta, 61: 3461-3475.

King, A.L. and Howard, W.R., 2001. Seasonality of foraminiferal flux in sediment traps at Chatham Rise, SW Pacific: Implications for paleotemperature estimates. Deep-Sea Research I, 48: 1687-1708.

King, A.L. and Howard, W.R., 2003. Planktonic foraminiferal flux seasonality in Subantarcitc sediment traps: A test for paleoclimate reconstructions. Paleoceanography, 18(1, 1019): doi:10.1029/2002PA000839.

Kopczynska, E.E., Dehairs, F., Elskens, M., and Wright, S., 2001. Phytoplankton and microzooplankton variability between the Subtropical and Polar Fronts south of Australia: Thriving under regenerative and new production in late summer. Journal of Geophysical Research, 106(C12): 31,597-31,609.

Labeyrie, L.D., Labracherie, M., Gorfti, N., Pichon, J.J., Vautravers, M., Arnold, M., Duplessy, J.-C., Paterne, M., Michel, E., Duprat, J., Caralp, M., and Turon, J.-L., 1996. Hydrographic changes of the Southern Ocean (southeast Indian sector) over the last 230 kyr. Paleoceanography, 11(1): 57-76.

Levitus, S. Levitus94: World Ocean Atlas 1994. 1994. NOAA Office of Global Programs and Lamont-Doherty Earth Observatory of Columbia University.

Matsumoto, K., Lynch-Stieglitz, J., and Anderson, R.F., 2001. Similar glacial and Holocene Southern Ocean hydrography. Paleoceanography, 16: 1-10.

Mix, A.C., 1987. The oxygen-isotope record of glaciation. In: W.F. Ruddiman and H. Wright (Editors), Geological Society of America, Boulder, Colorado., pp. 111-135.

Morley, J.J., 1989. Variations in high-latitude oceanographic fronts in the Southern Indian Ocean: An estimation based on faunal changes. Paleoceanography, 4: 547-554.

Mortyn, G.P. and Charles, C.D., 2003. Planktonic foraminiferal depth habitat and $\delta^{18}O$ calibrations: Plankton tow results from the Atlantic sector of the Southern Ocean. Paleoceanography, 18(2, 1037): doi: 10.1029/2001PA000637.

Mulitza, S., Dürkoop, A., Hale, W., Wefer, G., and Niebler, H.S., 1997. Planktonic foraminifera as recorders of past surface-water stratification. Geology, 25: 335-338.

Neil, H.L., 1997. Late Quaternary variability of surface and deep water masses - Chatham Rise, SW Pacific. Ph.D. Thesis, Univ. Waikato, Hamilton, New Zealand.

Nelson, C.S., Hendy, C.H., and Cuthbertson, A.M., 1994. Oxygen isotope evidence for climatic contrasts between Tasman Sea and Southwest Pacific Ocean during the late Quaternary. In: G.J. van der Lingen, K.M. Swanson, and R.J. Muir (Editors), A.A. Balkema, Brookfield, pp. 181-196.

Nodder, S. D. and Northcote, L. C., 2001. Episodic particulate fluxes at southern temperate mid-latitudes (42-45°S) in the Subtropical Front region, east of New Zealand. Deep-Sea Research I, 48: 833-864.

Orsi, A., Whitworth, T., and Nowlin, W.D., 1995. On the meridional extent and fronts of the Antarctic Circumpolar Current. Deep-Sea Research I, 42: 641-673.

Ortiż, J.D., Mix, A.C., and Collier, R.W., 1995. Environmental control of living symbiotic and asymbiotic foraminifera of the California Current. Paleoceanography, 10(6): 987-1009.

Parslow, J.S., Boyd, P.W., Rintoul, S.R., and Giffiths, F.B., 2001. A persistent subsurface chlorophyll maximum in the Interpolar Frontal Zone south of Australia: Seasonal progression and implications for phytoplankton-light-nutrient interactions. Journal of Geophysical Research, 106(C12): 31,543-31,557.

Prell, W.L., Hutson, W.H., and Williams, D.F., 1979. The subtropical convergence and late Quaternary circulation in the southern Indian Ocean. Marine Micropaleontology, 4: 225-234.

Rintoul, S.R. and Trull, T.W., 2001. Seasonal evolution of the mixed layer in the Subantarctic Zone south of Australia. Journal of Geophysical Research, 106(C12): 31,447-31,462.

Russell, A.D. and Spero, H.J., 2000. Field examination of the oceanic carbonate ion effect on stable isotopes in planktonic foraminifera. Paleoceanography, 15(1): 43-52.

Sautter, L.R. and Thunell, R.C., 1991. Seasonal variability in the $\delta^{18}O$ and $\delta^{13}C$ of planktonic foraminifera from an upwelling environment: Sediment trap results from the San Pedro Basin, Southern California Bight. Paleoceanography, 6(3): 307-334.

Spero, H.J., Bijma, J., Lea, D.W., and Bemis, B.E., 1997. Effect of seawater carbonate concentration on foraminiferal carbon and oxygen isotopes. Nature, 390: 497-500.

Trull, T., Bray, S., Manganini, S., Honjo, S., and François, R., 2001. Moored sediment trap measurements of carbon export in the Sub-Antarctic and Polar Frontal zones of the Southern Ocean, south of Australia. Journal of Geophysical Research, 106(C12): 31,489-31,510.

von Langen, P.J., Lea, D.W., and Spero, H.J., 2000. Effects of temperature on oxygen isotopic and Mg/Ca values in *Neogloboquadrina pachyderma* shells determined by live culturing. EOS transactions AGU, Fall Meeting Supplement.

Weaver, P.P.E., Neil, H., and Carter, L., 1997. Sea surface temperature estimates from the Southwest Pacific based on planktonic foraminifera and oxygen isotopes. Palaeogeography, Palaeoclimatology, Palaeoecology, 131: 241-256.

Williams, D.F., Bé, A.W.H., and Fairbanks, R.G., 1981. Seasonal stable isotopic variations in living planktonic foraminifera from Bermuda plankton tows. Palaeogeography, Palaeoclimatology, Palaeoecology, 33: 71-102.

CHAPTER 5

PLANKTONIC FORAMINIFERAL $\delta^{13}C$ FROM SOUTHERN OCEAN SEDIMENT TRAPS

"The microscopic organisms are very inferior in individual energy to lions and elephants, but in their united influences they are far more important than all of these animals"

C.G. Ehrenberg; 1862

Published as: King, A.L. and W.R. Howard, Planktonic foraminiferal $\delta^{13}C$ records from Southern Ocean sediment traps: New estimates of the oceanic Suess effect, *Global Biogeochemical Cycles,* 18, doi:10.1029/2003GB002162, in press.

Abstract

The carbon isotopic composition is measured for three species of planktonic foraminifera (*Globigerina bulloides, Globorotalia inflata* and *Neogloboquadrina pachyderma* (s.)) from Southern Ocean sediment traps. The sediment traps represent the annual flux of foraminifera in Subtropical to Polar Frontal environments from the western Pacific/Southern Australia sector. Comparison between the seasonal $\delta^{13}C$ composition of the foraminifera and estimated $\delta^{13}C$ of dissolved inorganic carbon (DIC) allows disequilibrium effects to be determined. Disequilibrium exhibits a latitudinal trend, with greatest offsets from equilibrium at lower latitudes. This effect causes a north to south increase in foraminiferal $\delta^{13}C$, while the $\delta^{13}C_{DIC}$ displays a decrease across these latitudes. Disequilibrium in *G. bulloides* can be accounted for by changes in temperature. The relationship between disequilibrium and temperature which we derive in this field study is consistent with the laboratory relationship of *Bemis et al.* [2000]. Corrected $\delta^{13}C$ for *G. bulloides* is closely correlated to seasonal changes in nutrients at each site, indicating the utility of *G. bulloides* $\delta^{13}C$ as a nutrient tracer in Southern Ocean environments. Comparison between flux-weighted sediment trap values and nearby core tops indicates a modern depletion in $\delta^{13}C$, which we attribute to the oceanic Suess effect. The imprint of this effect on the foraminiferal isotopes provides further evidence for the equilibration between surface waters and the atmosphere in the Subantarctic Zone.

Keywords: carbon isotopes, Southern Ocean, sediment traps, planktonic foraminifera disequilibrium, seasonal variability

5.1 Introduction

Carbon isotopic records from planktonic foraminifera are one of the many tools which are applied to reconstructions of the global carbon cycle. Determining past changes in the carbon cycle is key to our understanding of paleoclimate forcing, and also provides an insight into how the oceans may respond to present and future changes to the climate system. The Southern Ocean is central to our understanding of the global carbon cycle since the Subantarctic Zone (SAZ) is considered to be one of the strongest sinks for atmospheric CO_2, with deep penetration associated with the formation of Subantarctic Mode Water and Antarctic Intermediate Water [*Metzl et al.*, 1999].

Field and laboratory studies show that foraminifera exhibit disequilibrium effects during the incorporation of $\delta^{13}C$ into their shell calcite. The strongest effects shown in laboratory studies are associated with changes in the calcification temperature [eg. *Bemis et al.*, 2000] and the carbonate ion concentration of seawater [*Spero et al.*, 1997; *Bemis et al.*, 2000; *Russell and Spero*, 2000]. In this study, we provide one of the first field evaluations of laboratory culture-derived estimates of isotopic disequilibrium in planktonic foraminifera. We assess the relative influence of temperature and carbonate ion concentration on the $\delta^{13}C$ composition of *Globigerina bulloides*, *Neogloboquadrina pachyderma* (s.) and *Globorotalia inflata* obtained from sediment traps.

The foraminiferal records also provide insight into the role of the oceans in the modern carbon cycle. Recent ocean geochemical studies have sought to determine the magnitude of the oceanic uptake of atmospheric CO_2. Many of these studies have centered around the change in $\delta^{13}C$ of the surface oceans [eg. *Quay et al.*, 1992; *Beveridge and Shackleton*, 1994; *Heimann and Maier-Reimer*, 1996; *Bacastow et al.*, 1996; *Gruber et al.*, 1999; *Bauch et al.*, 2000; *Ortiz et al.*, 2000; *Takahashi et al.*, 2000; *McNeil et al.*, 2001a; *Quay et al.*, 2003]. The atmospheric $\delta^{13}C$ composition has become depleted by ~1.5‰ since the industrial revolution due to the burning of ^{13}C-depleted fossil fuels [*Keeling et al.*, 1995]. Uptake of this anthropogenic CO_2 by the oceans will cause a depletion in the oceanic $\delta^{13}C$ content. Comparison between modern sediment trap and core top foraminiferal $\delta^{13}C$ records provides a unique opportunity to determine the uptake of atmospheric CO_2 by the oceans over the entire time span since the industrial revolution. Application of this approach in the Eastern Atlantic reveals a modern depletion in $\delta^{13}C$ of the upper water column of ~0.62‰ [*Beveridge and Shackleton*, 1994], and in the Arctic Ocean of ~0.9‰ [*Bauch et al.*, 2000]. Water-column $\delta^{13}C_{DIC}$ measurements in the SAZ

region south of Australia indicate a depletion during the last 20 years of ~0.32‰, highlighting the potential importance of this region as a sink for atmospheric CO_2 [*McNeil et al.*, 2001a]. Understanding the ocean's role in the uptake and storage of anthropogenic CO_2 provides important constraints for understanding the modern carbon cycle and our predictions of future climate change.

In this study, we use the carbon isotopic composition recorded by planktonic foraminifera in an array of Southern Ocean sediment traps to fulfill two main aims. Firstly, we determine how well various species of planktonic foraminifera record seasonal changes in the surface carbon chemistry, and secondly, we apply the isotopic record from the sediment traps and nearby core tops to determine recent changes in the uptake of anthropogenic CO_2. This study provides the first calibration within the Subantarctic Zone of foraminiferal $\delta^{13}C$ records against observations on seasonal time scales, and tests fundamental assumptions of the $\delta^{13}C$ foraminiferal record.

5.2 Methods

5.2.1 Sediment trap moorings

Two sediment traps were moored north and south of Chatham Rise for approximately one year during 1996 and 1997. The South Chatham Rise (SCR) record spans the interval 9th June 1996 to 15th May 1997 while the deployment at North Chatham Rise (NCR) covers the interval from 14th September 1996 to 15th May 1997. Here we present results from the 1000 m traps at both sites.

Moorings from a separate deployment from the Australian sector of the Southern Ocean are also presented here. Sediment trap moorings were deployed between September 1997 and February 1998 along 142°E longitude in the central SAZ (47°S), at the SAF (51°S) and within the PFZ (54°S) (Figure 1) [see *Bray et al.*, 2000 and *Trull et al.*, 2001]. Moorings at 47°S were redeployed during the following year between 15th March 1998 and 5th February 1999, while traps at 54°S were deployed between 24th March 1998 and 5th February 1999. In this second deployment at 54°S, however, material was only collected in the first sample cup. Here we present results from the 1997 and 1998 deployments for traps at 3850 m at 47°S (47-3800), 3080 m at 51°S (51-3100) and 830 m at 54°S (54-800).

The Australian sector and Chatham Rise deployments both used McLane PARFLUX Mk 7G-21 time-incremental sediment traps. For sampling intervals and other details of the trap deployments at Chatham Rise refer to *Nodder and Northcote* [2001] and

King and Howard [2001] and for the Australian sector deployments to *Bray et al.* [2000] and *King and Howard* [2003].

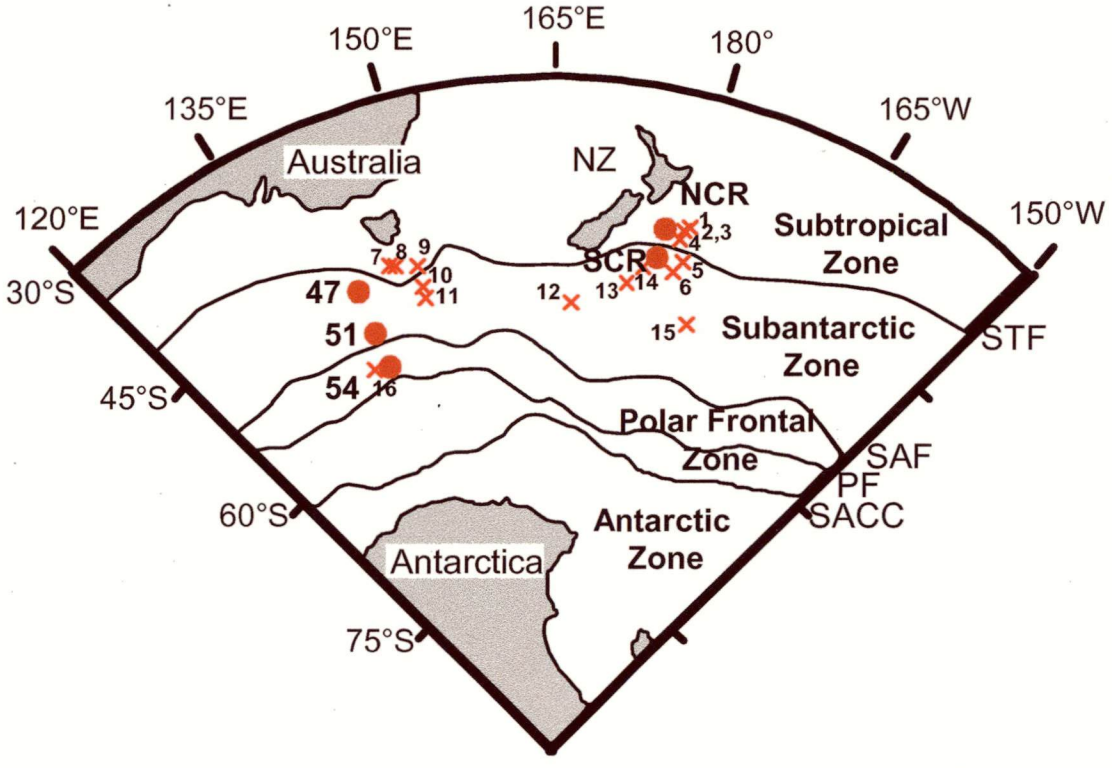

Figure 1: Trap (•) and core top (x) locations in relation to water masses and fronts. Core tops are as follows: 1: W266-K; 2: R657-K; 3: S924-K; 4: W268-P; 5: U939-P; 6: W272-P, 7: MD972-106-G; 8: SO136-165-BX; 9: SO136-161-BX; 10: SO136-153-BX; 11: SO136-147-BX; 12: D84-D 13: H564-G; 14:Q216-G; 15: Q585-G; 16: ELT36-1-PH. (G refers to gravity core, K to Kasten core, BX to box core, D to dredge, PH to phleger core and PC to piston core). Figure adapted from L. Armand pers. comm., with frontal locations based on *Orsi et al.*[1995]. Core 1 from *Neil* [1997], cores 3, 12, 13, 14 and 15 from *Weaver et al.* [1997].

5.2.2 Isotopic analysis

The carbon and oxygen isotopic composition of three species were obtained for the sediment traps (viz. *Globigerina bulloides, Neogloboquadrina pachyderma* (s.) and *Globorotalia inflata*). Ten specimens in the 250-355 µm size fraction were analysed per sample for *G. bulloides* and *G. inflata*, and 15-20 specimens in the 150-250 µm size fraction were analysed for *N. pachyderma* (s.). Prior to analysis, samples were rinsed and sonicated in methanol, and then roasted at 375°C for 60 mins to eliminate any water and volatile organic compounds.

The carbon and oxygen isotopic ratios were measured on two machines. The Chatham Rise samples were analysed at the Central Sciences Laboratory, University

of Tasmania on an individual reaction-vial automated carbonate line coupled to a Micromass Optima mass spectrometer. Analytical precision was ±0.08 for $\delta^{13}C$ and ±0.09 for $\delta^{18}O$ (N = 51). Most of the Australian sector samples were analysed on a Micromass Optima at UC Davis [see *Bemis et al.*, 2002 for methods]. The average analytical precision for these measurements was ±0.05 for $\delta^{13}C$, and ±0.06 for $\delta^{18}O$ (N = 28). The isotopic ratios are reported as per mil (‰) deviations from the Pee Dee belemnite (PDB) standard using Carrara marble as a laboratory standard.

5.2.3 Calculation of $\delta^{13}C$ for dissolved inorganic carbon

Measurements of $\delta^{13}C$ of dissolved inorganic carbon ($\delta^{13}C_{DIC}$) have been acquired during various seasons at the trap sites, though few during the actual deployment periods. $\delta^{13}C_{DIC}$ measurements within the SAZ region south of Tasmania were collected during February 1999, March 1998, July 1998 and November 1995 [*McNeil*, 2001c]. At Chatham Rise, $\delta^{13}C$ measurements were obtained during February 1996 on cruise P15S [*Quay et al.*, 2003]. Further estimates of $\delta^{13}C_{DIC}$ for the Australian sector traps have been made based on nutrient data collected on surveys during January 1995, July 1995 and September 1996. For the Chatham Rise traps nutrient data is available from CTD measurements at 44°S during February 1995, May 1997, August 1998 and October 1993, and at 42°S during March 1995, May 1997, June 1993, August 1998, October 1993 and November 1997.

We have calculated $\delta^{13}C_{DIC}$ from the nutrient data using the equation of *Broecker and Maier-Reimer* [1992]:

$$\delta^{13}C_{DIC} - \delta^{13}C_{MO} = (\Delta_{photo}/\Delta CO_{2\,MO})(C/P_{org})(PO_4 - PO_{4\,MO})$$

In this equation MO stands for mean ocean, Δ_{photo} is the carbon isotope separation during marine photosynthesis and C/P_{org} is the carbon to phosphorus ratio in marine organic matter. This equation accounts for the biological portion of the cycle, with the relationship between biological production and $\delta^{13}C_{DIC}$ remaining constant regardless of whether pre-formed phosphorus is present. The same relationship could be calculated on the basis of nitrate concentrations, but this calculation provides a poorer calibration to measured $\delta^{13}C_{DIC}$ for this data set.

Δ_{photo} and $C{:}P_{org}$ vary with latitude. We have estimated Δ_{photo} throughout the season at the trap sites based on the relationship to temperature derived from the Southern Ocean data of *Popp et al.* [1999]:

$$\Delta_{photo} = 0.7547*T - 29.53\ (R^2 = 0.88)$$

Values of Δ_{photo} calculated from this equation range from -15 to -28‰ and are consistent with more recent measurements of *Lourey et al.* [2004]. For C/P_{org} we have used a value of 100 at NCR, SCR and 47°S, consistent with average measurements within the SAZ [*Lourey and Trull*, 2001], while at 51°S and 54°S we apply the Redfield value of 106 [*Broecker and Maier-Reimer*, 1992]. Measurements of nutrient utilisation in the PFZ imply a C/P_{org} of 46.5 [*Lourey and Trull*, 2001], however, calculation of $\delta^{13}C_{DIC}$ using this value yields $\delta^{13}C_{DIC}$ values which are extremely depleted compared to the measured $\delta^{13}C_{DIC}$ for this region. The mean ocean values used are as follows: ΣCO_{2MO} 2200 µm; $\delta^{13}C_{MO}$ 0.5; and $PO_{4\,MO}$ 2.2 µmol/kg.

Variations in $\delta^{13}C_{DIC}$ reflect changes in biological production, air-sea exchange and mixing between water masses. It is important to constrain the relative influence of these parameters so we can better interpret $\delta^{13}C$ records from the Southern Ocean. The $\delta^{13}C$ of surface waters in the SAZ is most strongly influenced by variations in biological productivity, where biological cycling accounts for ~81% of the total change in DIC [*McNeil et al.*, 2001b]. However, the strength of the biological effect on $\delta^{13}C$ varies throughout the year and between sites.

Equilibrium calcite is enriched relative to $\delta^{13}C_{DIC}$ by ~1.3‰ within a temperature range of 15 to 25°C and at a pH of 8.15 [*Bemis et al.*, 2000]. However, we compare $\delta^{13}C_{foram}$ directly with $\delta^{13}C_{DIC}$ values since we are trying to assess how well foraminiferal calcite records the $\delta^{13}C$ of DIC.

5.2.4 Comparison between trap and core top $\delta^{13}C$ values

We compare trap $\delta^{13}C$ values to published core top values and analyses which we have made on additional core tops. The published core tops all use *G. bulloides*, providing a much larger core top data base for this species than for *G. inflata* or *N. pachyderma* (s.). Sources of the published material are shown on the figures.

To compare the sediment trap values to the core tops we obtained a flux-weighted $\delta^{13}C$ average for the three foraminiferal species. The flux-weighted value ($\hat{I}$) is calculated for each sediment trap by multiplying each isotope value (I) by the percentage abundance (f) of the species (i) in that cup, and then summing all values together to produce a single value for each trap deployment as follows:

$$\hat{I} = \sum_{1}^{n} f_i I_i / \Sigma f$$

These flux-weighted values are an approximation of a 'core top' value, assuming that seasonal flux patterns have remained similar to present over the time span

represented by each core top [see *Mix*, 1987]. This calculation also assumes that the proportion of shells in the size fraction used for isotopic analysis is consistent with the total shell flux for each species.

5.3 Oceanographic Setting

The five sediment traps were moored in distinct environments of the Pacific/Southern Ocean (Figure 1). These zones are characterised as Subtropical, Subantarctic, Subantarctic Front and Polar Front. Two traps were moored within the Subantarctic Zone (SAZ). One was located east of New Zealand, and the other south of Tasmania, Australia. Each of the traps are associated with major oceanic fronts which mark the transition between water masses with unique temperature, salinity and nutrient characteristics.

Traps moored at 42° and 44°S at North and South Chatham Rise east of New Zealand are separated by the Subtropical Front (STF). This front separates Subantarctic waters which are characteristically cold, low salinity, and nutrient-rich waters, from warm, saline, nutrient-depleted Subtropical waters [*Deacon*, 1982;*Heath*, 1985; *Belkin and Gordon*, 1996]. Nutrient concentrations continue to increase to the south into the Polar Frontal Zone.

The southward increase in nutrient concentrations is reflected in the increasing concentration of dissolved inorganic carbon (DIC) as well as in the depletion in the $\delta^{13}C$ content of DIC. $\delta^{13}C$ values decrease between the 47°S and 54°S trap sites by up to 1.2‰ [*McNeil et al.*, 2001b]. The depletion in nutrient concentrations in the SAZ relative to the PFZ reflects the higher biological uptake in the SAZ as indicated by measurements of total water-column production [*Griffiths et al.*, 1999] and higher mass flux collected in sediment traps at 47°S (0.8 g C m^{-2} at 1000 m) compared to 54°S (0.5 g C m^{-2} at 800 m) [*Trull et al.*, 2001]. Nitrate depletions are twice as large in the SAZ as the PFZ, with an average depletion of 510 mmol N m^{-2} in the SAZ and 250 mmol N m^{-2} in the PFZ [*Lourey and Trull*, 2001]. Ekman transport across the fronts supplies Antarctic surface waters (ASW) rich in DIC and low in $\delta^{13}C$ to the SAZ and PFZ [*McNeil et al.*, 2001b], and nutrient and DIC-rich waters are also supplied to the PFZ through the upwelling of waters containing remineralised organic matter [*Gruber et al.*, 1999].

The Chatham Rise region east of New Zealand has lower nutrient concentrations than the SAZ, implying more enriched $\delta^{13}C$. There is also a slight contrast in nutrient concentrations across the STF at Chatham Rise. Nutrient concentrations are lower at

North Chatham Rise than at South Chatham Rise, consistent with the higher export production at NCR than SCR [*Nodder and Northcote*, 2001].

In this study we analyse the $\delta^{13}C$ of planktonic foraminifera from sites within the Subtropical Zone, Subantarctic Zone, Subantarctic Front and the Polar Frontal Zone to determine seasonal variability in the $\delta^{13}C$ of sea water in these regions. Biological production is highly seasonal within these areas, with most production occurring during the austral spring and summer. Production at these times follows winter nutrient resupply to the surface. In the SAZ, nutrients are resupplied via deep winter mixing (<400 m) and the northward spreading of near-surface waters across the SAF [*Rintoul and Trull*, 2001]. In the SAF and PFZ winter mixing is much shallower (200m at the SAF, and 150 m in the PFZ) resulting in a much lower seasonal range in nutrient concentrations.

5.4 Results

5.4.1 Measured versus calculated $\delta^{13}C_{DIC}$

$\delta^{13}C_{DIC}$ values calculated using the equation of *Broecker and Maier-Reimer* (1992) compare well (within 0.2‰) to measurements taken in this sector between 39° and 51°S [*McNeil*, 2001c; *Quay et al.*, 2003] (Figure 2). The calculated values between 52° and 54°S, however, show a depletion of up to 0.3‰ compared to the measurements. Surface nutrient concentrations between 52° and 54°S are very high, while measured $\delta^{13}C_{DIC}$ values are relatively enriched compared to the estimates. The enrichment in $\delta^{13}C$ despite high nutrient concentrations most likely reflects the outgassing of CO_2 (relatively enriched in ^{12}C) to the atmosphere during summer within the PFZ [*Metzl et al.*, 1991]. In the following section we apply the measured and calculated $\delta^{13}C_{DIC}$ values to determine the foraminiferal $\delta^{13}C$ disequilibrium. At 54°S we apply only the measured $\delta^{13}C$ values (obtained during November, February and March) to avoid errors caused by the relatively poor calibration between the estimated and measured $\delta^{13}C$ values at this latitude.

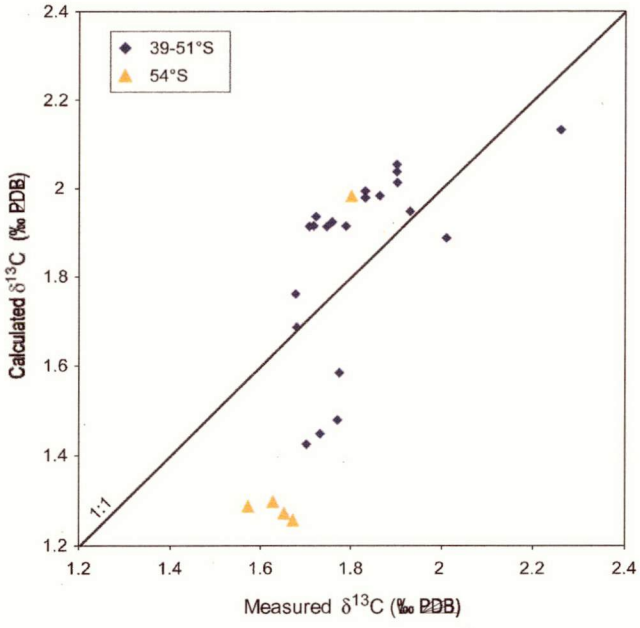

Figure 2: Measured against calculated $\delta^{13}C_{DIC}$ values between 39° and 54°S. Calculations are based on PO_4 measurements [*Tilbrook pers. comm.*] using the equation of *Broecker and Maier-Reimer* [1992]. Measured $\delta^{13}C_{DIC}$ values are derived from *McNeil* [2001c]. Estimated $\delta^{13}C_{DIC}$ from 54°S (triangles) are offset by up to 0.3‰ relative to measurements, while estimates across all other sites (diamonds) are within 0.2‰.

5.4.2 Latitudinal trends in $\delta^{13}C_{DIC}$ and $\delta^{13}C_{foram}$

Comparison between the $\delta^{13}C_{DIC}$ and the $\delta^{13}C$ measured in the foraminifera allows evaluation of disequilibrium effects for each of the three species. Water-column $\delta^{13}C_{DIC}$ displays a depletion in values from north to south, with summer values ranging from 2.0‰ at 42°S to 1.5‰ at 54°S (Figure 3a). This latitudinal depletion reflects the higher biological productivity in the SAZ compared to the PFZ, as well as the input of nutrient-rich, $\delta^{13}C$-depleted Antarctic surface waters into the PFZ. The $\delta^{13}C$ values from the foraminifera analysed from the 5 sediment traps, however, indicate an enrichment in values from north to south. *G. bulloides* increases by up to 1.8‰, and we observe $\delta^{13}C$ enrichments towards the more southerly sites for *G. inflata* and *N. pachyderma* (s.) as well (Figures 3a and b).

The contrast in the latitudinal trends in $\delta^{13}C_{DIC}$ and $\delta^{13}C_{foram}$ implies that disequilibrium decreases towards the south. All sites exhibit a depletion in $\delta^{13}C_{foram}$ compared to $\delta^{13}C_{DIC}$, with larger offsets at the more northerly sites in each sector. Disequilibrium offsets for *G. bulloides* at SCR are up to 2.2‰, and at NCR up to 3.1‰. At 47°S, foraminiferal $\delta^{13}C$ is depleted by as much as 2.6‰ and 2.1‰ for *G. bulloides* and *N. pachyderma* (s.) respectively. At 54°S, by contrast, *G. bulloides* is offset from $\delta^{13}C_{DIC}$ by 1.0-1.5‰, and *N. pachyderma* (s.) is offset by 0.5 to 0.9‰

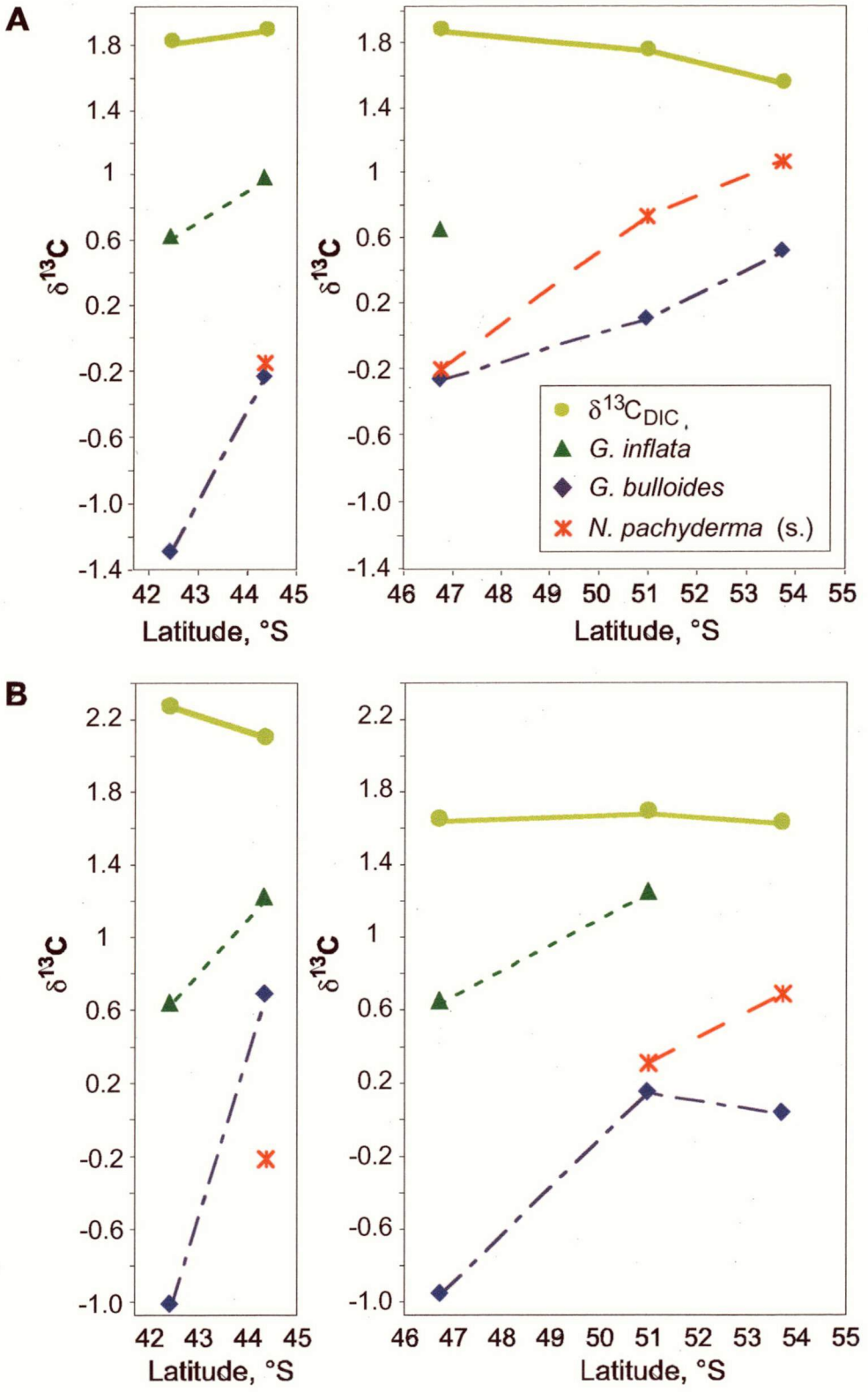

Figure 3: The latitudinal trend in $\delta^{13}C_{DIC}$ and $\delta^{13}C$ for *G. bulloides*, *G. inflata* and *N. pachyderma* (s.) across the Chatham Rise and Australian sector sediment traps. The $\delta^{13}C_{DIC}$ displays a general depletion in monthly averaged values across sites (a) during February and (b) in November, while each of the foraminiferal species display an enrichment in $\delta^{13}C$ from the northern to more southerly sites.

from $\delta^{13}C_{DIC}$. The gradient in disequilibrium across these sites is such that the trend in $\delta^{13}C_{foram}$ is the reverse of the latitudinal trend in $\delta^{13}C_{DIC}$. The average latitudinal $\delta^{13}C$ gradient from north to south across the sites during austral summer is +1.8‰ for *G. bulloides*, while the $\delta^{13}C$ gradient for DIC is -0.4‰. These results highlight the extreme importance of taking disequilibrium effects into account in the interpretation of foraminiferal $\delta^{13}C$ records.

5.4.3 Disequilibrium in $\delta^{13}C$ of planktonic foraminifera

Disequilibrium effects in $\delta^{13}C_{foram}$ are commonly attributed to 1) calcification temperature [eg. *Bemis et al.*, 2000]; 2) the activity of algal symbionts [*Bemis et al.*, 2000]; 3) the carbonate ion concentration of seawater [*Spero et al.*, 1997; *Bemis et al.*, 2000; *Russell and Spero*, 2000]; 4) the foraminiferal shell size [*Curry and Matthews*, 1981; *Williams et al.*, 1981; *Oppo and Fairbanks*, 1989; *Donner and Wefer*, 1994; *Ravelo and Fairbanks*, 1995; *Spero and Lea*, 1996]; 5) the isotopic composition of the foraminiferal diet [*Spero and Lea*, 1996; *Kohfeld et al.*, 2000]; 6) life habitat and ontogenetic migration [*Hemleben and Bijma*, 1994]; and 7) genotype variation [*Bauch et al.*, 2003; *Huber et al.*, 1997; *Darling et al.*, 2000; *Stewart et al.*, 2001; *Kucera and Darling*, 2002]. It is not possible to determine genotypic variation from these samples, and depth habitat has been assessed on the basis of the $\delta^{18}O$ results (see Chapter 4). The effect of diet is thought to be small (a 0 - 0.08‰ shift in foraminiferal $\delta^{13}C$ for each 1‰ change in dietary $\delta^{13}C$) [*Spero and Lea*, 1996]. Dietary corrections for *N. pachyderma* (s.) at Subantarctic latitudes of the South Atlantic indicate a very small effect on foraminiferal $\delta^{13}C$ based on the $\delta^{13}C$ content of phytoplankton [*Kohfeld et al.*, 2000]. Since we have no way of determining the $\delta^{13}C$ composition of the foraminiferal diet we do not attempt to evaluate this effect. In this study we have minimised the effects of size by using shells from the 250-355μm size fraction for both *G. bulloides* and *G. inflata*, and from the 150-250μm fraction for *N. pachyderma* (s.). For some cups there was not enough material to analyse *G. bulloides* and *G. inflata* from just the 250-355μm fraction so shells from the 150-355μm fraction were incorporated. For these samples there does not appear to be any relationship between disequilibrium and shell size. None of the species used in this study harbor algal symbionts, so the main sources of disequilibrium are most likely to be temperature and the carbonate ion concentration of the sea water, with the effect of genotypic variability unknown.

Temperature and $[CO_3^{2-}]$ covary in the water-column, but the mechanisms through which the two effects cause disequilibrium in foraminiferal $\delta^{13}C$ are quite different. Temperature affects the foraminiferal metabolism of organic compounds, with faster

metabolism at higher temperatures causing a greater incorporation of respired ^{12}C-enriched carbon into the shell calcite [*Bemis et al.*, 2000]. Conditions of higher pH (and $[CO_3^{2-}]$) cause significant changes to the ambient chemistry of the foraminiferal microenvironment, and most likely lead to changes in the shell $\delta^{13}C$ composition. Although the mechanisms are not fully understood, it is believed that under higher pH there is a higher proportion of respired, isotopically light CO_2 relative to bulk CO_2 in the foraminiferal microenvironment [*Zeebe et al.*, 1999]. This results in the enhanced uptake of relatively depleted CO_2 into the foraminiferal test . It is difficult to independently assess the relative influence of temperature and $[CO_3^{2-}]$ on foraminiferal $\delta^{13}C$ disequilbrium from field studies, however, by comparing measured disequilibrium in *G. bulloides* with disequilibrium observed during laboratory experiments it may be possible to determine the relative influence of these two effects.

The $[CO_3^{2-}]$ of the surface waters decreases gradually between 42°S and 54°S. We have estimated $[CO_3^{2-}]$ for the sediment trap sites based on the relationship between $[CO_3^{2-}]$ and temperature derived during transects conducted between 44°S and 65°S during January 1995, March 1998 and September 1996, and from WOCE lines P15S and P14S east and south of New Zealand during February 1996 [*Tilbrook* pers. comm.]. This data yields a relationship between temperature and $[CO_3^{2-}]$ as follows:

$$[CO_3^{2-}] = 0.126T^2 + 3.7332T + 105.15 \quad (R^2 = 0.965)$$

This relationship differs from that derived from the GEOSECS data [*Östlund et al.*, 1987], reflecting the decrease in $[CO_3^{2-}]$ since 1978 due to the uptake of anthropogenic CO_2 in this region [*McNeil et al.* , 2001a]. This new equation indicates that for the sediment trap sites the average $[CO_3^{2-}]$ is ~65 µmol/kg higher at NCR than 54°S, and 25 µmol/kg higher at NCR than at 47°S.

Increases in $[CO_3^{2-}]$ cause the $\delta^{13}C$ in foraminifera to become depleted relative to $\delta^{13}C_{DIC}$ [*Spero et al.*, 1997; *Bijma et al.*, 1999]. We apply the *Spero et al.* [1997] 12 chamber carbonate ion correction across cups for which we have measured $\delta^{13}C_{DIC}$ and/or have calculations based on nutrient measurements (Figure 4). The application of this slope (-0.014 / µmolkg^{-1}) causes a slight reduction in $\delta^{13}C$ disequilbrium across 42°S, 44°S and 47°S, with little impact on values at 51°S and 54°S.

The effects of temperature on $\delta^{13}C$ values for foraminifera are large in comparison to the $[CO_3^{2-}]$ effect. *Bemis et al.* [2000] found that the $\delta^{13}C$ disequilibrium ($\delta^{13}C_{foram} - \delta^{13}C_{DIC}$) for 12 chambered *G. bulloides* varies by -0.11‰ per °C over a temperature range of 15-24 °C. Assuming that the slope calculated by *Bemis et al.* [2000] remains

constant over the temperature range at the trap sites (4-18°C), we calculate a temperature-driven depletion in $\delta^{13}C$ of as much as 2.7‰ at NCR, 2.4‰ at SCR, 2‰ at 47°S and 1.3‰ at 54°S (Figure 4). The temperature corrected $\delta^{13}C$ values for *G. bulloides* are close to equilibrium with $\delta^{13}C_{DIC}$ (average offset of -0.16‰). However, if we combine the temperature and $[CO_3^{2-}]$ corrections, the resulting values for *G. bulloides* are enriched relative to equilibrium. This result implies that for this dataset temperature is the dominant effect driving *G. bulloides* disequilibrium. The relationship which we derive between *G. bulloides* disequilibrium and temperature across each of the traps sites is almost indistinguishable from the *Bemis et al.* [2000] laboratory relationship (Figure 5). This result confirms the application of laboratory derived relationships in field studies, and illustrates the robustness of the *Bemis et al.* [2000] relationship beyond the laboratory temperature range, with consistency observed to 4°C.

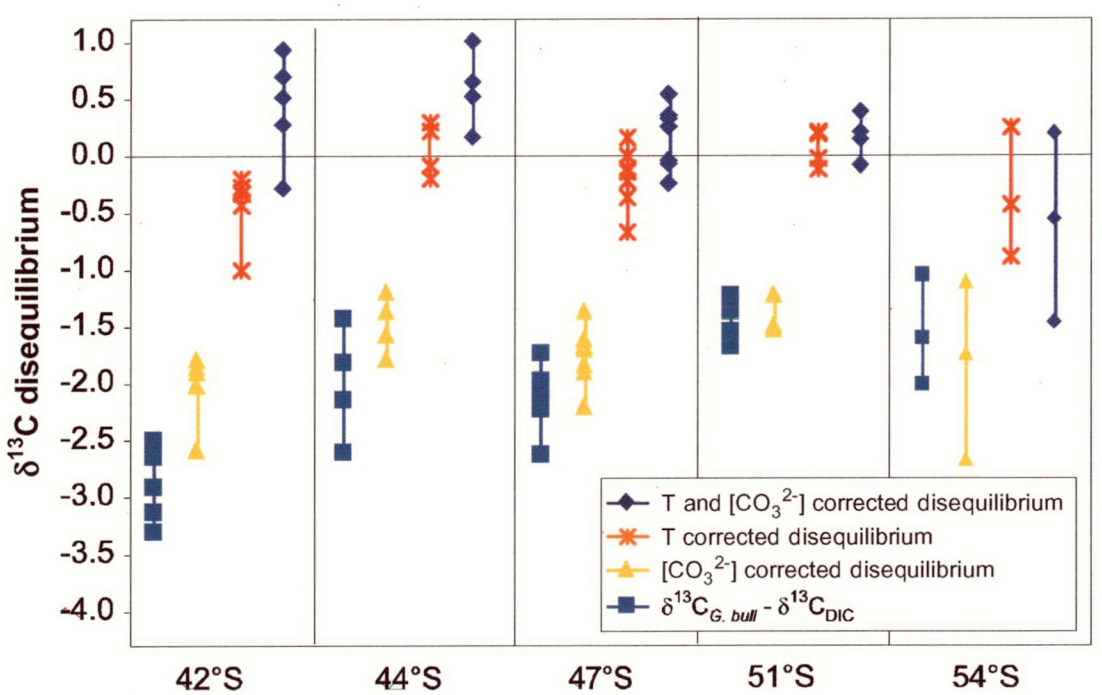

Figure 4: Calculation of disequilibrium in $\delta^{13}C$ for *G. bulloides* based on the 12 chamber relationships for temperature [*Bemis et al.*, 2000] and $[CO_3^{2-}]$ [*Spero et al.*, 1997]. Disequilibrium is expressed as $\delta^{13}C_{G.\ bulloides} - \delta^{13}C_{DIC}$. A latitudinal trend in disequilibrium is observed for *G. bulloides*, with disequilibrium decreasing to the south. The temperature correction reduces the latitudinal effect in disequilibrium, and brings $\delta^{13}C$ values for *G. bulloides* very close to equilibrium. Combining the effects of temperature and $[CO_3^{2-}]$ causes a slightly larger offset from equilibrium at these sites. Note that foraminiferal values have been averaged for the months corresponding to the CTD measurements.

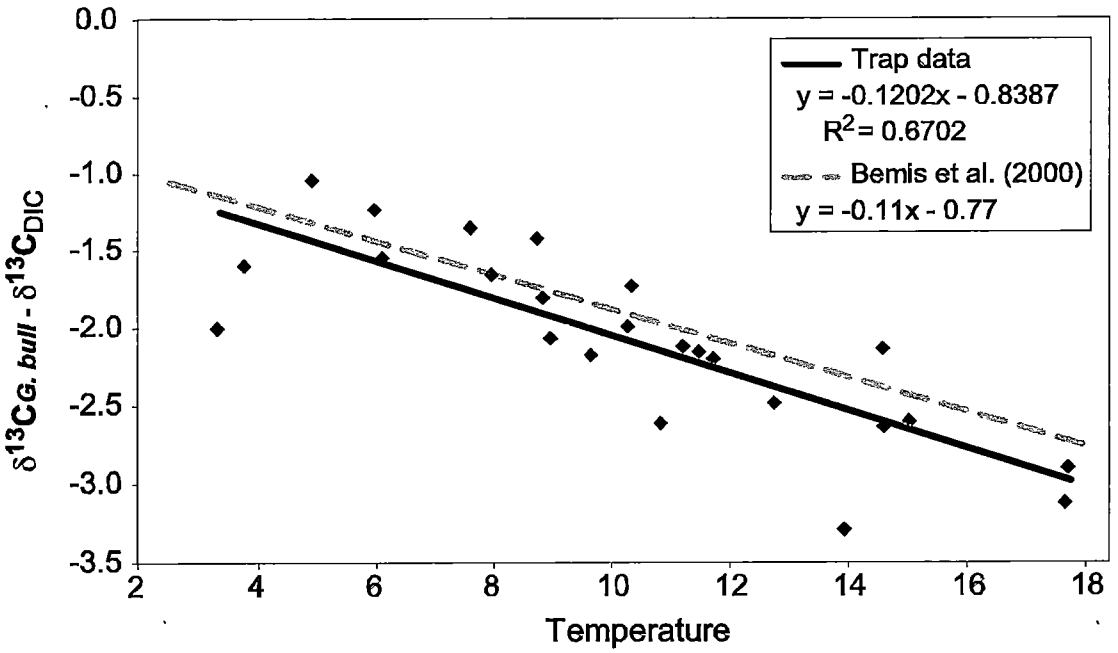

Figure 5: Temperature against $\delta^{13}C$ disequilibrium for *G. bulloides*. The relationship between $\delta^{13}C$ disequilibrium for *G. bulloides* and temperature at these sites is almost indistinguishable from the laboratory relationship determined by *Bemis et al.* [2000]. This suggests that temperature can fully account for disequilibrium offsets in *G. bulloides* at these sites.

The result that temperature seems to be the dominant factor driving disequilibrium in *G. bulloides* at these sites is surprising given the consistency of the carbonate ion effect in laboratory [eg. *Spero et al.*, 1997; *Bemis et al.*, 2000;] and field studies [*Russell and Spero*, 2000; Itou et al., 2001; Bauch et al., 2002]. Recalibration of the *Bemis et al.* [2000] temperature relationship to the cooler range observed at our sites may reveal the effect of carbonate ion concentration on $\delta^{13}C$ disequilibrium across this transect. However, to incorporate the carbonate ion effect would require a major reduction in the slope of the *Bemis et al.* [2000] temperature relationship, and a reassessment of the slope of the *Spero et al.* [1997] carbonate ion calibration. The recalibration of these relationships for the Southern Ocean may be justified if evidence for genotypic variation can be found to distinguish between Southern Ocean *G. bulloides* and those cultured in laboratory experiments (from the Southern California Bight).

To obtain $\delta^{13}C$ values for *G. bulloides* which are seasonally and spatially consistent in our dataset, we have applied the *Bemis et al.* [2000] temperature correction across the whole dataset, and use this to test the effectiveness of $\delta^{13}C_{foram}$ as a tracer of $\delta^{13}C_{DIC}$.

There are no laboratory-derived disequilibrium calibrations for *G. inflata* or *N. pachyderma* (s.). Disequilibrium effects are species-specific and several variables may be operating at once, so it is difficult to determine valid corrections for either of these species. One way in which we can establish the approximate magnitude of the disequilibrium offsets in these species is by aligning the $\delta^{13}C$ values against the corrected *G. bulloides* values during spring, when vertical differences in $\delta^{13}C$ are small and habitat depth therefore irrelevant. This adjustment implies that *G. inflata* is offset from $\delta^{13}C$ equilibrium by ~0.3 to 0.9‰ across the sites and *N. pachyderma* (s.) is offset by 0.3‰ to 2.4‰ between 54°S and SCR. Average offsets from corrected *G. bulloides* values are 0.6‰ for *G. inflata* and 1.4‰ for *N. pachyderma* (s.).

Another way to account for disequilibrium is to apply known *G. bulloides* corrections to *G. inflata* and *N. pachyderma* (s.). By applying the *G. bulloides* [CO_3^{2-}] and temperature correction slopes we can test how well these relationships account for disequilibrium in *G. inflata* and *N. pachyderma* (s.), and we may be able to establish the influence of temperature and [CO_3^{2-}] on their carbon isotopic disequilibrium (Figure 6). For *G. inflata*, the *G. bulloides* [CO_3^{2-}] and temperature corrections produce a much larger disequilibrium offset than observed, but it seems that application of a temperature relationship could eliminate the latitudinal trend in $\delta^{13}C$ disequilibrium. The overestimation of the temperature effect on disequilibrium partly reflects the lower temperature range within this species subsurface habitat. For *N. pachyderma* (s.), neither calibration taken alone can fully account for the latitudinal trend in disequilibrium, however, if both calibrations are applied then the resulting disequilibrium is nearly constant across the full latitudinal range, although still offset from equilibrium. Our results contrast with those of *Bauch et al.* [2002] who suggest that the *G. bulloides* [CO_3^{2-}] slope of *Spero et al.* [1997] can fully account for $\delta^{13}C$ disequilibrium in *N. pachyderma* (s.). *Lea et al.* [1999] suggest that the response of *N. pachyderma* (s.) to carbonate ion concentration may be twice as strong as for *G. bulloides*, however, this would overestimate disequilibrium for *N. pachyderma* (s.) in our dataset.

Field evaluation of disequilibrium effects is hindered by the inter-correlation among variables, however, this study illustrates that both [CO_3^{2-}] and temperature effects may be required to account for latitudinal and seasonal variations in disequilibrium for Southern Ocean *N. pachyderma* (s.). Laboratory studies should therefore focus on the effects of both [CO_3^{2-}] and temperature on *N. pachyderma* (s.) [eg. *von Langen et al.*, 2000] and temperature on *G. inflata*.

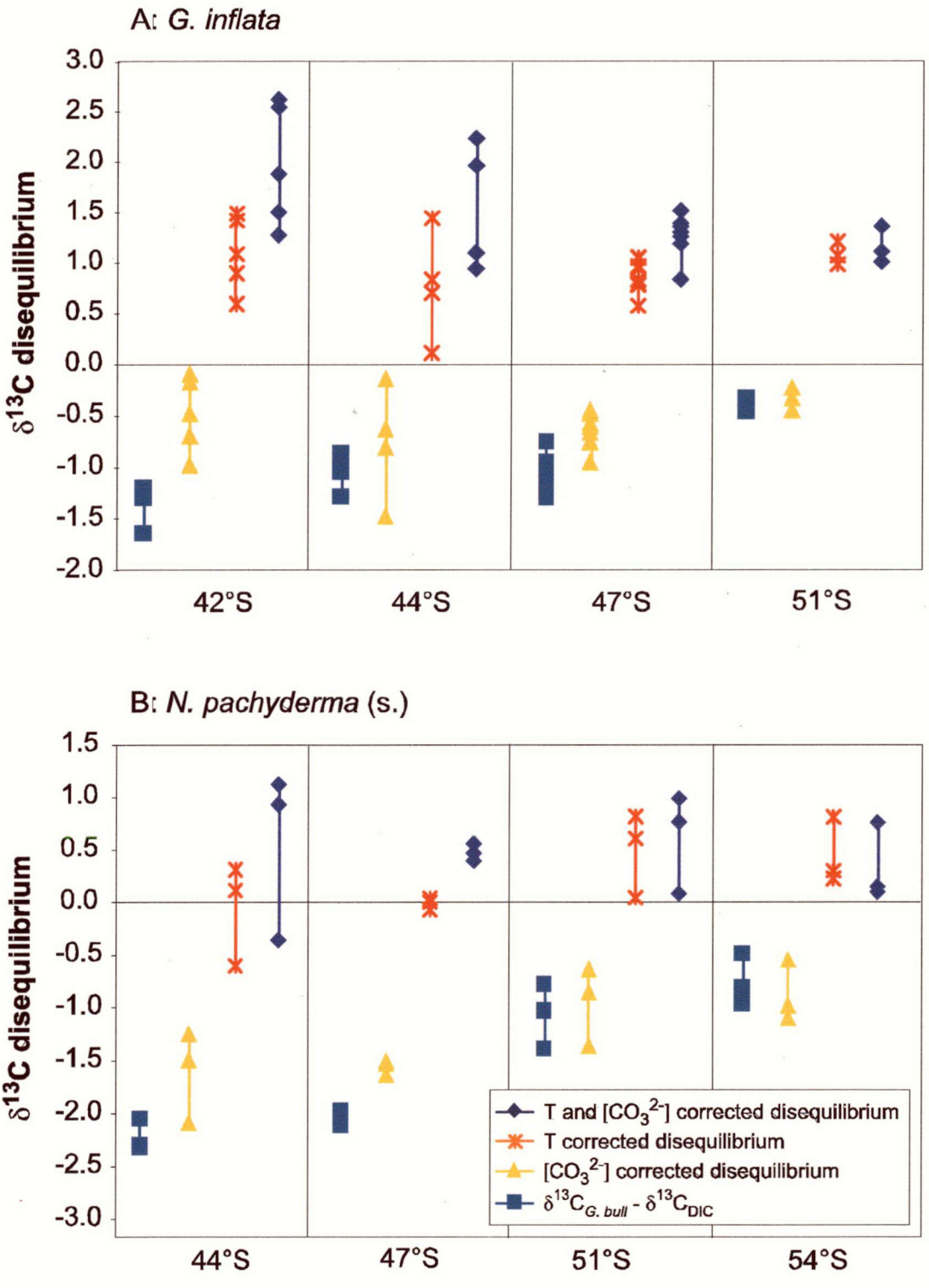

Figure 6: Disequilibrium in $\delta^{13}C$ for *G. inflata* (a) and *N. pachyderma* (s.) (b) based on the *G. bulloides* 12 chamber relationship for temperature [*Bemis et al.*, 2000] and $[CO_3^{2-}]$ [*Spero et al.*, 1997]. Disequilibrium is expressed relative to $\delta^{13}C_{DIC}$. Temperature-corrected disequilibrium in *G. inflata* is overestimated due to the subsurface habitat for *G. inflata*. The disequilibrium for *N. pachyderma* (s.) after correcting for both temperature and $[CO_3^{2-}]$ is within 1.2‰, and the latitudinal trend is removed.

Since disequilibrium effects do not vary greatly during the season at each site (up to 0.6‰ for *N. pachyderma* (s.) and 0.45‰ for *G. inflata*) we can use the uncorrected $\delta^{13}C$ records from *G. inflata* and *N. pachyderma* (s.) to evaluate the seasonal amplitude in $\delta^{13}C$ recorded by each species. We will not make comparisons between sites for these species however, given the latitudinal variations in disequilibrium.

5.4.4 Seasonal variability in $\delta^{13}C$: Unraveling the $\delta^{13}C_{foram}$ record

Seasonal variations in $\delta^{13}C$ obtained from the sediment traps for *G. bulloides*, *G. inflata* and *N. pachyderma* (s.) provide the opportunity to evaluate the utility of these $\delta^{13}C$ records as a proxy for the seasonal cycle in $\delta^{13}C_{DIC}$. Since the $\delta^{13}C_{DIC}$ in this region contains a strong biological imprint [*McNeil et al.*, 2001b], we compare the seasonal $\delta^{13}C_{foram}$ records to measurements of mass flux. Offsets between $\delta^{13}C_{foram}$ and mass flux may reflect the influence of air-sea exchange and water mass mixing on the $\delta^{13}C_{DIC}$. The recorded bloom events may also slightly lag the changes in foraminiferal $\delta^{13}C$ due to the relatively fast sinking speeds of the foraminifera.

Chatham Rise

At NCR, *G. bulloides* shows greatest enrichments in $\delta^{13}C$ during October/November, with increases also occurring from February through to April (Figure 7a). This pattern is consistent with peaks in biological production which are most pronounced during October, and relatively high throughout the summer as well. Lowest production occurs during November to December which is when $\delta^{13}C$ values are relatively depleted. At SCR, $\delta^{13}C$ values for *G. bulloides* increase throughout September and October with peaks between November and February (Figure 7b). The spring increase in $\delta^{13}C$ is consistent with peak mass flux at this time, while the high summer values occur despite low mass flux. The enrichment in $\delta^{13}C$ during summer at this site reflects the stratification of the water-column at this time which prevents vertical mixing and the replenishment of nutrients. Nutrient-depleted, ^{13}C-enriched waters are therefore maintained throughout the summer. $\delta^{13}C$ estimates based on nutrient concentrations from this site also predict a relative enrichment in $\delta^{13}C$ of surface waters during the summer. The consistency between the foraminiferal $\delta^{13}C$ and nutrient based calculations demonstrates that the $\delta^{13}C$ seasonal cycle at this site is most closely associated with changes in nutrients. Thus the impact of air-sea exchange appears to be small at these sites, but may dampen the enrichment in $\delta^{13}C$ caused by nutrient uptake by biota.

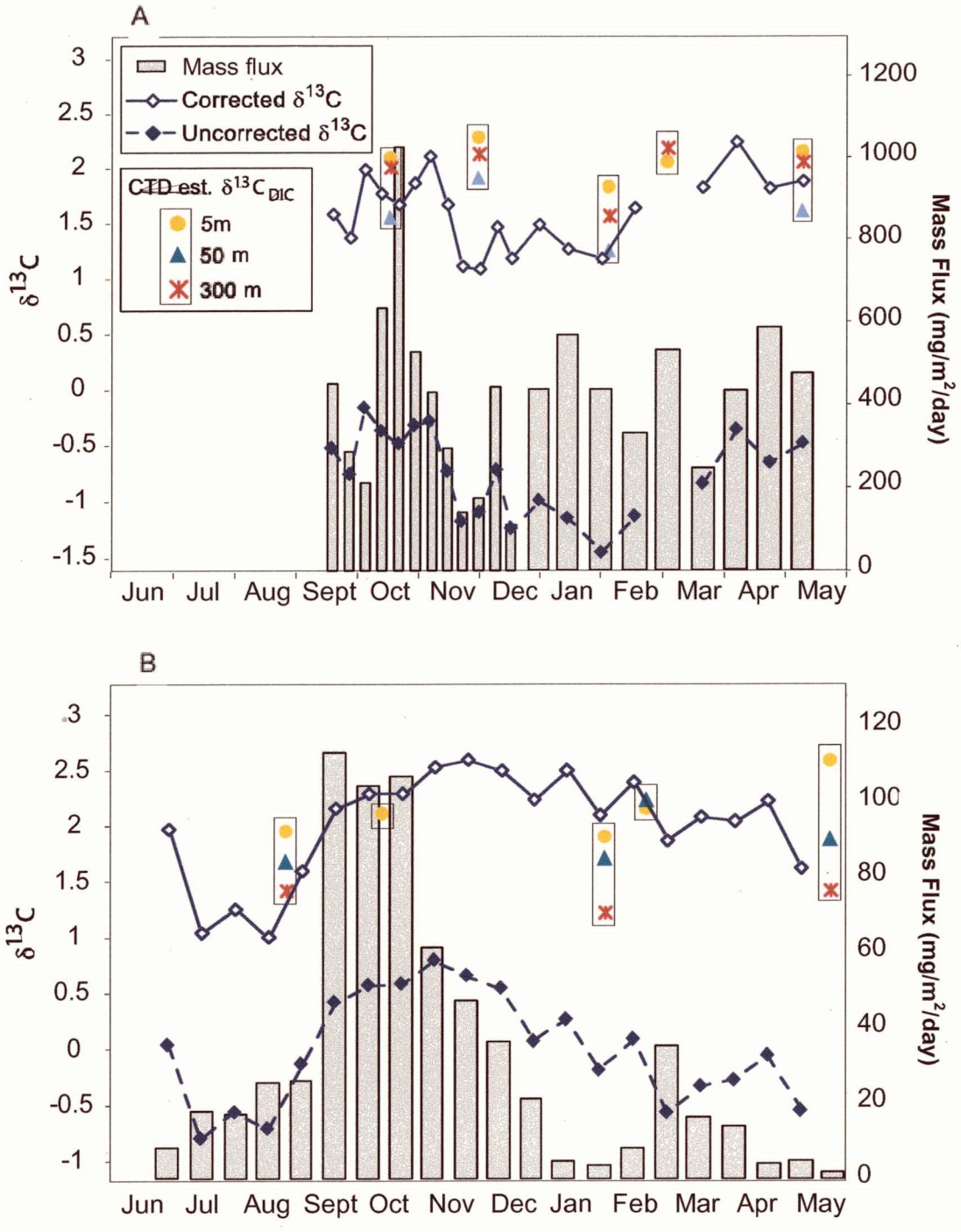

Figure 7: Mass flux versus $\delta^{13}C$ for *G. bulloides* at NCR (a) and SCR (b). Enrichments in $\delta^{13}C$ can mostly be related to increases in biological production (increased mass flux). The $\delta^{13}C$ enrichments during summer also relate to the intense stratification of the water-column at this time which prevents the resupply of nutrient-rich, $\delta^{13}C$-depleted waters at this time. Corrected $\delta^{13}C$ values are calculated on the basis of the temperature calibration of *Bemis et al.* [2000].

The seasonal cycle of $\delta^{13}C$ at NCR for *G. inflata* is very similar to that of *G. bulloides*, although with a much lower amplitude (0.45‰ for *G. inflata* vs 1.3‰ for

G. bulloides) (Figure 8a). The low variability in $\delta^{13}C$ for *G. inflata* reflects the deeper habitat for this species, as also indicated by the $\delta^{18}O$ record (see Chapter 4). The deeper habitat also causes a larger offset between $\delta^{13}C$ for *G. bulloides* and *G. inflata* during the summer months when stratification is more intense.

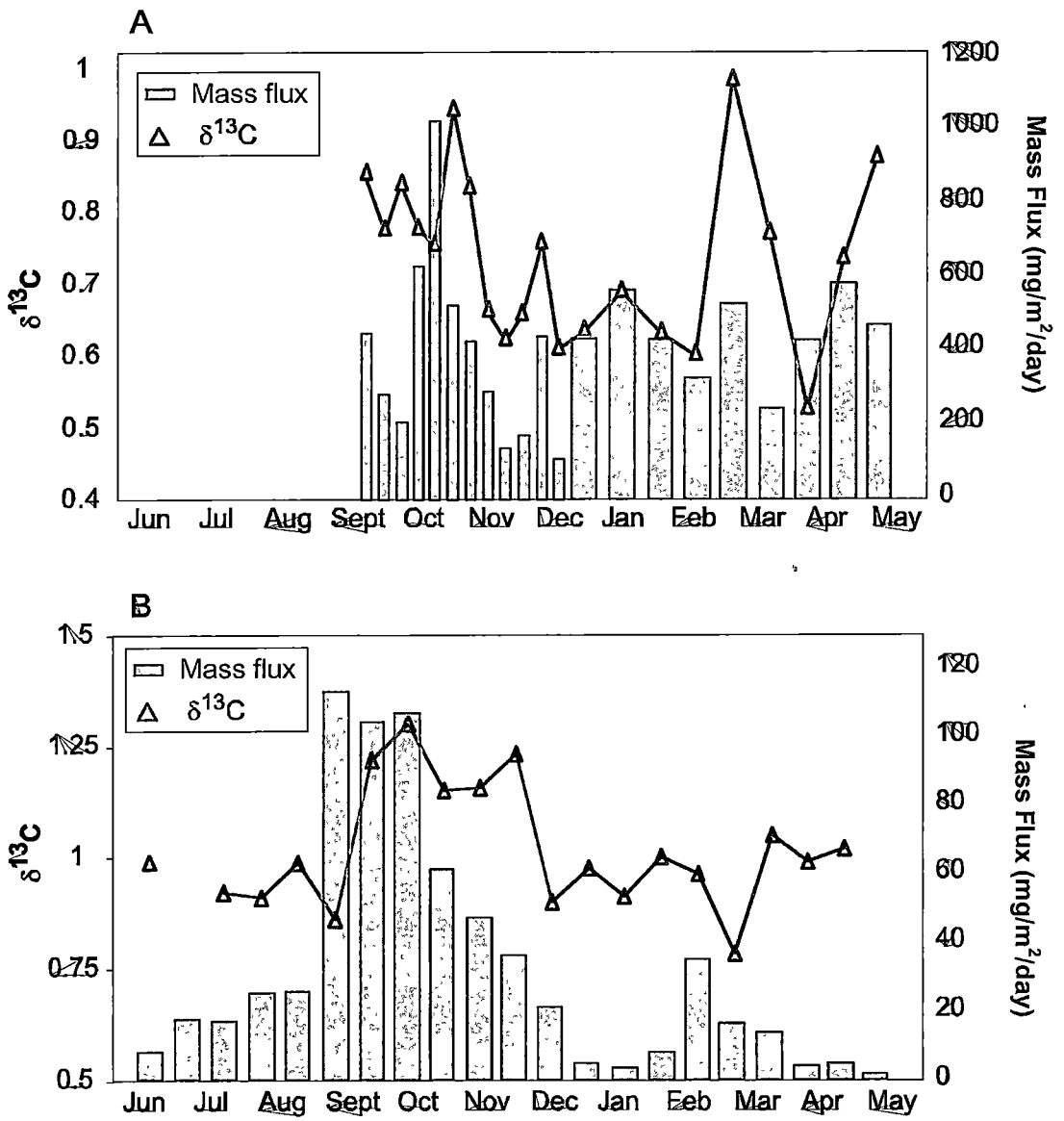

Figure 8: Mass flux versus $\delta^{13}C$ for *G. inflata* at NCR (a) and SCR (b). The seasonal amplitude in $\delta^{13}C$ is much lower for *G. inflata* than for *G. bulloides*. This implies a deeper habitat depth for *G. inflata*, which also causes depletion in summer $\delta^{13}C$ for this species due to the large depletion in $\delta^{13}C$ with depth.

At SCR, there is also a large contrast in the seasonal amplitude recorded by *G. bulloides* and *G. inflata*. *G. inflata* records a seasonal range of 0.5‰ (Figure 8b) while *G. bulloides* exhibits a range of 1.5‰ (Figure 7b). Both species record an increase in $\delta^{13}C$ during spring as mass flux increases, but *G. inflata* then drops to

very depleted $\delta^{13}C$ during the summer, reflecting the depleted $\delta^{13}C$ beneath the thermocline.

The $\delta^{13}C$ record for *Neogloboquadrina pachyderma* (s.) is difficult to interpret given the paucity of data points. However, the record from SCR does indicate a slight increase in $\delta^{13}C$ during spring, with relatively depleted values throughout the summer and increasing values during autumn (Figure 9). This spring enrichment and the low seasonal amplitude suggest a subsurface habitat, though probably shallower than *G. inflata* given the larger seasonal range for *N. pachyderma* (s.). The depth contrast between *N. pachyderma* (s.) and *G. inflata* is consistent with results obtained from South Atlantic plankton tows [*Mortyn and Charles*, 2003].

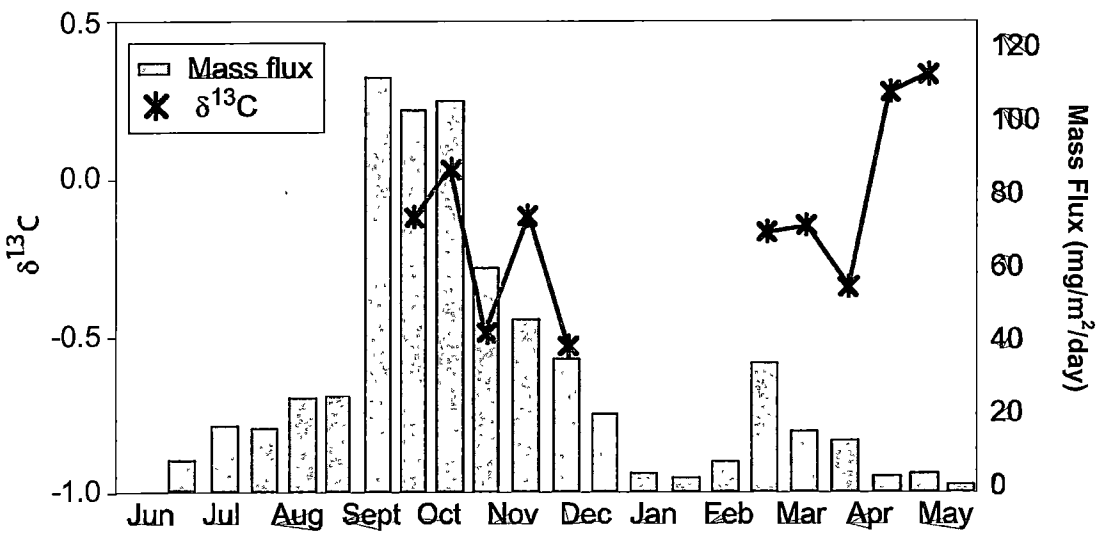

Figure 9: Mass flux versus $\delta^{13}C$ for *N. pachyderma (s.)* at SCR. Data are sparse for this species at SCR, but there is evidence for a slight increase in $\delta^{13}C$ during spring, with relatively depleted values throughout the summer and increasing values during autumn. This pattern is consistent with changes in mass flux.

47°S

G. bulloides $\delta^{13}C$ shows reasonable correlation to mass flux at 47°S (Figure 10a). $\delta^{13}C$ values are generally depleted during October/November 1997 when mass flux is also low, and mass flux and $\delta^{13}C$ both gradually increase until February. The $\delta^{13}C$ of *G. bulloides* reaches maximum values about a month prior to the maximum in mass flux. This indicates that the enrichment in $\delta^{13}C$ during summer probably reflects the influence of other factors in addition to biological production. The increasing stratification of the water-column during summer reduces mixing to the upper 50 m [*Rintoul and Trull*, 2001]. This diminishes the resupply of $\delta^{13}C$-depleted

waters to the surface, contributing to the maintenance of $\delta^{13}C$-enriched surface waters. Air-sea exchange and CO_2 invasion partly offsets the summer enrichment in $\delta^{13}C$, with the latter effect most pronounced in the northern SAZ [*McNeil et al.*, 2001b]. The depletion in $\delta^{13}C$ during May to August probably reflects the restoration of nutrients and $\delta^{13}C$-depleted waters to the surface via deep mixing to depths of >400 m [*Rintoul and Trull*, 2001]. $\delta^{13}C$ for *G. bulloides* increases during September, just prior to the spring increase in mass flux in the 1998 deployment.

The $\delta^{13}C$ of *G. inflata* (Figure 10b) displays a much smaller seasonal range than *G. bulloides*, and the correlation between *G. inflata* $\delta^{13}C$ and mass flux is poor. $\delta^{13}C$ values for this species are most depleted during January and February, which is when mass flux and therefore biological production is greatest. The high production at this time is reflected in an enrichment in the $\delta^{13}C$ of surface waters. The depleted January values, as well as the low seasonal range in $\delta^{13}C$ (0.3‰ compared to 0.5‰ for surface waters) suggest that this species calcifies at depth. Measured $\delta^{13}C_{DIC}$ during January and February at 150 m is depleted by 0.4-0.5‰ relative to the surface, reflecting the stronger stratification at this time. During September, by contrast, there is little gradient in $\delta^{13}C$ between the surface and 150 m. Surface $\delta^{13}C$ increases between September and January, while measurements at 150 m indicate a depletion in $\delta^{13}C$ values over this interval. Species living at depth will therefore record a depletion in $\delta^{13}C$ despite the enrichment observed in surface waters across this time interval.

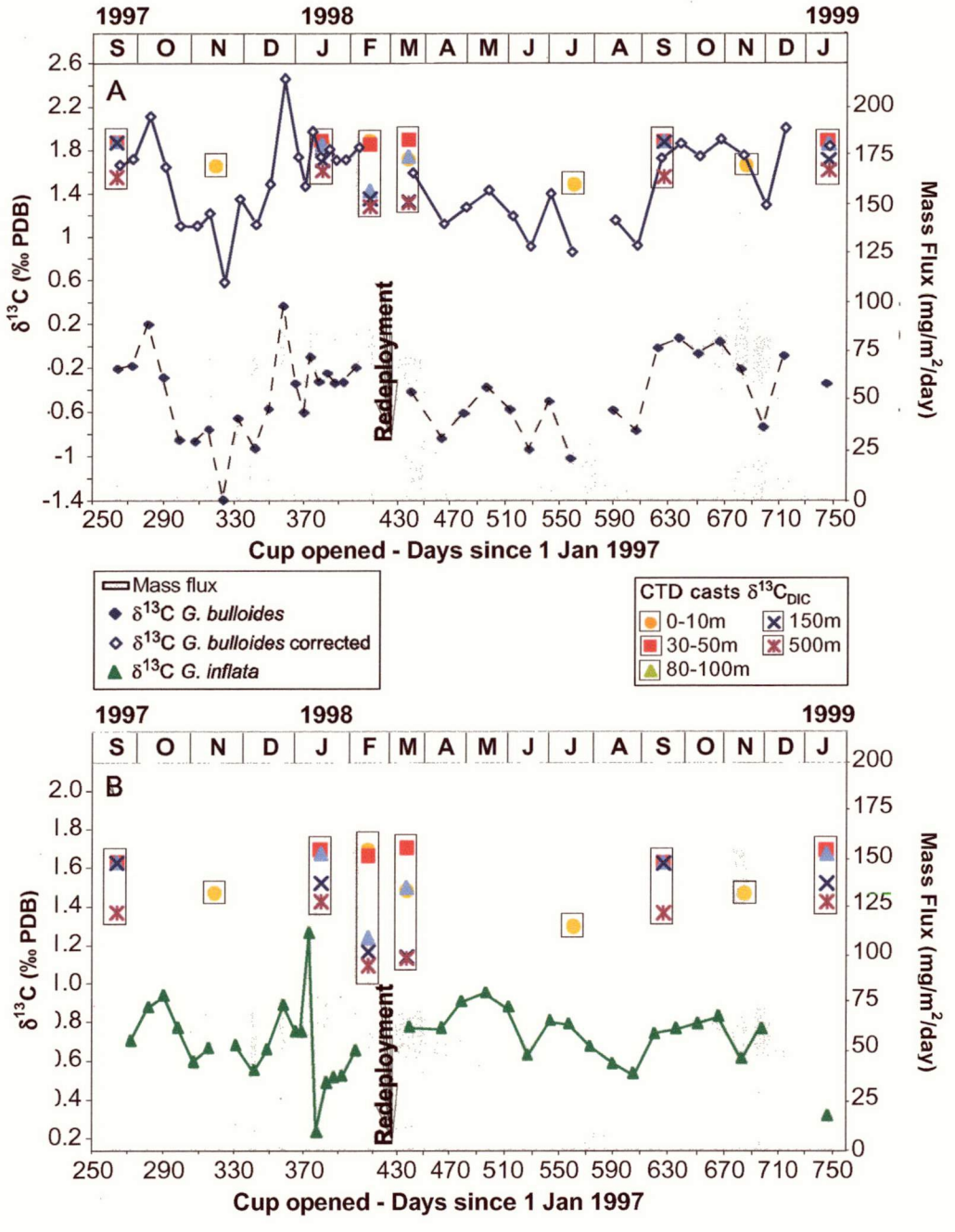

Figure 10: Mass flux versus $\delta^{13}C$ for *G. bulloides* (a) and *G. inflata* (b) at 47°S. The correlation between mass flux and $\delta^{13}C$ for *G. bulloides* is quite close, with the long enrichment during summer also reflecting the depletion in surface water $\delta^{13}C$ as stratification intensifies. *G. inflata* exhibits a lower amplitude in $\delta^{13}C$ than *G. bulloides*, suggesting that this species dwells at depth.

51°S

The $\delta^{13}C$ composition of *G. bulloides* at 51°S (Figure 11a) exhibits a smaller seasonal range than at 47°S (~0.7‰ compared to 1.2‰). Winter mixing in the SAF region is much less intense that in the SAZ, with relatively shallow mixed layer

depths (~200 m) and therefore this region experiences less intense vertical resupply of nutrients and carbon during winter [*Rintoul and Trull*, 2001]. The dominant processes which influence the $\delta^{13}C$ of surface waters in the SAF region are biological production and horizontal advection [*McNeil et al.*, 2001b]. Advection of waters from the PFZ during summer causes a relative enrichment in $\delta^{13}C$ which should enhance any enrichment due to biological production.

The relationship between $\delta^{13}C$ of *G. bulloides* and mass flux is difficult to determine at this site. *G. bulloides* exhibits a slight increase in $\delta^{13}C$ during October as mass flux increases, but then becomes more depleted during November despite consistently high mass flux. Slight increases in mass flux during December and January/February are associated with a slight increase in $\delta^{13}C$, but values are higher than during September and October, despite the relatively low mass flux. The relatively high summer $\delta^{13}C$ most likely reflects the entrainment of southern sourced waters with higher $\delta^{13}C$ into this region [*McNeil et al.*, 2001b]. The foraminiferal $\delta^{13}C$ record therefore implies that the isotopic values are decoupled from the seasonal cycle at the sediment trap site.

The $\delta^{13}C$ for *G. inflata* (Figure 11b) exhibits almost exactly the same pattern as for *G. bulloides* during September to November, with a depletion of 0.4-0.5‰ compared to the corrected *G. bulloides* values. This depletion increases to ~1.0‰ during December however, suggesting that this species inhabits deeper waters during the summer, as at the other sites. The trend in *N. pachyderma* (s.) values (Figure 11c) is consistent with the trend exhibited by *G. bulloides* throughout the record, with a slightly different amplitude. The difference in amplitude reflects either slightly different habitat depths, or a difference in their response to disequilibrium effects.

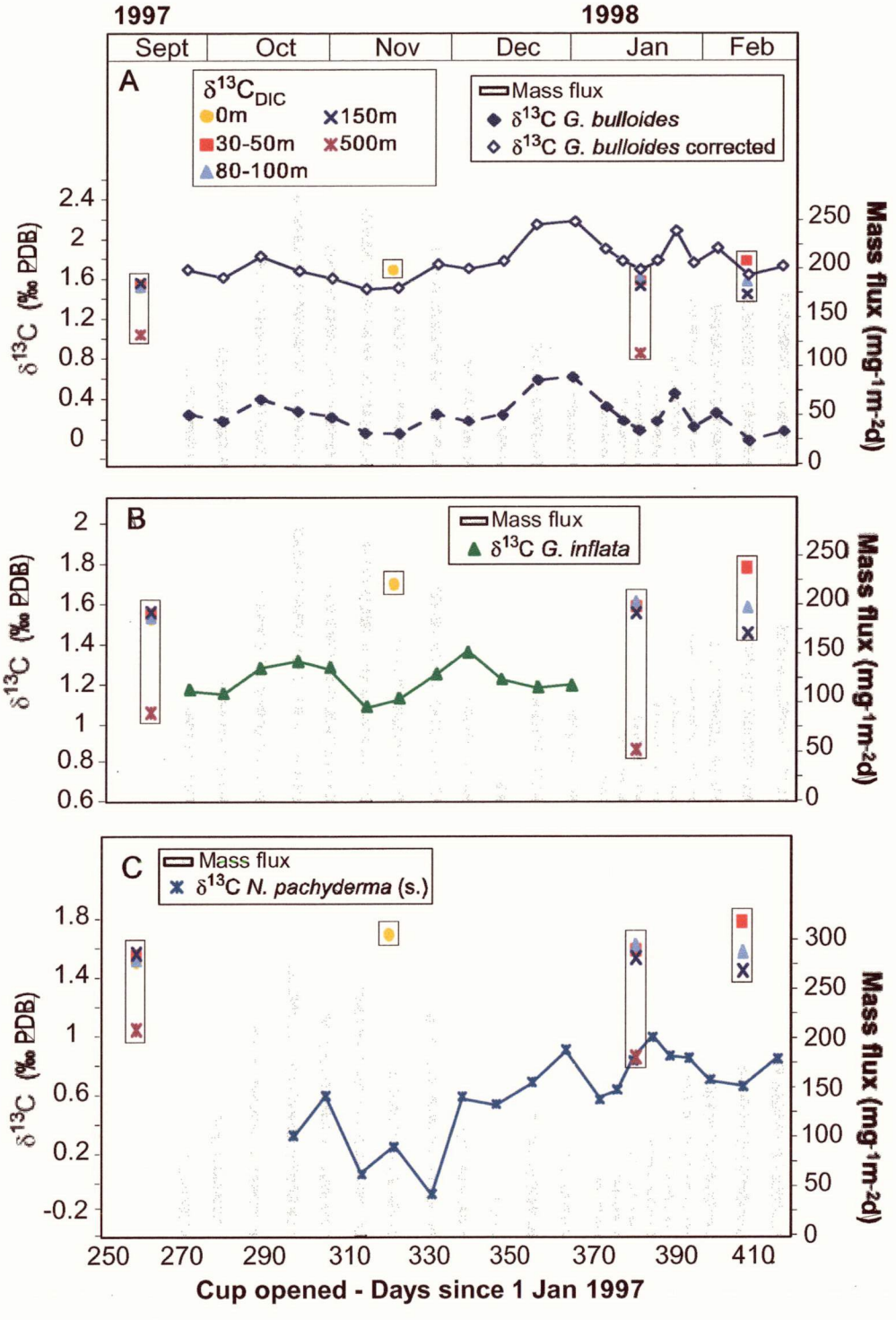

Figure 11: Mass flux versus $\delta^{13}C$ for *G. bulloides* (a), *G. inflata* (b) and *N. pachyderma* (s.) (c) at 51°S. The $\delta^{13}C$ values for *G. bulloides* exhibit a low amplitude at this site, and the relative enrichment in summer occurs despite low mass flux. This indicates that the $\delta^{13}C$ signature is strongly influenced by vertical mixing at this site, with shallow mixing in summer causing an enrichment in $\delta^{13}C$. *G. inflata* also shows a low amplitude in $\delta^{13}C$, and the depletion in values during summer imply that this species lives at depth. *N. pachyderma* (s.) displays a similar trend in $\delta^{13}C$ to *G. bulloides*, with an offset of ~1.1‰. This indicates that these species live at similar depths.

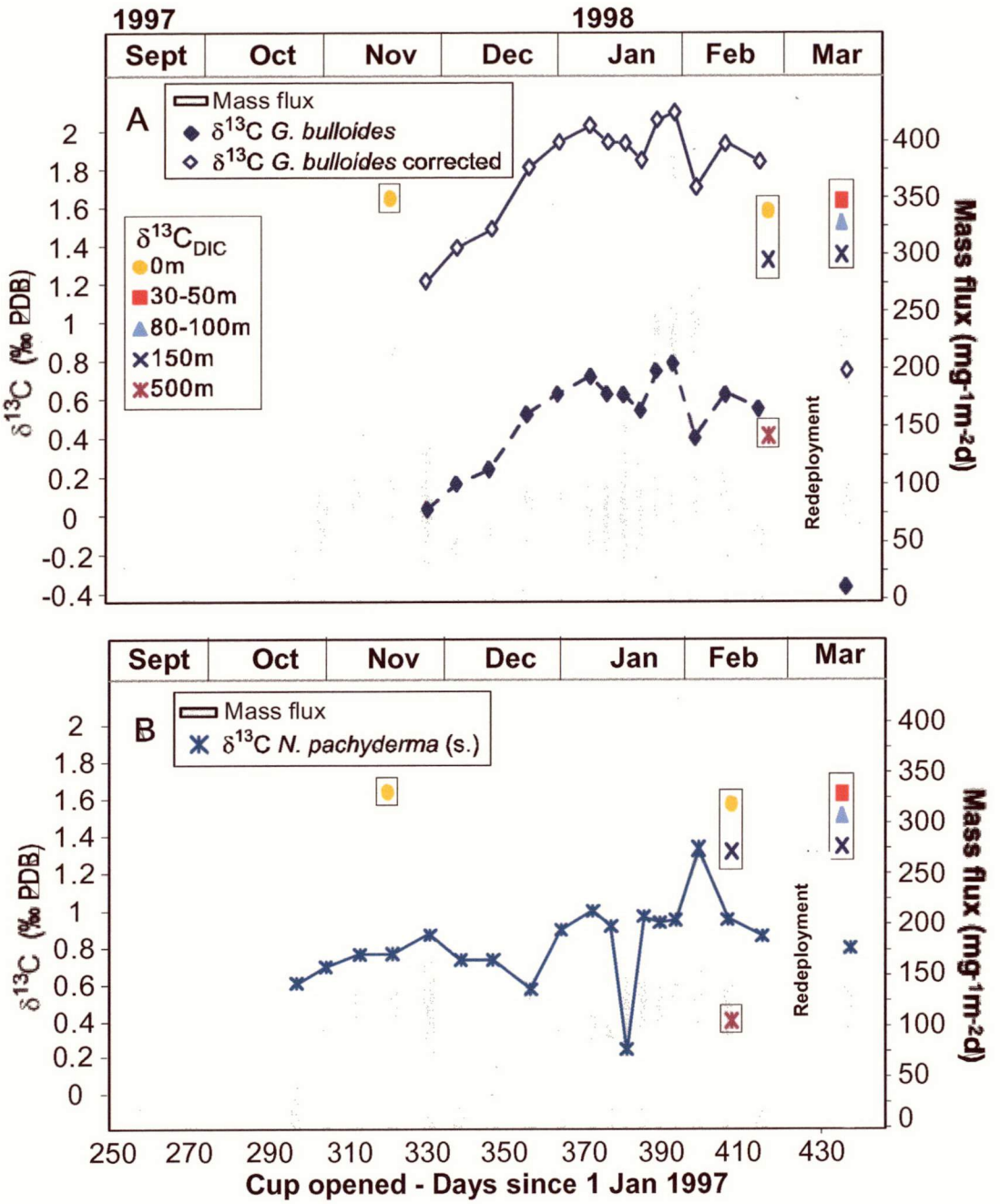

Figure 12: Mass flux versus $\delta^{13}C$ for *G. bulloides* (a), and *N. pachyderma* (s.) (b) at 54°S. The seasonal range in $\delta^{13}C$ is low for both species at this site, reflecting the weak vertical mixing during the winter which prevents the resupply of nutrients and $\delta^{13}C$ depleted waters to the surface. *N. pachyderma* (s.) exhibits an even lower amplitude in $\delta^{13}C$ than *G. bulloides*, and more depleted values during summer. This indicates that *N. pachyderma* (s.) dwells deeper than *G. bulloides*.

54°S

$\delta^{13}C$ values for *G. bulloides* increase gradually from depleted values in November, to most enriched values through January and February (Figure 12a). The seasonal range

in $\delta^{13}C$ for *G. bulloides* (~0.95‰) is relatively low compared to the SAZ sites (~1.4‰ at 47°S), despite the larger amplitude variation in mass flux at 54°S. The low seasonal range in $\delta^{13}C$ at 54°S reflects the weak vertical mixing during the winter which prevents the resupply of nutrients and $\delta^{13}C$-depleted waters to the surface. Mixing in winter reaches to a depth of ~150 m [*Rintoul and Trull*, 2001]. Model results indicate that most organic matter is remineralised below the depth of the winter mixed layer, implying that nutrients are not effectively resupplied to the upper ocean [*Wang et al.*, 2001]. However, the model also predicts that the loss of $[PO_4]$ is balanced by horizontal resupply in association with Ekman transport caused by the high eastward wind stress. The gradual increase of $[PO_4]$ during the summer reflects this supply of nutrients and $\delta^{13}C$-depleted waters into the region, although $\delta^{13}C$ values may also be driven by air-sea exchange during summer as suggested by the offset between the nutrient based estimates and measurements of $\delta^{13}C_{DIC}$.

The seasonal $\delta^{13}C$ range for *N. pachyderma* (s.) (~0.55‰) (Figure 12b) is even smaller than for *G. bulloides*. $\delta^{13}C$ values for *G. bulloides* and *N. pachyderma* (s.) are within 0.3‰ during November, and then diverge during summer with *N. pachyderma* (s.) exhibiting more depleted values. This pattern suggests that this species dwells at depth at this site, in contrast to the similar habitat depths inferred at the more northerly sites.

5.4.5 Summary

$\delta^{13}C$ measurements and mass fluxes across the five sediment trap sites illustrate the relative relationship between $\delta^{13}C$ and biological production. The relationship between $\delta^{13}C$ and biological production is not always direct, however, *McNeil et al.* [2001b] have shown that biological drawdown accounts for most of the change in $\delta^{13}C_{DIC}$ in this region. The comparison between foraminiferal $\delta^{13}C$ and biological production is particularly strong at 47°S for *G. bulloides*, while values at 51°S and 54°S reveal the dampening effect caused by changes in vertical and horizontal advection and air-sea exchange. The close correspondence between $\delta^{13}C_{foram}$ and the $\delta^{13}C_{DIC}$ predicted on the basis of nutrient concentrations indicates that these three species of foraminifera capture the range and trends in nutrient concentrations, with varying offsets from equilibrium $\delta^{13}C$.

5.4.6 Comparison to core tops

The flux-weighted sediment trap values allow comparison between the traps and the core tops. The relationship between the traps and several of the core tops has previously been established on the basis of the foraminiferal assemblages [*King and*

Howard, 2001; *King and Howard*, 2003]. Low dissimilarities between the core top and sediment trap assemblages indicate that the core tops represent the modern conditions of the sediment trap deployments. By comparing the isotopic composition between the traps and the core tops, we can further test the relationship between core top sediments and modern oceanographic conditions. Core top material is often used to establish a correlation between paleoclimate proxies and climatic or oceanographic variables such as temperature, stratification, circulation, or the seawater chemical composition, and these correlations are then applied to interpretations down the core. For this reason, it is important to assess the similarity between the core top fossil material and modern biological components.

For this analysis we have produced two separate flux-weighted values at 47°S for the 1997 and 1998 deployments. The flux-weighted $\delta^{13}C$ values obtained for the two deployments are within 0.02 – 0.07‰ of each other for all three species. The close match between the two deployments suggests that the 1997 deployment is representative of the annual cycle at these sites, despite the shorter collection period of September to February.

For calculation of the flux-weighted values we have used the uncorrected values for *G. bulloides*. There is a large range in latitudes amongst the core top sites, so we compare the latitudinal trend obtained from the sediment traps to the core tops at their latitude. This allows the offset from the modern values to be determined for each core top site.

The comparison between the flux-weighted sediment trap $\delta^{13}C$ values and the core tops for *G. bulloides* is shown in Figure 13a. *G. bulloides* exhibits a fairly large scatter in core top values, with most core tops enriched in $\delta^{13}C$ compared to the latitudinal trend of the sediment traps. The significance of the enrichment in the core tops will be discussed in a separate section in relation to the oceanic Suess effect. *G. inflata* and *N. pachyderma* (s.) show a smaller scatter in values overall, although with fewer sites (Figures 13b and c). Maximum offsets between the latitudinal trend in $\delta^{13}C$ and the core tops are 0.75‰ for *G. bulloides* (with most values within 0.5‰), 0.55‰ for *G. inflata* (with most core tops within 0.2‰), and 0.6‰ for *N. pachyderma* (s.) (most within 0.25‰). *N. pachyderma* (s.) is the only species for which we observe large depletions in the core top $\delta^{13}C$ relative to the latitudinal trend.

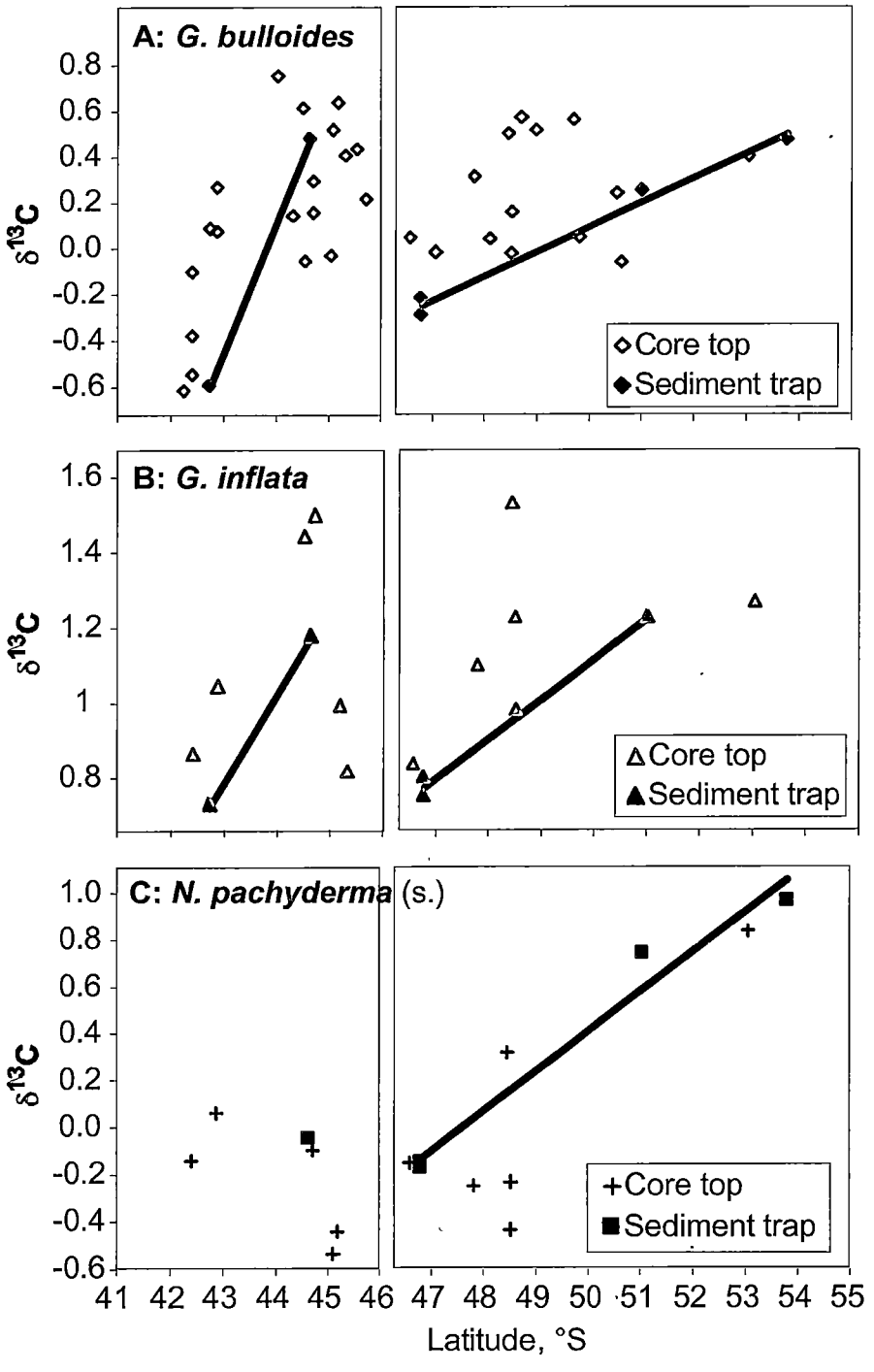

Figure 13: Core top versus weighted sediment trap $\delta^{13}C$ for *G. bulloides* (a), *G. inflata* (b) and *N. pachyderma* (s.) (c) for the Chatham Rise and Australian sector deployments. The $\delta^{13}C$ values generally display a depletion relative to the latitudinal trend obtained from the sediment trap for *G. bulloides* and *G. inflata*, while *N. pachyderma* (s.) exhibits more variation in core top $\delta^{13}C$ values. The line indicates the latitudinal trend.

5.5 Discussion

5.5.1 Implications for interpreting paleoclimate records

These sediment trap records highlight the critical importance of taking disequilibrium effects into account when interpreting $\delta^{13}C$ records from planktonic foraminifera. Disequilibrium is strongest in *G. bulloides* and *N. pachyderma* (s.), the two species most commonly used in paleo-reconstructions. Of the disequilibrium effects, temperature has the largest effect on $\delta^{13}C$, and causes an increase in disequilibrium with increasing temperature. Disequilibrium offsets are therefore less pronounced in the PFZ, but still >1‰ relative to $\delta^{13}C_{DIC}$.

The latitudinal trend in disequilibrium reveals the danger of interpreting uncorrected $\delta^{13}C$ records from foraminifera. The uncorrected data imply a sharp increase in $\delta^{13}C$ with latitude, whereas the corrected $\delta^{13}C$ values for *G. bulloides* indicate that $\delta^{13}C$ gradually decreases with latitude. These effects need to be accounted for in down-core paleo-nutrient reconstructions.

5.5.2 The oceanic Suess effect

Since the industrial revolution the $\delta^{13}C$ composition of the atmosphere has become progressively depleted by ~1.5‰ due to the burning of fossil fuels which have a very low $\delta^{13}C$ content [*Keeling et al.,* 1995]. Of the 7 billion tons of CO_2 which have been emitted due to the burning of fossil fuels and tropical forests, about 3.4 billion tons are known to stay in the atmosphere [*Kerr*, 1992]. The fate of the remaining 3 to 4 billion tons is uncertain, but the oceans most certainly play a role. Various techniques have been employed to study the contribution of the oceans to the uptake of anthropogenic CO_2. Many studies have centered around the change in $\delta^{13}C$ of the surface oceans, or proxies for this [eg. *Quay et al.*, 1992*; Beveridge and Shackleton*, 1994*; Heimann and Maier-Reimer*, 1996*; Bacastow et al.*, 1996*; Gruber et al.*, 1999*; Bauch et al*, 2000*; Ortiz et al.,* 2000; *Takahashi et al.*, 2000*;McNeil et al.*, 2001a; *Quay et al.,* 2003]. The isotopic composition of the oceans should have become lighter through time due to the enhanced uptake of atmospheric CO_2 which has a more depleted $\delta^{13}C$ composition. Determining the amplitude of $\delta^{13}C$ change over the whole time period since pre-Industrial times has only been possible in a few studies, including those based on foraminiferal $\delta^{13}C$ [*Beveridge and Shackleton*, 1994*; Bauch et al*, 2000] and $\delta^{13}C_{DIC}$ - nutrient profiles [*Ortiz et al.*, 2000]. In this study we provide the first Southern Ocean estimate of $\delta^{13}C$ depletion since prior to the Industrial Revolution.

The Subantarctic Zone is key to our understanding of CO_2 uptake, since a disproportionate amount of the anthropogenic carbon inventory has accumulated in this area (40-45 μmol kg^{-1} since the pre-industrial revolution) [*Sabine et al.*, 2002]. Deep winter mixing in the SAZ also makes it a prime location for the deep sequestration of atmospheric CO_2. Measurements of $\delta^{13}C_{DIC}$ across all major ocean basins have indicated that the largest uptake of atmospheric CO_2 occurs near the Subantarctic Front [*Gruber et al.*, 1999], with a depletion in $\delta^{13}C_{DIC}$ of up to 0.32‰ over 20 years between 1978 and 1998 in the Australian sector [*McNeil et al.*, 2001a]. Maximum depletion in $\delta^{13}C$ within the SAZ occurs between depths of 100 and 500 m, with a maximum penetration depth of up to 700-900 m. The depletion in $\delta^{13}C$ diminishes dramatically across the SAF (at 50-52°S), and southward through the Antarctic Zone.

The anthropogenic depletion in $\delta^{13}C$ within the SAZ should also be recorded by planktonic foraminifera. Foraminifera collected in the sediment traps will record the present $\delta^{13}C$ content at their calcification depth, while core top sediments will contain a larger proportion of material representing conditions prior to the industrial revolution. Foraminifera therefore provide a unique opportunity to determine the oceanic uptake of $\delta^{13}C$ throughout the entire time span since prior to the industrial revolution. The utility of foraminifera in recording the oceanic Suess effect has been demonstrated by *Beveridge and Shackleton* [1994] in the Eastern Atlantic and by *Bauch et al.* [2000] in the Arctic Ocean.

There is a large scatter in the core top $\delta^{13}C$ (Figure 13) and $\delta^{18}O$ (Figure 14) values compared to the weighted sediment trap values, with the $\delta^{13}C$ values generally enriched relative to the sediment traps. Some variability in the $\delta^{13}C$ and $\delta^{18}O$ of the core tops compared to the traps is expected due to interannual variability. Climatological SSTs [*Levitus*, 1994] differ from the observed AVHRR temperatures [*AVHRR*, 1999] during the deployment period by up to 1°C at 47°S and 1.5°C at 51° and 54°S. These temperature differences are equivalent to an interannual variability in $\delta^{18}O$ of ~0.25 – 0.38‰ (based on the $\delta^{18}O$ – temperature relationship of *Epstein et al.* [1953]). We take a slightly more conservative approach, however, and only use $\delta^{13}C$ values from those core tops which have a $\delta^{18}O$ that is within 0.15‰ of the weighted sediment trap values. This allows us to capture measurements from those core tops which are most similar to the sediment traps.

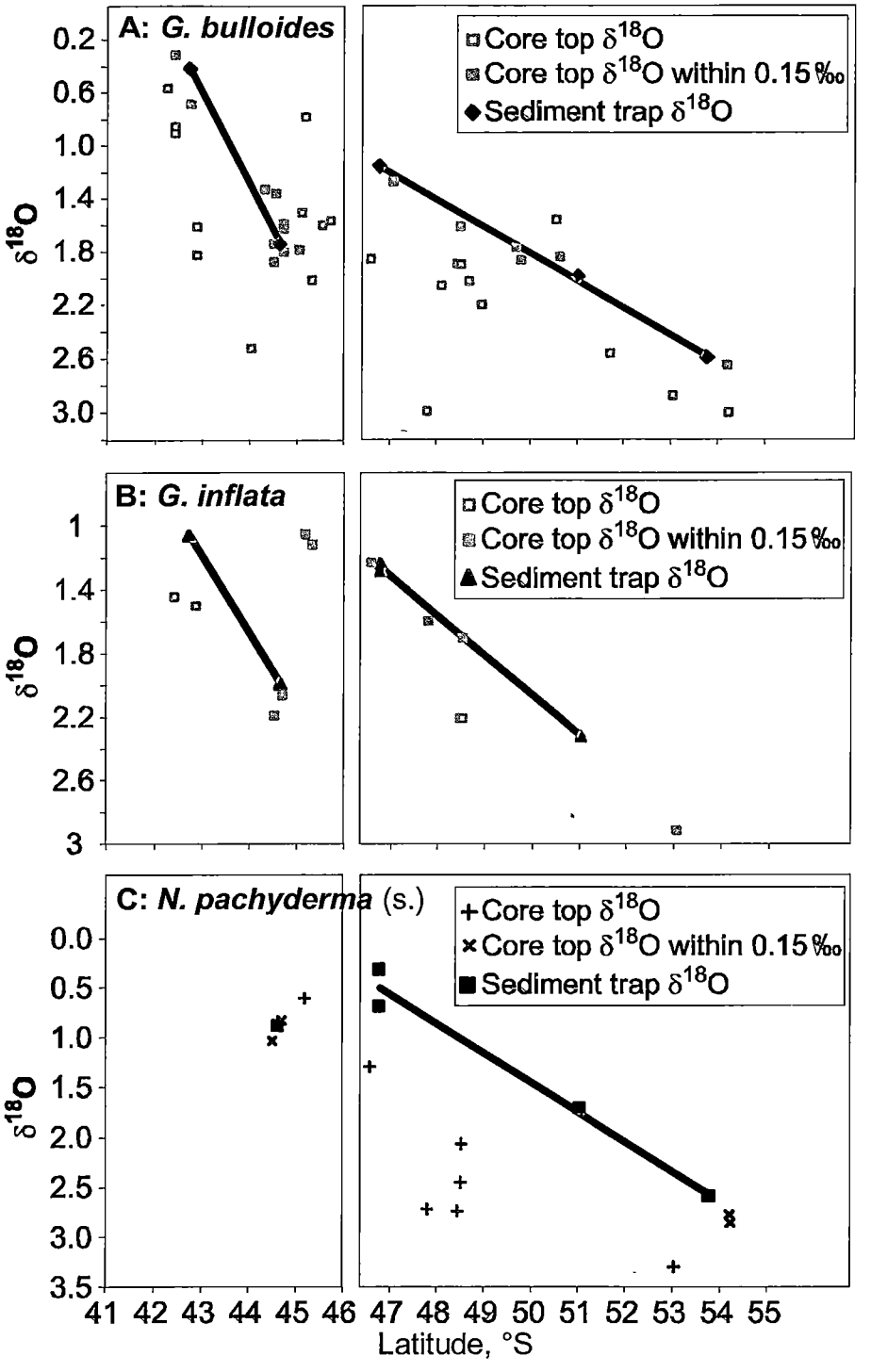

Figure 14: Core top versus weighted sediment trap $\delta^{18}O$ for *G. bulloides* (a), *G. inflata* (b) and *N. pachyderma* (s.) (c) for the Chatham Rise and Australian sector deployments. Core tops with a $\delta^{18}O$ within 0.15‰ of the sediment traps (shown by the shaded symbols for *G. bulloides* and *G. inflata* and by crosses for *N. pachyderma* (s.)) are considered to represent conditions similar to that of the sediment trap deployments. The $\delta^{13}C$ records from these sites are therefore used to establish the strength of the oceanic Suess effect. The line indicates the latitudinal trend.

There are six core top sites within the SAZ and Chatham Rise sites which meet our criteria for oxygen isotopic similarity and have a negative $\Delta\delta^{13}C$ for *G. bulloides* and *G. inflata* ($\Delta\delta^{13}C$ represents the weighted sediment trap $\delta^{13}C$ minus the core top $\delta^{13}C$) (Table 1). The average $\Delta\delta^{13}C$ across these six sites for *G. bulloides* is -0.44‰ and for *G. inflata* -0.21‰. Sites at which $\Delta\delta^{13}C$ is negative for both *G. bulloides* and *G. inflata* have higher $\Delta\delta^{13}C$ than the average across the other sites. There are also three sites for which the sediment trap $\delta^{18}O$ values are within 0.15‰ for *G. bulloides*, while the $\Delta\delta^{13}C$ is positive. Inclusion of these sites would decrease the average $\Delta\delta^{13}C$ for *G. bulloides* to -0.20‰, however, this reduction in the sediment trap to core top contrast is mainly influenced by the very positive $\Delta\delta^{13}C$ obtained from site Q216. It is not clear why the core top value from this site exhibits such a low $\delta^{13}C$. Dating of the core top material in future work may help to better constrain our selection of core tops. Apart from the poor result from this one site, it appears that the oceanic Suess effect is recorded by *G. bulloides* and *G. inflata*, and we record a slightly higher Suess effect for *G. bulloides* than that determined for the last 20 years within the SAZ (-0.32‰) [*McNeil et al.*, 2001a]. The depletion recorded by both *G. bulloides* and *G. inflata* primarily represents the spring-time signal, when the water-column is deeply mixed, increasing the sequestration of anthropogenic CO_2 at depth.

There are only two sites at which *N. pachyderma* (s.) exhibits a $\delta^{18}O$ difference of <0.15‰ between the sediment trap and core tops, and both of these sites have a positive $\Delta\delta^{13}C$. Samples of *N. pachyderma* (s.) are more likely to incorporate glacial material due to the low Holocene abundance of this species within the SAZ compared to its high abundance during the last glacial. The larger sample size for *N. pachyderma* (s.) (15 to 20 shells per analysis, compared to 10 for *G. bulloides* and *G. inflata*) also increases the likelihood of incorporating older material. Glacial sediments will have relatively depleted $\delta^{13}C$ values and enriched $\delta^{18}O$, as is observed for many of the core top samples for *N. pachyderma* (s.) (Figures 13 and 14). It is therefore difficult to determine the oceanic Suess effect from *N. pachyderma* (s.) at these latitudes.

The depletion in $\delta^{13}C$ recorded by the planktonic foraminifera is a minimum estimate of the uptake of anthropogenic CO_2 because the timescale required for $\delta^{13}C$ equilibration with the atmosphere is ~ 10 times longer than for the equilibrium uptake of CO_2 from the atmosphere [*Lynch-Steiglitz et al.*, 1995]. Our calculation of the Suess effect may also need to be reassessed, and indeed may be an underestimate, if future calibrations of foraminiferal $\delta^{13}C$ disequilibrium reveal that a carbonate ion

effect is required across these latitudes. *Kohfeld et al.* [2000] estimate a $[CO_3^{2-}]$ decrease since the pre-industrial era in the subantarctic South Atlantic of ~30μmol/kg. If we apply the carbonate ion relationship of *Spero et al.* [1997] then the decrease in $[CO_3^{2-}]$ during pre-industrial times would imply a relative enrichment in the sediment trap samples of up to 0.40‰ compared to core tops, partly masking the anthropogenic depletion in $\delta^{13}C$. This would imply a Suess effect in the SAZ of more than 1‰. However, at the moment our best estimate of the Suess effect in the SAZis –0.65‰, which is considerably higher than the estimated uptake during the last 20 years in this sector from measurements of $\delta^{13}C_{DIC}$ [*McNeil et al.*, 2001a]. Our estimate provides further evidence for the importance of the SAZ as a sink for atmospheric CO_2 since the industrial revolution.

Core	Latitude	*G. bulloides*		*G. inflata*		*N. pachyderma (s.)*	
		$\Delta\delta^{18}O$	$\Delta\delta^{13}C$	$\Delta\delta^{18}O$	$\Delta\delta^{13}C$	$\Delta\delta^{18}O$	$\Delta\delta^{13}C$
MD972-106	45°9.6'S	**+0.05**	**-0.65**	**-0.1**	**-0.2**	-0.6	0
SO136-165	45°18'S	-1.15	-0.75	**-0.1**	**-0.4**	NA	NA
SO136-161	46°33'S	-0.7	-0.3	**0**	**-0.08**	-0.9	+0.05
H564 [1]	47°04'S	**-0.02**	**-0.2**	NA	NA	NA	NA
SO136-153	47°46.8'S	-1.6	-0.4	**-0.05**	**-0.2**	-2.0	-0.25
SO136-147	48°30'S	-0.35	-0.2	**0**	**-0.05**	-1.0	-0.4
Q585 [1]	49°40.2'S	**0**	**-0.5**	NA	NA	NA	NA
D84 [1]	49°46.8'S	-0.07	+0.05	NA	NA	NA	NA
ELT36-1PH	53°1.1	-0.4	+0.05	-0.1	+0.2	-0.9	-0.1
W266 [2]	42°13.4'S	-0.15	+0.023	NA	NA	NA	NA
S924 [1]	42°23'S	**+0.11**	**-0.21**	NA	NA	NA	NA
U939	44°29.7'S	**-0.14**	**-0.47**	-0.2	-0.26	-0.14	+0.05
W272	44°41.2'S	**-0.06**	**-0.39**	**-0.07**	**-0.32**	+0.05	+0.49
Q216 [1]	45°1.5'S	+0.04	+0.509	NA	NA	NA	NA

Table 1: $\Delta\delta^{18}O$ and $\Delta\delta^{13}C$ for *G. bulloides*, *G. inflata* and *N. pachyderma* (s.). $\Delta\delta^{18}O$ and $\Delta\delta^{13}C$ represents the weighted sediment trap value minus the core top isotopic composition. Bold text represents sites at which $\Delta\delta^{18}O$ is $< \pm 0.15$‰ and $\Delta\delta^{13}C$ is < 0‰. Negative $\Delta\delta^{13}C$ values represent the uptake of anthropogenic CO_2. Values are calculated relative to the latitudinal trends inferred from the weighted trap values. Entries below the lower line are for sites measured relative to the Chatham Rise traps. Published core tops are from [1]*Weaver et al.* [1997] and [2]*Neil* [1997].

5.6 Conclusions

The $\delta^{13}C$ composition of planktonic foraminifera measured in 5 Southern Ocean sediment traps reveal disequilibrium in all species, which is strongest at lower latitudes. Disequilibrium has been corrected for *G. bulloides* by applying the temperature relationship of *Bemis et al.* [2000]. This laboratory relationship appears to fully capture the $\delta^{13}C$ disequilibrium observed for *G. bulloides* in this field study. The corrected $\delta^{13}C$ values show a good correlation to $\delta^{13}C_{DIC}$ and to nutrient concentrations, indicating that the $\delta^{13}C$ composition of *G. bulloides* is an effective tracer of nutrients in these Southern Ocean environments. Comparison between the flux-weighted isotopic composition and regional core tops within the SAZ indicates a depletion in $\delta^{13}C$ for *G. bulloides* and *G. inflata* since the pre-industrial age. This reflects the reduction in $\delta^{13}C$ of surface waters by up to 0.65‰ within the SAZ due to the uptake of anthropogenic CO_2.

5.7 References

AVHRR, Advanced Very High Resolution Radiometer. AVHRR sea surface temperature data. 99. NOAA/NASA. 1999.

Bacastow, R.B., Keeling, C.D., Lueker, T.J., Wahlen, M. and Mook, W.G., The ^{13}C Suess effect in the world surface oceans and its implications for oceanic uptake of CO_2: Analysis of observations at Bermuda, *Global Biogeochemical Cycles*, 10, 335-346, 1996.

Bauch, D., Carstens, J., Wefer, G. and Thiede, J., The imprint of anthropogenic CO_2 in the Arctic Ocean: evidence from planktic $\delta^{13}C$ data from watercolumn and sediment surfaces, *Deep-Sea Research II*, 47, 1791-1808, 2000.

Bauch, D., Erlenkeuser, H. Winckler, G. Pavlova, G. and Thiede, J., Carbon isotopes and habitat of polar planktic foraminifera in the Okhotsk Sea: the 'carbonate ion effect' under natural conditions, *Marine Micropaleontology*, 45, 83-99, 2002.

Bauch, D., Darling, K., Simstich, J., Bauch, H.A., Eriendeuser H. and Kroon, D., Palaeoceanographic implications of genetic variation in living North Atlantic *Neogloboquadrina pachyderma*, *Nature*, 424, 299-302, 2003.

Belkin, I.M. and Gordon, A.L., Southern Ocean fronts from the Greenwich meridian to Tasmania, *Journal of Geophysical Research*, 101, 3675-3696, 1996.

Bemis, B.E., Spero, H.J., Lea, D.W. and Bijma, J., Temperature influence on the carbon isotopic composition of *Globigerina bulloides* and *Orbulina Universa* (planktonic foraminifera), *Marine Micropaleontology*, 38, 213-228, 2000.

Bemis, B.E., Spero, H.J. and Thunell, R.C., Using species-specific paleotemperature equations with foraminifera: A case study in the Southern California Bight, *Marine Micropaleontology*, 46, 405-430, 2002.

Beveridge, N.A.S. and Shackleton, N.J., Carbon isotopes in recent planktonic foraminifera: A record of anthropogenic CO_2 invasion of the surface ocean, *Earth and Planetary Science Letters*, 126, 259-273, 1994.

Bijma, J., Spero, H.J. and Lea, D.W., Reassessing foraminiferal stable isotope geochemistry: Impact of the oceanic carbonate system (experimental results), Use of proxies in paleoceanography: Examples from the South Atlantic, edited by G. Fischer and G. Wefer, pp. 489-512, Springer-Verlag, Berlin, 1999.

Bray, S., Trull, T., and Manganini, S. SAZ project moored sediment traps: Results of the 1997-1998 deployments. 2000. Antarctic CRC, Hobart.

Broecker, W.S. and Maier-Reimer, E., The influence of air-sea exchange on the carbon isotope distribution in the sea, *Global Biogeochemical Cycles*, 6, 315-320, 1992.

Curry, W.B. and Matthews, R.K., Equilibrium ^{18}O fractionation in small size fraction planktic foraminifera: evidence from Recent Indian Ocean sediments, *Marine Micropaleontology*, 6, 327-337, 1981.

Darling, K.F., Wade, C.M., Stewart, I.A., Kroon, D., Dingle, R. and Brown, A.J.L., Molecular evidence for genetic mixing of Artic and Antarctic subpolar populations of planktonic foraminifers, *Nature*, 405, 43-47, 2000.

Deacon, G.E.R., Physical and biological zonation in the Southern Ocean, *Deep-Sea Research*, 29, 1-15, 1982.

Donner, B. and Wefer, G., Flux and stable isotope composition of *Neogloboquadrina pachyderma* and other planktonic foraminifers in the Southern Ocean (Atlantic sector), *Deep-Sea Research I*, 41, 1733-1743, 1994.

Epstein, S., Buchsbaum, R., Lowenstam, H.A. and Urey, H.C., Revised carbonate-water isotopic temperature scale, *Geological Society of America Bulletin*, 64, 1315-1326, 1953.

Griffiths, F.B., Bates, T.S., Quinn, P.K., Clementson, L.A. and Parslow, J.S., The oceanographic context of the first aerosol characterization experiment (ACE 1): A physical, chemical, and biological overview, *Journal of Geophysical Research*, 104, 21,649-21,671, 1999.

Gruber, N., Keeling, C.D., Bacastow, R.B., Guenther, P.R., Lueker, T.J., Wahlen, M., Meijer, H.A.J., Mook, W.G. and Stocker, T.F., Spatiotemporal patterns of carbon-13 in the global surface oceans and the oceanic Suess effect, *Global Biogeochemical Cycles*, 13, 307-335, 1999.

Heath, R.A., A review of the physical oceanography of the seas around New Zealand - 1982, *New Zealand Journal of Marine and Freshwater Research*, 19, 79-124, 1985.

Heimann, M. and Maier-Reimer, E., On the relations between the oceanic uptake of CO_2 and its carbon isotopes, *Global Biogeochemical Cycles*, 10, 89-110, 1996.

Hembleben, C. and Bijma, J., Foraminiferal population dynamics and stable carbon isotopes. Carbon Cycling in the Glacial Ocean: Constraints on the Ocean's Role in Global Change, edited by Zahn, R., Pedersen, T.F., Kaminski, M. and Labeyrie, L., pp. 145-166, NATO ASI. Elsevier, Fellhorst, 1994.

Huber, B.T., Bijma J. and Darling, K., Cryptic speciation in the living planktonic foraminifer *Globigerinella siphonifera* (d'Orbigny), *Paleobiology*, 23, 33-62, 1997.

Itou, M., Ono, T., Oba, T., and Noriki, S. Isotopic composition and morphology of living *Globorotalia scitula*: a new proxy of sub-intermediate ocean carbonate chemistry?, *Marine Micropaleontology*, 42, 189-210, 2001.

Keeling, C.D., Whorf, T.P., Wahlen, M., and van der Plicht, J., Interannual extremes in the rate of rise of atmospheric carbon dioxide since 1980, *Nature*, 375, 666-670, 1995.

Kerr, R.A., Fugitive carbon dioxide: It's not hiding in the ocean, *Science*, 256, 35, 1992.

King, A.L. and Howard, W.R., Seasonality of foraminiferal flux in sediment traps at Chatham Rise, SW Pacific: Implications for paleotemperature estimates, *Deep-Sea Research I*, 48, 1687-1708, 2001.

King, A.L. and Howard, W.R., Planktonic foraminiferal flux seasonality in Subantarctic sediment traps: A test for paleoclimate reconstructions, *Paleoceanography*, 18(1), 1019, doi:10.1029/2002PA000839, 2003.

Kohfeld, K.E., Anderson, R.F. and Lynch-Stieglitz, J., Carbon isotopic disequilibrium in polar planktonic foraminifera and its impact on modern and Last Glacial Maximum reconstructions, *Paleoceanography*, 15, 53-64, 2000.

Kucera, M. and Darling, K.F., Cryptic species of planktonic foraminifera: their effect on palaeoceanographic reconstructions, *Philosophical Transactions of the Royal Society of London Series a-Mathematical Physical and Engineering Sciences,* 360(1793), 695-718, 2002.

Levitus, S. Levitus94: World Ocean Atlas 1994. 94. NOAA Office of Global Programs and Lamont-Doherty Earth Observatory of Columbia University. 2000.

Lourey, M.J. and Trull, T.W., Seasonal nutrient depletion and carbon export in the Subantarctic and Polar Frontal Zones of the Southern Ocean south of Australia, *Journal of Geophysical Research*, 106, 31,463-31,488, 2001.

Lourey, M.J., Trull, T.W. and Tilbrook, B., Sensitivity of $\delta^{13}C$ of Southern Ocean suspended and sinking organic matter to temperature, nutrient utilization, and atmospheric CO_2, *Deep-Sea Research I*, 51, 281-305, 2004.

Lynch-Steiglitz, J., Stocker, T.F., Broecker, W.S. and Fairbanks, R.G., The influence of air-sea exchange on the isotopic composition of oceanic carbon: Observations and modeling, *Global Biogeochemical Cycles*, 9, 653-665, 1995.

McNeil, B.I., Matear, R.J. and Tilbrook, B., Does carbon 13 track anthropogenic CO_2 in the Southern Ocean?, *Global Biogeochemical Cycles*, 15, 597-613, 2001a.

McNeil, B.I., Tilbrook, B. and Matear, R.J., Carbon export in the sub-Antarctic zone, South of Australia based on seasonal changes in DIC and $\delta^{13}C_{DIC}$, *Deep-Sea Research*, 2001b.

McNeil, B.I., Stable isotopes as tracers of carbon cycling in the Southern Ocean,

PhD thesis, University of Tasmania, Hobart, Australia, 2001c.

Metzl, N., Tilbrook, B. and Poisson, A., The annual fCO_2 cycle and the air-sea CO_2 flux in the sub-Antarctic Ocean, *Tellus*, 51B, 849-861, 1999.

Mix, A.C. The oxygen-isotope record of glaciation, The Geology of North America, edited by Ruddiman, W. F. and Wright H., pp. 111-135, Geological Society of America, Boulder, Colorado, 1987.

Mortyn, G.P. and Charles, C.D., Planktonic foraminiferal depth habitat and $\delta^{18}O$ calibrations: Plankton tow results from the Atlantic sector of the Southern Ocean. *Paleoceanography,* 18(2), 1037, doi: 10.1029/2001PA000637, 2003.

Neil, H.L., Late Quaternary variability of surface and deep water masses - Chatham Rise, SW Pacific, PhD thesis, University of Waikato, Hamilton, New Zealand, 1997.

Nodder, S.D. and Northcote, L.C., Episodic particulate fluxes at southern temperate mid-latitudes (42-45°S) in the Subtropical Front region, east of New Zealand, *Deep-Sea Research I*, 48, 833-864, 2001.

Oppo, D.W. and Fairbanks, R.G., Carbon isotope composition of tropical surface water during the past 22,000 years, *Paleoceanography*, 4, 333-351, 1989.

Orsi, A., Whitworth, T. and Nowlin, W.D., On the meridional extent and fronts of the Antarctic Circumpolar Current, *Deep-Sea Research I*, 42, 641-673, 1995.

Ortiz, J.D., Mix, A.C., Wheeler, P.A. and Key, R.M, Anthropogenic CO_2 invasion into the northeast Pacific based on concurrent $\delta^{13}C_{DIC}$ and nutrient profiles from the California Current, *Global Biogeochemical Cycles*, 14, 917-929, 2000.

Östlund, H.G., Craig, H., Broecker, W.S., and Spenser, D. GEOSECS Atlantic, Pacific and Indian Ocean expeditions: Shorebased Data and Graphics. 87. Washington D.C., National Science Foundation.

Popp, B.N., Trull, T., Kenig, F., Wakeham, S.G., Rust, T.M., Tilbrook, B., Griffiths, F.B., Wright, S.W., Marchant, H.J., Bidigare, R.R. and Laws, E.A., Controls on the carbon isotopic composition of Southern Ocean phytoplankton, *Global Biogeochemical Cycles*, 13, 827-843, 1999.

Quay, P.D., Tilbrook, B. and Wong, C.S., Oceanic uptake of fossil fuel CO_2: Carbon-13 evidence, *Science*, 256, 74-79, 1992.

Quay, P., Sonnerup, R., Westby, T., Stutsman, J. and McNichol, A. Changes in the $^{13}C/^{12}C$ of dissolved inorganic carbon in the ocean as a tracer of anthropogenic CO_2 uptake, *Global Biogeochemical Cycles*, 17(1), 1004, doi:10.1029/2001GB001817, 2003.

Ravelo, A.C. and Fairbanks, R.G., Carbon isotopic fractionation in multiple species of planktonic foraminifera from core-tops in the tropical Atlantic, *Journal of*

Foraminiferal Research , 25, 53-74, 1995.

Rintoul, S.R. and Trull, T.W., Seasonal evolution of the mixed layer in the Subantarctic Zone south of Australia, *Journal of Geophysical Research*, 106, 31,447-31,462, 2001.

Russell, A.D. and Spero, H.J., Field examination of the oceanic carbonate ion effect on stable isotopes in planktonic foraminifera, *Paleoceanography*, 15, 43-52, 2000.

Sabine, C.L., Feely, R.A., Key, R.M., Bullister, J.L., Millero, F.J., Lee, K., Peng, T.-H., Tilbrook, B., Ono, T. and Wong, C.S., Distribution of anthropogenic CO_2 in the Pacific Ocean, *Global Biogeochemical Cycles*, 16(4)1083, doi:10.1029/2001GB001639, 2002.

Spero, H.J., Bijma, J., Lea, D.W., and Bemis, B.E., Effect of seawater carbonate concentration on foraminiferal carbon and oxygen isotopes, *Nature*, 390, 497-500, 1997.

Spero, H.J. and Lea, D.W., Experimental determination of stable isotope variability in *Globigerina bulloides*: implications for paleoceanographic reconstructions, *Marine Micropaleontology*, 28, 231-246, 1996.

Stewart, I.A., Darling, K.F., Kroon, D., Wade, C.M., Troelstra, S.R., Genotypic variability in subarctic Atlantic planktic foraminifera, *Marine Micropaleontology*, 43(1-2), 143-153, 2001.

Takahashi, Y., Matsumoto, E. and Watanabe, Y.W., The distribution of $\delta^{13}C$ in total dissolved inorganic carbon in the central North Pacific Ocean along 175°E and implications for anthropogenic CO_2 penetration, *Marine Chemistry*, 69, 237-251, 2000.

Trull, T., Bray, S., Manganini, S., Honjo, S. and François, R., Moored sediment trap measurements of carbon export in the Sub-Antarctic and Polar Frontal zones of the Southern Ocean, south of Australia, *Journal of Geophysical Research*, 106, 31,489-31,510, 2001.

von Langen, P.J., Lea, D.W., and Spero, H.J., Effects of temperature on oxygen isotopie and Mg/Ca values in *Neogloboquadrina pachyderma* shells determined by live culturing, *EOS Transactions AGU*, Fall Meeting Supplement, 2000.

Wang, X., Matear, R.J. and Trull, T.W., Modeling seasonal phosphate export and resupply in the Subantarctic and Polar Frontal Zones in the Australian sector of the Southern Ocean., *Journal of Geophysical Research*, 106, 31,525-31,542, 2001.

Weaver, P.P.E., Neil, H., and Carter, L., Sea surface temperature estimates from the Southwest Pacific based on planktonic foraminifera and oxygen isotopes,

Palaeogeography, Palaeoclimatology, Palaeoecology, 131, 241-256, 1997.

Williams, D.F., Bé, A.W.H., and Fairbanks, R.G., Seasonal stable isotopic variations in living planktonic foraminifera from Bermuda plankton tows, *Palaeogeography, Palaeoclimatology, Palaeoecology*, 33, 71-102, 1981.

Zeebe, R.E., Bijma, J. and Wolf-Gladrow, D.A., A diffusion-reaction model of carbon isotope fractionation in foraminifera, *Marine Chemistry*, 64, 199-227, 1999.

CHAPTER 6

ISOTOPIC ANALYSIS OF INDIVIDUAL FORAMINIFERA FROM CHATHAM RISE TRAPS

"Nature never breaks her own laws"
Leonardo da Vinci (1452-1519)

6.1 Introduction

The interpretation of foraminiferal isotopic records is hindered by uncertainty regarding the seasonal weighting contained within sedimentary records, and potential changes in species seasonal flux patterns through time. The analysis of individual foraminifera from sediments may allow a better understanding of the seasonal amplitude of isotopic values, and therefore of the seasonal weighting contained in pooled measurements. However, intraspecific isotopic variability due to habitat depth or changes in disequilibrium offsets are unknown. In this study individual *G. bulloides* and *G. inflata* were analysed from the sediment traps to establish the intraspecies variability within each cup and to test variations in relation to inferred habitat depth, size and morphology. In this chapter I also discuss results from the analysis of individual foraminifera from Chatham Rise core tops (Bemis, 2000) to determine the success with which individuals from this region can capture the seasonal isotopic range.

6.2 Methods

The oxygen and carbon isotopic composition of individual specimens of *G. bulloides* and *G. inflata* were measured for specific intervals at NCR and SCR. At NCR, individuals were analysed from cups during September/October, December and April, and at SCR from September, February and March. These intervals were chosen to capture intraspecific variations across the seasons and during periods of different stratification. Prior to analysis the maximum length and weight of all specimens was measured. The specimens analysed were at least 355μm long and weighed no less than 10μg. All individuals were analysed on the Micromass Optima at UC Davis. The isotopic ratios are reported as per mil (‰) deviations from the Pee Dee belemnite (PDB) standard using Carrara marble as a laboratory standard.

Additional measurements of *G. bulloides* from these cups were made to determine the isotopic variability associated with changes in morphology. The morphological characteristics of these specimens were analysed under Scanning Electron Microscope (SEM) at the ANU Electro Microscopy Unit. Two distinct morphologies were observed at SCR, an open and very fine shelled form and a compacted heavily calcified form. Shells exhibiting a mixture of these features were also observed.

6.3 Results

Initial analyses of *G. bulloides* and *G. inflata* from cups 12 and 19 at NCR yielded $\delta^{18}O$ and $\delta^{13}C$ values which were extremely offset from the pooled values, particularly for $\delta^{13}C$ (pale symbols on Figures 1-4). Reanalysed specimens from these cups show much greater consistency with the pooled values. The large offsets in these initial analyses, which were all obtained during the same machine run, suggest that there may have been analytical error in these measurements. In the following discussion I exclude these samples.

6.3.1 Comparison between pooled and individual $\delta^{18}O$ and implied depth variability

Individual specimens of *G. bulloides* show good consistency to the pooled values at NCR, exhibiting a range of 0.3‰ during October and up to 0.4‰ during April (Figure 1a). This range may be equivalent to habitat depths ranging from 0 to 75 m during both periods. At SCR, wider variability is observed. Sixteen individuals were measured from cup 7, and this yielded a range in $\delta^{18}O$ of 0.56‰ (Figure 1b). This range in $\delta^{18}O$ would be equivalent to habitat depths ranging from the surface to 500 m, although some specimens are depleted relative to equilibrium surface $\delta^{18}O$. Some of the specimens from cup 7 may represent a remnant of the July to August population when $\delta^{18}O$ values were relatively depleted. The wide $\delta^{18}O$ range may also reflect the range in disequilibrium for *G. bulloides* at any one time. Disequilibrium in *G. bulloides* relative to the Epstein equation exhibits a scatter of ±0.28‰ over the whole trap data set (see Chapter 4), equivalent to the range in the individual values in cup 7. Values from cup 17 in February/March show a larger range in $\delta^{18}O$ of 1.15‰. This scatter is greater than the error margin obtained in relation to the Epstein equilibrium equation and equates to a depth range of 0 to 100 m.

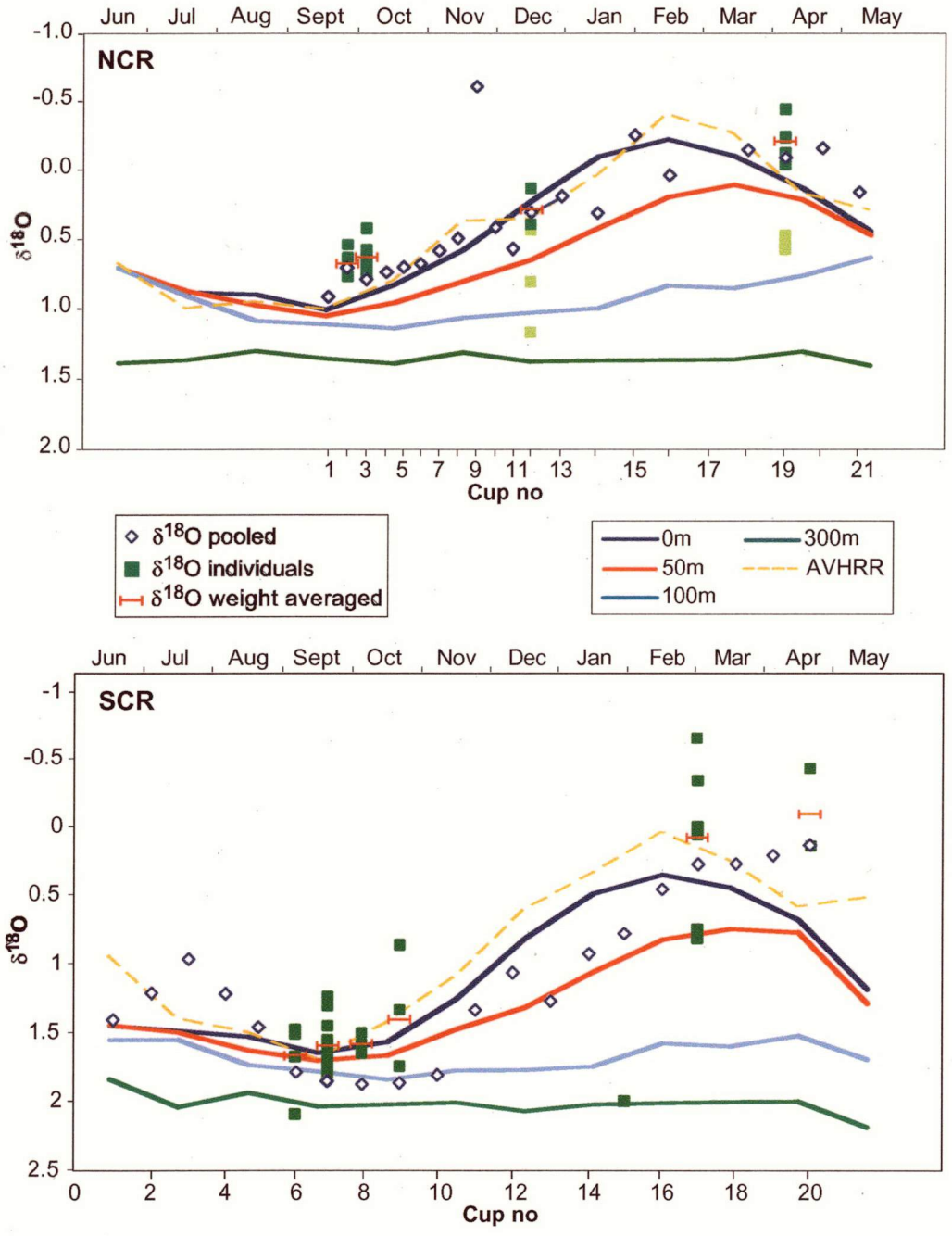

Figure 1: Individual and pooled $\delta^{18}O$ values for *G. bulloides* at NCR (A) and SCR (B). The red bars show the average $\delta^{18}O$ value for the pooled samples in each cup based on shell weight. Also plotted are the equilibrium $\delta^{18}O$ values estimated with the equation of Epstein et al. (1953). Equilibrium values have been adjusted according to the results from Chapter 4. The pale squares represent the individual $\delta^{18}O$ values suspected to be poorly calibrated. The individual $\delta^{18}O$ values are generally well-centred over the pooled measurements, particularly when the weight of the individuals is taken into account.

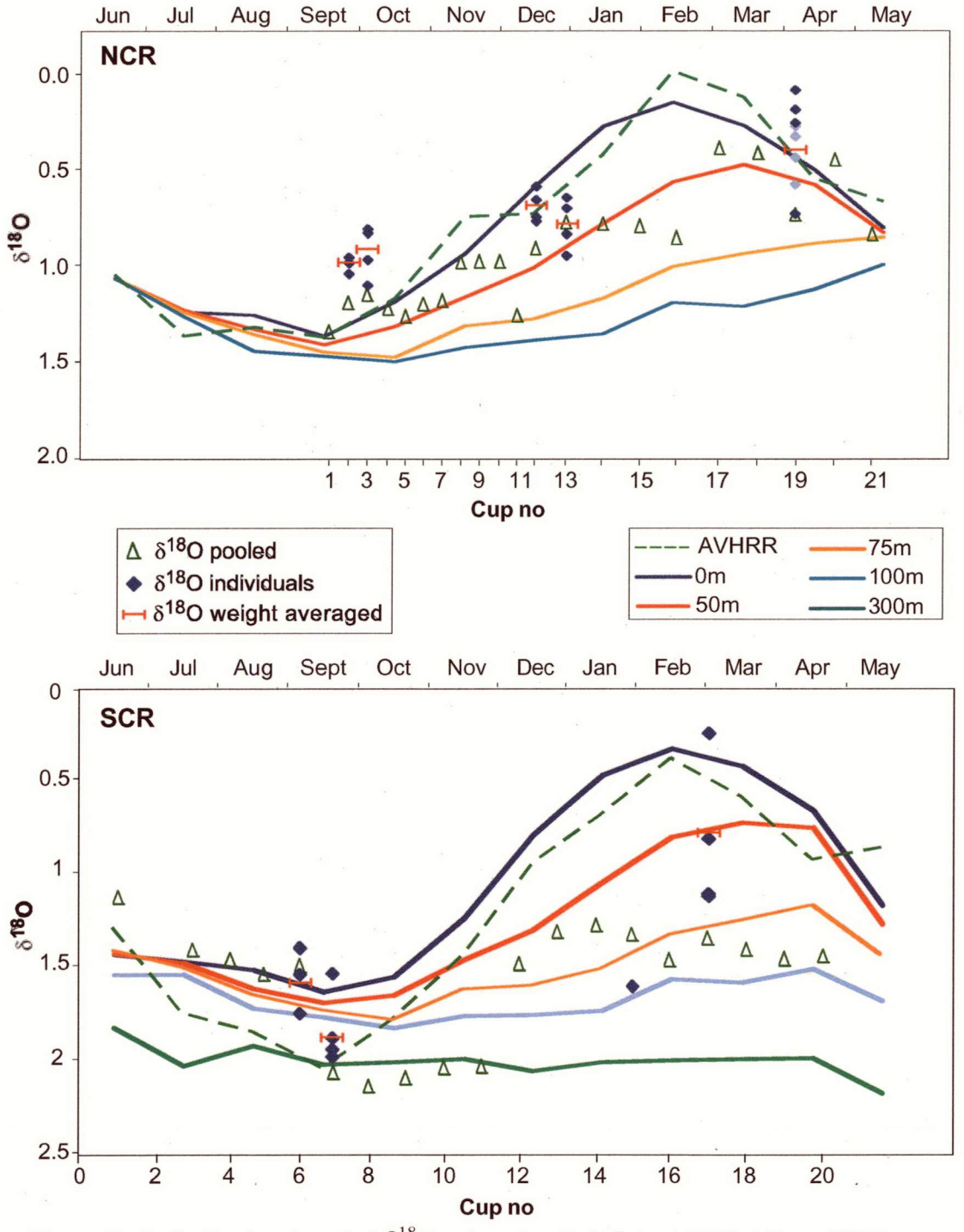

Figure 2: Individual and pooled $\delta^{18}O$ values for *G. inflata* at NCR (A) and SCR (B) with equilibrium $\delta^{18}O$ values (Epstein et al., 1953). The red bars show the average $\delta^{18}O$ value for the pooled samples in each cup based on shell weight. The pale diamonds represent the individual $\delta^{18}O$ values suspected to be poorly calibrated.

Average values obtained from the individual specimens, when averaged according to the weight of each shell, generally show a good correlation to the pooled $\delta^{18}O$ values for *G. bulloides*. Offsets between these weight averaged values and the pooled values are within 0.15‰ at NCR and 0.45‰ at SCR. This result implies that the pooled *G. bulloides* values are obtained from specimens with a similar range in $\delta^{18}O$ as demonstrated for the individual samples.

G. inflata displays a range in individual $\delta^{18}O$ values of 0.1 to 0.3‰ throughout the season at NCR (Figure 2a). Assuming that the most depleted values represent surface equilibrium, inferred habitat depths for individual *G. inflata* range from the surface to 75 m. A similar pattern is observed at SCR. Individual samples analysed from cup 7 (October) exhibit a range of 0.44‰, and a range of 0.88‰ is observed from cup 17 during February/March (Figure 2b). These results are consistent with a depth range for *G. inflata* of 0 to 75 m.

The weight averaged $\delta^{18}O$ values for *G. inflata* are within 0.3‰ of the pooled values at NCR and 0.5‰ at SCR. Larger offsets are observed during summer, reflecting the wider depth range of individual *G. inflata* at this time.

6.3.2 Comparison between pooled and individual $\delta^{13}C$

Individual $\delta^{13}C$ values for *G. bulloides* at NCR are generally centered over the pooled values, particularly in comparison to the weight averaged values (Figure 3). One individual from cup 3 is offset by 1.6‰, yet the weight averaged value is within 0.25‰ of the pooled value. The largest offset between the weight averaged and pooled value occurs in cup 12 (0.9‰). Weight averaged $\delta^{13}C$ values at SCR are within 0.1 - 0.3‰ of the pooled values. Individual *G. bulloides* from cup 7 have an overall $\delta^{13}C$ range of 1.8‰, yet there is a good correspondence between the pooled and weight averaged value (within 0.3‰). This implies that the pooled value may also be composed of individuals with a large $\delta^{13}C$ range. The $\delta^{13}C$ amplitude obtained from cup 7 is slightly larger than the seasonal amplitude across the whole record. As observed for the $\delta^{18}O$ values, the depleted $\delta^{13}C$ values obtained from this cup probably represent part of the remnant winter population.

Variability in individual *G. inflata* is minimal at both NCR and SCR. The weight averaged $\delta^{13}C$ values are within 0.25‰ of the pooled values (Figure 4). This small

variation reflects the relative consistency in the habitat depth for this species, as also seen from the $\delta^{18}O$ results.

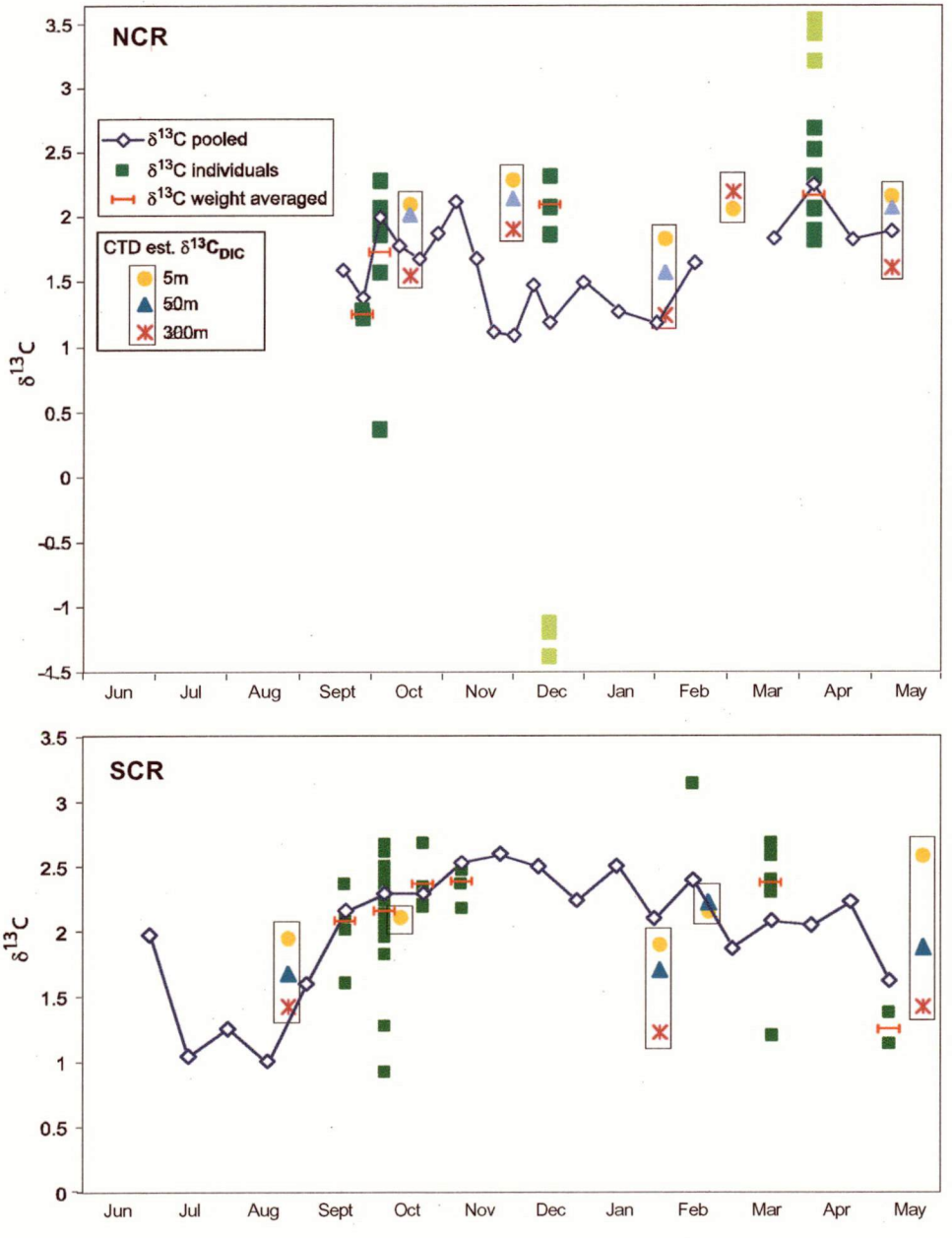

Figure 3: Individual and pooled $\delta^{13}C$ values for *G. bulloides* at NCR (A) and SCR (B). The red bars show the average $\delta^{13}C$ value for the pooled samples in each cup based on shell weight. Also shown are the equilibrium $\delta^{13}C$ values estimated from nutrient data in CTD casts. The pale squares represent poorly calibrated data. The broad spread of data points in SCR cup 7 towards more depleted values may represent individuals from the remnant winter population. There is generally a good correspondence between the weighted and pooled $\delta^{13}C$ values.

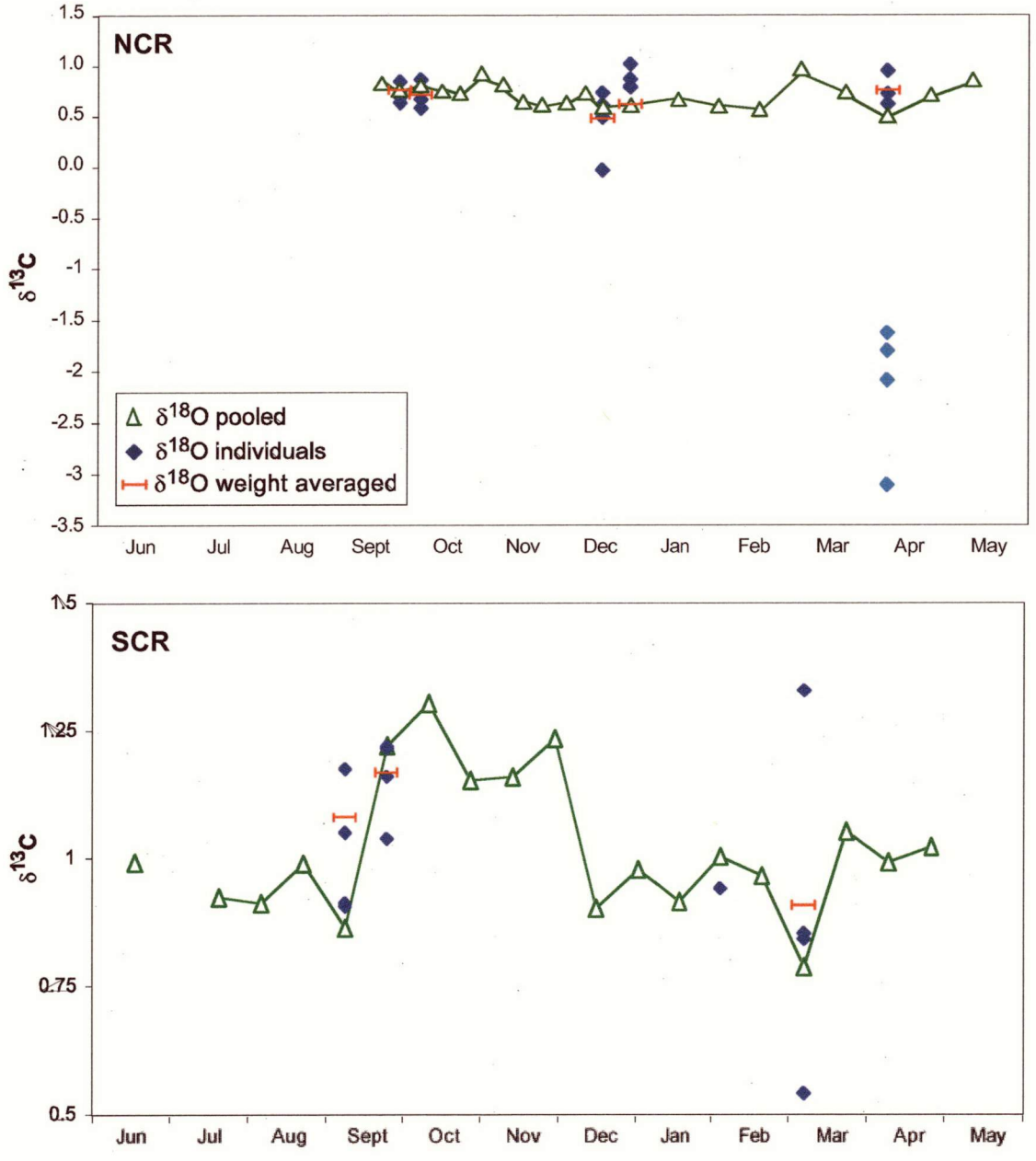

Figure 4: Individual and pooled $\delta^{13}C$ values for *G. inflata* at NCR (A) and SCR (B). The red bars show the average $\delta^{13}C$ value for the pooled samples in each cup based on shell weight. Also shown are the equilibrium $\delta^{13}C$ values estimated from nutrient data in CTD casts. The pale diamonds represent poorly calibrated data. The weighted $\delta^{13}C$ values from individual *G. inflata* are generally very close to the pooled measurements.

6.3.3 Summary of intraspecific variability

Comparison between the pooled and individual $\delta^{18}O$ and $\delta^{13}C$ values indicates that the intraspecific variability is relatively minor, particularly for *G. inflata*. Variability amongst individual samples is greater for *G. bulloides*, but generally within the disequilibrium range observed across the whole sediment trap data set for $\delta^{18}O$. Variations between individual samples may be explained by differences in depth between individuals, with the implied depth range well within the depth variability observed in Southern Ocean plankton tows (Mortyn and Charles, 2003). However, intraspecific variability may also reflect differences in disequilibrium due to size or morphological variations, as tested in the following sections.

6.3.4 Variations in isotopic composition with shell size

Variations in shell size have been cited as one of the many causes of $\delta^{18}O$ and $\delta^{13}C$ variability in *G. bulloides* (Curry and Matthews, 1981;Donner and Wefer, 1994;Oppo and Fairbanks, 1989;Spero and Lea, 1996). To assess the effect of size on isotopic variability in this study, 28 individual *G. bulloides* were analysed from cups 6 to 9 at SCR (Figure 5). Cups 6 to 9 exhibit little difference in pooled $\delta^{18}O$ (0.09‰) and $\delta^{13}C$ values (0.3‰) so variations in individual *G. bulloides* should reflect either changes in habitat depth or disequilibrium, possibly associated with changes in shell size.

Individual *G. bulloides* from these four cups range in length from 345 to 660μm. The isotopic variation in these samples is 1.25‰ for $\delta^{18}O$ and 1.8‰ for $\delta^{13}C$. Despite the large range in isotopic composition and size for these samples, there is no clear relationship between a specimens length and its $\delta^{18}O$ or $\delta^{13}C$ composition (Figure 5). The large isotopic range observed from cup 7 may also reflect the mixing of winter and spring populations as discussed earlier, but exclusion of these samples does not improve the relationship between size and $\delta^{18}O$ or $\delta^{13}C$.

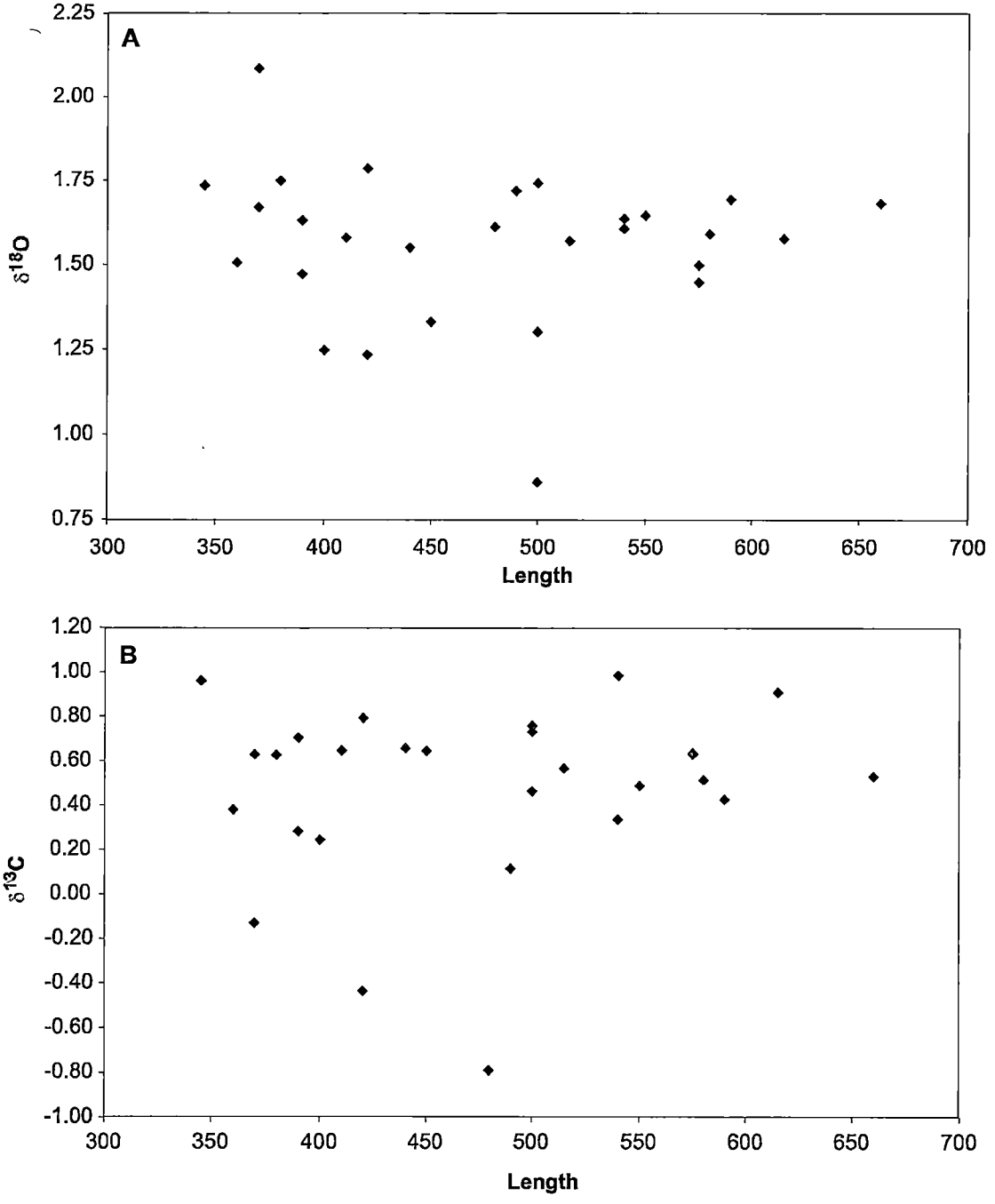

Figure 5: Individual *G. bulloides* $\delta^{18}O$ (A) and $\delta^{13}C$ (B) values plotted against length for cups 6 to 9 from SCR. There is no correlation between either $\delta^{18}O$ or $\delta^{13}C$ and size in this data set.

This result appears contrary to the many other studies which have demonstrated the strong influence of size on $\delta^{18}O$ and $\delta^{13}C$ disequilibrium. However, we have already limited size variability by only analysing foraminifera larger than 345 μm. *G. bulloides* grown under controlled laboratory conditions indicate that $\delta^{13}C$ disequilibrium is greatest in juvenile chambers (chambers 1 – 10) with little isotopic variation in the larger chambers, equivalent to shell sizes >300 μm (Spero and Lea, 1996). The analysis of individual *G. bulloides* from the >300 μm size fraction in the current study may therefore be above the limit for size-related disequilibrium effects. The $\delta^{18}O$ composition measured from individual chambers grown under laboratory conditions does, however, display a uniform decrease in $\delta^{18}O$ with increasing chamber position/shell size for shells up to ~441 μm (Spero and Lea, 1996). The results from this study do not support this trend, suggesting that there are other factors influencing intraspecific $\delta^{18}O$ and $\delta^{13}C$ variability at Chatham Rise.

6.3.5 Isotopic variability and changes in morphology

Morphological variations in *G. bulloides* have been suggested as a potential cause of isotopic disequilibrium (Sautter and Thunell, 1991; Darling et al., 2000; Bemis et al., 2002; Kucera and Darling, 2002; Bauch et al., 2003). Sediment traps from the San Pedro Basin collected two distinct morphotypes of *G. bulloides*: encrusted and normal forms (Sautter and Thunell, 1991). Encrusted *G. bulloides* at these sites were enriched in both $\delta^{18}O$ and $\delta^{13}C$ compared to the dominant normal form. Down-core records from the nearby Southern California Bight indicate a change from normal forms during interglacial periods to encrusted forms during cold glacial intervals, with an associated offset from the expected isotopic gradient (Bemis et al., 2002). Genetic analysis of normal and encrusted *G. bulloides* from the Southern California Bight region demonstrate that the two morphotypes represent genetically distinct populations (Kucera et al., 2001).

Morphotypic variation in *G. bulloides* is observed at the Chatham Rise sites. The encrusted form of this species is very compacted with a small aperture and thick shell (Plate 1), while the normal form is characterised by a large open aperture, inflated chambers and a fine texture (Plate 2). The encrusted form is common at SCR, but absent at NCR. At SCR both the encrusted and normal form of *G. bulloides* is present throughout the year, allowing comparisons between their isotopic composition. There are also some specimens which are heavily calcified, but in contrast to the true encrusted form have an open morphology. These are referred to as mixed morphotypes. In this section I combine SEM characterisation of the *G. bulloides* morphotypes with their

isotopic composition to test whether the morphotypic variations are associated with changes in $\delta^{18}O$ and $\delta^{13}C$ values at SCR.

The encrusted and mixed *G. bulloides* morphotype at SCR exhibits a slight enrichment in $\delta^{18}O$ compared to the normal form, but there is considerable overlap in cups 7 and 8 (Figure 6a). The greatest offset between these two forms occurs in cups 17 and 20, with the normal forms depleted by up to 0.8‰ compared to the encrusted form and by at least 0.7‰ compared to the corrected surface $\delta^{18}O$ equilibrium. The depleted $\delta^{18}O$ values for these specimens are consistent with equilibrium $\delta^{18}O$ at NCR, which suggests that these specimens may have been advected across the Subtropical Front from near the NCR site. If this is the case, then it implies that the encrustation of *G. bulloides* has little effect on its $\delta^{18}O$ composition at these sites. This conclusion is supported by the fact that, despite the difference in dominant morphotypes between NCR and SCR, pooled samples from both sites exhibit a similar offset in $\delta^{18}O$ relative to the Epstein equation (see Chapter 4). This would not be expected if morphotypic variations were causing $\delta^{18}O$ disequilibrium.

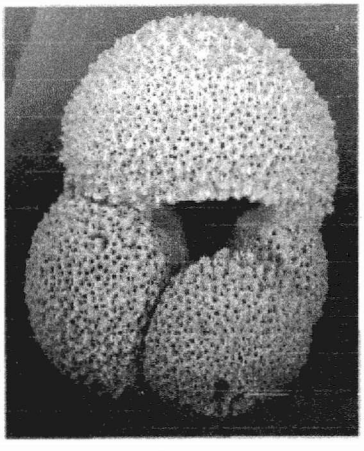

Plate 1: An example of the encrusted, compact *G. bulloides* morphotype at SCR. This specimen was collected in cup 8.

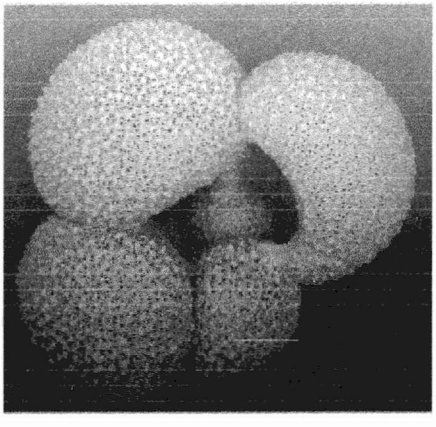

Plate 2: An example of the open, lightly calcified form of *G. bulloides* at SCR. This specimen is also from cup 8.

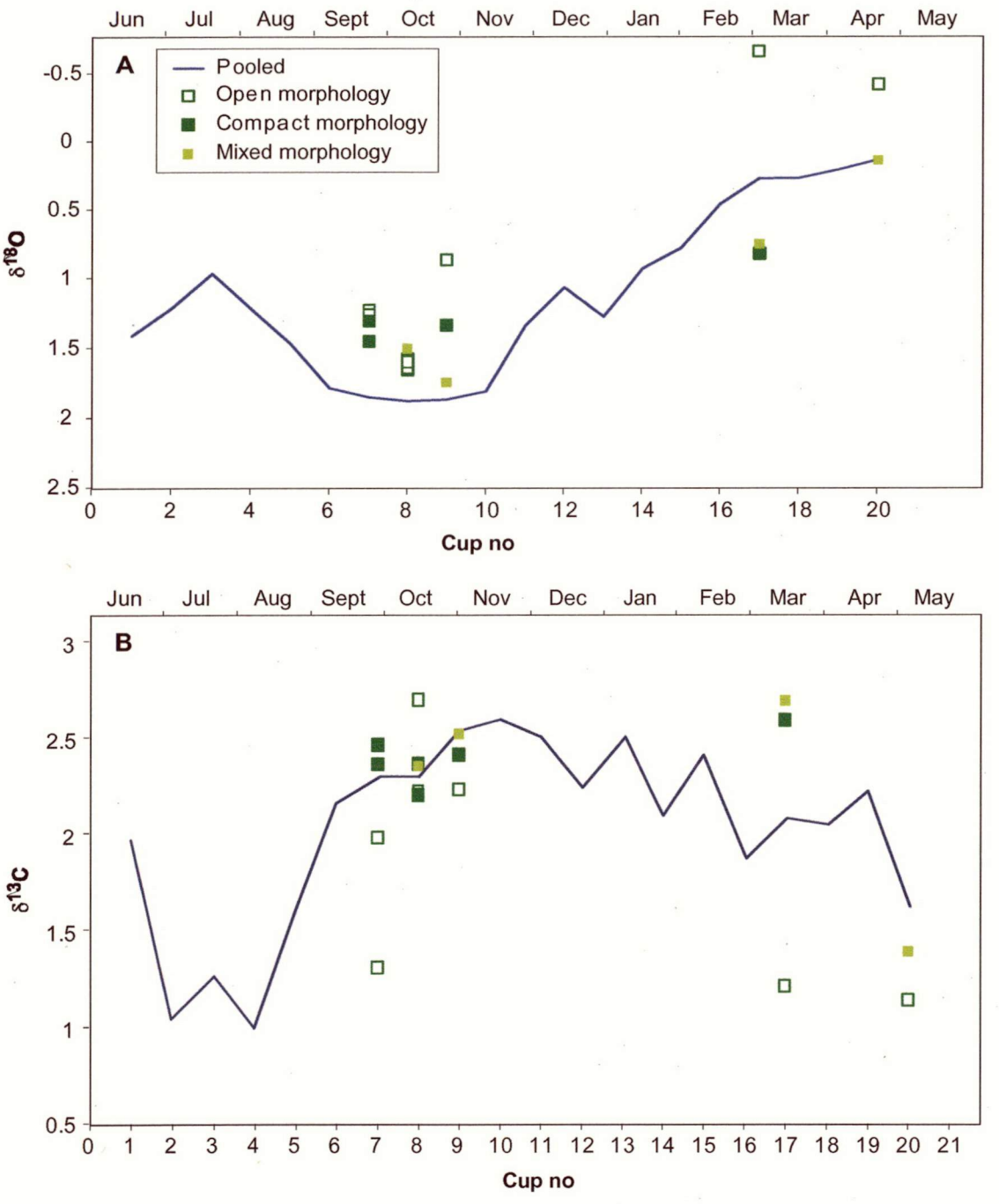

Figure 6: Morphotypes of *G. bulloides* are plotted with the pooled values (shown by the line) for $\delta^{18}O$ (A) and $\delta^{13}C$ (B). Two distinct morphotypes occur at SCR. An encrusted/compact form (large solid square) and an open form (open square). An intermediate form also occurs (small solid square). There is no consistent relationship between $\delta^{18}O$ or $\delta^{13}C$ values and morphotypic variation in *G. bulloides* for these samples.

The $\delta^{13}C$ composition of encrusted and mixed morphotypes of *G. bulloides* shows a slight tendency towards more enriched values relative to the normal form, however $\delta^{13}C$ values for both forms show considerable overlap in cup 8 (Figure 6b). Offsets between the encrusted and normal forms are again greatest for cup 17 and the $\delta^{13}C$ of the normal form in cup 17 is depleted relative to equilibrium, consistent with the $\delta^{18}O$ results. The offset from equilibrium at SCR for these 'normal' specimens further supports the suggestion that they may be sourced from north of Chatham Rise. The larger $\delta^{13}C$ range in cup 7 probably reflects mixing with the winter population, as already discussed.

6.3.6 Summary of results

The results from the analysis of individual *G. bulloides* and *G. inflata* from the Chatham Rise sediment traps indicates that intraspecific variability is most likely controlled by differences in depth between individuals. There is no relationship between isotopic variability and either changes in size or morphology, leaving advection between sites and depth variability as the most likely causes of intraspecific variability. Individual *G. bulloides* exhibit a depth range of 0 – 100 m and *G. inflata* a range of 0 - 75 m at these two sites.

6.4 Discussion

6.4.1 Seasonal signals from individual isotopic analysis

The primary objective in the analysis of individual foraminifera is to capture the seasonal amplitude in the isotopic record. As seen in Chapters 4 and 5, sedimentary isotopic records obtained from north and south of Chatham Rise are weighted towards the season of maximum production observed in the traps for each species. To properly interpret down-core records it is therefore necessary to determine the consistency of this seasonal weighting. One way in which this may be achieved is by comparison between the pooled isotopic values and the range in the individual analyses, assuming that the individuals reflect the seasonal isotopic range. In this study the intraspecific variability at any one time is small relative to the overall seasonal range, so individuals analysed in down-core records may capture the seasonal isotopic amplitude. However, a further constraint for obtaining a good seasonal record from individual analyses is that the species must be sufficiently productive throughout the year to be sampled across the season through random selection. Regions with very strong seasonal weighting in species fluxes will require the analysis of a greater number of specimens than in regions where production is spread more evenly across the seasons. In this section I compare the range in $\delta^{18}O$ from individual *G. bulloides* and *G. inflata* in Chatham Rise core tops (Bemis, 2000) to the

seasonal range observed in the sediment traps to assess how well individual analyses from this region capture the seasonal amplitude in $\delta^{18}O$.

Individual *G. bulloides* and *G. inflata* were analysed from core tops at sites R657 and W272 located north and south of Chatham Rise respectively (Bemis, 2000). At site R657 (NCR) the analysis of 7 *G. inflata* specimens yielded a $\delta^{18}O$ range of 0.48-1.12‰. This represents a 'seasonal' $\delta^{18}O$ amplitude of 0.66‰ at this site whereas the trap at NCR reveals a seasonal range for this species of 0.97‰. The range in 7 individual *G. inflata* at site W272 (SCR) was 0.38‰, much smaller than the seasonal range of 1.0‰ obtained from analysis of this species in the SCR sediment trap. At both SCR and NCR individual analysis of *G. inflata* underestimates the true seasonal amplitude which should be recorded by this species. The $\delta^{18}O$ amplitude obtained from W272 compares only to the range in individual values obtained at SCR from cups collected during September and October (cups 7 and 8), when flux of *G. inflata* is greatest. A larger sample size is required to capture the seasonal amplitude in *G. inflata* at these sites.

There were no individual analyses of *G. bulloides* from R657, but at W272 25 individual *G. bulloides* were analysed, yielding a $\delta^{18}O$ range of 0.58‰. This value is much lower than the seasonal range obtained from the SCR sediment trap (1.74‰ for *G. bulloides*). The individual *G. bulloides* analysed captures only the range observed within cups 7 and 8 in the sediment trap. These two cups represent 73% of the *G. bulloides* flux at this site, so it is not surprising that the individuals selected from the sedimentary record are representative of isotopic values during this interval. The small seasonal range obtained from core W272, despite the relatively large sample size, highlights the need for very large sample sizes in order to capture the full seasonal range from individual analyses.

The difficulty of capturing the seasonal range in $\delta^{18}O$ is exacerbated by the relatively large shell size required for the analysis of individual foraminifera. Current techniques require specimens of at least 10μg, or size fractions generally >355 μm for *G. bulloides*. At Chatham Rise, shell production in this larger size fraction is highly seasonal. At SCR, fractions >355μm were collected only during September and October, and even fluxes in the 250-355μm size fraction are mainly restricted to the period between September and November. At NCR, specimens >355μm were found only during January, with one specimen >355μm also counted from the May cup. On the basis of these flux patterns to the sediment traps, it may not be possible to obtain the seasonal isotopic range from analysis of individual *G. bulloides* in these regions.

Individual *G. inflata* provide greater opportunity for obtaining a seasonal isotopic signal. This species tends to have greater mass/size than *G. bulloides*, so specimens from the 250-355μm fraction may provide enough calcite to be analysed individually. At NCR, the >355μm size fraction was present during September, October, December, March and April, however, fluxes during January and February were low in all size fractions. The >355μm size fraction was present in the sediment trap at SCR during September to November, with low fluxes in the 250-355μm size fraction throughout the remainder of the record. The underestimation of the seasonal $\delta^{18}O$ range from core top *G. inflata*, despite its presence throughout the record at SCR, highlights the need for much larger sample sizes and possibly smaller size fractions in the analysis of individual foraminifera.

6.5 Conclusions

Analysis of individual *G. bulloides* and *G. inflata* from the Chatham Rise traps indicates that intraspecific variability is small relative to the seasonal range in $\delta^{18}O$ and $\delta^{13}C$ for these two species. Variations in $\delta^{18}O$ and $\delta^{13}C$ for *G. bulloides* show no correlation to changes in size or morphology, so it is likely that the isotopic range for this species reflects advection of specimens from north of the Subtropical Front and differences in habitat depth. The $\delta^{18}O$ range for *G. bulloides* is equivalent to depths ranging between 0 and100 m, while *G. inflata* is inferred to have a depth range of 0 - 75 m. Analysis of individual *G. bulloides* and *G. inflata* in Chatham Rise core tops (Bemis, 2000) yields a small range in $\delta^{18}O$ values compared to the seasonal amplitude. This confirms the strong seasonal weighting preserved in these core top sediments, as observed from the sediment trap deployment. The seasonal weighting of isotopic records therefore needs to be considered in the interpretation of individual as well as pooled foraminiferal samples.

6.6 References

Bauch, D., Darling, K., Simstich, J., Bauch, H.A., Eriendeuser H. and Kroon, D., 2003. Palaeoceanographic implications of genetic variation in living North Atlantic *Neogloboquadrina pachyderma*, Nature, 424: 299-302.

Bemis, B.E., 2000. Controls on the Oxygen and Carbon Isotopic Composition of Planktonic Foraminifera: Implications for Paleoceanographic Reconstructions.University of California, Davis.

Bemis, B.E., Spero, H.J., and Thunell, R.C., 2002. Using species-specific paleotemperature equations with foraminifera: A case study in the Southern California Bight. Marine Micropaleontology, 46: 405-430.

Curry, W.B. and Matthews, R.K., 1981. Equilibrium ^{18}O fractionation in small size fraction planktic foraminifera: evidence from Recent Indian Ocean sediments. Marine Micropaleontology, 6: 327-337.

Darling, K.F., Wade, C.M., Stewart, I.A., Kroon, D., Dingle, R. and Brown, A.J.L., Molecular evidence for genetic mixing of Artic and Antarctic subpolar populations of planktonic foraminifers, *Nature*, 405, 43-47, 2000.

Donner, B. and Wefer, G., 1994. Flux and stable isotope composition of *Neogloboquadrina pachyderma* and other planktonic foraminifers in the Southern Ocean (Atlantic sector). Deep-Sea Research I, 41: 1733-1743.

Epstein, S., Buchsbaum, R., Lowenstam, H.A., and Urey, H.C., 1953. Revised carbonate-water isotopic temperature scale. Geological Society of America Bulletin, 64: 1315-1326.

Kucera, M. and Darling, K.F., Cryptic species of planktonic foraminifera: their effect on palaeoceanographic reconstructions, *Philosophical Transactions of the Royal Society of London Series a-Mathematical Physical and Engineering Sciences,* 360(1793), 695-718, 2002.

Kucera, M., Darling, K. Wade, C., von Langen, P. and Pak, D., 2001. Seasonal dynamics of cryptic species of planktonic foraminifera in Santa Barbara Channel during 1999. 7th International Conference on Paleoceanography, Sapporo, Japan.

Mortyn, G.P. and Charles, C.D., 2003. Planktonic foraminiferal depth habitat and $\delta^{18}O$ calibrations: Plankton tow results from the Atlantic sector of the Southern Ocean. Paleoceanography, 18(2, 1037): doi: 10.1029/2001PA000637.

Oppo, D.W. and Fairbanks, R.G., 1989. Carbon isotope composition of tropical surface water during the past 22,000 years. Paleoceanography, 4: 333-351.

Sautter, L.R. and Thunell, R.C., 1991. Seasonal variability in the δ18O and $\delta^{13}C$ of planktonic foraminifera from an upwelling environment: Sediment trap results from

the San Pedro Basin, Southern California Bight. Paleoceanography, 6(3): 307-334.
Spero, H.J. and Lea, D.W., 1996. Experimental determination of stable isotope variability in *Globigerina bulloides*: implications for paleoceanographic reconstructions. Marine Micropaleontology, 28: 231-246.

CHAPTER 7

CONCLUSIONS

The farther back you can look, the farther forward you are likely to see

Winston Churchill

7.1 Introduction

The Southern Ocean plays an important role in the global climate system, providing a link between each of the major ocean basins through the circulation of deep water masses. The significance of this region during climatic cycles of the Pleistocene is also highlighted by evidence for the glacial draw down of atmospheric CO_2 (Knox and McElroy, 1984). Planktonic foraminifera form a key component in many reconstructions of past Southern Ocean climate and oceanographic variability (eg. Charles and Fairbanks, 1990; Charles and Fairbanks, 1992; Howard and Prell, 1992; Labeyrie et al., 1996; Hodell et al., 2000). The composition of foraminiferal shells provides a record of surface water chemistry, while changes in species abundances can provide information about the movement of surface water masses, and therefore variations in temperature. Comparisons between foraminiferal and other biotic and chemical tracers, however, are at times contradictory (compare Howard and Prell, 1994; Howard and Prell, 1992; Charles et al., 1991; Charles and Fairbanks, 1990; Rosenthal et al., 2000; Rosenthal et al., 1995; Kumar et al., 1995; Elderfield and Rickaby, 2000). Inconsistencies between different proxies highlight the need for better calibration of climatic tracers in the Southern Ocean. The goal of this study has therefore been to establish the utility of planktonic foraminifera as tracers of climatic and chemical change in the surface waters of the Southern Ocean. In this section I summarise the results from this thesis, and test their application to a down-core record before providing some suggestions for future research.

7.2 Biotic estimates of sea-surface temperature

Various temperature equations have been developed to derive estimates of sea-surface temperature (SST) change from foraminiferal assemblages. In this study I assessed the accuracy of one commonly employed technique, the Modern Analog Technique (MAT). Techniques such as the MAT rely on the assumption that the core top sediments represent modern foraminiferal production, and furthermore, that these assemblages can

be associated with modern climatic conditions, and in particular temperature. The utility of the MAT was tested in this study by first establishing the similarity between the core top sediments and the modern biota with use of the dissimilarity index. The comparison between the trap assemblages and nearby core tops indicated a low dissimilarity (0.04 to 0.17) at all sites apart from 54°S. The close similarity between the core top and sediment trap assemblages highlights the stability of seasonal cycles during the Holocene. The higher dissimilarities (0.16 to 0.6) between the trap and core top assemblages from the Polar Frontal region reveals the need for better core top analogues from this region. The higher dissimilarities may also reflect dissolution of the core top material, however core tops in this study showed little fragmentation, suggesting good preservation.

The association between foraminiferal assemblages and modern observed climatic conditions was tested by comparing estimated MAT temperatures to observed AVHRR (1999) temperatures at each trap site. This comparison revealed the consistency of the MAT over a wide range of environments. At the Chatham Rise traps the MAT captured the seasonal range in observed temperatures, with estimates within 2.7°C of the observed temperature at NCR and 1.3°C at SCR. These offsets from observation are well within the standard deviation derived from the 10 closest analogue sites. For the remaining trap deployments SST estimates were within 1.2°C at 47°S (1997 deployment) and 2.2°C (1998 deployment), 2.9°C at 51°S, and 4.5°C at 54°S. The 54°S site is the only site at which the offset between the MAT estimate and the observed temperature is larger than the standard deviation of the estimate. This again reflects the lack of good analogue sites in the core top data base for Polar Frontal environments.

7.3 Implications of seasonal cycles in foraminiferal production

The sediment trap deployments also provided the opportunity to establish seasonal variations in foraminiferal fluxes and the implications for our interpretation of sedimentary records. A distinct seasonal succession of species was observed at each site. *G. bulloides* exhibited highest productivity during spring to early summer, while *N. pachyderma* (s. and d.) tended to be most productive during summer to autumn. Consistent seasonal flux patterns between each site were closely associated with seasonal changes in surface water stratification and food availability. Despite consistency in the timing of species production patterns between the sites, relative abundances of species varied markedly. The overall foraminiferal assemblage can be more closely associated with changes in parameters such as temperature.

The seasonality of foraminiferal flux and their preferred habitat depth has important implications for interpretation of isotopic records. To determine the preservation of the seasonal flux signal in sedimentary records, the flux data from the sediment traps was combined with the isotopic records to derive a flux-weighted isotopic value. This value was compared to the isotopic value obtained from nearby core top sediments. Comparison between the $\delta^{18}O$ composition of the core tops and the flux-weighted values from the sediment traps indicated the strength of the seasonal signal in the core tops, particularly for *G. bulloides* and *G. inflata* once habitat depth was accounted for. The sediment trap deployments therefore captured seasonal production patterns as recorded by the core tops.

The dominant seasonal production patterns are consistent between each site for *G. bulloides*, *G. inflata* and *N. pachyderma* (s.), however, slight differences in the overall fluxes between sites impact on the flux-weighted isotopic values. As a result, the latitudinal gradient in $\delta^{18}O$ values between each site is not always consistent with the latitudinal gradient in $\delta^{18}O$ observed during any one season. At SCR, for instance, over 80% of the flux for *G. bulloides* occurs during September and October, while at the other sites, flux is also high during summer, despite the spring flux remaining dominant. This variation in flux pattern at SCR results in a steep latitudinal gradient in $\delta^{18}O$ north and south of this site.

These results highlight the importance of capturing seasonal flux patterns before interpreting isotopic records. One way in which this has been attempted is through the analysis of individual foraminifera. Individual foraminifera analysed from SCR and NCR reveal the influence of habitat depth variations on intraspecific variability, although the range in isotopic values are generally considerably smaller than the seasonal range in $\delta^{18}O$ at these sites. The difficulty of capturing the seasonal signal from individual foraminifera in sedimentary records is the need for large number of individuals to capture the seasonal range at sites with strong seasonal flux patterns. Analysis of 25 individual *G. bulloides* from core top sediments in the SCR region (Bemis, 2000) yielded a range in $\delta^{18}O$ equivalent only to the intraspecies variability observed within one sediment trap cup. It will therefore be difficult to obtain seasonal information from analysis of individual foraminifera at these sites.

The seasonal $\delta^{18}O$ range may be obtained by comparison between $\delta^{18}O$ values recorded by species with distinct seasonal fluxes. *G. bulloides* and *N. pachyderma* (s.) have

largely distinct fluxes, during spring and summer respectively. The seasonal amplitude recorded between these species, however, is dampened by minor fluxes throughout the year. The $\delta^{18}O$ contrast between these species only partly captures the seasonal amplitude at these sites.

7.4 Application of foraminiferal isotopic records

The $\delta^{18}O$ record from foraminifera provides an important tracer of both temperature and salinity. There are a large array of temperature equations which are applied to the interpretation of foraminiferal records and a key aim of this thesis was to determine the validity of these equations in Southern Ocean environments. The results from this study indicate that the equation of Epstein et al. (1953) provides the greatest consistency across all sites, with constant offsets from equilibrium. Each of the other equations examined display inconsistent offsets from equilibrium. Using the Epstein equation, we can apply an offset of -0.37‰ to the $\delta^{18}O$ values for *G. bulloides*, yielding an accuracy of ±0.28‰ compared to equilibrium. For *N. pachyderma* (s.), $\delta^{18}O$ values are offset from equilibrium by -0.50±0.28‰.

Comparison between the equilibrium $\delta^{18}O$ values and the $\delta^{18}O$ for each species through the season can be used to constrain the habitat depth for these species. *G. bulloides* and *N. pachyderma* (s.) both tend to inhabit near-surface waters, while *G. inflata* dwells at depth (~50 m). The habitat depth for *G. bulloides* and *N. pachyderma* (s.) may be associated with the relatively shallow depth of the chlorophyll maximum in these regions. The contrast between the $\delta^{18}O$ content of *G. bulloides* and *G. inflata* in core tops sediments reflects the difference in their depth, providing a record of thermal stratification during spring to early summer.

In this study we tested the utility of foraminiferal $\delta^{13}C$ as a nutrient tracer in Southern Ocean environments. The interpretation of *G. bulloides* $\delta^{13}C$ records is hampered by strong disequilibrium in this species, with disequilibrium also observed for *N. pachyderma* (s.) and *G. inflata*. Disequilibrium is most extreme at lower latitudes, with offsets of up to 3.1‰ observed for *G. bulloides*. The latitudinal trend in disequilibrium results in a sharp contrast between foraminiferal $\delta^{13}C$ records and $\delta^{13}C$ of dissolved inorganic carbon (DIC). The foraminifera record a north to south increase in $\delta^{13}C$, whereas the $\delta^{13}C_{DIC}$ decreases across the sites. The interpretation of foraminiferal $\delta^{13}C$ records will therefore be misleading if disequilibrium effects are not taken into account.

Disequilibrium in $\delta^{13}C$ for *G. bulloides* is most strongly influenced by temperature, revealing a relationship consistent to the laboratory correction determined by Bemis et al. (2000). *G. inflata* and *N. pachyderma* (s.) also exhibit disequilibrium which may be accounted for by variations in temperature and $[CO_3^{2-}]$, however, separation of these effects requires culturing under controlled laboratory conditions.

Comparison between the core top and flux-weighted sediment trap $\delta^{13}C$ values reveals a $\delta^{13}C$ depletion in the traps relative to the core tops. This relative depletion is greatest for *G. bulloides* for sites within the Subantarctic Zone, with *G. inflata* also displaying consistently depleted values in this region. The modern depletion in $\delta^{13}C$ reflects the oceanic uptake of anthropogenic CO_2 from the atmosphere. The atmospheric $\delta^{13}C$ content has decreased by ~1.5‰ since the industrial revolution due to the release of isotopically light carbon from the burning of fossil fuels and tropical forests. The SAZ region has been previously determined as a strong sink for atmospheric CO_2, and the results from this study highlight the importance of the region for CO_2 uptake. *G. bulloides* displays a depletion of up to 0.66‰. This indicates substantial equilibration between the atmosphere and surface ocean within the SAZ. Since the SAZ region is a zone of very deep winter mixing (to depths >400 m), it is likely that the CO_2 is sequestered to depth. $\delta^{13}C$ depletion in *G. inflata* confirms that the anthropogenic signature is recorded to depths of at least 50 m. The results from this study highlight the important control that this zone has on the atmospheric CO_2 balance.

7.5 Application to a down-core record

In this section I apply the results from the sediment traps to the interpretation of the isotopic and faunal SST records from core RC11-120 in the Southern Indian Ocean. This core is located just south of the STF (at 43°31'S), and provides a climatic history from the present to almost 300 ka. Isotopic data from this core are obtained from Shackleton and Pisias (1985) using *G. bulloides* in the 355 - 425μm size fraction. SST data is derived from a radiolarian transfer function (Hays et al., 1976) which is consistent with foraminiferal based estimates during isotope stages 6-5 (Howard and Prell, 1984). The timing of oxygen isotope stages has been determined based on the time scale of Imbrie et al. (1984).

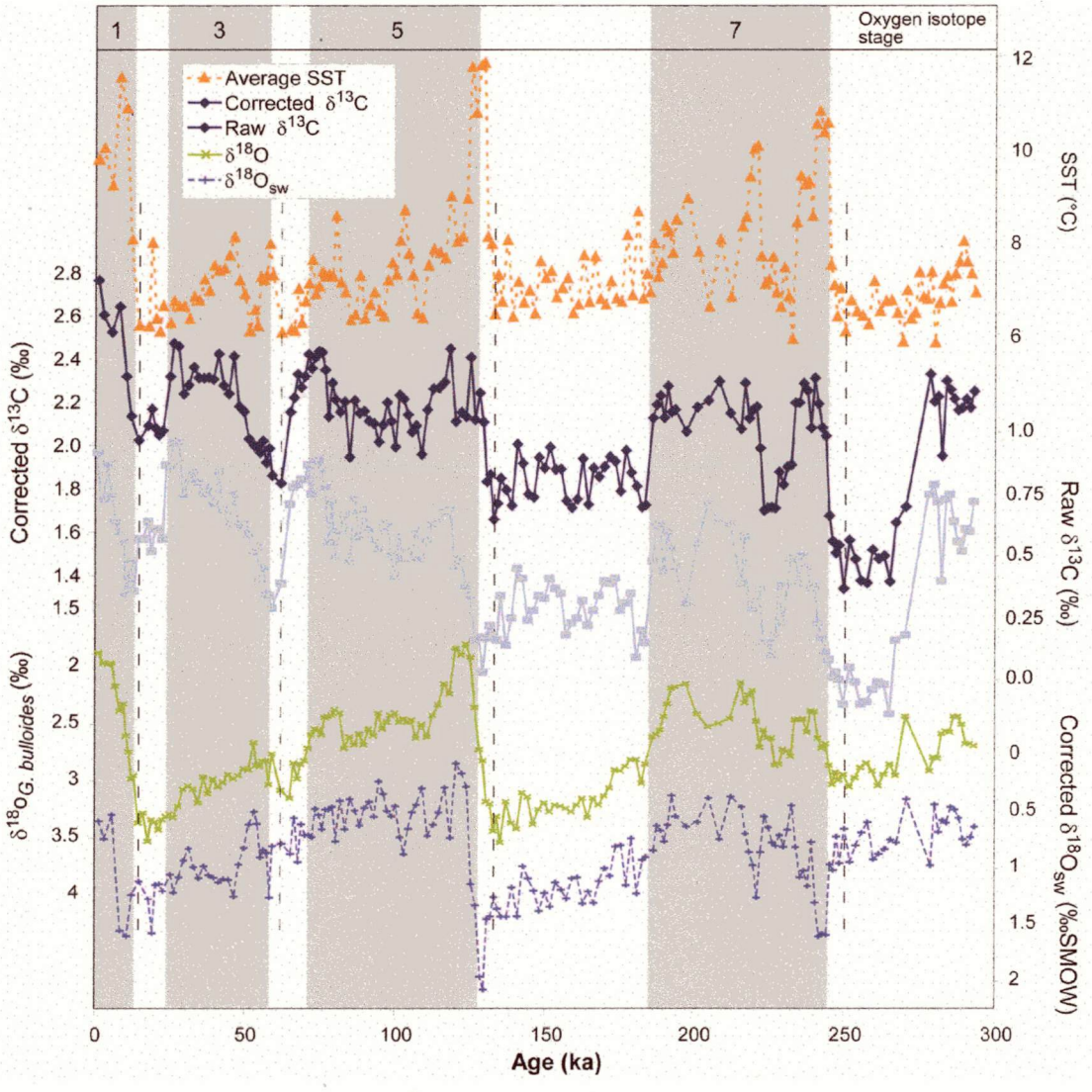

Figure 1: Sea-surface temperature and the *G. bulloides* isotopic records from RC11-120 in the Southern Indian Ocean. New estimates of $\delta^{13}C$ and $\delta^{18}O_{sw}$ have been obtained by applying the appropriate disequilibrium offsets and accounting for the spring flux signal in *G. bulloides* as determined from the sediment traps. The summer and winter radiolarian SST estimates have been averaged to obtain the 'spring' signal. Changes in SST and the corrected $\delta^{13}C$ records occur ~4-5 kyr prior to the retreat of Northern Hemisphere ice sheets, as indicated by the estimated $\delta^{18}O_{sw}$. Isotopic data are from Shackleton and Pisias (1985), SST data are from a radiolarian transfer function (Hay et al., 1976) and the time scale is based on Imbrie et al. (1984).

The sediment trap results indicate that *G. bulloides* productivity is strongly weighted towards spring, and that isotopic values are similarly weighted towards these spring values. I have therefore calculated an average value from the summer and winter radiolarian SST estimates to better capture temperature conditions during spring (Figure 1). These 'spring' temperature estimates agree well with the *G. bulloides* Mg/Ca temperature estimates also obtained from this core (Mashiotta et al., 1999). The maximum Holocene temperature from the Mg/Ca results is ~12.85°C, while the average radiolarian SST estimate is 11.55°C. The minimum LGM values are ~6.8° and 6.1°C for the Mg/Ca and average radiolarian estimates respectively. The close correspondence between these two independent sets of SST estimates reveals the consistency of *G. bulloides* spring production down the core, with the result that both the Mg/Ca values and the isotopic values are weighted towards conditions during spring.

The interpretation of planktonic foraminiferal $\delta^{18}O$ records is hampered in down-core records by the uncertainty in separating the effects due to changes in temperature and the isotopic composition of sea water. Changes in the $\delta^{18}O$ of sea water ($\delta^{18}O_{sw}$) largely reflect the growth and retreat of Northern Hemisphere ice sheets on glacial-interglacial timescales. Deep-sea benthic $\delta^{18}O$ and sea-level records suggest that the glacial $\delta^{18}O_{sw}$ was enriched by 1.1 to 1.3‰ relative to the Holocene (Chappell and Shackleton, 1986; Shackleton and Opdyke, 1973; Fairbanks, 1989), but variations within each cycle and the timing of events are more difficult to determine. The temperature calibration for *G. bulloides* $\delta^{18}O$ obtained from the sediment traps in this study allows a new estimate of the temperature component contained within the $\delta^{18}O_{G\ bulloides}$ record, and therefore an estimate of the $\delta^{18}O_{sw}$.

The temperature equation of Epstein et al. (1953) is applied to the $\delta^{18}O_{G\ bulloides}$ record with an offset of 0.37‰ to obtain an estimate of the temperature component contained within the RC11-120 record. This value is subtracted from the original $\delta^{18}O_{G\ bulloides}$ value to obtain an estimate of $\delta^{18}O_{sw}$ (‰SMOW). The resulting $\delta^{18}O_{sw}$ indicates relatively large changes in the sea water composition on glacial-interglacial timescales, with the highest amplitude recorded across the Stage 6/5 transition (2‰) (Figure 1). The maximum amplitude between the LGM and Holocene is 1.1‰. This value is slightly higher than the maximum estimate based on the Mg/Ca record (~1.0‰) (Mashiotta et al., 1999), and consistent with estimates based on benthic $\delta^{18}O$ records (Chappell and Shackleton, 1986; Fairbanks, 1989; Shackleton and Opdyke, 1973). Previous comparison between biotic and isotopic temperatures from Southern Ocean cores have

conflicted due to the relatively low amplitude of the planktonic $\delta^{18}O$ record, which does not allow for the temperature change recorded by the biota (Howard and Prell, 1992; Charles and Fairbanks, 1990). By accounting for the appropriate seasonal weighting in the $\delta^{18}O$ record the isotopic record at RC11-120 allows for the magnitude of the biotic and Mg/Ca temperature estimates from this site as well as the glacial-interglacial change in ice volume.

The timing of climatic events in the Southern Ocean can be determined by comparison between the temperature and $\delta^{18}O_{sw}$ records. Several studies indicate that changes in Southern Ocean climate lead changes in the volume of Northern Hemisphere ice sheets by several thousand years (Howard and Prell, 1992; Hays et al., 1976; Charles et al., 1996; Mashiotta et al., 1999). The comparison between the radiolarian SST record and the estimated $\delta^{18}O_{sw}$ is consistent with these earlier results, revealing the warming of the surface ocean ~4-5 kyr prior to the melting of Northern Hemisphere ice sheets.

The $\delta^{13}C$ record obtained from *G. bulloides* in the sediment traps proved to be an effective proxy for productivity, and hence changes in the concentration of atmospheric CO_2. This study also revealed that the offset between the $\delta^{13}C$ composition of *G. bulloides* and equilibrium at these Southern Ocean sites can be accounted for by the temperature correction of Bemis et al. (2000). I therefore provide corrected $\delta^{13}C$ values for RC11-120 by applying the Bemis et al. (2000) temperature equation. The corrected $\delta^{13}C$ record from *G. bulloides* reveals distinct changes across the glacial-interglacial boundaries, with slightly larger amplitude than for the uncorrected values (Figure 1). The major change in the corrected $\delta^{13}C$ values, however, is in the timing of these transitions. The corrected $\delta^{13}C$ values imply that the timing of $\delta^{13}C$ changes correspond to major transitions in temperature at this site. The uncorrected $\delta^{13}C$ record, by contrast, suggests that the $\delta^{13}C$ of surface waters lags major changes in SST by 3-4 kyr. The close correspondence between the corrected $\delta^{13}C$ and SST records reflects the close coupling between temperature and atmospheric CO_2 as also observed in the Vostok ice core (Barnola et al., 1987).

This revised record supports the opinion that the warming of Southern Ocean surface waters and the decrease in surface water productivity (and increase in CO_2) occurs several thousand years prior to the retreat of polar ice sheets (Howard and Prell, 1992; Hays et al., 1976; Charles et al., 1996; Mashiotta et al., 1999). This conclusion confirms the key role of the Southern Ocean in global climate change and also provides a

timeframe for the mechanisms which may drive the collapse of Northern Hemisphere ice sheets.

7.6 Future directions for research

This study has highlighted several areas which would benefit from further research. The analysis of modern foraminiferal fluxes and isotopic composition in this study has provided important constraints for interpretation of down-core sediments, but their application would be strengthened by additional Southern Ocean sediment trap studies. The results from this study mark the first detailed analysis of planktonic foraminifera from Southern Ocean sediment traps across Subtropical to Polar Frontal environments. Further sediment trap studies in other sectors of the Southern Ocean would help to better calibrate the relationships between foraminiferal proxies and sea-surface conditions.

Interpretation of down-core isotopic records requires a knowledge of each species season of maximum production and its preferred habitat depth. These preferences may vary between regions, so additional data sets from other sectors of the Southern Ocean would help to better constrain seasonal flux patterns and their driving mechanisms. Changes in seasonal flux patterns may affect the reliability of the MAT, so it is important to continue calibrations of this and other transfer functions. Future calibration of the MAT would benefit greatly from a larger Southern Ocean core top data base, particularly the addition of sites south of the Polar Front.

The deployment of multiple depth stratified plankton tow nets in Southern Ocean transects would provide a much better constraint on habitat depth for each species, therefore allowing a better calibration of the $\delta^{18}O$ and $\delta^{13}C$ records. No such studies have been conducted in the Southern Ocean so far.

This study has shown the significant gains which can be made through the application of laboratory calibrations to field data. Further field testing of laboratory isotopic calibrations would help to better define disequilibrium effects and variations between regions. The analysis of $\delta^{13}C$ disequilibrium in *N. pachyderma* (s.) and *G. inflata* reveal possible associations to both temperature and the carbonate ion concentration of the sea water. Both of these species are commonly used in down-core records, yet this data set reveals significant offsets from equilibrium. Valuable information about disequilibrium effects in these two species could be obtained from laboratory cultures.

The isotopic data from this study reveal some significant differences to laboratory-derived relationships. These differences may reflect the calibration of the laboratory relationships to slightly warmer conditions, or they may be due to genotypic variability between the Southern Ocean and laboratory foraminifera. These possibilities could be investigated by culturing foraminifera over a cooler temperature range, by culturing Southern Ocean foraminifera, and by collecting foraminifera for genetic analysis.

Additional insights in our interpretation of Southern Hemisphere paleoclimate have been gained through the application of the results from this sediment trap study to the down-core record at RC11-120. Knowledge of the seasonal distribution of *G. bulloides* and of its isotopic temperature calibration allowed a better estimate of the temperature component contained within the down-core $\delta^{18}O$ record, and therefore a better estimate of the $\delta^{18}O_{sw}$. The application of appropriate disequilibrium corrections to the $\delta^{13}C$ record also provided a new interpretation of the sequence of events across glacial-interglacial cycles in this core. Future studies of down-core records from the Southern Ocean may also benefit from the application of these sediment trap results.

A weakness of this study was the lack of well-dated core tops which could provide a better constraint on estimates of the oceanic Suess effect. The selection of core tops was restricted according to their similarity to modern oxygen isotopic composition, and this approach was mostly successful in providing core tops with a negative $\delta^{13}C$ content attributable to the Suess effect. A better estimate of the Suess effect could be obtained by using radiocarbon dated core tops. The relatively high magnitude of the Suess effect determined from the sediment trap and core top isotopes highlights the potential success of this technique for determining the uptake of anthropogenic CO_2 in the Southern Ocean over the entire time span since the industrial revolution. Once we have a better constrain on these estimates we will be able to better predict the ongoing role of the Southern Ocean in the global carbon cycle.

7.7 Conclusion

This study set out to test some of the commonly used techniques in the interpretation of paleoclimate records from planktonic foraminifera. The results from the analysis of sediment trap material confirms the array of environmental information that can be captured from both biotic and geochemical techniques in modern environments. The distribution of foraminiferal faunas relate well to distributions in a global core top data base, allowing the estimation of sea-surface temperatures from assemblage data. Oxygen

isotopic records also provide valid estimates of temperature, with a slight but constant offset from the Epstein et al. (1953) equation. The carbon isotopic records closely reflect changes in productivity in this region, and disequilibrium effects can be corrected with the temperature relationship of Bemis et al. (2000). Isotopic records are strongly weighted towards the season of maximum production for each species, so it is important to determine seasonal flux patterns. Application of these biotic and isotopic relationships to down-core records should provide new insights into Southern Ocean paleoclimate variability.

7.8 References

AVHRR, Advanced Very High Resolution Radiometer. 1999. AVHRR sea surface temperature data. NOAA/NASA.

Barnola, J. M.; Raynaud, D.; Korotkevich, Y. S., and Lorius, C. 1987. Vostok ice core provides 160,000-year record of atmospheric CO2. Nature, 329: 408-414.

Bemis, B.E., 2000. Controls on the Oxygen and Carbon Isotopic Composition of Planktonic Foraminifera: Implication for Paleoceanographic Reconstructions. Ph.D. Thesis, University of California, Davis.

Bemis, B.E., Spero, H.J., Lea, D.W., and Bijma, J., 2000. Temperature influence on the carbon isotopic composition of *Globigerina bulloides* and *Orbulina Universa* (planktonic foraminifera). Marine Micropaleontology, 38: 213-228.

Chappell, J. and Shackleton, N.J., 1986. Oxygen isotopes and sea level. Nature, 324: 137-140.

Charles, C.D. and Fairbanks, R.G., 1990. Glacial to interglacial changes in the isotopic gradients of Southern Ocean surface water. In: U. Bleil and J. Thiede (Editors), Geological History of the Polar Oceans: Arctic Versus Antarctic. Kluwer, Boston, Mass., pp. 519-538.

Charles, C.D. and Fairbanks, R.G., 1992. Evidence from Southern Ocean sediments for the effect of North Atlantic deep-water flux on climate. Nature, 355: 416-419.

Charles, C.D., Froelich, P.N., Zibello, M.A., Mortlock, R.A., and Morley, J.J., 1991. Biogenic opal in Southern Ocean sediments over the last 450,000 years: Implications for surface water chemistry and circulation. Paleoceanography, 6: 697-728.

Charles, C.D., Lynch-Stieglitz, J., Ninnemann, U.S., and Fairbanks, R.G., 1996. Climate connections between the hemispheres revealed by deep sea sediment core/ice core correlations. Earth and Planetary Science Letters, 142: 19-27.

Elderfield, H. and Rickaby, R.E.M., 2000. Oceanic Cd/P ratio and nutrient utilization in the glacial Southern Ocean. Nature, 405: 305-310.

Epstein, S., Buchsbaum, R., Lowenstam, H.A., and Urey, H.C., 1953. Revised carbonate-water isotopic temperature scale. Geological Society of America Bulletin, 64: 1315-1326.

Fairbanks, R.G., 1989. A 17000 year glacio-eustatic sea level record: Influence of glacial melting rates on the Younger Dryas event and deep ocean circulation. Nature, 342: 637-642.

Hays, J.D., Imbrie, J., and Shackleton, N.J., 1976. Variations in the Earth's orbit: Pacemaker of the ice ages. Science, 194: 1121-1132.

Hodell, D.A., Charles, C.D., and Ninnemann, U.S., 2000. Comparison of interglacial

stages in the South Atlantic sector of the southern ocean for the past 450 kyr: implications for Marine Isotope Stage (MIS) 11. Global and Planetary Change, 24(1): 7-26.

Howard, W.R. and Prell, W.L., 1984. A comparison of radiolarian and foraminiferal paleoecology in the Southern Indian Ocean: New evidence for the interhemispheric timing of climatic change. Quaternary Research, 21: 244-263.

Howard, W.R. and Prell, W.L., 1992. Late Quaternary surface circulation of the Southern Indian Ocean and its relationship to orbital variations. Paleoceanography, 7: 79-118.

Howard, W.R. and Prell, W.L., 1994. Late Quaternary carbonate production and preservation in the Southern Ocean: Implications for oceanic and atmospheric carbon cycling. Paleoceanography, 9: 453-482.

Imbrie, J., Hays, J.D., Martinson, D.G., McIntyre, A., Mix, A.C., Morley, J.J., Pisias, N.G., Prell, W.L., and Shackleton, N.J., 1984. The orbital theory of Pleistocene climate: Support from a revised chronology of the marine $\delta^{18}O$ record. In: A.L. Berger, J. Imbrie, J. Hays, G. Kukla, and B. Saltzman (Editors), D. Riedel, Hingham, Mass., pp. 269-305.

Knox, F. and McElroy, M.B., 1984. Changes in atmospheric CO_2: Influence of the marine biota at high latitude. Journal of Geophysical Research, 89(D3): 4629-4637.

Kumar, N., Anderson, R.F., Mortlock, R.A., Froelich, P.N., Kubik, P., Dittrich-Hannen, B., and Suter, M., 1995. Increased biological productivity and export production in the glacial Southern Ocean. Nature, 378: 675-680.

Labeyrie, L.D., Labracherie, M., Gorfti, N., Pichon, J.J., Vautravers, M., Arnold, M., Duplessy, J.-C., Paterne, M., Michel, E., Duprat, J., Caralp, M., and Turon, J.-L., 1996. Hydrographic changes of the Southern Ocean (southeast Indian sector) over the last 230 kyr. Paleoceanography, 11(1): 57-76.

Mashiotta, T.A., Lea, D.W., and Spero, H.J., 1999. Glacial-interglacial changes in Subantarctic sea surface temperature and $\delta^{18}O$-water using foraminiferal Mg. Earth and Planetary Science Letters, 170: 417-432.

Rosenthal, Y., Boyle, E.A., Labeyrie, L.D., and Oppo, D., 1995. Glacial enrichments of authigenic Cd and U in Subantarctic sediments: A climatic control on the elements' oceanic budget? Paleoceanography, 10: 395-414.

Rosenthal, Y., Dahan, M., and Shemesh, A., 2000. Southern Ocean contributions to glacial-interglacial changes of atmospheric pCO_2: An assessment of carbon isotope records in diatoms. Paleoceanography, 15(1): 65-75.

Shackleton, N.J. and Opdyke, N.D., 1973. Oxygen isotope and paleomagnetic

stratigraphy of equatorial Pacific core V28-238: Oxygen isotope temperatures and ice volumes on a 10^5 year and 10^6 year scale. Quaternary Research, 3: 39-55.

Shackleton, N.J. and Pisias, N.G., 1985. Atmospheric carbon dioxide, orbital forcing, and climate. In: E.T. Sundquist and W.S. Broecker (Editors), The Carbon Cycle and Atmospheric CO_2: Natural Variations Archean to Present. AGU, Washington D.C., pp. 303-317.

APPENDIX I

Deployment duration and
total foraminiferal flux
expressed as shells/m^2/day
at 42°S, 44°S, 47°S, 51°S and 54°S
for all trap depths.

NCR 300

Cup	Split	Trap opened	Trap closed	Shell flux/m^2/day
1	0.25	14/09/96 15.00	22/09/96 12:00	2956.00
2	0.25	22/09/96 12:00	30/09/96 19.30	3328 01
3	0.25	30/09/96 19:30	08/10/96 12.00	2456.01
4	0.125	08/10/96 12:00	17/10/96 00:00	6172.45
5	0.125	17/10/96 00:00	25/10/96 12:00	0.00
6	0.25	25/10/96 12:00	02/11/96 4 30	1.00
7	0 125	02/11/96 4:30	11/10/96 12:00	5.34
8	0 25	11/10/96 12.00	18/11/96 09.00	1.14
9	N/A	18/11/96 09·00	26/11/96 12 00	N/A
10	N/A	26/11/96 12 00	04/12/96 13.30	N/A
11	N/A	04/12/96 13:30	12/12/96 12 00	N/A
12	N/A	12/12/96 12:00	20/12/96 18:00	N/A
13	N/A	20/12/96 18:00	05/01/97 22:30	N/A
14	0.083	05/01/97 22.30	21/1/97 3.00	290.66
15	0 25	21/1/97 3:00	07/02/97 7:30	325.65
16	0 25	07/02/97 7 30	23/2/97 12:00	92 50
17	0.25	23/2/97 12:00	11/03/97 16.30	49 00
18	0.25	11/03/97 16:30	27/3/97 21·00	154.00
19	N/A	27/3/97 21:00	13/4/97 1:30	N/A
20	0.25	13/4/97 1:30	29/4/97 6:00	26.00
21	0 125	29/4/97 6:00	15/5/97 12.00	0.00

NCR 1000

Cup	Split	Trap opened	Trap closed	Shell flux/m^2/day
1	0 25	14/09/96 15 00	22/09/96 12:00	3784 00
2	0 25	22/09/96 12.00	30/09/96 19:30	2816 00
3	0 25	30/09/96 19.30	08/10/96 12.00	6032 00
4	0.25	08/10/96 12·00	17/10/96 00:00	6129 78
5	0 25	17/10/96 00 00	25/10/96 12:00	2560 00
6	0 25	25/10/96 12·00	02/11/96 4 30	1892.00
7	0 25	02/11/96 4:30	11/10/96 12:00	1258 67
8	0 25	11/10/96 12·00	18/11/96 09:00	1284 57
9	0.25	18/11/96 09·00	26/11/96 12:00	934.00
10	0 25	26/11/96 12·00	04/12/96 13:30	1024 00
11	0 25	04/12/96 13:30	12/12/96 12:00	9152 00
12	0 25	12/12/96 12·00	20/12/96 18:00	2168.00
13	0.25	20/12/96 18:00	05/01/97 22:30	354 00
14	0.25	05/01/97 22:30	21/1/97 3:00	179 00
15	0.25	21/1/97 3:00	07/02/97 7:30	91.76
16	0.25	07/02/97 7 30	23/2/97 12:00	59.50
17	0.25	23/2/97 12·00	11/03/97 16.30	143.00
18	0.25	11/03/97 16:30	27/3/97 21:00	422.00
19	0.25	27/3/97 21:00	13/4/97 1·30	3523.76
20	0.25	13/4/97 1:30	29/4/97 6.00	1032.00
21	0.25	29/4/97 6·00	15/5/97 12:00	1212.00

SCR 300

Cup	Split	Trap opened	Trap closed	Shell flux/m^2/day
1	0.125	09/06/96 12 00	25/06/96 16:30	0.00
2	0.25	25/06/96 16.30	11/07/96 21:00	194.50
3	0.125	11/07/96 21.00	28/07/96 01 40	0 00
4	0 25	28/07/96 01:40	13/08/96 06:15	6.50
5	0.25	13/08/96 06:15	29/08/96 10:50	218.50
6	0.25	29/08/96 10.50	14/09/96 15:20	904.00
7	0.25	14/09/96 15.20	30/09/96 20:00	16172.06
8	0 25	30/09/96 20:00	17/10/96 00 30	3358.12
9	0 25	17/10/96 00:30	02/11/96 5:00	3.00
10	0.25	02/11/96 5:00	18/11/96 9·40	0.00
11	0.25	18/11/96 9.40	04/12/96 14:15	0.00
12	0.25	04/12/96 14.15	20/12/96 18.50	130 50
13	0.125	20/12/96 18:50	05/01/97 23·20	5.00
14	0.125	05/01/97 23:20	22/1/97 4:00	0.00
15	0.125	22/1/97 4:00	07/02/97 8·30	0.00
16	0.25	07/02/97 8:30	23/2/97 13.00	0 50
17	N/A	23/2/97 13·00	11/03/97 17·40	N/A
18	0.125	11/03/97 17:40	27/3/97 22.10	0.00
19	0.25	27/3/97 22.10	13/4/97 2:45	0.00
20	0.125	13/4/97 2:45	29/4/97 7 20	0.00
21	0 125	29/4/97 7:20	15/5/97 12:00	8 00

SCR 1000

Cup	Split	Trap opened	Trap closed	Shell flux/m^2/day
1	0.25	09/06/96 12:00	25/06/96 16:30	522.50
2	0 25	25/06/96 16:30	11/07/96 21:00	237.50
3	0.25	11/07/96 21:00	28/07/96 01:40	258.82
4	0.25	28/07/96 01:40	13/08/96 06:15	195 00
5	0.25	13/08/96 06·15	29/08/96 10·50	462.00
6	0.25	29/08/96 10 50	14/09/96 15.20	1348.00
7	0.125	14/09/96 15 20	30/09/96 20:00	4862.00
8	0 25	30/09/96 20:00	17/10/96 00:30	5064.94
9	0.25	17/10/96 00:30	02/11/96 5.00	1188.00
10	0.25	02/11/96 5.00	18/11/96 9:40	619.50
11	0.25	18/11/96 9.40	04/12/96 14·15	491.00
12	0.25	04/12/96 14 15	20/12/96 18.50	167.50
13	0.25	20/12/96 18 50	05/01/97 23:20	170.00
14	0.25	05/01/97 23.20	22/1/97 4·00	168 94
15	0.25	22/1/97 4:00	07/02/97 8:30	310 50
16	0.25	07/02/97 8·30	23/2/97 13:00	680.50
17	0.25	23/2/97 13:00	11/03/97 17:40	1195.00
18	0 25	11/03/97 17·40	27/3/97 22.10	1245 00
19	0 25	27/3/97 22:10	13/4/97 2 45	537.41
20	0.25	13/4/97 2:45	29/4/97 7:20	531.00
21	0.125	29/4/97 7:20	15/5/97 12:00	0 00

SAZ 47°S, 1000m

Cup	Split	Trap opened	Trap closed	Shell flux/m^2/day
1	0.1	22-Sep-97 23:00	1-Oct-97 11:00	263.53
2	0.1	1-Oct-97 11:00	9-Oct-97 23:00	512.94
3	0 1	9-Oct-97 23:00	18-Oct-97 11 00	1195.29
4	0.1	18-Oct-97 11:00	26-Oct-97 23:00	964.71
5	0.1	26-Oct-97 23:00	4-Nov-97 11:00	322 35
6	0.1	4-Nov-97 11:00	12-Nov-97 23:00	411.76
7	0.1	12-Nov-97 23:00	21-Nov-97 11·00	105.88
8	0 1	21-Nov-97 11:00	29-Nov-97 23·00	312.94
9	0.1	29-Nov-97 23 00	8-Dec-97 11 00	195.29
10	0.1	8-Dec-97 11.00	16-Dec-97 23:00	496.47
11	0.1	16-Dec-97 23.00	25-Dec-97 11:00	835.29
12	0.1	25-Dec-97 11:00	2-Jan-98 23:00	1480.00
13	0 1	2-Jan-98 23:00	7-Jan-98 5 00	1501.18
14	0.1	7-Jan-98 5 00	11-Jan-98 11 00	2249 41
15	0.1	11-Jan-98 11·00	15-Jan-98 17:00	2550 59
16	0.1	15-Jan-98 17·00	19-Jan-98 23:00	578 82
17	0.1	19-Jan-98 23.00	24-Jan-98 5:00	1195.29
18	0.1	24-Jan-98 5:00	28-Jan-98 11:00	978 82
19	0.1	28-Jan-98 11:00	5-Feb-98 23:00	1087 06
20	0.1	5-Feb-98 23:00	14-Feb-98 11.00	0
21	0.1	14-Feb-98 11:00	22-Feb-98 23:00	0

SAZ 47°S, 3800m

Cup	Split	Trap opened	Trap closed	Shell flux/m^2/day
1	0.1	22-Sep-97 23.00	1-Oct-97 11:00	167.058824
2	0.1	1-Oct-97 11 00	9-Oct-97 23:00	736.470588
3	0.1	9-Oct-97 23·00	18-Oct-97 11·00	712.941176
4	0.1	18-Oct-97 11.00	26-Oct-97 23·00	950.588235
5	0.1	26-Oct-97 23 00	4-Nov-97 11·00	428.235294
6	0 1	4-Nov-97 11:00	12-Nov-97 23:00	816.470588
7	0.1	12-Nov-97 23:00	21-Nov-97 11:00	581 176471
8	0 1	21-Nov-97 11:00	29-Nov-97 23:00	247.058824
9	0.1	29-Nov-97 23:00	8-Dec-97 11:00	352.941176
10	0.1	8-Dec-97 11:00	16-Dec-97 23.00	449.411765
11	0.1	16-Dec-97 23.00	25-Dec-97 11.00	736.470588
12	0.1	25-Dec-97 11.00	2-Jan-98 23:00	1103.52941
13	0.1	2-Jan-98 23.00	7-Jan-98 5:00	837.647059
14	0 1	7-Jan-98 5·00	11-Jan-98 11·00	1910.58824
15	0.1	11-Jan-98 11·00	15-Jan-98 17.00	3256.47059
16	0.1	15-Jan-98 17 00	19-Jan-98 23 00	2385.88235
17	0.1	19-Jan-98 23:00	24-Jan-98 5:00	1741.17647
18	0.1	24-Jan-98 5·00	28-Jan-98 11:00	823.529412
19	0 1	28-Jan-98 11 00	5-Feb-98 23·00	1042.35294
20	0.1	5-Feb-98 23 00	14-Feb-98 11 00	1804 70588
21	0.1	14-Feb-98 11.00	22-Feb-98 23:00	0

SAZ 47°S, 3800m, 1998 redeployment

Cup	Split	Trap opened	Trap closed	Shell flux/m^2/day
1	0.2	16-Mar-02 12:00	10-Apr-02 00:00	1660 41
2	0.2	10-Apr-02 00:00	25-Apr-02 12·00	593.55
3	0.2	25-Apr-02 12:00	11-May-02 00:00	1340.00
4	0 3	11-May-02 00:00	26-May-02 12:00	1356.56
5	0 2	26-May-02 12 00	11-Jun-02 00:00	833 55
6	0.2	11-Jun-02 00.00	26-Jun-02 12:00	434.84
7	0.2	26-Jun-02 12:00	12-Jul-02 00:00	392.26
8	0.2	12-Jul-02 00.00	27-Jul-02 12 00	181.29
9	0.2	27-Jul-02 12·00	12-Aug-02 00·00	138.06
10	0.2	12-Aug-02 00:00	27-Aug-02 12:00	108 39
11	0 2	27-Aug-02 12:00	12-Sep-02 00:00	134 19
12	0.3	12-Sep-02 00:00	27-Sep-02 12:00	167.31
13	0.2	27-Sep-02 12:00	13-Oct-02 00·00	689.68
14	0.2	13-Oct-02 00:00	28-Oct-02 12:00	967.74
15	0 2	28-Oct-02 12·00	13-Nov-02 00:00	840.65
16	0.2	13-Nov-02 00:00	28-Nov-02 12:00	458.06
17	0.2	28-Nov-02 12:00	14-Dec-02 00 00	169.03
18	0.2	14-Dec-02 00 00	29-Dec-02 12·00	87.74
19	0.2	29-Dec-02 12.00	14-Jan-03 00.00	62.58
20	0.2	14-Jan-03 00·00	29-Jan-03 12:00	332 90
21	NA	29-Jan-03 12.00	14-Feb-03 00:00	NA

SAF 51°S, 3300m

Cup	Split	Trap opened	Trap closed	Shell flux/m^2/day
1	0.1	22-Sep-97 23:00	1-Oct-97 11:00	802.352941
2	0 1	1-Oct-97 11:00	9-Oct-97 23:00	715.294118
3	0.1	9-Oct-97 23·00	18-Oct-97 11:00	6611.76471
4	0.1	18-Oct-97 11·00	26-Oct-97 23:00	8811.76471
5	0.1	26-Oct-97 23.00	4-Nov-97 11:00	9691.76471
6	0.1	4-Nov-97 11:00	12-Nov-97 23 00	5383.52941
7	0.1	12-Nov-97 23 00	21-Nov-97 11·00	5369.41176
8	0 1	21-Nov-97 11.00	29-Nov-97 23:00	5651.76471
9	0.1	29-Nov-97 23:00	8-Dec-97 11:00	2407.05882
10	0.1	8-Dec-97 11:00	16-Dec-97 23:00	745.882353
11	0.1	16-Dec-97 23 00	25-Dec-97 11·00	2809.41176
12	0.1	25-Dec-97 11.00	2-Jan-98 23:00	3322.35294
13	0.1	2-Jan-98 23 00	7-Jan-98 5 00	4268.23529
14	0.1	7-Jan-98 5:00	11-Jan-98 11:00	484 705882
15	0.1	11-Jan-98 11:00	15-Jan-98 17:00	3727.05882
16	0.1	15-Jan-98 17:00	19-Jan-98 23:00	2560
17	0 1	19-Jan-98 23:00	24-Jan-98 5:00	3044.70588
18	0.1	24-Jan-98 5.00	28-Jan-98 11.00	2678
19	0.1	28-Jan-98 11 00	5-Feb-98 23:00	2449.41176
20	0.1	5-Feb-98 23·00	14-Feb-98 11:00	1484.70588
21	0.1	14-Feb-98 11 00	22-Feb-98 23:00	3536 47059

PFZ 54°S, 800m

Cup	Split	Trap opened	Trap closed	Shell flux/m^2/day
1	0.1	22-Sep-97 23:00	1-Oct-97 11:00	0
2	0 1	1-Oct-97 11:00	9-Oct-97 23 00	0
3	0 1	9-Oct-97 23 00	18-Oct-97 11 00	0
4	0.1	18-Oct-97 11:00	26-Oct-97 23 00	195.294118
5	0.1	26-Oct-97 23:00	4-Nov-97 11.00	1590.58824
6	0.1	4-Nov-97 11:00	12-Nov-97 23:00	1122.35294
7	0.1	12-Nov-97 23:00	21-Nov-97 11:00	2571.76471
8	0.1	21-Nov-97 11:00	29-Nov-97 23:00	8409 41176
9	0.1	29-Nov-97 23 00	8-Dec-97 11:00	2343 52941
10	0.1	8-Dec-97 11:00	16-Dec-97 23.00	1495 12605
11	0.1	16-Dec-97 23:00	25-Dec-97 11.00	2098.82353
12	0 1	25-Dec-97 11:00	2-Jan-98 23:00	3731.76471
13	0.1	2-Jan-98 23:00	7-Jan-98 5:00	3204 70588
14	0.1	7-Jan-98 5:00	11-Jan-98 11 00	2268 23529
15	0.1	11-Jan-98 11 00	15-Jan-98 17 00	2249.41176
16	0.1	15-Jan-98 17.00	19-Jan-98 23:00	2188.23529
17	0.1	19-Jan-98 23:00	24-Jan-98 5 00	4296.47059
18	0.1	24-Jan-98 5.00	28-Jan-98 11:00	8814.11765
19	0.1	28-Jan-98 11 00	5-Feb-98 23.00	7324.70588
20	0.1	5-Feb-98 23.00	14-Feb-98 11:00	5529.41176
21	0.1	14-Feb-98 11:00	22-Feb-98 23 00	2491.77448
1-98	0.2	24-Mar-98 12 00	10-Apr-98 00.00	1105.16129

PFZ 54°S, 1500m

Cup	Split	Trap opened	Trap closed	Shell flux/m^2/day
1	0.1	22-Sep-97 23·00	1-Oct-97 11·00	12.9411765
3	0.1	9-Oct-97 23·00	18-Oct-97 11:00	111.764706
5	0.1	26-Oct-97 23·00	4-Nov-97 11 00	482.352941
6	0.1	4-Nov-97 11:00	12-Nov-97 23:00	738.823529
7	0.1	12-Nov-97 23:00	21-Nov-97 11:00	1894.11765
8	0.1	21-Nov-97 11:00	29-Nov-97 23 00	2927.05882
9	0.1	29-Nov-97 23 00	8-Dec-97 11:00	4018.82353
10	0.1	8-Dec-97 11·00	16-Dec-97 23.00	1936.47059
11	0.1	16-Dec-97 23:00	25-Dec-97 11:00	2115.29412
12	0.1	25-Dec-97 11:00	2-Jan-98 23:00	1489.41176
13	0.1	2-Jan-98 23·00	7-Jan-98 5 00	4668.23529
14	0.1	7-Jan-98 5:00	11-Jan-98 11:00	1087 05882
15	0.1	11-Jan-98 11:00	15-Jan-98 17·00	1251.76471
16	0 1	15-Jan-98 17 00	19-Jan-98 23.00	720
17	0.1	19-Jan-98 23.00	24-Jan-98 5 00	837.647059
18	0.1	24-Jan-98 5.00	28-Jan-98 11:00	837.647059
19	0.1	28-Jan-98 11:00	5-Feb-98 23:00	1134.11765
20	0 1	5-Feb-98 23 00	14-Feb-98 11.00	609 411765
21	0 1	14-Feb-98 11:00	22-Feb-98 23 00	595.294351
1-98	0.2	24-Mar-98 12:00	10-Apr-98 00:00	1373 54839

APPENDIX II

Total planktonic foraminiferal fluxes collected in each sediment trap cup at 42°S, 44°S, 47°S, 51°S and 54°S for all trap depths.

NCR 300

Cup	Split	*O. Univ.*	*G. ruber*	*G. aequil.*	*G. calida*	*G. bull.*	*G. falc.*	*G. quinq.*	*N. pachy* (s.)	*N. pachy* (d.)	*N. dut.*	*G. infl.*	*G. trunc.* (s.)	*G. trunc.* (d.)	*G. crass.*	*G. hirs.*	*G. scit.*	*G. glut.*	*G. Uvula*	*unknown*
1	0.25	0	0	3	6	142	0	4	10	76	21	2643	25	1	0	0	7	18	0	0
2	0.25	40	0	0	0	152	0	8	16	280	88	2600	56	8	0	0	0	80	0	0
3	0.25	48	0	0	0	208	0	8	48	232	40	1784	8	0	0	0	8	72	0	0
4	0.125	56	0	16	8	408	0	48	72	504	40	1888	24	0	0	0	32	376	0	0
5	0.125	0	0	0	0	0	0	0	0	0	0	0	0	0	0	0	0	0	0	0
6	0.25	0	0	0	0	0	0	0	0	0	0	1	0	0	0	0	0	0	0	0
7	0 125	0	0	0	0	0	0	0	1	2	0	0	0	0	0	0	0	0	0	0
8	0.25	0	0	0	0	0	0	0	1	0	0	0	0	0	0	0	0	0	0	0
9	N/A	N/A	N/A	N/A	N/A	N/A	N/A	N/A	N/A	N/A	N/A	N/A	N/A	N/A	N/A	N/A	N/A	N/A	N/A	N/A
10	N/A	N/A	N/A	N/A	N/A	N/A	N/A	N/A	N/A	N/A	N/A	N/A	N/A	N/A	N/A	N/A	N/A	N/A	N/A	N/A
11	N/A	N/A	N/A	N/A	N/A	N/A	N/A	N/A	N/A	N/A	N/A	N/A	N/A	N/A	N/A	N/A	N/A	N/A	N/A	N/A
12	N/A	N/A	N/A	N/A	N/A	N/A	N/A	N/A	N/A	N/A	N/A	N/A	N/A	N/A	N/A	N/A	N/A	N/A	N/A	N/A
13	N/A	N/A	N/A	N/A	N/A	N/A	N/A	N/A	N/A	N/A	N/A	N/A	N/A	N/A	N/A	N/A	N/A	N/A	N/A	N/A
14	0.083	1	0	0	3	28	0	15	13	25	5	70	0	0	3	0	21	9	0	0
15	0.25	14	0	0	0	50	0	10	10	44	4	496	0	0	40	0	14	10	0	0
16	0.25	2	0	1	0	17	0	0	0	13	0	146	0	0	1	0	5	0	0	0
17	0.25	0	0	0	0	12	0	1	4	8	2	65	0	0	1	0	3	2	0	0
18	0.25	4	0	0	0	29	0	3	0	21	1	241	3	0	0	0	3	3	0	0
19	N/A	N/A	N/A	N/A	N/A	N/A	N/A	N/A	N/A	N/A	N/A	N/A	N/A	N/A	N/A	N/A	N/A	N/A	N/A	N/A
20	0.25	0	0	0	0	7	0	1	1	4	1	33	0	0	0	0	4	1	0	0
21	0 125	0	0	0	0	0	0	0	0	0	0	0	0	0	0	0	0	0	0	0

NCR 1000

Cup	Split	*O. univ.*	*G. ruber*	*G. aequil.*	*G. calida*	*G. bull.*	*G. falc.*	*G. quinq.*	*N. pachy.* (s.)	*N. pachy* (d.)	*N. dut.*	*G. infl.*	*G. trunc.* (s.)	*G. trunc.* (d.)	*G. crass.*	*G. hirs.*	*G. scit.*	*G. glut.*	*G. uvula*	*unknown*
1	0.25	8	0	8	0	416	0	0	72	568	32	2408	0	0	0	0	176	96	0	0
2	0.25	8	0	8	16	224	40	16	48	464	72	1720	0	0	0	0	168	32	0	0
3	0.25	144	0	0	16	752	16	16	48	1232	112	3136	16	0	0	0	496	48	0	0
4	0.25	768	0	32	0	496	0	80	144	864	48	3760	32	0	0	0	288	384	0	0
5	0.25	16	0	24	40	256	0	56	8	208	16	1440	16	0	0	0	280	200	0	0
6	0.25	12	0	20	4	292	0	100	20	224	4	976	8	0	0	0	136	72	0	24
7	0.25	28	0	8	20	428	0	68	8	116	4	648	4	0	0	0	24	48	0	12
8	0.25	12	0	4	8	248	0	40	32	104	0	604	12	0	0	0	12	40	0	8
9	0.25	8	2	0	6	228	0	32	14	94	2	514	8	0	0	0	6	18	0	2
10	0 25	32	0	0	8	316	0	68	12	192	12	360	0	0	0	0	8	16	0	0
11	0 25	64	0	16	32	1632	64	288	304	1904	208	4464	32	0	0	0	0	128	0	16
12	0 25	8	0	0	8	112	0	8	16	160	8	1848	0	0	0	0	0	0	0	0
13	0 25	4	2	0	4	136	8	12	10	128	4	366	2	0	0	0	6	22	0	4
14	0.25	3	0	1	0	66	3	8	3	50	4	191	2	0	0	0	21	5	0	1
15	0 25	1	13	0	3	72	0	19	4	23	1	36	0	0	3	0	16	4	0	0
16	0 25	0	1	1	0	33	0	7	12	17	1	33	0	0	1	0	8	5	0	0
17	0.25	0	5	2	2	12	0	0	2	21	1	213	0	0	0	0	28	0	0	0
18	0.25	4	4	0	0	20	0	6	8	50	6	708	0	0	0	0	38	0	0	0
19	0.25	32	0	0	0	800	0	32	0	448	32	6048	0	0	0	0	96	0	0	0
20	0.25	0	8	0	0	600	8	0	72	280	8	1024	8	0	0	0	16	32	0	8
21	0.25	24	0	8	0	344	0	0	16	328	8	1632	24	0	0	0	32	8	0	0

SCR 1000

Cup	Split	*O. univ.*	*G. ruber*	*G. aequil.*	*G. calida*	*G. bull.*	*G. falc.*	*G. quinq.*	*N. pachy (s.)*	*N. pachy (d.)*	*N. dut.*	*G. infl.*	*G. trunc. (s.)*	*G. trunc. (d.)*	*G. crass.*	*G. hirs.*	*G. scit.*	*G. glut.*	*G. uvula*	*unknown*
1	0 25	1	0	0	0	83	0	18	6	320	2	55	251	7	0	0	106	196	0	0
2	0.25	2	0	0	0	53	0	22	2	142	1	4	80	3	0	0	32	134	0	0
3	0.25	0	0	0	0	127	0	22	8	63	0	29	104	0	0	0	75	122	0	0
4	0.25	3	0	0	0	122	0	22	5	40	0	29	64	1	0	1	53	50	0	0
5	0.25	1	0	0	0	416	6	106	16	136	0	71	84	0	0	0	57	31	0	0
6	0.25	10	0	0	0	1340	0	144	40	560	0	292	63	2	0	0	81	164	0	0
7	0 125	1	0	0	0	3265	0	144	88	476	0	600	37	0	0	0	46	205	0	0
8	0.25	16	0	0	0	7008	0	352	384	1144	0	1510	24	0	0	0	39	286	0	0
9	0.25	21	0	0	0	837	0	156	52	456	0	631	61	1	0	0	43	118	0	0
10	0.25	5	0	0	0	381	0	126	26	298	0	264	61	0	0	0	5	71	0	0
11	0 25	111	0	0	0	314	0	120	42	146	0	53	103	1	0	0	7	85	0	0
12	0.25	16	0	0	0	130	0	44	19	55	1	10	36	0	0	0	4	18	0	2
13	0.25	69	0	0	0	75	0	42	12	38	0	28	58	1	0	0	3	14	0	0
14	0.25	45	0	0	0	71	0	40	18	63	3	46	54	0	0	1	5	13	0	0
15	0.25	88	0	0	0	88	0	111	23	178	14	35	43	2	0	2	8	29	0	0
16	0.25	21	0	0	0	216	0	172	48	786	17	33	30	0	0	0	3	35	0	0
17	0.25	51	0	0	0	230	0	224	48	1690	75	47	11	0	0	0	11	2	0	0
18	0.25	14	0	0	0	169	0	163	42	1791	183	24	21	0	0	0	26	55	0	2
19	0.25	15	0	0	0	126	0	72	48	712	94	38	7	0	0	0	9	21	0	0
20	0 25	11	0	0	0	115	0	56	36	689	66	40	7	0	0	0	15	27	0	0
21	0 125	0	0	0	0	0	0	0	0	0	0	0	0	0	0	0	0	0	0	0

SCR 300

Cup	Split	*O. univ.*	*G. ruber*	*G. aequil.*	*G. calida*	*G. bull.*	*G. falc.*	*G. quinq.*	*N. pachy* (s.)	*N. pachy* (d.)	*N. dut.*	*G. infl.*	*G. trunc.* (s.)	*G. trunc.* (d.)	*G. crass.*	*G. hirs.*	*G. scit.*	*G. glut.*	*G. uvula*	*unknown*
1	0.125	0	0	0	0	0	0	0	0	0	0	0	0	0	0	0	0	0	0	0
2	0.25	5	0	0	0	25	0	7	19	50	1	2	173	0	0	0	1	106	0	0
3	0.125	0	0	0	0	0	0	0	0	0	0	0	0	0	0	0	0	0	0	0
4	0 25	0	0	0	0	0	0	0	0	0	0	3	2	0	0	0	0	8	0	0
5	0 25	0	0	0	0	117	0	48	8	40	0	30	135	0	0	0	0	58	1	0
6	0.25	4	0	0	0	688	60	64	8	280	0	372	188	0	0	0	4	140	0	0
7	0.25	0	0	0	0	0	0	0	0	0	0	0	0	0	0	0	0	0	0	0
8	0.25	0	0	0	0	0	0	0	0	0	0	0	0	0	0	0	0	0	0	0
9	0.25	0	0	0	0	2	0	0	0	0	0	4	0	0	0	0	0	0	0	0
10	0.25	0	0	0	0	0	0	0	0	0	0	0	0	0	0	0	0	0	0	0
11	0 25	0	0	0	0	0	0	0	0	0	0	0	0	0	0	0	0	0	0	0
12	0.25	34	0	0	0	69	0	2	3	8	0	17	112	0	0	0	0	16	0	0
13	0.125	4	0	0	0	1	0	0	0	0	0	0	0	0	0	0	0	0	0	0
14	0.125	0	0	0	0	0	0	0	0	0	0	0	0	0	0	0	0	0	0	0
15	0.125	0	0	0	0	0	0	0	0	0	0	0	0	0	0	0	0	0	0	0
16	0.25	0	0	0	0	0	0	0	0	0	0	0	0	0	0	0	0	1	0	0
17		N/A	N/A	N/A	N/A	N/A	N/A	N/A	N/A	N/A	N/A	N/A	N/A	N/A	N/A	N/A	N/A	N/A	N/A	0
18	0.125	0	0	0	0	0	0	0	0	0	0	0	0	0	0	0	0	0	0	0
19	0.25	0	0	0	0	0	0	0	0	0	0	0	0	0	0	0	0	0	0	0
20	0.125	0	0	0	0	0	0	0	0	0	0	0	0	0	0	0	0	0	0	0
21	0.125	3	0	0	0	4	0	0	0	1	0	0	0	0	0	0	0	0	0	0

APPENDIX II

Total planktonic foraminiferal fluxes collected in each sediment trap cup at 42°S, 44°S, 47°S, 51°S and 54°S for all trap depths.

NCR 300

Cup	Split	*O. Univ.*	*G. ruber*	*G. aequil.*	*G. calida*	*G. bull.*	*G. falc.*	*G. quinq.*	*N. pachy* (s.)	*N. pachy* (d.)	*N. dut.*	*G. infl.*	*G. trunc.* (s.)	*G. trunc.* (d.)	*G. crass.*	*G. hirs.*	*G. scit.*	*G. glut.*	*G. Uvula*	*unknown*
1	0.25	0	0	3	6	142	0	4	10	76	21	2643	25	1	0	0	7	18	0	0
2	0.25	40	0	0	0	152	0	8	16	280	88	2600	56	8	0	0	0	80	0	0
3	0.25	48	0	0	0	208	0	8	48	232	40	1784	8	0	0	0	8	72	0	0
4	0.125	56	0	16	8	408	0	48	72	504	40	1888	24	0	0	0	32	376	0	0
5	0 125	0	0	0	0	0	0	0	0	0	0	0	0	0	0	0	0	0	0	0
6	0.25	0	0	0	0	0	0	0	0	0	0	1	0	0	0	0	0	0	0	0
7	0.125	0	0	0	0	0	0	0	1	2	0	0	0	0	0	0	0	0	0	0
8	0 25	0	0	0	0	0	0	0	1	0	0	0	0	0	0	0	0	0	0	0
9	N/A	N/A	N/A	N/A	N/A	N/A	N/A	N/A	N/A	N/A	N/A	N/A	N/A	N/A	N/A	N/A	N/A	N/A	N/A	N/A
10	N/A	N/A	N/A	N/A	N/A	N/A	N/A	N/A	N/A	N/A	N/A	N/A	N/A	N/A	N/A	N/A	N/A	N/A	N/A	N/A
11	N/A	N/A	N/A	N/A	N/A	N/A	N/A	N/A	N/A	N/A	N/A	N/A	N/A	N/A	N/A	N/A	N/A	N/A	N/A	N/A
12	N/A	N/A	N/A	N/A	N/A	N/A	N/A	N/A	N/A	N/A	N/A	N/A	N/A	N/A	N/A	N/A	N/A	N/A	N/A	N/A
13	N/A	N/A	N/A	N/A	N/A	N/A	N/A	N/A	N/A	N/A	N/A	N/A	N/A	N/A	N/A	N/A	N/A	N/A	N/A	N/A
14	0.083	1	0	0	3	28	0	15	13	25	5	70	0	0	3	0	21	9	0	0
15	0.25	14	0	0	0	50	0	10	10	44	4	496	0	0	40	0	14	10	0	0
16	0.25	2	0	1	0	17	0	0	0	13	0	146	0	0	1	0	5	0	0	0
17	0.25	0	0	0	0	12	0	1	4	8	2	65	0	0	1	0	3	2	0	0
18	0 25	4	0	0	0	29	0	3	0	21	1	241	3	0	0	0	3	3	0	0
19	N/A	N/A	N/A	N/A	N/A	N/A	N/A	N/A	N/A	N/A	N/A	N/A	N/A	N/A	N/A	N/A	N/A	N/A	N/A	N/A
20	0.25	0	0	0	0	7	0	1	1	4	1	33	0	0	0	0	4	1	0	0
21	0.125	0	0	0	0	0	0	0	0	0	0	0	0	0	0	0	0	0	0	0

NCR 1000

Cup	Split	*O. univ.*	*G. ruber*	*G. aequil.*	*G. calida*	*G. bull.*	*G. falc.*	*G. quinq.*	*N. pachy.* (s.)	*N. pachy* (d.)	*N. dut.*	*G. infl.*	*G. trunc.* (s.)	*G. trunc.* (d.)	*G. crass.*	*G. hirs.*	*G. scit.*	*G. glut.*	*G. uvula*	*unknown*
1	0.25	8	0	8	0	416	0	0	72	568	32	2408	0	0	0	0	176	96	0	0
2	0.25	8	0	8	16	224	40	16	48	464	72	1720	0	0	0	0	168	32	0	0
3	0 25	144	0	0	16	752	16	16	48	1232	112	3136	16	0	0	0	496	48	0	0
4	0.25	768	0	32	0	496	0	80	144	864	48	3760	32	0	0	0	288	384	0	0
5	0.25	16	0	24	40	256	0	56	8	208	16	1440	16	0	0	0	280	200	0	0
6	0.25	12	0	20	4	292	0	100	20	224	4	976	8	0	0	0	136	72	0	24
7	0.25	28	0	8	20	428	0	68	8	116	4	648	4	0	0	0	24	48	0	12
8	0.25	12	0	4	8	248	0	40	32	104	0	604	12	0	0	0	12	40	0	8
9	0.25	8	2	0	6	228	0	32	14	94	2	514	8	0	0	0	6	18	0	2
10	0 25	32	0	0	8	316	0	68	12	192	12	360	0	0	0	0	8	16	0	0
11	0 25	64	0	16	32	1632	64	288	304	1904	208	4464	32	0	0	0	0	128	0	16
12	0.25	8	0	0	8	112	0	8	16	160	8	1848	0	0	0	0	0	0	0	0
13	0.25	4	2	0	4	136	8	12	10	128	4	366	2	0	0	0	6	22	0	4
14	0 25	3	0	1	0	66	3	8	3	50	4	191	2	0	0	0	21	5	0	1
15	0.25	1	13	0	3	72	0	19	4	23	1	36	0	0	3	0	16	4	0	0
16	0.25	0	1	1	0	33	0	7	12	17	1	33	0	0	1	0	8	5	0	0
17	0 25	0	5	2	2	12	0	0	2	21	1	213	0	0	0	0	28	0	0	0
18	0.25	4	4	0	0	20	0	6	8	50	6	708	0	0	0	0	38	0	0	0
19	0.25	32	0	0	0	800	0	32	0	448	32	6048	0	0	0	0	96	0	0	0
20	0.25	0	8	0	0	600	8	0	72	280	8	1024	8	0	0	0	16	32	0	8
21	0 25	24	0	8	0	344	0	0	16	328	8	1632	24	0	0	0	32	8	0	0

SCR 300

Cup	Split	*O. univ.*	*G. ruber*	*G. aequil.*	*G. calida*	*G. bull.*	*G. falc.*	*G. quinq.*	*N. pachy* (s.)	*N. pachy* (d.)	*N. dut.*	*G. infl.*	*G. trunc.* (s.)	*G. trunc.* (d.)	*G. crass.*	*G. hirs.*	*G. scit.*	*G. glut.*	*G. uvula*	*unknown*
1	0.125	0	0	0	0	0	0	0	0	0	0	0	0	0	0	0	0	0	0	0
2	0.25	5	0	0	0	25	0	7	19	50	1	2	173	0	0	0	1	106	0	0
3	0.125	0	0	0	0	0	0	0	0	0	0	0	0	0	0	0	0	0	0	0
4	0.25	0	0	0	0	0	0	0	0	0	0	3	2	0	0	0	0	8	0	0
5	0.25	0	0	0	0	117	0	48	8	40	0	30	135	0	0	0	0	58	1	0
6	0.25	4	0	0	0	688	60	64	8	280	0	372	188	0	0	0	4	140	0	0
7	0.25	0	0	0	0	0	0	0	0	0	0	0	0	0	0	0	0	0	0	0
8	0 25	0	0	0	0	0	0	0	0	0	0	0	0	0	0	0	0	0	0	0
9	0.25	0	0	0	0	2	0	0	0	0	0	4	0	0	0	0	0	0	0	0
10	0.25	0	0	0	0	0	0	0	0	0	0	0	0	0	0	0	0	0	0	0
11	0.25	0	0	0	0	0	0	0	0	0	0	0	0	0	0	0	0	0	0	0
12	0.25	34	0	0	0	69	0	2	3	8	0	17	112	0	0	0	0	16	0	0
13	0.125	4	0	0	0	1	0	0	0	0	0	0	0	0	0	0	0	0	0	0
14	0.125	0	0	0	0	0	0	0	0	0	0	0	0	0	0	0	0	0	0	0
15	0.125	0	0	0	0	0	0	0	0	0	0	0	0	0	0	0	0	0	0	0
16	0.25	0	0	0	0	0	0	0	0	0	0	0	0	0	0	0	0	1	0	0
17		N/A	N/A	N/A	N/A	N/A	N/A	N/A	N/A	N/A	N/A	N/A	N/A	N/A	N/A	N/A	N/A	N/A	N/A	0
18	0.125	0	0	0	0	0	0	0	0	0	0	0	0	0	0	0	0	0	0	0
19	0.25	0	0	0	0	0	0	0	0	0	0	0	0	0	0	0	0	0	0	0
20	0 125	0	0	0	0	0	0	0	0	0	0	0	0	0	0	0	0	0	0	0
21	0.125	3	0	0	0	4	0	0	0	1	0	0	0	0	0	0	0	0	0	0

SCR 1000

Cup	Split	*O. univ.*	*G. ruber*	*G. aequil.*	*G. calida*	*G. bull.*	*G. falc.*	*G. quinq.*	*N. pachy* (s.)	*N. pachy* (d.)	*N. dut.*	*G. infl.*	*G. trunc.* (s.)	*G. trunc.* (d.)	*G. crass.*	*G. hirs.*	*G. scit.*	*G. glut.*	*G. uvula*	*unknown*
1	0.25	1	0	0	0	83	0	18	6	320	2	55	251	7	0	0	106	196	0	0
2	0.25	2	0	0	0	53	0	22	2	142	1	4	80	3	0	0	32	134	0	0
3	0.25	0	0	0	0	127	0	22	8	63	0	29	104	0	0	0	75	122	0	0
4	0.25	3	0	0	0	122	0	22	5	40	0	29	64	1	0	1	53	50	0	0
5	0 25	1	0	0	0	416	6	106	16	136	0	71	84	0	0	0	57	31	0	0
6	0.25	10	0	0	0	1340	0	144	40	560	0	292	63	2	0	0	81	164	0	0
7	0.125	1	0	0	0	3265	0	144	88	476	0	600	37	0	0	0	46	205	0	0
8	0.25	16	0	0	0	7008	0	352	384	1144	0	1510	24	0	0	0	39	286	0	0
9	0.25	21	0	0	0	837	0	156	52	456	0	631	61	1	0	0	43	118	0	0
10	0.25	5	0	0	0	381	0	126	26	298	0	264	61	0	0	0	5	71	0	0
11	0.25	111	0	0	0	314	0	120	42	146	0	53	103	1	0	0	7	85	0	0
12	0.25	16	0	0	0	130	0	44	19	55	1	10	36	0	0	0	4	18	0	2
13	0.25	69	0	0	0	75	0	42	12	38	0	28	58	1	0	0	3	14	0	0
14	0.25	45	0	0	0	71	0	40	18	63	3	46	54	0	0	1	5	13	0	0
15	0.25	88	0	0	0	88	0	111	23	178	14	35	43	2	0	2	8	29	0	0
16	0.25	21	0	0	0	216	0	172	48	786	17	33	30	0	0	0	3	35	0	0
17	0.25	51	0	0	0	230	0	224	48	1690	75	47	11	0	0	0	11	2	0	0
18	0.25	14	0	0	0	169	0	163	42	1791	183	24	21	0	0	0	26	55	0	2
19	0.25	15	0	0	0	126	0	72	48	712	94	38	7	0	0	0	9	21	0	0
20	0.25	11	0	0	0	115	0	56	36	689	66	40	7	0	0	0	15	27	0	0
21	0.125	0	0	0	0	0	0	0	0	0	0	0	0	0	0	0	0	0	0	0

SAZ 47°S, 1000m

Cup	Split	*O. Univ.*	*G. ruber*	G. calida	G. bull.	*G. falc.*	*G. quinq.*	*N. pachy* (s.)	*N. pachy* (d.)	*N. dut.*	*G. infl.*	*G. trunc.* (s.)	*G. trunc.* (d.)	*G. hirs.*	*G. scit.*	*G. glut.*	*G. Uvula*	*unknown*
1	0.1	0	0	0	57	2	2	1	4	0	15	10	0	0	15	5	0	1
2	0.1	0	0	0	113	3	11	0	23	1	30	10	0	0	11	16	0	0
3	0.1	1	0	0	172	9	24	9	117	0	93	28	0	3	8	44	0	0
4	0.1	0	0	0	104	1	7	3	90	0	148	22	0	1	15	19	0	0
5	0.1	1	0	0	20	0	1	3	29	0	34	18	0	0	16	15	0	0
6	0 1	0	0	0	29	0	30	6	21	0	41	27	0	0	10	11	0	0
7	0.1	0	0	0	13	0	4	1	6	0	9	4	0	0	4	4	0	0
8	0.1	0	0	0	22	0	28	2	18	0	23	21	0	0	12	7	0	0
9	0.1	1	0	0	20	0	25	6	10	2	6	9	0	0	2	2	0	0
10	0.1	0	0	0	43	0	79	4	17	0	30	23	0	0	4	11	0	0
11	0.1	38	0	0	80	1	70	23	47	0	40	41	2	0	6	7	0	0
12	0.1	4	0	0	85	3	54	145	181	5	48	37	2	0	17	48	0	0
13	0.1	0	0	0	33	4	2	40	127	0	38	29	1	0	6	39	0	0
14	0.1	10	0	0	69	0	25	77	212	14	22	6	1	0	8	34	0	0
15	0.1	4	0	0	90	0	23	60	227	15	43	31	2	0	4	43	0	0
16	0.1	2	0	0	18	0	10	17	41	2	9	7	0	0	2	15	0	0
17	0.1	14	0	0	28	0	29	37	75	7	20	14	0	0	0	30	0	0
18	0.1	9	0	0	45	0	20	23	55	3	16	15	1	0	1	20	0	0
19	0.1	23	0	0	73	0	49	60	130	10	36	29	1	0	1	50	0	0
20	0.1	0	0	0	0	0	0	0	0	0	0	0	0	0	0	0	0	0
21	0.1	0	0	0	0	0	0	0	0	0	0	0	0	0	0	0	0	0

SAZ 47°S, 3800m

Cup	Split	*O. Univ.*	*G. ruber*	*G. calida*	*G. bull.*	*G. falc.*	*G. quinq.*	*N. pachy (s.)*	*N. pachy (d.)*	*N. dut.*	*G. infl.*	*G. trunc. (s.)*	*G. trunc. (d.)*	*G. hirs.*	*G. scit.*	*G. glut.*	*G. Uvula*	*unknown*
1	0.1	1	0	0	49	3	3	0	2	0	5	4	0	0	0	4	0	0
2	0.1	2	0	0	208	7	2	1	7	0	43	28	1	0	0	14	0	0
3	0.1	0	0	0	121	3	3	2	42	1	94	19	0	0	2	14	0	2
4	0.1	1	1	0	130	0	19	6	84	2	107	19	0	0	3	31	0	1
5	0.1	0	0	0	32	0	11	1	48	0	48	17	0	0	7	18	0	0
6	0 1	0	0	1	70	2	28	5	72	1	81	31	0	0	13	42	0	1
7	0 1	0	0	0	68	0	39	2	32	0	48	29	3	0	6	17	0	3
8	0.1	0	0	0	15	0	32	1	16	0	6	12	0	0	13	9	0	1
9	0 1	0	0	0	33	0	21	0	10	0	31	32	0	0	15	7	0	1
10	0 1	0	0	0	29	0	68	4	23	0	12	16	1	0	22	16	0	0
11	0.1	3	0	1	48	0	134	6	39	0	21	24	0	0	17	20	0	0
12	0.1	24	0	0	84	0	181	26	47	0	40	30	1	0	9	26	0	1
13	0.1	2	0	0	27	0	43	21	32	1	22	21	0	0	2	7	0	0
14	0.1	1	0	1	53	0	50	68	102	5	53	26	1	0	13	32	0	1
15	0.1	0	0	0	93	0	69	110	251	11	64	25	2	0	13	52	0	2
16	0.1	2	0	2	50	0	43	92	216	6	36	15	0	0	4	41	0	0
17	0.1	4	0	0	36	0	37	70	135	6	16	15	0	0	9	39	0	3
18	0.1	4	0	0	9	0	19	43	59	0	12	5	0	0	4	20	0	0
19	0.1	8	0	0	28	0	59	71	156	6	27	27	0	0	10	51	0	0
20	0.1	1	0	0	62	0	74	76	368	4	56	84	6	0	6	28	0	2
21	0.1	0	0	0	0	0	0	0	0	0	0	0	0	0	0	0	0	0

SAZ 47°S, 3800m, 1998 redeployment

Cup	Split	*O. Univ.*	*G. ruber*	*G. calida*	*G. bull.*	*G. falc.*	*G. quinq.*	*N. pachy* (s.)	*N. pachy* (d.)	*N. dut.*	*G. infl.*	*G. trunc.* (s.)	*G. trunc.* (d.)	*G. hirs.*	*G. scit.*	*G. glut.*	*G. Uvula*	*unknown*
1	0.2	100	0	8	464	0	616	155	1784	144	418	204	21	0	48	98	0	8
2	0.2	17	0	1	105	0	90	24	428	20	159	41	2	0	8	21	0	4
3	0.2	16	0	0	337	1	0	100	1063	16	357	66	5	0	13	87	0	16
4	0 3	37	0	3	505	8	80	96	1704	56	272	109	0	0	8	260	0	16
5	0.2	13	0	0	135	4	12	36	580	0	228	79	0	0	0	204	0	1
6	0 2	11	0	1	53	0	4	12	248	4	125	51	0	0	2	161	0	2
7	0.2	11	0	2	40	2	16	24	144	0	132	84	1	0	0	152	0	0
8	0.2	16	0	0	40	2	8	8	40	0	57	70	0	0	4	36	0	0
9	0 2	6	0	0	23	0	8	4	24	1	33	84	3	0	1	27	0	0
10	0 2	12	0	0	29	0	6	0	19	1	21	60	0	0	2	18	0	0
11	0.2	6	0	1	53	2	3	3	21	1	27	73	0	0	5	13	0	0
12	0 3	25	0	1	228	11	5	1	7	0	22	60	2	0	2	24	0	1
13	0.2	23	0	0	749	20	22	0	20	0	102	74	1	0	0	56	0	2
14	0 2	18	0	0	935	36	28	0	40	0	249	57	4	0	17	112	0	4
15	0 2	5	0	0	565	24	164	8	148	0	184	85	1	0	5	113	0	1
16	0 2	5	0	0	218	6	116	10	118	0	52	70	0	0	24	91	0	0
17	0.2	0	0	0	73	0	19	2	28	0	23	31	0	0	54	29	0	3
18	0 2	3	0	0	16	1	24	0	6	0	3	16	2	0	20	37	0	8
19	0.2	2	0	0	29	0	19	0	8	0	10	4	0	0	10	15	0	0
20	0.2	9	0	0	149	1	151	13	132	1	19	10	0	0	8	18	0	5
21	NA	NA	NA	NA	NA	NA	NA	NA	NA	NA	NA	NA	NA	NA	NA	NA	NA	NA

SAF 51°S, 3300m

Cup	Split	*O. Univ.*	*G. ruber*	*G. calida*	*G. bull.*	*G. falc.*	*G. quinq.*	*N. pachy* (s.)	*N. pachy* (d.)	*N. dut.*	*G. infl.*	*G. trunc.* (s.)	*G. trunc.* (d.)	*G. hirs.*	*G. scit.*	*G. glut.*	*G. Uvula*	*unknown*
1	0.1	0	0	0	129	2	53	1	4	0	83	12	0	2	0	55	0	0
2	0.1	0	0	0	176	3	22	2	5	0	66	8	0	0	0	22	0	0
3	0.1	0	0	0	2144	0	80	28	16	0	396	32	0	0	0	114	0	0
4	0 1	0	0	0	2813	0	68	44	4	0	588	20	0	0	0	208	0	0
5	0.1	0	0	0	2205	0	168	48	8	0	1396	20	4	0	0	270	0	0
6	0 1	0	0	0	1458	0	76	14	8	0	602	12	0	0	0	118	0	0
7	0.1	0	0	0	1191	0	100	28	4	0	735	24	4	0	0	192	0	4
8	0.1	0	0	0	1603	0	108	28	20	0	495	12	0	0	0	136	0	0
9	0.1	0	0	0	458	0	122	24	26	0	285	16	0	0	0	90	0	2
10	0.1	0	0	0	138	0	37	24	28	0	36	16	2	0	0	36	0	0
11	0.1	0	0	0	564	0	168	172	124	0	74	20	1	0	0	70	0	1
12	0.1	0	0	0	440	0	184	392	232	0	78	23	2	0	0	61	0	0
13	0 1	0	0	0	235	0	72	292	232	0	14	16	0	0	0	46	0	0
14	0.1	0	0	0	17	0	10	27	46	0	1	1	0	0	0	1	0	0
15	0 1	0	0	0	161	0	44	284	246	0	0	8	1	0	0	48	0	0
16	0.1	0	0	0	148	0	38	108	174	0	1	11	0	0	0	62	0	2
17	0.1	0	0	0	187	0	42	146	148	0	5	15	0	0	0	102	0	2
18	0.1	0	0	0	105	0	60	228	88	0	2	12	2	0	0	72	0	0
19	0 1	0	0	0	225	0	198	318	144	0	5	21	4	0	0	124	0	2
20	0.1	2	0	0	111	0	164	192	48	0	5	10	0	0	0	91	8	0
21	0.1	0	0	0	414	0	432	368	116	0	13	15	1	0	8	136	0	0

PFZ 54°S, 800m

Cup	Split	*O. Univ.*	*G. ruber*	*G. calida*	*G. bull.*	*G. falc.*	*G. quinq.*	*N. pachy* (s.)	*N. pachy* (d.)	*N. dut.*	*G. infl.*	*G. trunc.* (s.)	*G. trunc.* (d.)	*G. hirs.*	*G. scit.*	*G. glut.*	*G. Uvula*	*unknown*
1	0.1	0	0	0	0	0	0	0	0	0	0	0	0	0	0	0	0	0
2	0.1	0	0	0	0	0	0	0	0	0	0	0	0	0	0	0	0	0
3	0 1	0	0	0	0	0	0	0	0	0	0	0	0	0	0	0	0	0
4	0.1	0	0	0	2	0	24	50	0	0	1	0	0	0	0	6	0	0
5	0 1	0	0	0	8	0	106	491	19	0	6	0	0	0	0	46	0	0
6	0.1	0	0	0	3	0	67	367	14	0	1	0	0	0	0	24	0	1
7	0 1	0	0	0	10	0	316	683	40	0	4	0	0	0	0	40	0	0
8	0.1	0	0	0	30	0	2352	944	104	0	24	0	0	0	0	120	0	0
9	0.1	0	0	0	231	0	352	184	20	0	61	0	0	0	0	148	0	0
10	0.1	0	0	0	51	0	363	119	5	0	29	0	0	0	0	69	0	0
11	0.1	0	0	0	179	0	420	164	0	0	16	0	0	0	0	113	0	0
12	0.1	0	0	0	262	0	356	860	44	0	4	11	0	0	0	45	0	4
13	0 1	0	0	0	85	0	90	444	24	0	8	2	0	0	0	24	0	4
14	0.1	0	0	0	56	0	80	292	36	0	2	0	0	0	0	16	0	0
15	0.1	0	0	0	64	0	53	330	18	0	1	0	0	0	0	12	0	0
16	0.1	0	0	0	56	0	56	290	46	0	5	0	0	0	0	12	0	0
17	0.1	0	0	0	81	0	32	708	64	0	4	0	0	0	0	20	0	4
18	0.1	0	0	0	77	0	44	1624	100	0	0	0	0	0	0	20	0	8
19	0.1	0	0	0	120	0	176	2601	152	0	0	0	0	0	0	64	0	0
20	0.1	0	0	0	89	0	64	2081	96	0	0	0	0	0	0	16	0	4
21	0.1	0	0	0	49	0	118	820	44	0	0	2	0	0	0	26	0	0
1-98	0.2	0	0	0	77	0	544	1036	8	0	0	0	0	0	0	48	0	0

PFZ 54°S, 1500m

Cup	Split	*O. Univ.*	*G. ruber*	G. calida	G. bull.	*G. falc.*	*G. quinq.*	*N. pachy* (s.)	*N. pachy* (d.)	*N. dut.*	*G. infl.*	*G. trunc.* (s.)	*G. trunc.* (d.)	*G. hirs.*	*G. scit.*	*G. glut.*	*G. Uvula*	*unknown*
1	0.1	0	0	0	0	0	5	2	0	0	1	0	0	0	0	3	0	0
3	0 1	0	0	0	1	0	17	65	3	0	2	0	0	0	0	7	0	0
5	0.1	0	0	0	2	0	11	174	5	0	2	0	0	0	1	10	0	0
6	0.1	0	0	0	2	0	28	252	11	0	1	0	0	0	0	18	0	2
7	0 1	0	0	0	15	0	150	540	28	0	0	0	0	0	0	72	0	0
8	0 1	0	0	0	8	0	520	584	36	0	4	0	0	0	0	92	0	0
9	0 1	0	0	0	99	0	1208	288	29	0	7	0	0	0	0	77	0	0
10	0 1	0	0	0	29	0	566	142	10	0	9	0	0	0	0	67	0	0
11	0.1	0	0	0	79	0	648	93	8	0	23	0	0	0	0	48	0	0
12	0 1	0	0	0	81	0	336	168	14	0	4	2	0	0	0	28	0	0
13	0.1	0	0	0	150	0	172	616	22	0	6	4	2	0	0	20	0	0
14	0 1	0	0	0	24	0	56	140	3	0	2	0	0	0	0	6	0	0
15	0 1	0	0	0	21	0	79	147	10	0	0	0	0	0	0	9	0	0
16	0.1	0	0	0	26	0	29	85	6	0	0	0	0	0	0	7	0	0
17	0.1	0	0	0	9	0	30	117	12	0	2	0	0	0	0	7	0	1
18	0.1	0	0	0	6	0	20	128	19	0	0	0	0	0	0	5	0	0
19	0.1	0	0	0	32	0	45	382	17	0	0	0	0	0	0	6	0	0
20	0 1	0	0	0	6	0	28	214	5	0	0	0	0	0	0	6	0	0
21	0.1	0	0	0	11	0	35	189	8	0	0	0	0	0	0	9	0	1
1-98	0.2	0	0	0	73	0	624	1272	64	0	8	0	0	0	0	48	0	40

APPENDIX II

Total planktonic foraminiferal fluxes collected in each sediment trap cup at 42°S, 44°S, 47°S, 51°S and 54°S for all trap depths.

NCR 300

Cup	Split	*O. Univ.*	*G. ruber*	*G. aequil.*	*G. calida*	*G. bull.*	*G. falc.*	*G. quinq.*	*N. pachy* (s.)	*N. pachy* (d.)	*N. dut.*	*G. infl.*	*G. trunc.* (s.)	*G. trunc.* (d.)	*G. crass.*	*G. hirs.*	*G. scit.*	*G. glut.*	*G. Uvula*	*unknown*
1	0.25	0	0	3	6	142	0	4	10	76	21	2643	25	1	0	0	7	18	0	0
2	0.25	40	0	0	0	152	0	8	16	280	88	2600	56	8	0	0	0	80	0	0
3	0 25	48	0	0	0	208	0	8	48	232	40	1784	8	0	0	0	8	72	0	0
4	0.125	56	0	16	8	408	0	48	72	504	40	1888	24	0	0	0	32	376	0	0
5	0.125	0	0	0	0	0	0	0	0	0	0	0	0	0	0	0	0	0	0	0
6	0.25	0	0	0	0	0	0	0	0	0	0	1	0	0	0	0	0	0	0	0
7	0.125	0	0	0	0	0	0	0	1	2	0	0	0	0	0	0	0	0	0	0
8	0 25	0	0	0	0	0	0	0	1	0	0	0	0	0	0	0	0	0	0	0
9	N/A	N/A	N/A	N/A	N/A	N/A	N/A	N/A	N/A	N/A	N/A	N/A	N/A	N/A	N/A	N/A	N/A	N/A	N/A	N/A
10	N/A	N/A	N/A	N/A	N/A	N/A	N/A	N/A	N/A	N/A	N/A	N/A	N/A	N/A	N/A	N/A	N/A	N/A	N/A	N/A
11	N/A	N/A	N/A	N/A	N/A	N/A	N/A	N/A	N/A	N/A	N/A	N/A	N/A	N/A	N/A	N/A	N/A	N/A	N/A	N/A
12	N/A	N/A	N/A	N/A	N/A	N/A	N/A	N/A	N/A	N/A	N/A	N/A	N/A	N/A	N/A	N/A	N/A	N/A	N/A	N/A
13	N/A	N/A	N/A	N/A	N/A	N/A	N/A	N/A	N/A	N/A	N/A	N/A	N/A	N/A	N/A	N/A	N/A	N/A	N/A	N/A
14	0 083	1	0	0	3	28	0	15	13	25	5	70	0	0	3	0	21	9	0	0
15	0.25	14	0	0	0	50	0	10	10	44	4	496	0	0	40	0	14	10	0	0
16	0.25	2	0	1	0	17	0	0	0	13	0	146	0	0	1	0	5	0	0	0
17	0 25	0	0	0	0	12	0	1	4	8	2	65	0	0	1	0	3	2	0	0
18	0.25	4	0	0	0	29	0	3	0	21	1	241	3	0	0	0	3	3	0	0
19	N/A	N/A	N/A	N/A	N/A	N/A	N/A	N/A	N/A	N/A	N/A	N/A	N/A	N/A	N/A	N/A	N/A	N/A	N/A	N/A
20	0 25	0	0	0	0	7	0	1	1	4	1	33	0	0	0	0	4	1	0	0
21	0.125	0	0	0	0	0	0	0	0	0	0	0	0	0	0	0	0	0	0	0

NCR 1000

Cup	Split	*O. univ.*	*G. ruber*	*G. aequil.*	*G. calida*	*G. bull.*	*G. falc.*	*G. quinq.*	*N. pachy.* (s.)	*N. pachy* (d.)	*N. dut.*	*G. infl.*	*G. trunc.* (s.)	*G. trunc.* (d.)	*G. crass.*	*G. hirs.*	*G. scit.*	*G. glut.*	*G. uvula*	*unknown*
1	0 25	8	0	8	0	416	0	0	72	568	32	2408	0	0	0	0	176	96	0	0
2	0.25	8	0	8	16	224	40	16	48	464	72	1720	0	0	0	0	168	32	0	0
3	0.25	144	0	0	16	752	16	16	48	1232	112	3136	16	0	0	0	496	48	0	0
4	0.25	768	0	32	0	496	0	80	144	864	48	3760	32	0	0	0	288	384	0	0
5	0.25	16	0	24	40	256	0	56	8	208	16	1440	16	0	0	0	280	200	0	0
6	0 25	12	0	20	4	292	0	100	20	224	4	976	8	0	0	0	136	72	0	24
7	0.25	28	0	8	20	428	0	68	8	116	4	648	4	0	0	0	24	48	0	12
8	0.25	12	0	4	8	248	0	40	32	104	0	604	12	0	0	0	12	40	0	8
9	0.25	8	2	0	6	228	0	32	14	94	2	514	8	0	0	0	6	18	0	2
10	0.25	32	0	0	8	316	0	68	12	192	12	360	0	0	0	0	8	16	0	0
11	0.25	64	0	16	32	1632	64	288	304	1904	208	4464	32	0	0	0	0	128	0	16
12	0.25	8	0	0	8	112	0	8	16	160	8	1848	0	0	0	0	0	0	0	0
13	0.25	4	2	0	4	136	8	12	10	128	4	366	2	0	0	0	6	22	0	4
14	0.25	3	0	1	0	66	3	8	3	50	4	191	2	0	0	0	21	5	0	1
15	0 25	1	13	0	3	72	0	19	4	23	1	36	0	0	3	0	16	4	0	0
16	0.25	0	1	1	0	33	0	7	12	17	1	33	0	0	1	0	8	5	0	0
17	0.25	0	5	2	2	12	0	0	2	21	1	213	0	0	0	0	28	0	0	0
18	0.25	4	4	0	0	20	0	6	8	50	6	708	0	0	0	0	38	0	0	0
19	0.25	32	0	0	0	800	0	32	0	448	32	6048	0	0	0	0	96	0	0	0
20	0.25	0	8	0	0	600	8	0	72	280	8	1024	8	0	0	0	16	32	0	8
21	0.25	24	0	8	0	344	0	0	16	328	8	1632	24	0	0	0	32	8	0	0

SCR 300

Cup	Split	*O. univ.*	*G. ruber*	*G. aequil.*	*G. calida*	*G. bull.*	*G. falc.*	*G. quinq.*	*N. pachy* (s.)	*N. pachy* (d.)	*N. dut.*	*G. infl.*	*G. trunc.* (s.)	*G. trunc.* (d.)	*G. crass.*	*G. hirs.*	*G. scit.*	*G. glut.*	*G. uvula*	*unknown*
1	0.125	0	0	0	0	0	0	0	0	0	0	0	0	0	0	0	0	0	0	0
2	0.25	5	0	0	0	25	0	7	19	50	1	2	173	0	0	0	1	106	0	0
3	0.125	0	0	0	0	0	0	0	0	0	0	0	0	0	0	0	0	0	0	0
4	0.25	0	0	0	0	0	0	0	0	0	0	3	2	0	0	0	0	8	0	0
5	0.25	0	0	0	0	117	0	48	8	40	0	30	135	0	0	0	0	58	1	0
6	0 25	4	0	0	0	688	60	64	8	280	0	372	188	0	0	0	4	140	0	0
7	0.25	0	0	0	0	0	0	0	0	0	0	0	0	0	0	0	0	0	0	0
8	0 25	0	0	0	0	0	0	0	0	0	0	0	0	0	0	0	0	0	0	0
9	0.25	0	0	0	0	2	0	0	0	0	0	4	0	0	0	0	0	0	0	0
10	0.25	0	0	0	0	0	0	0	0	0	0	0	0	0	0	0	0	0	0	0
11	0.25	0	0	0	0	0	0	0	0	0	0	0	0	0	0	0	0	0	0	0
12	0 25	34	0	0	0	69	0	2	3	8	0	17	112	0	0	0	0	16	0	0
13	0.125	4	0	0	0	1	0	0	0	0	0	0	0	0	0	0	0	0	0	0
14	0 125	0	0	0	0	0	0	0	0	0	0	0	0	0	0	0	0	0	0	0
15	0.125	0	0	0	0	0	0	0	0	0	0	0	0	0	0	0	0	0	0	0
16	0 25	0	0	0	0	0	0	0	0	0	0	0	0	0	0	0	0	1	0	0
17		N/A	N/A	N/A	N/A	N/A	N/A	N/A	N/A	N/A	N/A	N/A	N/A	N/A	N/A	N/A	N/A	N/A	N/A	0
18	0.125	0	0	0	0	0	0	0	0	0	0	0	0	0	0	0	0	0	0	0
19	0.25	0	0	0	0	0	0	0	0	0	0	0	0	0	0	0	0	0	0	0
20	0.125	0	0	0	0	0	0	0	0	0	0	0	0	0	0	0	0	0	0	0
21	0.125	3	0	0	0	4	0	0	0	1	0	0	0	0	0	0	0	0	0	0

SCR 1000

Cup	Split	*O. univ.*	*G. ruber*	*G. aequil.*	*G. calida*	*G. bull.*	*G. falc.*	*G. quinq.*	*N. pachy* (s.)	*N. pachy* (d.)	*N. dut.*	*G. infl.*	*G. trunc.* (s.)	*G. trunc.* (d.)	*G. crass.*	*G. hirs.*	*G. scit.*	*G. glut.*	*G. uvula*	*unknown*
1	0.25	1	0	0	0	83	0	18	6	320	2	55	251	7	0	0	106	196	0	0
2	0.25	2	0	0	0	53	0	22	2	142	1	4	80	3	0	0	32	134	0	0
3	0.25	0	0	0	0	127	0	22	8	63	0	29	104	0	0	0	75	122	0	0
4	0 25	3	0	0	0	122	0	22	5	40	0	29	64	1	0	1	53	50	0	0
5	0.25	1	0	0	0	416	6	106	16	136	0	71	84	0	0	0	57	31	0	0
6	0.25	10	0	0	0	1340	0	144	40	560	0	292	63	2	0	0	81	164	0	0
7	0 125	1	0	0	0	3265	0	144	88	476	0	600	37	0	0	0	46	205	0	0
8	0.25	16	0	0	0	7008	0	352	384	1144	0	1510	24	0	0	0	39	286	0	0
9	0.25	21	0	0	0	837	0	156	52	456	0	631	61	1	0	0	43	118	0	0
10	0.25	5	0	0	0	381	0	126	26	298	0	264	61	0	0	0	5	71	0	0
11	0.25	111	0	0	0	314	0	120	42	146	0	53	103	1	0	0	7	85	0	0
12	0 25	16	0	0	0	130	0	44	19	55	1	10	36	0	0	0	4	18	0	2
13	0.25	69	0	0	0	75	0	42	12	38	0	28	58	1	0	0	3	14	0	0
14	0.25	45	0	0	0	71	0	40	18	63	3	46	54	0	0	1	5	13	0	0
15	0.25	88	0	0	0	88	0	111	23	178	14	35	43	2	0	2	8	29	0	0
16	0.25	21	0	0	0	216	0	172	48	786	17	33	30	0	0	0	3	35	0	0
17	0.25	51	0	0	0	230	0	224	48	1690	75	47	11	0	0	0	11	2	0	0
18	0 25	14	0	0	0	169	0	163	42	1791	183	24	21	0	0	0	26	55	0	2
19	0.25	15	0	0	0	126	0	72	48	712	94	38	7	0	0	0	9	21	0	0
20	0.25	11	0	0	0	115	0	56	36	689	66	40	7	0	0	0	15	27	0	0
21	0.125	0	0	0	0	0	0	0	0	0	0	0	0	0	0	0	0	0	0	0

SAZ 47°S, 1000m

Cup	Split	*O. Univ.*	*G. ruber*	G. calida	G. bull.	*G. falc.*	*G. quinq.*	*N. pachy* (s.)	*N. pachy* (d.)	*N. dut.*	*G. infl.*	*G. trunc.* (s.)	*G. trunc.* (d.)	*G. hirs.*	*G. scit.*	*G. glut.*	*G. Uvula*	*unknown*
1	0 1	0	0	0	57	2	2	1	4	0	15	10	0	0	15	5	0	1
2	0 1	0	0	0	113	3	11	0	23	1	30	10	0	0	11	16	0	0
3	0 1	1	0	0	172	9	24	9	117	0	93	28	0	3	8	44	0	0
4	0.1	0	0	0	104	1	7	3	90	0	148	22	0	1	15	19	0	0
5	0 1	1	0	0	20	0	1	3	29	0	34	18	0	0	16	15	0	0
6	0.1	0	0	0	29	0	30	6	21	0	41	27	0	0	10	11	0	0
7	0.1	0	0	0	13	0	4	1	6	0	9	4	0	0	4	4	0	0
8	0.1	0	0	0	22	0	28	2	18	0	23	21	0	0	12	7	0	0
9	0.1	1	0	0	20	0	25	6	10	2	6	9	0	0	2	2	0	0
10	0 1	0	0	0	43	0	79	4	17	0	30	23	0	0	4	11	0	0
11	0.1	38	0	0	80	1	70	23	47	0	40	41	2	0	6	7	0	0
12	0.1	4	0	0	85	3	54	145	181	5	48	37	2	0	17	48	0	0
13	0.1	0	0	0	33	4	2	40	127	0	38	29	1	0	6	39	0	0
14	0 1	10	0	0	69	0	25	77	212	14	22	6	1	0	8	34	0	0
15	0.1	4	0	0	90	0	23	60	227	15	43	31	2	0	4	43	0	0
16	0.1	2	0	0	18	0	10	17	41	2	9	7	0	0	2	15	0	0
17	0.1	14	0	0	28	0	29	37	75	7	20	14	0	0	0	30	0	0
18	0.1	9	0	0	45	0	20	23	55	3	16	15	1	0	1	20	0	0
19	0.1	23	0	0	73	0	49	60	130	10	36	29	1	0	1	50	0	0
20	0.1	0	0	0	0	0	0	0	0	0	0	0	0	0	0	0	0	0
21	0 1	0	0	0	0	0	0	0	0	0	0	0	0	0	0	0	0	0

SAZ 47°S, 3800m

Cup	Split	*O. Univ.*	*G. ruber*	*G. calida*	*G. bull.*	*G. falc.*	*G. quinq.*	*N. pachy* (s.)	*N. pachy* (d.)	*N. dut.*	*G. infl.*	*G. trunc.* (s.)	*G. trunc.* (d.)	*G. hirs.*	*G. scit.*	*G. glut.*	*G. Uvula*	*unknown*
1	0.1	1	0	0	49	3	3	0	2	0	5	4	0	0	0	4	0	0
2	0 1	2	0	0	208	7	2	1	7	0	43	28	1	0	0	14	0	0
3	0.1	0	0	0	121	3	3	2	42	1	94	19	0	0	2	14	0	2
4	0 1	1	1	0	130	0	19	6	84	2	107	19	0	0	3	31	0	1
5	0.1	0	0	0	32	0	11	1	48	0	48	17	0	0	7	18	0	0
6	0 1	0	0	1	70	2	28	5	72	1	81	31	0	0	13	42	0	1
7	0 1	0	0	0	68	0	39	2	32	0	48	29	3	0	6	17	0	3
8	0.1	0	0	0	15	0	32	1	16	0	6	12	0	0	13	9	0	1
9	0.1	0	0	0	33	0	21	0	10	0	31	32	0	0	15	7	0	1
10	0 1	0	0	0	29	0	68	4	23	0	12	16	1	0	22	16	0	0
11	0.1	3	0	1	48	0	134	6	39	0	21	24	0	0	17	20	0	0
12	0.1	24	0	0	84	0	181	26	47	0	40	30	1	0	9	26	0	1
13	0 1	2	0	0	27	0	43	21	32	1	22	21	0	0	2	7	0	0
14	0.1	1	0	1	53	0	50	68	102	5	53	26	1	0	13	32	0	1
15	0.1	0	0	0	93	0	69	110	251	11	64	25	2	0	13	52	0	2
16	0.1	2	0	2	50	0	43	92	216	6	36	15	0	0	4	41	0	0
17	0.1	4	0	0	36	0	37	70	135	6	16	15	0	0	9	39	0	3
18	0.1	4	0	0	9	0	19	43	59	0	12	5	0	0	4	20	0	0
19	0 1	8	0	0	28	0	59	71	156	6	27	27	0	0	10	51	0	0
20	0.1	1	0	0	62	0	74	76	368	4	56	84	6	0	6	28	0	2
21	0.1	0	0	0	0	0	0	0	0	0	0	0	0	0	0	0	0	0

SAZ 47°S, 3800m, 1998 redeployment

Cup	Split	*O. Univ.*	*G. ruber*	*G. calida*	*G. bull.*	*G. falc.*	*G. quinq.*	*N. pachy* (s.)	*N. pachy* (d.)	*N. dut.*	*G. infl.*	*G. trunc.* (s.)	*G. trunc.* (d.)	*G. hirs.*	*G. scit.*	*G. glut.*	*G. Uvula*	*unknown*
1	0.2	100	0	8	464	0	616	155	1784	144	418	204	21	0	48	98	0	8
2	0.2	17	0	1	105	0	90	24	428	20	159	41	2	0	8	21	0	4
3	0 2	16	0	0	337	1	0	100	1063	16	357	66	5	0	13	87	0	16
4	0.3	37	0	3	505	8	80	96	1704	56	272	109	0	0	8	260	0	16
5	0 2	13	0	0	135	4	12	36	580	0	228	79	0	0	0	204	0	1
6	0 2	11	0	1	53	0	4	12	248	4	125	51	0	0	2	161	0	2
7	0.2	11	0	2	40	2	16	24	144	0	132	84	1	0	0	152	0	0
8	0.2	16	0	0	40	2	8	8	40	0	57	70	0	0	4	36	0	0
9	0 2	6	0	0	23	0	8	4	24	1	33	84	3	0	1	27	0	0
10	0.2	12	0	0	29	0	6	0	19	1	21	60	0	0	2	18	0	0
11	0 2	6	0	1	53	2	3	3	21	1	27	73	0	0	5	13	0	0
12	0.3	25	0	1	228	11	5	1	7	0	22	60	2	0	2	24	0	1
13	0.2	23	0	0	749	20	22	0	20	0	102	74	1	0	0	56	0	2
14	0.2	18	0	0	935	36	28	0	40	0	249	57	4	0	17	112	0	4
15	0.2	5	0	0	565	24	164	8	148	0	184	85	1	0	5	113	0	1
16	0.2	5	0	0	218	6	116	10	118	0	52	70	0	0	24	91	0	0
17	0.2	0	0	0	73	0	19	2	28	0	23	31	0	0	54	29	0	3
18	0 2	3	0	0	16	1	24	0	6	0	3	16	2	0	20	37	0	8
19	0.2	2	0	0	29	0	19	0	8	0	10	4	0	0	10	15	0	0
20	0.2	9	0	0	149	1	151	13	132	1	19	10	0	0	8	18	0	5
21	NA	NA	NA	NA	NA	NA	NA	NA	NA	NA	NA	NA	NA	NA	NA	NA	NA	NA

SAF 51°S, 3300m

Cup	Split	*O. Univ.*	*G. ruber*	*G. calida*	*G. bull.*	*G. falc.*	*G. quinq.*	*N. pachy (s.)*	*N. pachy (d.)*	*N. dut.*	*G. infl.*	*G. trunc. (s.)*	*G. trunc. (d.)*	*G. hirs.*	*G. scit.*	*G. glut.*	*G. Uvula*	*unknown*
1	0.1	0	0	0	129	2	53	1	4	0	83	12	0	2	0	55	0	0
2	0 1	0	0	0	176	3	22	2	5	0	66	8	0	0	0	22	0	0
3	0.1	0	0	0	2144	0	80	28	16	0	396	32	0	0	0	114	0	0
4	0.1	0	0	0	2813	0	68	44	4	0	588	20	0	0	0	208	0	0
5	0 1	0	0	0	2205	0	168	48	8	0	1396	20	4	0	0	270	0	0
6	0 1	0	0	0	1458	0	76	14	8	0	602	12	0	0	0	118	0	0
7	0.1	0	0	0	1191	0	100	28	4	0	735	24	4	0	0	192	0	4
8	0.1	0	0	0	1603	0	108	28	20	0	495	12	0	0	0	136	0	0
9	0.1	0	0	0	458	0	122	24	26	0	285	16	0	0	0	90	0	2
10	0 1	0	0	0	138	0	37	24	28	0	36	16	2	0	0	36	0	0
11	0.1	0	0	0	564	0	168	172	124	0	74	20	1	0	0	70	0	1
12	0.1	0	0	0	440	0	184	392	232	0	78	23	2	0	0	61	0	0
13	0.1	0	0	0	235	0	72	292	232	0	14	16	0	0	0	46	0	0
14	0.1	0	0	0	17	0	10	27	46	0	1	1	0	0	0	1	0	0
15	0 1	0	0	0	161	0	44	284	246	0	0	8	1	0	0	48	0	0
16	0.1	0	0	0	148	0	38	108	174	0	1	11	0	0	0	62	0	2
17	0.1	0	0	0	187	0	42	146	148	0	5	15	0	0	0	102	0	2
18	0 1	0	0	0	105	0	60	228	88	0	2	12	2	0	0	72	0	0
19	0 1	0	0	0	225	0	198	318	144	0	5	21	4	0	0	124	0	2
20	0.1	2	0	0	111	0	164	192	48	0	5	10	0	0	0	91	8	0
21	0 1	0	0	0	414	0	432	368	116	0	13	15	1	0	8	136	0	0

PFZ 54°S, 800m

Cup	Split	*O. Univ.*	*G. ruber*	G. calida	*G. bull.*	*G. falc.*	*G. quinq.*	*N. pachy* (s.)	*N. pachy* (d.)	*N. dut.*	*G. infl.*	*G. trunc.* (s.)	*G. trunc.* (d.)	*G. hirs.*	*G. scit.*	*G. glut.*	*G. Uvula*	*unknown*
1	0.1	0	0	0	0	0	0	0	0	0	0	0	0	0	0	0	0	0
2	0 1	0	0	0	0	0	0	0	0	0	0	0	0	0	0	0	0	0
3	0.1	0	0	0	0	0	0	0	0	0	0	0	0	0	0	0	0	0
4	0.1	0	0	0	2	0	24	50	0	0	1	0	0	0	0	6	0	0
5	0.1	0	0	0	8	0	106	491	19	0	6	0	0	0	0	46	0	0
6	0.1	0	0	0	3	0	67	367	14	0	1	0	0	0	0	24	0	1
7	0 1	0	0	0	10	0	316	683	40	0	4	0	0	0	0	40	0	0
8	0 1	0	0	0	30	0	2352	944	104	0	24	0	0	0	0	120	0	0
9	0 1	0	0	0	231	0	352	184	20	0	61	0	0	0	0	148	0	0
10	0.1	0	0	0	51	0	363	119	5	0	29	0	0	0	0	69	0	0
11	0.1	0	0	0	179	0	420	164	0	0	16	0	0	0	0	113	0	0
12	0 1	0	0	0	262	0	356	860	44	0	4	11	0	0	0	45	0	4
13	0.1	0	0	0	85	0	90	444	24	0	8	2	0	0	0	24	0	4
14	0 1	0	0	0	56	0	80	292	36	0	2	0	0	0	0	16	0	0
15	0.1	0	0	0	64	0	53	330	18	0	1	0	0	0	0	12	0	0
16	0.1	0	0	0	56	0	56	290	46	0	5	0	0	0	0	12	0	0
17	0.1	0	0	0	81	0	32	708	64	0	4	0	0	0	0	20	0	4
18	0.1	0	0	0	77	0	44	1624	100	0	0	0	0	0	0	20	0	8
19	0.1	0	0	0	120	0	176	2601	152	0	0	0	0	0	0	64	0	0
20	0.1	0	0	0	89	0	64	2081	96	0	0	0	0	0	0	16	0	4
21	0.1	0	0	0	49	0	118	820	44	0	0	2	0	0	0	26	0	0
1-98	0 2	0	0	0	77	0	544	1036	8	0	0	0	0	0	0	48	0	0

PFZ 54°S, 1500m

Cup	Split	*O. Univ.*	*G. ruber*	*G. calida*	*G. bull.*	*G. falc.*	*G. quinq.*	*N. pachy* (s.)	*N. pachy* (d.)	*N. dut.*	*G. infl.*	*G. trunc.* (s.)	*G. trunc.* (d.)	*G. hirs.*	*G. scit.*	*G. glut.*	*G. Uvula*	*unknown*
1	0.1	0	0	0	0	0	5	2	0	0	1	0	0	0	0	3	0	0
3	0 1	0	0	0	1	0	17	65	3	0	2	0	0	0	0	7	0	0
5	0.1	0	0	0	2	0	11	174	5	0	2	0	0	0	1	10	0	0
6	0 1	0	0	0	2	0	28	252	11	0	1	0	0	0	0	18	0	2
7	0.1	0	0	0	15	0	150	540	28	0	0	0	0	0	0	72	0	0
8	0.1	0	0	0	8	0	520	584	36	0	4	0	0	0	0	92	0	0
9	0 1	0	0	0	99	0	1208	288	29	0	7	0	0	0	0	77	0	0
10	0 1	0	0	0	29	0	566	142	10	0	9	0	0	0	0	67	0	0
11	0.1	0	0	0	79	0	648	93	8	0	23	0	0	0	0	48	0	0
12	0.1	0	0	0	81	0	336	168	14	0	4	2	0	0	0	28	0	0
13	0.1	0	0	0	150	0	172	616	22	0	6	4	2	0	0	20	0	0
14	0.1	0	0	0	24	0	56	140	3	0	2	0	0	0	0	6	0	0
15	0.1	0	0	0	21	0	79	147	10	0	0	0	0	0	0	9	0	0
16	0.1	0	0	0	26	0	29	85	6	0	0	0	0	0	0	7	0	0
17	0.1	0	0	0	9	0	30	117	12	0	2	0	0	0	0	7	0	1
18	0.1	0	0	0	6	0	20	128	19	0	0	0	0	0	0	5	0	0
19	0.1	0	0	0	32	0	45	382	17	0	0	0	0	0	0	6	0	0
20	0.1	0	0	0	6	0	28	214	5	0	0	0	0	0	0	6	0	0
21	0.1	0	0	0	11	0	35	189	8	0	0	0	0	0	0	9	0	1
1-98	0 2	0	0	0	73	0	624	1272	64	0	8	0	0	0	0	48	0	40

APPENDIX III

Carbon and isotopic composition for selected species of planktonic foraminifera at 42°S, 44°S, 47°S, 51°S and 54°S.

42°S, NCR 1000

	G. BULLOIDES		*G. INFLATA*		*N. PACHYDERMA* (d.)		*G. QUINQUELOBA*	
Cup	$\delta^{13}C$	$\delta^{18}O$	$\delta^{13}C$	$\delta^{18}O$	$\delta^{13}C$	$\delta^{18}O$	$\delta^{13}C$	$\delta^{18}O$
1	-0.5280	0.9125	0 8566	1.3674	0.0426	0 8424	NA	NA
2	-0 7591	0 7020	0.7780	1.2152	0.2333	0.8490	NA	
3	-0.1647	0.7862	0.8407	1 1725	-0.0204	0 7838	-1.4723	0.4194
4	-0.3741	0.7335	0.7800	1.2443	-0 2362	0.9191	-1 4571	0.9167
5	-0 4842	0.6962	0.7566	1.2871	-0.0792	0 9571	-1.5993	1.1488
6	-0.3237	0.6736	0.9453	1.2226	-0.0254	0.8645	-1 5365	0 6814
7	-0.2921	0 5780	0.8363	1 2030	-0.1470	0.7110	-1.4890	0.5896
8	-0.7362	0 4878	0.6648	1.0042	-0 1083	0 6413	-1.6315	0.6803
9	-1.1919	-0.6167	0.6258	0 9989	0.0107	0.5428	-1.6677	0.5207
10	-1 1057	0.4074	0.6602	0 9990	-0.3038	0.4882	-1.6531	0.2824
11	-0.7277	0 5637	0.7593	1.2817	-0 1822	0 5006	-1 5322	0.3917
12	-1 2436	0.3016	0.6128	0 9289	-0.2001	0.4707	-0 9803	0 5977
13	-0.9937	0.1857	0 6372	0 7965	-0.0560	0.4964	-1 5907	0.4421
14	-1.1532	0.3030	0 6922	0 8059	-0.5093	0.5410	NA	NA
15	-1.4547	-0 2615	0 6340	0 8156	NA	NA	-1.3872	-0 0829
16	-1.1313	0 0286	-0 6050	0.8759	NA	NA	NA	NA
17	NA	NA	0.9874	0.4054	0 5124	-0.0317	NA	NA
18	-0.8442	-0.1548	0.7721	0.4310	0.0219	-0.1888	NA	NA
19	-0.3623	-0 0978	0.5296	0 7559	-0.2818	0.0146	-1.3486	-0.1797
20	-0.6548	-0 1698	0.7375	0 4667	-0.0648	0.0805	-0.7977	0.6665
21	-0 4821	0.1520	0.8789	0.8580	-0.0149	0 3130	NA	NA

44°S, SCR 1000

	G. BULLOIDES		*G. INFLATA*		*N. PACHYDERMA* (s.)		*N. PACHYDERMA* (d.)		*G. QUINQUELOBA*	
Cup	$\delta^{13}C$	$\delta^{18}O$	$\delta^{13}C$	$\delta^{18}O$	$\delta^{13}C$	$\delta^{18}O$	$\delta^{13}C$	$\delta^{18}O$	$\delta^{13}C$	$\delta^{18}O$
1	0 042	1 406	0.993	1.137	NA	NA	0.5803	0.8452	-0.158	1 499
2	-0.791	1.210	NA	NA	NA	NA	0 3308	0 8480	-0.452	1.061
3	-0 558	0 962	0.924	1.420	NA	NA	0.6005	1.0204	-0.527	1.169
4	-0 708	1.216	0.912	1.471	NA	NA	0.5514	1 2515	-1.031	1.000
5	-0.131	1.460	0.990	1.546	NA	NA	0.6500	1.7679	-0 9011	1.2345
6	0 4184	1.7845	0.8636	1.4818	NA	NA	0.4610	1.5018	-0.9320	1.2577
7	0.5723	1.8498	1.2233	2 0690	-0.100	1.262	0.4948	1 4048	-0.8437	1.3749
8	0 5843	1.8728	1.3062	2.1418	0 051	1.332	0.5902	1.4913	-0.8873	1.3956
9	0.7946	1.8639	1.1541	2.0978	-0.466	0.346	0.6503	1.4193	-0.6888	1.4979
10	0.6570	1 8053	1.1603	2 0451	-0.096	1.588	0 3926	1 8260	-0.5169	1.7332
11	0.5454	1 3335	1.236	2.037	-0.509	1 115	0.3660	1.3680	-0.8921	1.5120
12	0.0706	1.0620	0 902	1.492	NA	NA	0.4335	1.2393	-1.3976	0.0634
13	0 262	1.270	0.978	1.321	NA	NA	0 4416	1.2132	-0 8617	0.8477
14	-0.187	0.925	0.915	1 288	NA	NA	0.0150	0.9238	-0.9605	1.2312
15	0 088	0.776	1.003	1.337	NA	NA	-0.5782	0.3055	-1.4201	0.7025
16	-0 565	0.453	0.965	1 473	-0.149	0.512	-0 0091	0 4167	-1 1780	0.1635
17	-0.328	0.270	0.787	1 357	-0.1287	0.3857	0.3394	0.2242	-1.351	-0 100
18	-0.276	0.267	1.053	1 417	-0.3177	0.4047	0.3462	0.0851	-1.1848	0 7669
19	-0.053	0.206	0.993	1 466	0 2953	0.1327	0.2053	0.1674	-0.7942	0.2194
20	-0 545	0 129	1 023	1.453	0 3483	0 5357	0.4739	0 2572	-0.9863	0.2468
21	NA	NA	NA	NA	NA	NA	NA	NA	NA	NA

44°S, SCR 300

	G. BULLOIDES		*G. INFLATA*	
Cup	$\delta^{13}C$	$\delta^{18}O$	$\delta^{13}C$	$\delta^{18}O$
5	-0.343	1.501		
6	0.255	1.974	1.126	2.026
7	0.585	1.906	0.979	1.793
8	0.562	1.839		

42°S, NCR 1000 Individuals

SPECIES	CUP	$\delta^{13}C$ (VPDB)	$\delta^{18}O$ (VPDB)	MAX LENGTH (µm)	WEIGHT (µm)
G. bulloides	2	-0.87	0.62	415	9.5
G. bulloides	2	-0.90	0.53	390	6.5
G. bulloides	2	-0.92	0.75	465	18
G. bulloides	3	-0.19	0.41	575	11
G. bulloides	3	-0.08	0.62	530	9.6
G. bulloides	3	0.13	0.65	420	15
G. bulloides	3	-0.29	0.56	415	16
G. bulloides	3	-1.78	0.72	370	10.5
G. bulloides	3	-0.58	0.75	390	14.5
G. bulloides	12	-3.61	1.15	365	11
G. bulloides	12	-3.80	0.42	390	12
G. bulloides	12	-3.54	0.79	370	13
G. bulloides	12	-0.35	0.38	405	7.5
G. bulloides	12	-0.11	0.38	410	12.7
G. bulloides	12	-0.56	0.12	440	11
G. bulloides	19	0.09	-0.24	465	8.4
G. bulloides	19	-0.77	-0.46	500	9.4
G. bulloides	19	0.85	0.46	390	12.5
G. bulloides	19	0.61	0.51	390	14.5
G. bulloides	19	0.83	0.56	390	15.5
G. bulloides	19	0.94	0.49	420	17.5
G. bulloides	19	-0.53	-0.14	380	13.1
G. bulloides	19	-0 7	-0.26	445	15.8
G. bulloides	19	-0.28	-0.14	450	11.8
G. bulloides	19	-0.07	-0.05	455	11
G. inflata	2	0.64	0.96	430	23
G. inflata	2	0.74	0.99	380	15.5
G. inflata	2	0.86	0.99	390	22.5
G. inflata	2	0.69	1.05	380	16.5
G. inflata	3	0.68	0.83	432	25
G. inflata	3	0.87	1.10	380	16
G. inflata	3	0.79	0.82	370	18
G. inflata	3	0.59	0.97	420	21.5
G. inflata	12	-0.03	0.77	415	20
G. inflata	12	0.50	0.66	435	31.5
G. inflata	12	0.62	0.59	435	25.5
G. inflata	12	0.74	0.75	430	30
G. inflata	13	0.80	0.65	420	28
G. inflata	13	1.03	0.95	430	32.5
G. inflata	13	0.88	0.71	430	29.5
G. inflata	13	0.81	0.84	370	22.5
G. inflata	19	0.73	0.58	415	17.4
G. inflata	19	0.73	0.44	430	20.3
G. inflata	19	0.96	0.33	440	20.3
G. inflata	19	0.63	0.26	450	18.7

44°S, SCR 1000 Individuals

SPECIES	CUP	$\delta^{13}C$ (VPDB)	$\delta^{18}O$ (VPDB)	MAX LENGTH (µm)	WEIGHT (µm)
G. bulloides	6	0.63	1 67	370	16
G. bulloides	6	-0.13	2.09	370	13
G. bulloides	6	0.28	1.47	390	18
G. bulloides	6	0.38	1.50	360	14
G. bulloides	7	0.63	1.45	575	20.4
G. bulloides	7	0.73	1 30	500	19.1
G. bulloides	7	-0.44	1.23	420	9.2
G. bulloides	7	0.24	1.25	400	16.5
G. bulloides	7	0.63	1 75	380	18.5
G. bulloides	7	0.96	1.73	345	15
G. bulloides	7	0.70	1.63	390	11
G. bulloides	7	0.79	1.79	420	13
G. bulloides	7	0.56	1 57	515	27
G. bulloides	7	0.66	1.55	440	25
G. bulloides	7	-0.79	1.61	480	26
G. bulloides	7	0.11	1.72	490	33
G. bulloides	7	0.91	1 58	615	44.5
G. bulloides	7	0.43	1.69	590	42
G. bulloides	7	0.33	1.61	540	29
G. bulloides	7	0.53	1.68	660	52
G. bulloides	8	0.49	1.64	550	28.8
G. bulloides	8	0.98	1.64	540	22.8
G. bulloides	8	0.65	1.58	410	19.3
G. bulloides	8	0.51	1.59	580	23.9
G. bulloides	8	0.63	1.50	575	27.1
G. bulloides	9	0.64	1.33	450	17.5
G. bulloides	9	0.46	0.86	500	12.2
G. bulloides	9	0.76	1.74	500	25
G. bulloides	15	0.83	1.99	380	28
G. bulloides	17	0.17	0.81	360	9
G. bulloides	17	0.27	0.74	325	8
G. bulloides	17	-1.22	-0.66	390	5.5
G. bulloides	17	-0.05	0.05	415	15
G. bulloides	17	0.19	-0.34	490	11 5
G. bulloides	17	-0.11	0.00	480	13.5
G. bulloides	17	-0.01	0.05	500	17
G. bulloides	20	-1.03	-0.42	400	5.5
G. bulloides	20	-0.78	0.14	335	8

44°S, SCR 1000 Individuals cont.

SPECIES	CUP	$\delta^{13}C$ (VPDB)	$\delta^{18}O$ (VPDB)	MAX LENGTH (µm)	WEIGHT (µm)
G. inflata	6	0.91	1.54	395	18
G. inflata	6	0.91	1.40	345	12
G. inflata	6	1.05	1.40	380	15.5
G. inflata	6	1.17	1.75	445	38
G. inflata	7	1.04	1.99	415	27.5
G. inflata	7	1.22	1.88	440	52
G. inflata	7	1.16	1.54	430	16
G. inflata	7	1.22	1.95	415	39
G. inflata	15	0.94	1.60	390	25.5
G. inflata	17	0.85	1.12	390	18.5
G. inflata	17	0.54	0.81	410	20
G. inflata	17	0.84	1.11	390	17
G. inflata	17	1.33	0.24	465	22.5

47°S, SAZ

	G. BULLOIDES		*G. INFLATA*		*N. PACHYDMERMA* (s.)	
Cup	$\delta^{13}C$	$\delta^{18}O$	$\delta^{13}C$	$\delta^{18}O$	$\delta^{13}C$	$\delta^{18}O$
1	-0.195	1.451				
2	-0.171	1.500	0.713	1.441		
3	0.209	1.359	0.885	1 714		
4	-0.274	1.267	0.946	1.809		
5	-0.839	1.391	0.779	1.542		
6	-0.853	1.212	0.602	1.382		
7	-0.745	1.056	0.673	1.365		
8	-1.394	0.955				
9	-0.643	1.005	0.689	1 107		
10	-0.913	0.861	0.558	1.132		
11	-0.556	0.750	0.667	1.081		
12	0.379	1.127	0.897	1.114	-0.38	0.57
13	-0.330	0.857	0.762	1 247	-0.17	0.26
14	-0.589	0.880	0.758	1 068	-0.028	0.853
15	-0.085	0.952	1.272	-0.252	-0.144	0.857
16	-0.311	0.906	0.237	0.909	-0.068	0.779
17	-0.235	0.943	0.494	1.198	-0.143	0.810
18	-0.32	0.84	0.521	1.242	-0.220	0.678
19	-0.322	0.787	0.530	1.222	-0.3637	0.4499
20	-0.185	0.717	0.661	1.054	-0.189	0.592
21						

47°S, SAZ 1998

	G. BULLOIDES		*G. INFLATA*		*N. PACHYDMERMA* (s.)	
Cup	$\delta^{13}C$	$\delta^{18}O$	$\delta^{13}C$	$\delta^{18}O$	$\delta^{13}C$	$\delta^{18}O$
1	-0.40	0.810	0.783	1.143	-0.266	0.348
2	-0.83	0.604	0.778	0.878		
3	-0.597	0.821	0.916	1.198	-0.121	0.590
4	-0.37	0.827	0.960	1.262	-0.161	0.420
5	-0.56	0.843	0.887	1 264		
6	-0.92	0.984	0.638	1.221		
7	-0.49	0.821	0.815	1.102		
8	-1.01	0.936	0.797	1.383		
9			0.683	1.480		
10	-0.57	1.02	0.592	1.094		
11	-0.76	1 108	0.542	1 263		
12	0.00	1.41	0.749	1.396		
13	0.08	1.4104	0.775	1.573		
14	-0.06	1.286	0.800	1.622		
15	0.05	1.45	0.839	1.672		
16	-0.20	1.30	0.619	1 251		
17	-0.72	1.20	0.774	1.412		
18	-0.07	2.08				
19						
20	-0.33	0.891	0.325	0.846		
21						

51°S, SAF

	G. BULLOIDES		*G. INFLATA*		*N. PACHYDMERMA* (s.)	
Cup	$\delta^{13}C$	$\delta^{18}O$	$\delta^{13}C$	$\delta^{18}O$	$\delta^{13}C$	$\delta^{18}O$
1	0.255	1.911	1.184	2.226		
2	0.187	1.852	1.167	2 193		
3	0.408	1.911	1.293	2 286		
4	0.285	1.926	1.325	2.386	0.331	1.907
5	0.228	1.941	1.296	2.336	0.604	1.941
6	0.069	1.956	1.100	2.225	0.07	1.89
7	0.061	2.091	1.142	2.299	0.25	1.81
8	0.258	2.239	1.263	2.442	-0.07	1.70
9	0.189	2.084	1.371	2.536	0.598	1.837
10	0.247	2.238	1.237	2.171	0.55	1.61
11	0.601	2.262	1.197	2.393	0.696	1.797
12	0.629	2.069	1.205	2.284	0.916	1.906
13	0.331	1.949			0.576	2.000
14	0.19	1.49			0.65	1.63
15	0.096	1.592			0.842	1.960
16	0.186	1.572			1.002	1.844
17	0.468	1.871			0.875	1.789
18	0.131	1.579			0.861	1.520
19	0.268	1.622			0.713	1.531
20	-0.007	1.447			0.668	1.330
21	0.087	1.651			0.853	1.428

54°S, PFZ

	G. BULLOIDES		*N. PACHYDMERMA* (s.)	
Cup	$\delta^{13}C$	$\delta^{18}O$	$\delta^{13}C$	$\delta^{18}O$
1				
2				
3				
4			0.61	2 20
5			0.701	2.433
6			0.768	2.751
7			0.772	2.386
8	0.04	2.79	0.872	2.683
9	0.17	2.80	0.737	2.482
10	0.24	2.81	0.738	2.408
11	0.53	2.83	0.578	2.573
12	0.63	2.72	0.900	2.410
13	0.72	2.45	1.001	2.298
14	0.63	2.53	0.921	2.424
15	0.6274	2.5789	0.820	2.310
16	0.55	2.61	0.974	2.252
17	0.751	2.449	0.938	2.214
18	0.7921	2.6513	0.953	2.231
19	0.41	2.24	1.364	3.429
20	0.63	2.55	0.956	2.454
21	0.55	2.26	0.867	2.215
22	-0.38	2.13	0.805	2 151